NUCLEOSOME ASSEMBLY AND HISTONE H3 METHYLATION DURING DNA REPLICATION

TamarTom **Rolef Ben-Shahar**

A thesis submitted for the degree of Ph.D.

at

The University of London

July, 2004

Cancer Research UK London Research Institute,

Clare Hall Laboratories,

South Mimms, Hertfordshire, EN6 3LD

and

University College London,

Gower Street, London, WC1 6BT

ProQuest Number: 10014844

All rights reserved

INFORMATION TO ALL USERS
The quality of this reproduction is dependent upon the quality of the copy submitted.

In the unlikely event that the author did not send a complete manuscript
and there are missing pages, these will be noted. Also, if material had to be removed,
a note will indicate the deletion.

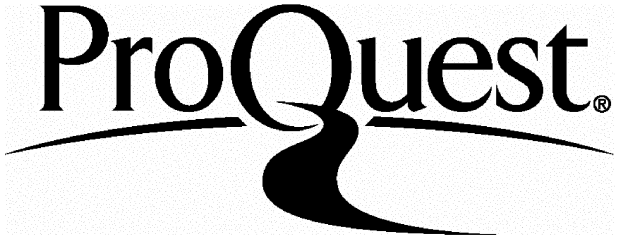

ProQuest 10014844

Published by ProQuest LLC(2016). Copyright of the Dissertation is held by the Author.

All rights reserved.
This work is protected against unauthorized copying under Title 17, United States Code.
Microform Edition © ProQuest LLC.

ProQuest LLC
789 East Eisenhower Parkway
P.O. Box 1346
Ann Arbor, MI 48106-1346

ACKNOWLEDGEMENTS

To begin with, I would like to acknowledge my mistakes, scientific and others. Hopefully the future will show that I have learned what I could from them.

My work has been funded by Cancer Research UK and with a B'NAI BRITH scholarship, and for that I am grateful. I would like to thank Alain Verreault for his supervision, for our scientific conversations and for allowing me to make my own mistakes. My gratitude is given to Munah Abdul-Rauf for being a colleague, collaborator, friend and sister; to Michal Goldberg, Niki Hawks and to other friends and colleagues in Clare-Hall. I would also like to thank the people at the service units here at Clare Hall, and in Lincoln Inn Fields. A special thanks to Yossi Gruenbaum for having faith in me, and to Wendy for her support.
My heart is always with Anath who gave me perspective in recent years.

Last but not least to Asaf, I thank you for everything.

ABSTRACT

Nucleosome assembly is essential for viability and entails a controlled mechanism by which newly synthesised histones are specifically deposited onto replicating DNA by assembly factors such as Chromatin Assembly Factor 1 (CAF1). CAF1 binds directly to Proliferating Cell Nuclear Antigen (PCNA), a processivity factor for DNA replication and repair, and this interaction is necessary to target its 'cargo', histones H3/H4, to newly synthesised DNA. Chapter 3 in this work presents the characterisation of the interaction between CAF1 and PCNA. This interaction is surprisingly complex, involving two distinct consensus PCNA binding motifs in the p150 subunit of CAF1, which are functionally distinct. Similar motifs are found in many other proteins involved in cell cycle control, DNA replication, DNA modification and various forms of DNA repair. I found some specificity in binding to PCNA, underscoring the existence of a regulatory mechanism which ensures that CAF1 and other PCNA-binding proteins act in a well-orchestrated manner at the replication fork.

In Chapters 4 and 5, I employed two different techniques to identify other factors involved in chromatin assembly in human cells and in yeast. Micro-array analysis in budding yeast revealed global changes in gene expression in chromatin assembly factors null mutants. Through this screen I identified Periodic Tryptophan Protein 1 (Pwp1) as a putative chromatin assembly factor.

The faithful replication and transfer of hereditary material to daughter cells includes not only accurate duplication of the parental DNA and chromosome architecture, but also the propagation of an epigenetic 'signature'. DNA replication offers a window of opportunity for cells to duplicate or modify the epigenetic state. For instance, DNA methylation is propagated during replication by the binding of the maintenance DNA Methyltransferase DNMT1 to PCNA. In Chapter 6, I used the budding yeast to examine a possible role for PCNA in directing the specialised histone H3 lysine 4 methyltransferase Set1 to newly assembled chromatin.

ABBREVIATIONS

2D	Two Dimensional
Ab	Antibody
Ade	Adenine
ACF	ATP utilising Chromatin assembly and remodelling Factor
ALB	Agarose Loading Buffer
Amp	Ampicillin
Apn2	AP nuclease 2
APS	Ammonium persulphate
ARS	Autonomously Replicating Sequence
Asf1	Anti-silencing factor 1
ATP	Adenosine 5'-triphosphate
BER	Base Excision Repair
BLAST	Basic Local Alignment Search Tool
Bp	Base pairs
BrDU	Bromodeoxyuridine
BSA	Bovine Serum Albumin
βME	β-Mercaptoethanol
CAC	Chromatin Assembly Complex
CAF1	Chromatin Assembly Factor 1
Cdc	Cell division cycle
CDK	Cyclin Dependent Kinase
CHRAC	Chromatin Accessibility Complex
D	Dimerisation Domain
DDK	Dbf4-dependent kinase
dH_2O	Distilled water
DEPC	Diethylpyrocarbonate
DMSO	Dimethyl sulphoxide
DNA	Deoxyribonucleic Acid
DNA-PK	DNA-Protein Kinase
DNMT	DNA Methyltransferase
dNTP	Deoxy N-5'-triphosphate
Δ	Deletion mutant
ECL	Enhanced Chemiluminescence
EDTA	Ethylene diamine tetra-acetic acid
EGFP	Enhanced GFP
ERFP	Enhanced RFP
ExPasy	Expert Protein Analysis System
FACT	Facilitates Chromatin Transcription
FBS	Foetal Bovine Serum
FEN1	Flap Endonuclease 1
FOA	5-Fluoro-orotic acid
FPLC	Fast performance liquid chromatography
GADD 45	Growth Arrest and DNA Damage induced protein 45
GAL	Galactose
GEB	GST Elution Buffer
GFP	Green Fluorescent Protein
GO	Gene Ontology
GST	Glutathione-S-transferase
HA	Haemagglutinin
HAST	Hda1-Affected Subtelomeric domains
HAT	Histone Acetyltransferase
HD1	Histone Deacetylase 1
HDAC	Histone Deacetylase
HEPES	N-(2-Hydroxyethyl) piperazine-N'-(2-ethanesulfonic acid)
Hir	Histone gene regulation
HLB	His Lysis Buffer
HML	Homothalic Mating type loci L
HMR	Homothalic Mating type loci R
HMT	Histone Methyltransferase
HP1	Heterochromatin Protein 1
HRP	Horseradish Preoxidase

HU	Hydroxyurea
IDCL	Inter-Domain Connecting Loop
IPTG	Isopropyl-β-D-thiogalactopyranoside
ISWI	Imitation Switch
Kan	Kanamycin
Kb	Kilo base
Kd	Dissociation constant
kDa	Kilo Dalton
LB	L Broth
Leu	Leucine
Lig1	DNA ligase I
mAb	Monoclonal antibody
MBD	Methyl-DNA binding
MCM	Micro-Chromosome Maintenance
MeCP	Methyl-CpG binding Protein
MIPS	Munich Information Centre for Protein Sequences
MLB	Mammalian Lysis Buffer
MLH	Mut L homologue
MMR	Mismatch Repair
MMS	Methylmethanesulfonate
MOI	Multiplicity Of Infection
MSH	Mut S homologue
MyD 118	Myeloid Differentiation primary response gene 118
NAP	Nucleosome Assembly Protein
NCBI	National Centre for Biotechnology Information
NER	Nucleotide Excision Repair
NGS	Normal Goat Serum
nt	nucleotides
NuRD	Nucleosome Remodelling histone Deacetylase complex
NURF	Nucleosome Remodelling Factor
OD	Optic Diffraction
ON	Overnight
Orc	Origin Recognition Complex
ORF	Open Reading Frame
pAb	Polyclonal antibody
PAS	Protein A Sepharose
PBM	PCNA Binding Motif
PBP	PCNA Binding Protein
PBS	Phosphate Buffered Saline
PBS-T	PBS + 1% Tween20
PBS-TB	PBS-T + 5% BSA
PBS-TM	PBS-T + 5% skimmed Milk
PCR	Polymerase Chain Reaction
PCNA	Proliferating Cell Nuclear Antigen
PEI	Polyethyleneimine
pI	Isoelectric point
PI	Protease Inhibitors
PMSF	Phenylmethylsulfonyl Fluoride
Pol	DNA polymerase
PP1	Protein Phosphatase 1
PPase	Protein Phosphatase
Pre-IC	Pre-Initiation Complex
Pre-RC	Pre-Replication Complex
PVP	Position-effect Variegation
PWP1	Periodic Tryptophan Protein 1
RAS	Retrovirus-Associated DNA Sequences
Rb	Retinoblastoma
RCAF	Replication-Coupling Assembly Factor
rDNA	Ribosomal DNA
RFC	Replication Factor C
RFP	Red Fluorescent Protein
RNA	Ribonucleic Acid
RNase HI	RNA nuclease HI
RPA	Replication Protein A
rpm	Revolutions per minute
rRNA	Ribosomal RNA

RT	Room Temperature
S100	Cytosolic Buffer
SAGE	Serial Analysis of Gene Expression
Sas2	Something About Silencing 2
SDM	Site Directed Mutagenesis
SDS-PAGE	Sodium Dodecyl Sulphate-Polyacrylamide Gel Electrophoresis
Set1	Su(var)3-9 – enhancer of zeste – trithorax 1
SGD	*Saccharomyces* Genome Database
Sir	Silent information regulator
siRNA	small interference RNA
Snf2/SNF2H	Sucrose non-fermenting yeast homologue-like 2
SSB	Single Strand Break
SsDNA	Single Stranded DNA
SUV39H1	Suppressor of Variegation 3-9 homologue 1
SV40	Simian Virus 40
TAFII	TATA-binding protein Associated Factor II
T Ag	T Antigen
TCA	Trichloroacetic Acid
TE	Tris EDTA solution
TEMED	N,N,N',N'-Tetramethylethylenediamine
Tm	Melting Temperature
tRNA	Transfer RNA
Tris	Tris (hydroxymethyl) aminomethane
Trp	Triptophan
TSA	Trichostatin
TSS	Transformation and Storage Solution
Tween 20	Polyoxyethylene (20) sorbitan monolaurate
Ubc9	Ubiquitin-like protein SUMO-1 conjugating enzyme
UNG2	Uracil N-Glycosylase 2
Ura	Uracil
UV	Ultraviolet
WICH	WSTF-ISWI Chromatin remodelling complex
Xic	X inactivation centre
Xist	Inactive X specific transcript
XPG	Xeroderma Pigmentosum G
YNB	Yeast Nitrogen Base
YPD	Yeast Peptone Dextrose

CONTENTS

Page

Acknowledgements 2
Abstract 3
Abbreviations 4
Contents 7
Tables and figures 10
Chapter 1 – Introduction
1.1 Historical Perspective 13
1.2 S phase and the eukaryotic cell cycle 14
1.3 DNA replication 14
1.3.1 Replication initiation 14
1.3.2 Multiple replication sites are activated throughout S phase 17
1.3.3 The process of DNA replication 20
1.3.4 DNA replication within the cell cycle context 27
1.4 A general view on genome duplication 28
1.4.1 DNA lesion bypass polymerases 29
1.4.2 DNA repair 29
1.4.3 DNA methylation following replication 31
1.4.4 Chromatin assembly following replication 31
1.4.4.1 Following the histones 34
1.4.4.2 ASF1 35
1.4.4.3 CAF1 36
1.4.4.4 CAF1 in DNA repair 41
1.4.4.5 The Hir proteins 43
1.4.4.6 Other histone chaperons 45
1.4.5 Replication related Chromatin remodelling 46
1.5 The assembly of specialised chromatin structures 47
1.5.1 Functionally specialised chromatin structures and epigenetic marks 47
1.5.2 Propagation of histone post-translational modification in proliferating cells 48
Chapter 2 – Materials and methods
2.1 Buffers 51
2.2 Basic DNA methods 55
2.3 RNA methods 58
2.4 Basic protein methods 59
2.5 *E. coli* methods 69
2.6 Baculoviruses and insects SF9 cells 70
2.7 Expression and purification of recombinant proteins 72
2.8 Protein-protein interaction assays 79
2.9 Yeast 79
2.10 Mammalian cells 83
2.11 Fluorescence and immunofluorescence microscopy 87
2.12 SV40 DNA replication and chromatin assembly assay 89
2.13 Enzymatic reactions 90
2.14 Word and Image processing and molecular biology computer programmes 91

2.15 WWW useful sites..... 92
Chapter 3 – Characterisation of the interaction between CAF1 and PCNA and it's implications
3.1 Introduction..... 93
3.2 CAF1 has three putative PCNA binding motifs..... 100
3.3 CAF1 binds PCNA *in vitro*..... 100
3.3.1 CAF1 binds PCNA *in vitro* via the first 467 residues in p150 100
3.3.2 p150 binds PCNA *in vitro* via PBM1..... 102
3.3.3 p150 PBM1, but not PBM2 nor the p60 PBM, binds to PCNA..... 103
3.4 The rationale behind PCNA mutagenesis..... 106
3.5 CAF1 and PCNA interact *in vitro* via PBM1 on p150 and hydrophobic residues on the PCNA IDCL..... 109
3.6 PBM mutations do not interfere with p150 binding to other proteins..... 110
3.7 PBM2 is essential for CAF1 dependent nucleosome assembly *in vitro*..... 111
3.7.1 P150ΔPBM2 but not p150ΔPBM1 is deficient in nucleosome assembly *in vitro*..... 114
3.7.2 P150ΔPBM1 binds weakly to PCNA in S100 extract..... 115
3.8 The interaction of p150 with PCNA does not seem to depend upon its phosphorylation state..... 118
3.9 Targeting CAF1 to DNA replication *in vivo*..... 124
3.9.1 PBM1 and PBM2 synergistically contribute to the targeting of p150 to DNA replication foci *in vivo*..... 124
3.9.2 PBM2 and the dimerisation domain are jointly crucial for targeting CAF1 to DNA replication foci *in vivo*..... 131
3.10 CAF1 PBM peptides preferentially inhibit nucleosome assembly over DNA synthesis..... 133
3.11 CAF1 PBM1 can convert DNA Ligase I into a preferential inhibitor of nucleosome assembly..... 142
3.12 Cac1 binding to PCNA in yeast..... 144
3.12.1 PBM1 binding to PCNA is conserved in yeast *cac1* and human p150..... 144
3.12.2 PBM1 is important for Cac1 function *in vivo*..... 144
3.12.2.1 *cac1 PBM1* mutation in *hirΔ* background confers slow growth..... 146
3.12.2.2 *cac1* PBM1 mutation in *hirΔ* background slightly increases mitotic chromosome loss rate..... 148
3.13 Conclusions and future objectives..... 152
3.13.1 Multiple PCNA binding sites on CAF1..... 152
3.13.2 Unresolved puzzles..... 154
3.13.3 The purpose of two distinct PBMs in CAF1..... 156
3.13.4 Regulation of PCNA binding by CAF1..... 158
3.13.5 The dimerisation of p150 molecules..... 161
3.13.6 The interaction of CAF1 with HP1..... 163
3.13.7 Understanding the sequence of events at the replication fork..... 164

Chapter 4 - A search for CAF1 binding proteins
4.1 Introduction..... 167
4.2 Multiple polypeptides co-precipitate with p60 and p150..... 169
4.3 2D gel and mass spectrometry analysis..... 173
4.4 DNA polymerase α/primase..... 178
4.5 Discussion..... 179
4.5.1 DNA polymerase α/primase, a potential CAF1 binding protein..... 180
4.5.2 Insights from 2D gel analysis..... 182
Chapter 5 – Preliminary expression analysis of *cac1* and *asf1* mutants and the search for novel nucleosome assembly factors
5.1 Introduction..... 183
5.2 Micro-array analysis..... 183
5.3 General analysis of micro-array data..... 184
5.4 Expression of genes of interest..... 191
5.4.1 Expression of genes in specific chromosomal domains..... 191
5.4.1.1 Subtelomeric regions..... 193
5.4.1.2 The *RDN1* locus..... 195
5.4.1.3 Other RNA genes..... 197
5.4.1.4 The silent mating type loci..... 199
5.4.1.5 Other chromosomal regions..... 199
5.4.2 Expression of genes in related pathways..... 201
5.4.3 Specific genes of interest have altered expression in *asf1 cac1* mutants..... 202
5.5 *PWP1* expression is reduced in *asf1 cac1* double mutants..... 203
5.6 Pwp1 level under different conditions..... 206
5.6.1 Pwp1 levels in wild type and mutant cells..... 206
5.6.2 Pwp1 levels after treatment with DNA damaging agents..... 206
5.7 Degradation of overexpressed Pwp1..... 207
5.8 Pwp1 binds histone H3 *in vivo*..... 210
5.9 Pwp1 binding to histone H3 increases in *hat1Δhat2Δ* cells..... 211
5.10 Conclusions and future objectives 214
5.10.1 Notes on the micro-array screen..... 214
5.10.1.1 Expression in subtelomeric regions..... 216
5.10.1.2 Expression from the *RDN1* locus..... 217
5.10.1.3 Expression of genes on chromosome 11..... 217
5.10.2 Pwp1 and nucleosome assembly: an open question 219
Chapter 6 – Does *S. cerevisiae* SET1 function in S phase via PCNA?
6.1 Introduction..... 224
6.2 Set1 contains a putative PCNA binding motif..... 227
6.3 Mutations in the Putative PBM of Set1 Cause a strong decrease in H3 K4 methylation *in vivo* 227
6.4 Mutations in PCNA may cause some loss of histone H3 K4 methylation..... 229
6.5 Pull down assays..... 232
6.6 Conclusions and future objectives 232
References..... 235
Appendix I – Cloning databases..... 264
Appendix II – Micro-array screen results..... 278

TABLES AND FIGURES

		Page
Chapter 1		
Figure 1.1	Initiation of DNA replication	15
Figure 1.2	DNA replication	16
Figure 1.3	Replication foci patterns in mammalian cells throughout S phase	19
Figure 1.4	PCNA structure	22
Figure 1.5	Lagging strand synthesis	26
Figure 1.6	The structure of the nucleosome core particle	32
Figure 1.7	CAF1 is composed of three subunits	38
Chapter 2		
Figure 2.1	Standard curve from Bradford protein reagent with BSA	59
Figure 2.2	Purification of C-His PCNA by gel filtration	68
Figure 2.3	Titration of baculovirus to SF9 cells for protein expression	71
Figure 2.4	Comparing expression of C-His PCNA in BL21 and in CodonPlus™	72
Figure 2.5	Purification of C-His p150	74
Figure 2.6	Purification of N-His Lig1 and PBM1-Lig1 and of GST-tagged proteins	75
Figure 2.7	Purification of recombinant CAF1 and T Antigen from SF9 cells	77
Figure 2.8	p150 expression *in vitro*	78
Figure 2.9	Phosphorylation of CAF1 by CDK2/A3	91
Table 2.1	Commonly used Protein gels	61
Table 2.2	Histone gels	61
Table 2.3	Tricine gels	61
Table 2.4	Primary antibodies used for Western blot analysis	65
Table 2.5	Peptides used in this work	67
Table 2.6	Protein expression in *E. coli* and purification procedures	73
Table 2.7	Mammalian cells used in this work	85
Table 2.8	Primary antibodies used for immunostaining	88
Table 2.9	SV40 DNA replication and chromatin assembly assay	89
Chapter 3		
Figure 3.1	CAF1 contains three putative PCNA binding motifs	99
Figure 3.2	p150 binds to PCNA	101
Figure 3.3	Binding of PBMs to PCNA	104
Figure 3.4	CAF1 p150 binds to the IDCL of PCNA via PBM1 *In vitro*	108
Figure 3.5	PBM mutations do not prevent p150 from interacting with other p150 target proteins	112
Figure 3.6	PBM2 but not PBM1, is important for nucleosome assembly during SV40 DNA replication *in vitro*	113
Figure 3.7	PCNA in the S100 extract binds weakly to p150ΔPBM1	117
Figure 3.8	CAF1 phosphorylation does not seem to affect PCNA binding *in vitro*	119

Figure 3.9 Phosphorylation of p150 does not appear to be involved in PCNA binding..... 123
Figure 3.10 Deletion of PBM1 and PBM2 interferes with localisation of GFP-p150 during early- and mid-S phase..... 126
Figure 3.11 Confocal microscopy images showing GFP-p150 mis-targeting during S phase due to deletion of PBM1 and PBM2..... 128
Figure 3.12 Both PBMs in p150 contribute to its localisation at DNA replication foci..... 132
Figure 3.13 Possible models for the sequence of events at the replication fork..... 135
Figure 3.14 Inhibition of DNA replication by PBM peptides in a T antigen dependent assay..... 137
Figure 3.15 p150 PBMs preferentially inhibit chromatin assembly over DNA synthesis in T antigen independent reactions 141
Figure 3.16 PBM1 can convert DNA Ligase I into a preferential inhibitor of chromatin assembly..... 143
Figure 3.17 The N-terminus of Cac1 can bind PCNA in a PBM1 dependent manner..... 145
Figure 3.18 The Cac1 PBM1 mutation confers a slow growth phenotype at 18°C in cells lacking Hir1 (*hir1Δ*), but not in wild-type cells (*HIR1*wt)..... 147
Figure 3.19 Assay to monitor the stability of a non-essential chromosome fragment..... 149
Figure 3.20 Putative mechanisms for PBM switching..... 159
Figure 3.21 Model for simultaneous nucleosome assembly onto both sister chromatids..... 162
Table 3.1 PCNA binding proteins..... 94
Table 3.2 PBM peptides used in this work..... 104
Table 3.3 Frequency of chromosome fragment CF III.L loss per mitotic division in yeast strains with Cac1 PBM mutations..... 150

Chapter 4
Figure 4.1 Immunoprecipitation of p150 and p60 from cell extracts 171
Figure 4.2 Preliminary analysis of immunprecipitated samples..... 172
Figure 4.3 2D gel analysis of proteins that co-immunoprecipitated with p150 from nuclear extract versus control..... 174
Figure 4.4 2D gel analysis of proteins that co-immunoprecipitated with p150 or p60 from nuclear extract..... 175
Figure 4.5 2D gel analysis of proteins that co-immunoprecipitated with p150 from nuclear versus chromatin extract..... 176
Figure 4.6 Figure 4.6: 2D gel analysis of proteins that co-immuno-precipitated with p150 or p60 from chromatin extract.... 177

Chapter 5
Figure 5.1 Comparison of expression in W303 versus *asf1Δ* cells.. 187
Figure 5.2 The distribution of entries with altered expression in the mutant strains..... 188
Figure 5.3 The distribution of annotated entries with strongly altered expression between the mutant strains..... 191

Figure 5.4 The genomic localisation of all available entries..... 192
Figure 5.5 The genomic localisation and expression of HAST entries..... 194
Figure 5.6 The distribution of subtelomeric entries with strongly altered expression between the mutant strains..... 195
Figure 5.7 The genomic localisation and expression of ribosomal RNA and tRNA genes..... 198
Figure 5.8 Genomic localisation and expression of specific groups of genes..... 200
Figure 5.9 The expression of Pwp1 is not influenced by mutations in chromatin assembly factors or DNA damage..... 205
Figure 5.10 Overexpressed Pwp1-HA3 is degraded in *cac1* mutant cells..... 209
Figure 5.11 PWP1 binds to higher amounts of histone H3 in *hat1Δhat2Δ* mutants than in wild type cells..... 213
Table 5.1 General overview of alterations in gene expression in mutant strains normalised to wild type cells..... 189
Table 5.2 PWP1 binding proteins..... 221
Chapter 6
Figure 6.1 SET1 has a putative PCNA binding motif..... 226
Figure 6.2 Mutations in the putative PBM of SET1 abolish H3 K4 methylation..... 228
Figure 6.3 *pol30* mutations may affect H3 K4 methylation by SET1..... 231
Appendix I
Table I.I Oligonucleotides used for cloning and site directed mutagenesis in this work..... 264
Table I.II plasmids used in this work..... 267
Table I.III Yeast strains used in this work..... 275
Appendix II
Table II.I Annotated genes whose expression is significantly altered in all three mutant strains relative to wild type... 278
Table II.II Annotated genes whose expression is significantly altered in *asf1Δ* and *asf1Δcac1Δ* relative to wild type... 286
Table II.III Annotated genes whose expression is significantly altered in *cac1Δ* and *asf1Δcac1Δ* relative to wild type... 288
Table II.IV Annotated genes whose expression is significantly altered in *asf1Δ* and *cac1Δ* relative to wild type..... 289
Table II.V Annotated genes whose expression is significantly altered in *asf1Δ* only relative to wild type..... 291
Table II.VI Annotated genes whose expression is significantly altered in *cac1Δ* only relative to wild type..... 292
Table II.VII Annotated genes whose expression is significantly altered in *asf1Δcac1Δ* only relative to wild type..... 293

CHAPTER 1 - INTRODUCTION

1.1 HISTORICAL PERSPECTIVE

Scientists in the late 19th century were the first to describe mitotic chromosomes, as seen under the microscope. Several decades later, Watson and Crick determined the structure of DNA (Watson and Crick, 1953). This paved the way for our modern understanding of life at a molecular level. In the following half-century, exhaustive studies shed light on the replication of DNA. The initial suggestion of Watson and Crick that semi-conservative DNA duplication could explain genetic inheritance was verified and many important aspects of DNA replication have been elucidated at the molecular level. However, it also became clear that, in eukaryotes, there is an additional level of complexity and regulation imposed by the physical structure in which the DNA is packaged in the cell. This structure, known as chromatin, includes the DNA, histones, non-histone proteins, and non-coding RNA (Adkins et al., 2004).

In the early days of chromatin research, "histones were commonly regarded as unpleasant proteins for rigorous studies" (Cook et al., 1956). The reason for this non-enviable reputation was that the strong non-specific affinity of histones for DNA often interfered with studies of DNA related processes such as transcription or replication.

However, it is now clear that histones not only serve for the compaction of DNA in the nucleus, but that they are also involved in many aspects of DNA metabolism including the regulation of gene expression.

Since this thesis is mainly concerned with the duplication of chromatin structure and its maintenance during DNA replication, in this introduction I wish to contextualise this within the "story" of the nucleus in S phase. I first describe DNA replication followed by an overview of other processes that also occur at the replication fork. Finally, our current knowledge of nucleosome assembly is described in detail.

1.2 S PHASE AND THE EUKARYOTIC CELL CYCLE

Proliferating cells undergo a very conserved and tightly regulated series of events that constitute the cell cycle. In most cells, this cycle consists of four distinct phases: G1, the first gap phase when cell growth occurs; S phase - when the genome is replicated; G2, a second gap phase, dedicated to chromosome and cell preparation for division; and M-phase or mitosis, when the physical segregation of chromosomes and cytokinesis produce two daughter cells.

The transitions between the various stages of the cell cycle are mediated by oscillations in the activity of cyclin-dependent kinases (CDKs) complexed with specific cyclins. Cyclin synthesis is necessary for phase entry, and CDK-cyclin inhibition or cyclin degradation is needed for phase exit (Murray and Hunt, 1993). The transition from late G1 to S phase necessitates the expression of many specific genes (Simon et al., 2001).

1.3 DNA REPLICATION

The major event taking place during S phase is the replication of the entire genome. DNA replication in eukaryotic cells is a complex process requiring the interplay of many proteins (for reviews see Jonsson and Hubscher, 1997; Waga and Stillman, 1998).

1.3.1 Replication initiation

Several mechanisms ensure that DNA replication occurs with high accuracy and fidelity once and only once per cell cycle. Much of this regulation occurs at the level of initiation of DNA replication (Bell and Dutta, 2002; Mendez and Stillman, 2003).

Replication initiates at specific sites along the genome termed 'origins of replication'. The eukaryotic origins of replication direct the formation of a number of protein complexes leading to the assembly of two divergent DNA replication forks. To reach this point, at least 20 different and mostly evolutionary conserved proteins function in the process of DNA replication initiation (Figure 1.1).

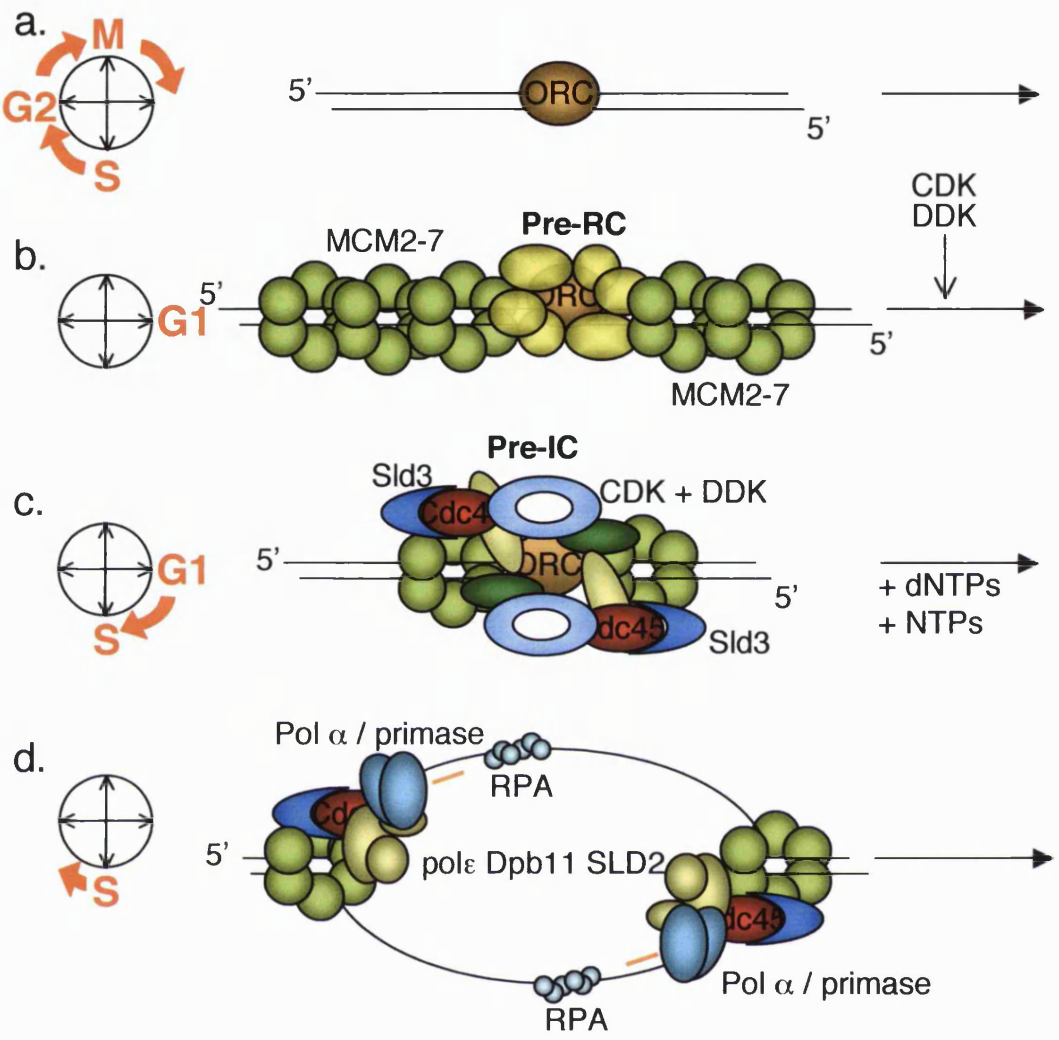

Figure 1.1: Initiation of DNA replication

The process of DNA replication initiation involves at least 20 different proteins.

a. The origin of recognition complex (ORC), is bound to origins of DNA replication throughout most of the cell cycle.

b. During late mitosis and early G1, pre-RCs are assembled at origins of replication. It is believed that the primary role of the pre-RC is loading MCM complexes onto chromatin.

c. Upon G1/S transition and throughout S phase, activity of protein kinases such as the S-phase CDK and DDK triggers the transition to competent pre-IC to begin active DNA synthesis. Several components of the pre-RC are removed while other bind to the complexes at origins. These include Cdc45, Sld3 and the CDK and DDK themselves.

d. The ultimate goal of the DNA replication initiation machinery is the assembly of the DNA replication polymerases. The MCM proteins which are part of the pre-IC, are found associated with the progressing replication forks following replication initiation. The MCM rings are believed to function as the DNA replication helicases. Cdc45 and Sld3 are thought to function in polymerase recruitment, and Cdc45 also becomes associated with the progressing DNA replication forks. Its association with the MCM proteins as well as the DNA polymerases suggests that it may coordinate the function of these complexes at the replication fork. RPA is recruited and binds to the ssDNA exposed by the unwinding of DNA at origins. DNA polymerase ε, together with Dpb11 and SLD2 are recruited to the initiation complex. Following this, the DNA polymerase α/primase complex (pol α/primase) is recruited, and utilising NTPs and dNTPs, this complex synthesises a short RNA-DNA primer. Here only the leading strand priming is shown, but lagging strand initiation occurs similarly.

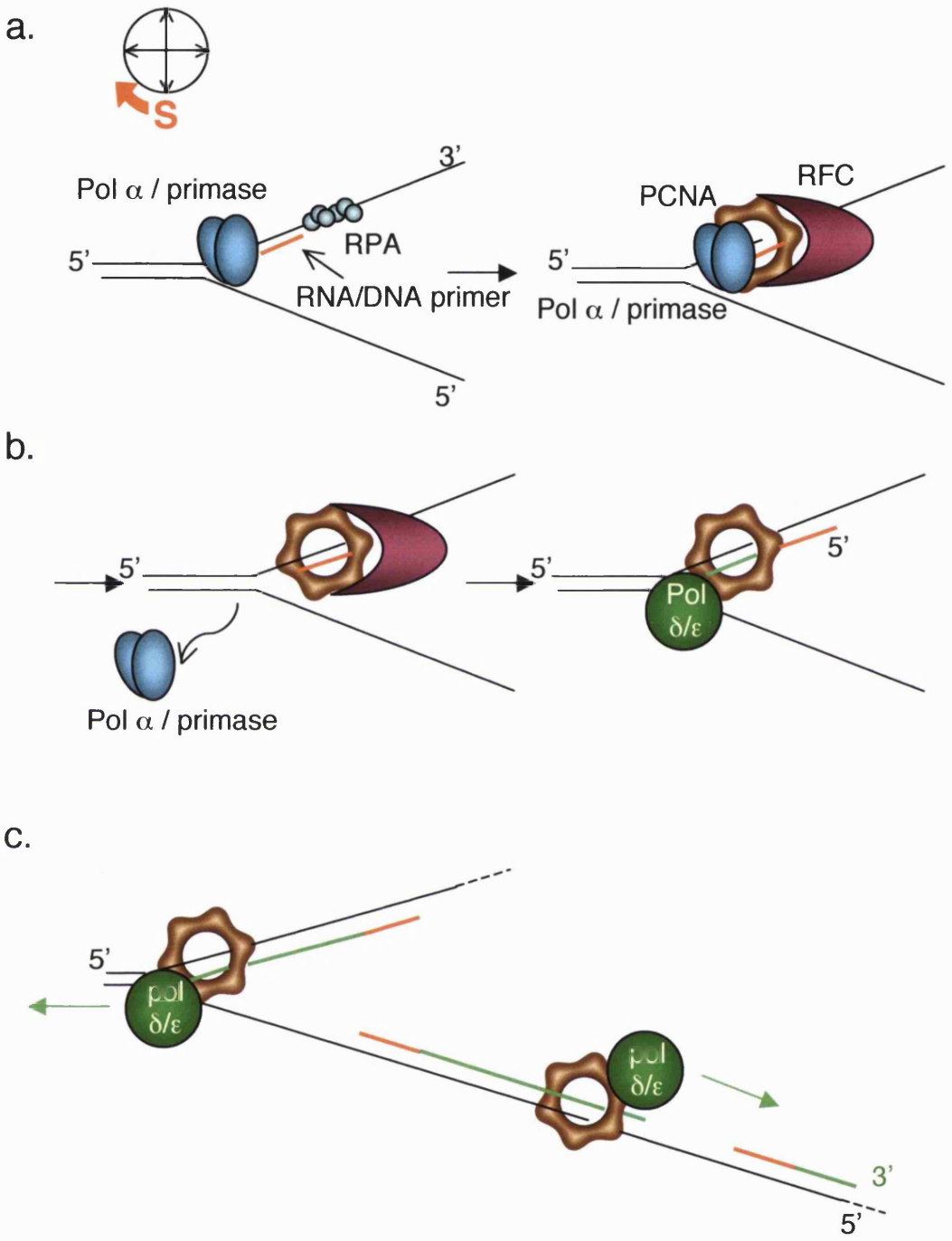

Figure 1.2: DNA replication
The events taking place at a leading strand of a single DNA replication fork are shown.
a. pol α/primas is recruited to the ssDNA protected by RPA, and synthesises an RNA-DNA primer. This is recognised by RFC which loads PCNA onto DNA.
b. pol α/primase is dissociated from DNA, and DNA polymerase δ or ε (pol δ/ε) can bind to the PCNA ring, and synthesise DNA processively from the RNA-DNA primer.
c. Similar events take place at the lagging strand. Because DNA synthesis occurs in a 5'-3' direction, lagging strand synthesis is discontinuous, whereby a fragment of roughly 200 bp is synthesised upstream of the previous fragment.

The initiation of DNA replication in eukaryotic cells is a two-step process. The assembly of pre-replicative complexes (pre-RCs), also known as 'origin licensing', occurs in late M-phase and G1 but another activation step is needed before initiation can occur. At the G1/S transition and throughout S phase, the conversion of pre-RC into pre-initiation complexes (pre-IC – Figure 1.1) is required before DNA synthesis can begin. This is governed by the activities of protein kinases such as the S phase CDKs and the Dbf4-Dependent Kinase (DDK, also known as Cdc7-Dbf4). The initiation process is concluded by the loading of the DNA polymerase holoenzymes (Figures 1.1-1.2).

After initiation of DNA replication from a particular origin, the pre-IC is dismantled and the origin switches to a non-competent state. The CDKs block re-initiation by targeting several components of the pre-RC/IC, preventing cells in the post-initiation state from forming new pre-IC complexes. Competence is restored in late mitosis by inhibiting CDK activity, and a new round of origin licensing takes place after sister chromatid segregation (Bell and Dutta, 2002; Mendez and Stillman, 2003).

1.3.2 Multiple replication sites are activated throughout S phase

Eukaryotic genomes are large, ranging from 10^7 to over 10^9 base pairs (bp), and are organised into multiple chromosomes. In mammalian cells, the replication fork progresses *in vivo* at an average rate of about 1.7 Kbp per minute (Berezney et al., 2000). Thus, were a single origin of replication responsible for the replication of each chromosome, it would have taken a human cell with roughly 3.2 billion bps of DNA more than 28 days to duplicate its genome. Consequently, to efficiently duplicate their large discontinuous genomes within the relatively short time span of S phase, eukaryotes have evolved a mechanism by which initiation of replication occurs at many sites along the chromosomal DNA. The use of numerous origins of DNA replication ensures that no stretch of DNA is left unreplicated beyond the normal duration of S phase (Hyrien et al., 2003). In budding yeast, there are roughly 460 active origins of replication (Wyrick et al., 1999), whereas the human genome contains an estimated $4x10^4$ origins (Berezney et al., 2000).

In most cells, origins are not all synchronously activated at the beginning of S phase. Instead, they fire in a reproducible temporal order throughout S phase, and can therefore be classified either as early- or late-firing origins. Similarly to origin licensing, the time of origin firing is determined in G1 (Goren and Cedar, 2003). Remarkably, there is a strong correlation between the level of gene transcription and their timing of replication (Goren and Cedar, 2003; McNairn and Gilbert, 2003). With a few notable exceptions (Kim et al., 2003; Schubeler et al., 2002), most active genes are located within early replicating euchromatin, while most heterochromatin (a condensed and inactive chromatin structure) is replicated late in S phase. The different replication timings of these two distinct types of chromatin structures may be important to propagate their unique features to daughter cells (Dillon and Festenstein, 2002; Flickinger, 2001).

During S phase, between 1 and 10 replicons are clustered together in structures known as replication factories or replication foci (Berezney et al., 2000). In mammalian cells, these factories can be visualised by immunofluorescence as well-defined foci in the nucleus (Fox et al., 1991; and Figure 1.3). Interestingly, cells exhibit distinct patterns of these foci as they progress through S phase and different segments of the genome are replicated (Spector, 2003). In early-S phase of human HeLa cells, approximately 750 replication foci are located throughout the nucleus with the exception of nucleoli. In mid-S phase, replication foci are more prominent along the nuclear periphery and peri-nucleolar regions. Late-S phase cells exhibit only a few large replication foci that are distributed throughout the nucleus and co-localise with pericentric heterochromatin. To generate this pattern, replication factories do not slide along the DNA, but rather disassemble and reassemble at adjacent sites (Berezney et al., 2000; Sporbert et al., 2002).

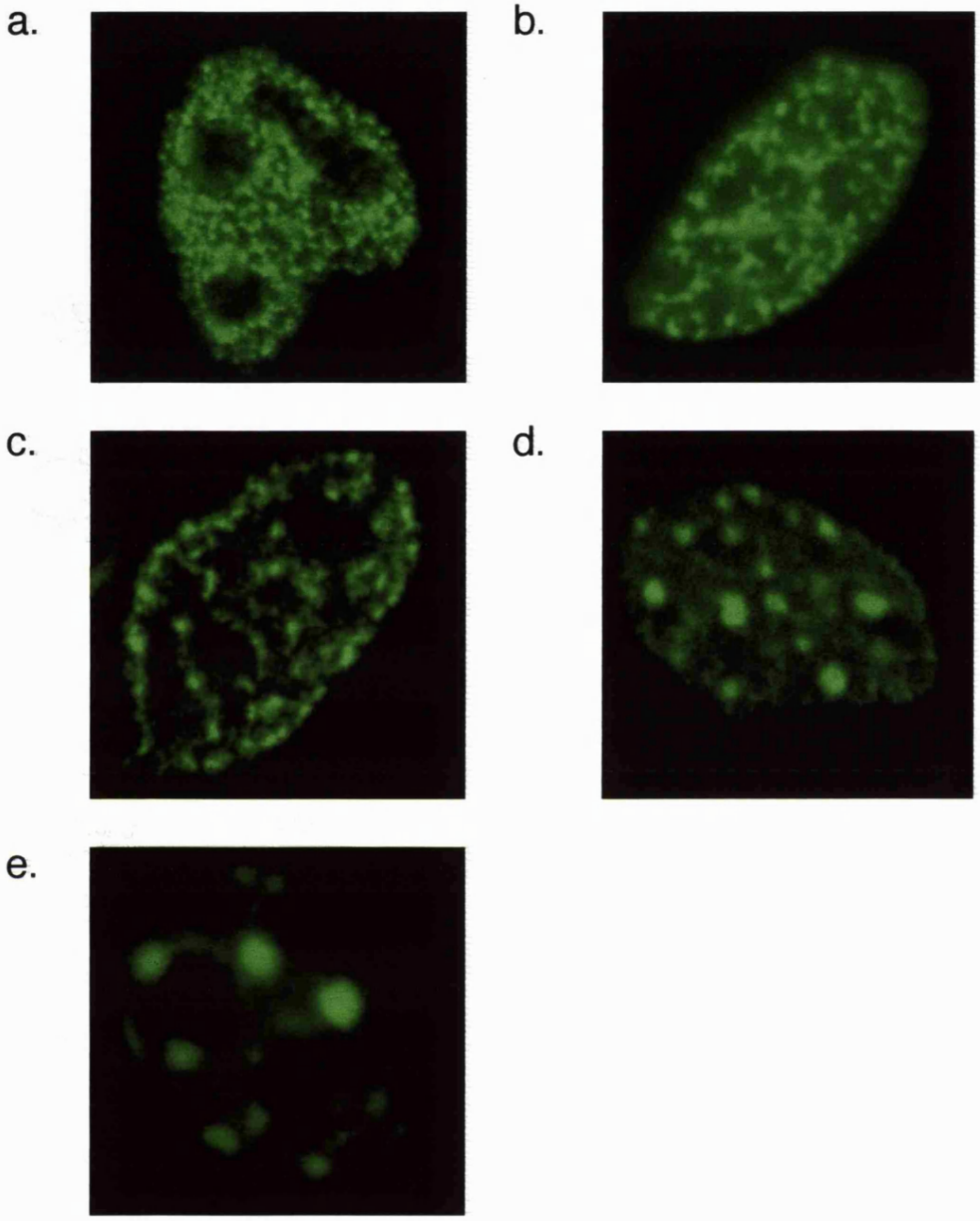

Figure 1.3: The patterns of DNA replication in mammalian cells throughout S phase
Five distinct patterns of DNA replication have been identified in mammalian cells (O'Keefe et al., 1992). Single optical sections taken by confocal laser scanning microscopy of fixed mouse NIH 3T3 cells in S phase are shown. Chromatin Assembly Factor 1 (CAF1 - see below) targets to replication foci throughout S phase and was used to illustrate the replication patterns. Cells were transfected with GFP-mCAF1 p150 expressing plasmid, and were processed and analysed 48 h later (see Chapter 2.11). During early- S phase, replication foci appear to be distributed at sites throughout the nucleoplasm, excluding the nucleolus (**a.**). As S phase progresses replication of euchromatin decreases and peripheral regions of heterochromatin begin to replicate (**b.**). During mid-S phase replication is restricted to of perinucleolar chromatin as well as peripheral areas of heterochromatin (**c.**). Later, interconnected patches of chromatin throughout the nuclear interior and at a few discrete sites at the periphery of the nucleus replicate, forming larger and fewer foci (**d.**). Finally replication occurs mostly at a few large regions of dense chromatin (**e.**).

1.3.3 The process of DNA replication

Each replication factory contains an average of five replicons, corresponding to ten replication forks (Berezney et al., 2000). Much of our understanding of events taking place at the replication fork comes from studies of the simian virus 40 (SV40), whose DNA is replicated by cellular proteins together with the viral T antigen (T Ag), and from genetic analyses in *Saccharomyces cerevisiae* (Waga and Stillman, 1998).

When the pre-RC becomes competent to initiate replication, the DNA double helix is locally unwound in the vicinity of the origin. This unwinding is catalysed by DNA helicases, which produce a single-stranded DNA (ssDNA) substrate that is protected and stabilised by the heterotrimeric ssDNA binding protein, replication protein A (RPA; Wold, 1997). RPA is able to wrap around long stretches of ssDNA, thus protecting the DNA that is exposed during DNA replication, recombination or repair (Figures 1.1d and 1.2a). RPA binding is followed by the loading of DNA polymerase α/primase complex (pol α/primase) onto DNA. This step, called primosome assembly, involves an interaction between pol α/primase and both RPA and a DNA helicase (T Ag during SV40 DNA replication or other endogenous helicases during cellular DNA replication). Pol α/primase is the only eukaryotic enzyme capable of initiating DNA chain synthesis *de novo* (Hubscher et al., 2002). The synthesis of the first stretch of nucleotides is initiated by primase, which synthesises a 10-nucleotide (nt) long RNA primer using DNA as template (Figure 1.2). Primase is replaced by pol α with which it is complexed, and pol α extends the RNA primer by adding 20-30 deoxyribonucleotides. The human pol α/primase consists of four subunits (p180, p70, p58 and p48), and similar subunits are found in all eukaryotes. The p180 subunit harbours the polymerase activity, and p48 the primase activity.

The primer-template junction is recognised by replication factor C (RFC). RFC is a heteropentameric ATPase that loads the sliding clamp Proliferating Cell Nuclear Antigen (PCNA) onto DNA. RFC is composed of one large

(p140/RFC1) and four smaller subunits (p40/RFC4, p38/RFC5, p37/RFC2, and p36/RFC3) that share considerable sequence similarity in their ATPase domains and are conserved in all eukaryotes (Mossi and Hubscher, 1998). PCNA is a homotrimer composed of ~30kDa subunits that associate in a head-to-tail fashion to form a closed ring structure (Figure 1.4; reviewed in Kelman, 1997; Kelman and Hurwitz, 1998; Tsurimoto, 1998; Tsurimoto, 1999),

In order to load PCNA onto DNA, RFC transiently disrupts the PCNA subunit interface and re-closes it when PCNA encircles DNA (Mossi and Hubscher, 1998). This ring can slide freely along the DNA (Figure 1.2; and Mozzherin et al., 1999; Yao et al., 1996), and is bound by DNA polymerases thus increasing processivity during elongation of DNA synthesis (Prelich and Stillman, 1988). However, PCNA also acts as platform to recruit several replication enzymes and a large number of other proteins (see Table 3.1), indicating that PCNA is essential not only in DNA replication, but also in coordinating replication with other processes. The primary amino acid (aa) sequence of PCNA is not highly conserved among species. Compared with human PCNA, aa sequence identity is 36%, 65% and 70% with yeast, plants and *Drosophila melanogaster*, respectively (Jonsson and Hubscher, 1997). Yeast and human PCNA nevertheless adopt an almost identical three-dimensional shape that is also very similar to the structures of the functional homologues of PCNA from *Escherichia coli* and bacteriophage T4 (*i.e.* the b-subunit of DNA polymerase III and the gp45 protein, respectively; Kelman, 1997). Each PCNA monomer consists of two globular domains, resulting in a trimeric ring with quasi-six-fold symmetry (figure 1.4). The two domains are nearly identical in structure, though they do not share sequence similarity (Krishna et al., 1994). The DNA sliding clamps are arranged in a two-layer structure. The outer layer is composed of b-sheets and loops with a highly negative electrostatic potential, which is ideal for interaction with other proteins. The inner layer, through which DNA is threaded, is composed of 12 α-helices with an array of basic residues positioned roughly perpendicular to the phosphodiester backbone of DNA. However, the helices do not interact strongly with DNA and thereby allow free sliding of PCNA along DNA (Gulbis et al., 1996; Krishna et al., 1994).

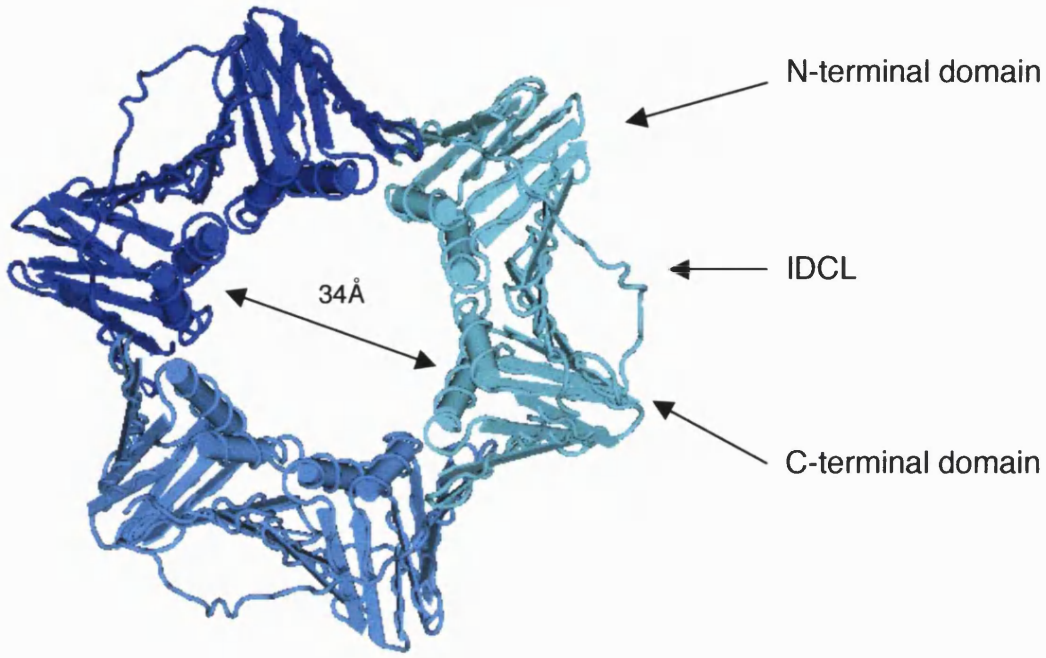

Figure 1.4: PCNA structure
The structure of a PCNA trimer ring, based on coordinates from Gulbis et al. (1996). The three monomers trimerising to form a ring are coloured in three different shades of blue. The N-terminal and C-terminal domains and the Inter-Domain Connecting Loop (IDCL) are marked. When PCNA is loaded onto DNA, DNA is threaded through the large cavity at the centre of the ring.

The two replication-associated DNA polymerases δ and ε (pol δ and pol ε) bind to PCNA loaded at the primer-template junction and function in front of the PCNA ring to drive DNA synthesis (Burgers, 1991; Mozzherin et al., 1999). PCNA serves as a processivity factor for both polymerases (Burgers, 1991; Lee et al., 1991; Tsurimoto and Stillman, 1991; reviewed in Tsurimoto, 1998; Tsurimoto 1999). The catalytic subunits of pol δ and ε both contain a 3'-5' proofreading exonuclease domain at their N-termini. This domain allows the enzymes to remove mis-incorporated nucleotides. Therefore DNA synthesis occurs with a low nucleotide mis-incorporation frequency of 10^{-4}-10^{-7}, ensuring faithful genome replication (Hubscher et al., 2002). The division of labour between these two DNA polymerases has been ground for heated debate. Pol δ seems to be the main replicative polymerase, and its proposed dimeric structure offers an attractive model for synchronous lagging and leading

strand synthesis (Hubscher et al., 2002). However, pol ε is also capable of processive and accurate DNA synthesis. In fact, it is becoming clear that pol ε catalytic activity, and not just its involvement in checkpoint activation is important for DNA replication *in vivo* (Fuss and Linn, 2002; Hubscher et al., 2002; Waga and Stillman, 1998).

Pol δ has at least three subunits in *S. cerevisiae* (Pol3, Pol31 and Pol33) and higher eukaryotes (p125, p50 and p66 in human cells), and at least four subunits in *Schizosaccaromyces pombe* (Pol3, Cdc1, Cdc27 and Cmd1). The large subunit harbours both the DNA polymerase and 3'-5' exonuclease proofreading activities (Hubscher et al., 2002). PCNA was primarily characterised as a processivity factor for this enzyme (Bravo et al., 1987; Prelich et al., 1987; Tan et al., 1986), and its binding site on PCNA has been mapped to the inter-domain connector loop (IDCL) using genetic and biochemical assays (Eissenberg et al., 1997; Fukuda et al., 1995; Jonsson et al., 1995; Oku et al., 1998; Zhang et al., 1998). However, other published work has revealed interactions between each of the three subunits of pol δ and PCNA in different species. It therefore seems that pol δ has at least two and possibly three PCNA binding surfaces.

Pol ε is a heterotetramer containing a 250 kDa subunit that harbours both the DNA polymerase and exonuclease activities (Hubscher et al., 2002), while one of the small subunits, p59, has a PCNA binding motif (Fuss and Linn, 2002). Apart from its role in DNA replication, pol ε participates in several DNA repair pathways as is the case for pol δ. However, unlike pol δ, pol e also serves as a sensor in the DNA damage checkpoint (Nyberg et al., 2002).

Synthesis of leading and lagging strands

The synthesis of the leading DNA strand is processive and proceeds continuously for at least 5-10 Kb. However, because DNA synthesis always occurs in the 5' to 3' direction, lagging strand synthesis is discontinuous and divided into short segments known as Okazaki fragments (Hubscher and Seo, 2001). DNA synthesis of every ~180 nt long Okazaki fragment continues until the polymerase encounters the primer of the previously synthesised Okazaki fragment (Figure 1.5b). Therefore, while initiation events happen 4×10^4 times on the leading strand (approximately the number of origins of DNA replication in a mammalian cell), this has to be repeated at the beginning of each Okazaki fragment (adding up to about 2×10^7 times in mammalian cells; Berezney et al., 2000). The mechanisms involved in priming leading strand synthesis and the synthesis of each Okazaki fragment are very similar.

Looping back of the lagging strand into the replisome has been postulated as a mechanism to explain how the dimeric polymerases can extend the two antiparallel strands of DNA in the same direction and at the same rate. During this process, the lagging strand polymerase from the end of one Okazaki fragment is recycled to the next RNA primer (Figure 1.5a; Hubscher and Seo, 2001). PCNA is essential for the coordinated synthesis of leading and lagging strands (Prelich and Stillman, 1988), and its omission from the SV40 replication system results in an accumulation of unligated short Okazaki fragments (Waga and Stillman, 1994).

After the lagging strand DNA polymerase encounters the RNA primer of the preceding fragment, a process called 'Okazaki fragment maturation' converts the lagging strand into a long continuous DNA product. Two different nucleases, RNase HI and a 5'-3' exo- and endonuclease called Flap endonuclease 1 (FEN1), are involved in the complete removal of the RNA primer (Figure 1.5c; Hubscher and Seo, 2001; Waga and Stillman, 1998). The endonuclease activity of RNase HI cleaves most of the initiator RNA, leaving a single ribonucleotide at the 5'-end of the RNA-DNA junction, which can be removed by the 5'-3' exonuclease activity of FEN1. Alternatively, following

strand displacement by the lagging strand DNA polymerase, the endonuclease activity of FEN1 can remove the entire RNA-containing 5'-flap, a structure for which it displays preference; this bypasses any requirement for RNase HI. FEN1 also binds to PCNA, which stimulates its activity 50 fold or more (Gomes and Burgers, 2000; Li et al., 1995; Tom et al., 2000; Warbrick et al., 1997; and see Table 3.1). Despite the well-established *in vitro* activities of these two enzymes, genetic analysis in yeast revealed that null RNase HI and FEN1 mutants are not lethal. This is due to the existence of a redundant pathway involving the participation of RPA and the helicase/endonuclease Dna2 in conjunction with either FEN1 or the exonuclease function of pol δ (Henneke et al., 2003a).

The nick created by the endonuclease activity is then ligated by another PCNA Binding Protein (PBP), DNA Ligase I (Lig1 - Figure 1.5d; Montecucco et al., 1998; see Table 3.1), which completes Okazaki fragment maturation (Hubscher and Seo, 2001; Waga and Stillman, 1998). Meanwhile, the next Okazaki fragment is being synthesised. Recent work suggests that PCNA is being recycled from one Okazaki fragment to the other, rather than new PCNA rings being reloaded every 200bp (Sporbert et al., 2002).

Unwinding of DNA in front of the DNA polymerase to create ssDNA templates is achieved by replication specific DNA helicases (von Hippel and Delagoutte, 2003). DNA superhelical tension, which is caused by the unwinding of the DNA double helix, is released mainly by DNA topoisomerase I, and the replicated DNA molecules are separated by DNA topoisomerase II (Wang, 2002).

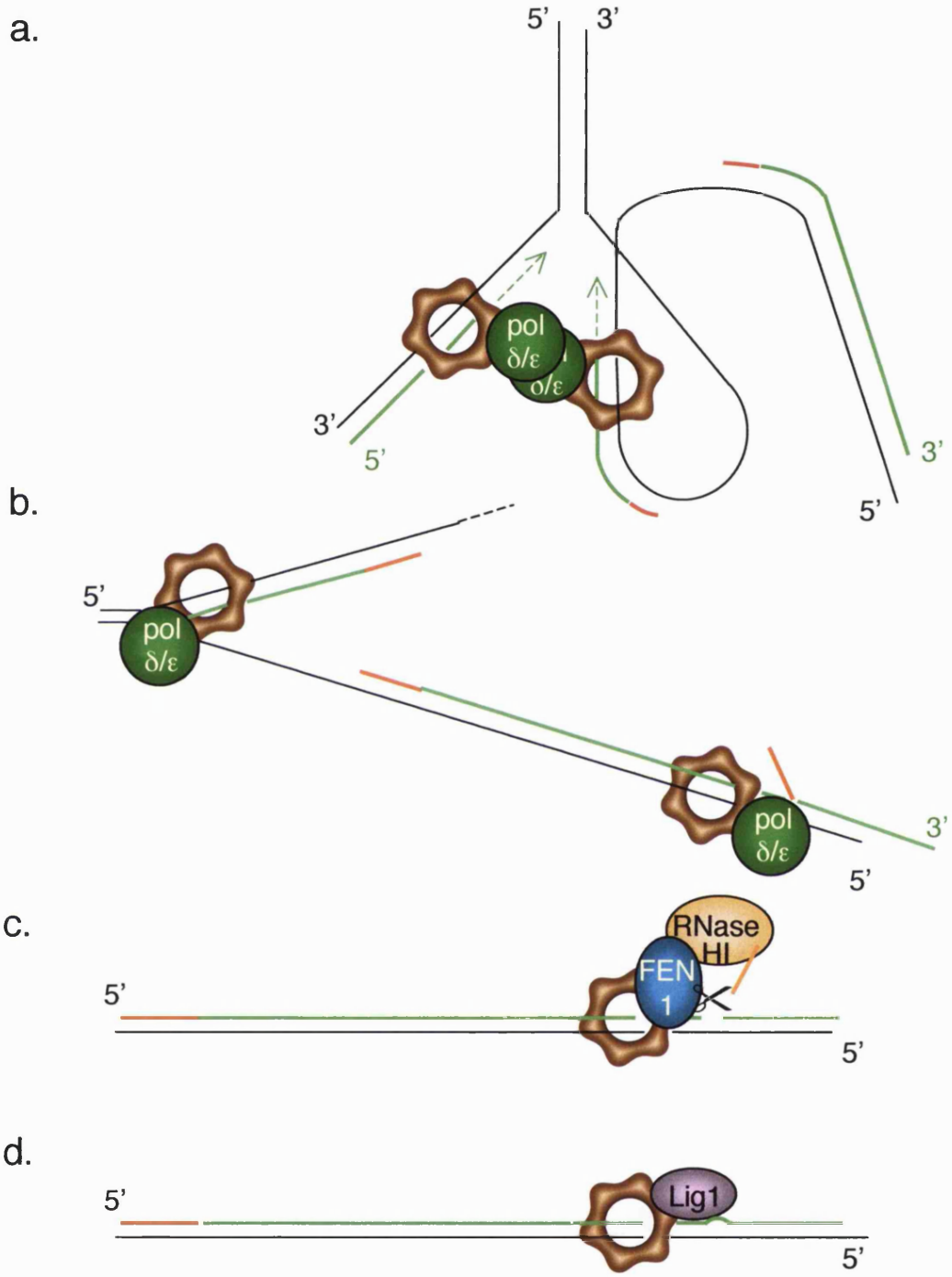

Figure 1.5: Lagging strand synthesis

a. To allow coordinated synthesis of the leading and lagging strands, the lagging strand is believed to loop back, so that although the DNA is being synthesised at opposite directions, the movement of the replication machinery in space is unidirectional.

b. The replication DNA polymerase (pol δ/ε) on the lagging strand reaches the previous Okazaki fragment and is able to continue synthesising DNA by strand displacement.

c. The RNA-DNA primer of the previous Okazaki fragment is removed. The main nucleases involved in this process are RNase HI which can cleave most of the RNA primer off, and FEN1 which has both endo- or exo-nucleatic activity, and has a flap structure preference. Such structures arise by pol δ/ε strand displacement.

d. Cleavage of the preceding Okazaki fragment results in a nick which is ligated by DNA ligase 1 (Lig1).

1.3.4 DNA replication within the cell cycle context

DNA replication is coordinated with other events in the cell cycle. This coordination is achieved by regulatory mechanisms that enforce the strict alternation of DNA replication and mitosis. Eukaryotic cells have evolved additional controls, known as 'checkpoints', that halt the normal course of cell cycle progression in response to conditions that are potentially detrimental to cell division. These mechanisms monitor the successful completion of cell cycle events.

The activity of many replication factors is modulated by specific post-translational modifications. In particular, phosphorylation inhibits the function of many replication proteins and/or blocks their association with PCNA (Henneke et al., 2003b). In fact CDK2 localises to sites of DNA replication via its own interaction with PCNA, keeping it in close proximity to potential substrates (Koundrioukoff et al., 2000). PCNA activity is itself regulated by post-translational modifications such as ubiquitylation, sumolation and acetylation (Hoege et al., 2002; Naryzhny et al., 2003; Naryzhny et al., 2004).

PCNA function is also regulated by the CDK inhibitor p21 (Sherr and Roberts, 1999). p21 is induced during mitogenic stimulation of mammalian cells and in response to DNA damage by the tumour suppression protein p53, as well as many other stimuli (Dotto, 2000). p21 forms a tight complex with cyclin-CDK through motifs in both its N- and C-termini. This interaction inhibits CDK activities that are required for G1/S progression, leading to cell cycle arrest. Through the C-terminus, p21 can also bind to PCNA, thus acting as a bridge between CDKs and PCNA (Chen et al., 1995; Nakanishi et al., 1995). The human papillomavirus oncoprotein (HPV-16 E7 protein) overcomes this inhibition by binding to the C-terminal region of p21, through a region that overlaps both the PCNA Binding domain and the second cyclin binding motif. Thus, E7 inhibits p21-induced cell cycle arrest, promoting viral replication (Funk et al., 1997; Jones et al., 1997).

In vitro, p21 can inhibit DNA replication in the SV40 replication system and in *Xenopus* cell extracts through its direct binding to PCNA (Dotto, 2000; Table 3.1). p21 has also been shown to inhibit MisMatch Repair (MMR; Umar et al., 1996), however the effect of p21 on PCNA dependent Nucleotide Excision Repair (NER) is controversial and unclear (Li et al., 1994; Pan et al., 1995; Podust et al., 1995; Shivji et al., 1994).

The structure of a complex between a p21-derived peptide and PCNA has been solved (Gulbis et al., 1996; and see Figure 3.4). The p21 peptide binds to PCNA in a stoichiometric manner with a dissociation constant (Kd) of 2.5 nM (Gibbs et al., 1997) and is able to prevent various replication factors from binding to PCNA (Chen et al., 1996; Chuang et al., 1997; Oku et al., 1998; Warbrick et al., 1997). These proteins share with p21 a consensus PCNA Binding Motif (PBM – Kelman and Hurwitz, 1998; Maga and Hubscher, 2003; Warbrick, 1998; Warbrick, 2000).

Other cell cycle regulators also bind to PCNA directly (see Table 3.1 for PBPs). For example, Cdk2 not only associates with PCNA through p21, but also binds to it directly. A ternary PCNA-Cdk2-cyclin A complex can phosphorylate the PCNA binding region of RFCp140 as well as Lig1, suggesting that Cdk2 may modify replication factors by associating with PCNA (Koundrioukoff et al., 2000).

1.4 A GENERAL VIEW OF GENOME DUPLICATION

In addition to DNA synthesis, several other processes take place at or near the replication fork. These include several forms of DNA repair such as the bypass of lesions in the DNA template as well as processes that repair nascent DNA, such as MMR and base excision repair (BER). Additionally, nascent DNA must be methylated and rapidly assembled into nucleosomes. Post-translational modifications of newly synthesised histones and DNA methylation are two types of epigenetic information that need to be re-established during each passage through S phase in proliferating cells.

1.4.1 DNA lesion bypass polymerases

Although DNA polymerases δ and ε are highly processive and accurate enzymes, they are not capable of copying DNA containing particular types of lesions. When the replication machinery encounters such lesions, specialised polymerases that can bypass the lesion need to be recruited to the replication fork. Certain lesions can only be bypassed at the cost of introducing mutations in the nascent DNA. Many DNA lesion bypass polymerases have been identified and each exhibits a preference for the bypass of specific types of lesions (Hubscher et al., 2002). Due to the importance of their immediate availability, bypass polymerases are constitutively present in replication factories throughout S phase. Interestingly, like the replicative polymerases, the DNA lesion bypass polymerases pol η and pol _ have been shown to target replication foci by binding to PCNA (Haracska et al., 2001a; Haracska et al., 2001b).

1.4.2 DNA repair

Different repair pathways have evolved to cope with specific DNA lesions, including the NER pathway; the BER pathway and the MMR pathway (Christmann et al., 2003; Lindahl and Wood, 1999). These three pathways function by excising a stretch of DNA containing the lesion, followed by DNA synthesis to restore the structure of DNA. The DNA synthesis step associated with many forms of DNA repair is catalysed by replication proteins. Therefore, mutations in many replication factors cause sensitivity to DNA damaging agents (Christmann et al., 2003).

NER deals with a variety of helix distorting lesions. During NER, after lesion recognition and excision of a stretch of DNA surrounding the lesion, the entire DNA elongation complex is loaded onto the DNA at the 5' end of the gap created, and functions in strand filling as in DNA replication (Costa et al., 2003). Intriguingly, the *Xeroderma pigmentosum* G (XPG) endonuclease, which functions in the preceding steps, is closely related to FEN1, and has also preference for flap-DNA structures. It is therefore possible that XPG

replaces FEN1 during NER, and indeed XPG also binds to PCNA (Gary et al., 1997).

BER is the main mechanism by which cells repair DNA alkylation and oxidative damage. The Uracil-DNA-glycosylase UNG2, functions during the first step of BER by scanning the DNA in search of uracil, a product of cytosine deamination. Importantly, UNG2 binds to PCNA via a PBM (Otterlei et al., 1999). Following removal of the damaged base and cleavage of the phosphodiester backbone by apurinic/apyrimidinic site endonuclease, BER can proceed as either a short patch (resynthesis of a single nucleotide) or a long patch pathway (resynthesis of 2-7 nucleotides). The excision step in long patch BER, which is carried out by FEN1, also requires PCNA (Gary et al., 1999). Furthermore, long patch BER utilises the replication elongation apparatus (Fortini et al., 2003). PCNA has also been shown to interact directly with DNA polymerase β (Kedar et al., 2002), suggesting that PCNA may also be required for short patch BER as well.

MMR takes place immediately behind the replication fork and corrects errors in DNA replication such as mis-incorporated bases and insertions or deletions in repetitive DNA elements (Buermeyer et al., 1999). Genetic analyses in yeast indicate the involvement of PCNA in MMR (Gu et al., 1998; Johnson et al., 1996; Lau et al., 2002; Umar et al., 1996). Mutations in PCNA increase frameshifts in simple sequence repeats by disrupting MMR (Ayyagari et al., 1995; Johnson et al., 1996; Kokoska et al., 1999). MutS Homologue (MSH) 2 dimerises with MSH3 or MSH6 to form two distinct mismatch recognition complexes. Importantly, both MSH2 and MSH3 as well as the MutL Homologue (MLH) 1 complex seem to interact with PCNA at least in part via PBMs (Gu et al., 1998; Johnson et al., 1996; Umar et al., 1996). PCNA has been shown to increase the specificity of mismatch recognition, and the recognition of a DNA mismatch by MSH2-MSH6 leads to their dissociation from PCNA. This has led to the proposal that MSH2-MSH6 may utilise PCNA for processive surveillance of the newly replicated DNA (Lau and Kolodner, 2003). PCNA might also allow the MMR machinery to determine which strand

should serve as a template during repair, or might trigger involvement of the 3' to 5' exonuclease activities of DNA polymerases in mismatch removal. Moreover, these interactions may be important *in vivo* for targeting the MMR complexes to newly synthesised DNA. After excision, at least part of the DNA elongation apparatus is recruited for gap filling (Gu et al., 1998). Taken together, these findings suggest a model in which PCNA acts to link the MMR complex to DNA polymerases at the replication fork, possibly facilitating recognition and repair of the nascent strand.

1.4.3 DNA methylation following replication

In mammalian cells, DNA methylation generally serves as a marker for transcriptional repression (Bird, 2002). The patterns of DNA methylation, primarily at sites of CpG, are maintained by the activity of DNA (5-cytosine) methyltransferase 1 (DNMT1), which copies existing methylation patterns from the parental strand during DNA replication and repair, whereas *de novo* DNA methylation largely occurs by DNMT3 family of methyltransferases. During S phase, DNMT1 localises to both early- and late-replication foci, along with an associated protein, DMAP1 (Rountree et al., 2000). Like many other replication factors, DNMT1 is targeted to the replication fork by binding to PCNA through a PBM (Chuang et al., 1997; Knox et al., 2000; Leonhardt et al., 1992).

1.4.4 Chromatin assembly following replication

The compartmentalisation of DNA within the nucleus of eukaryotic cells requires an extreme compaction of this highly charged polymer. Compaction is achieved through association of the DNA with a set of extremely basic histone proteins and non-histone proteins to form a structure known as chromatin (Wolffe, 1992).

The fundamental repeat unit of chromatin is the nucleosome core particle, which is composed of an octamer of the four core histones, H2A, H2B, H3, and H4, and 147 base pairs of DNA wound in 1.65 left-handed superhelical turns around the surface of the octamer (Luger et al., 1997; Figure 1.6). Neighbouring nucleosomes are separated by short segments of linker DNA. The N-terminal domains of the four core histones, known as histone "tails", protrude outside the core particle to contact DNA, other histones and non-histone proteins. These contacts contribute to the folding of the nucleosomal fibre into higher-order structures, and the recognition of histone tails by specific proteins that allows them to carry out post-translational modification of the tails or trigger changes in chromatin structure (Adkins et al., 2004).

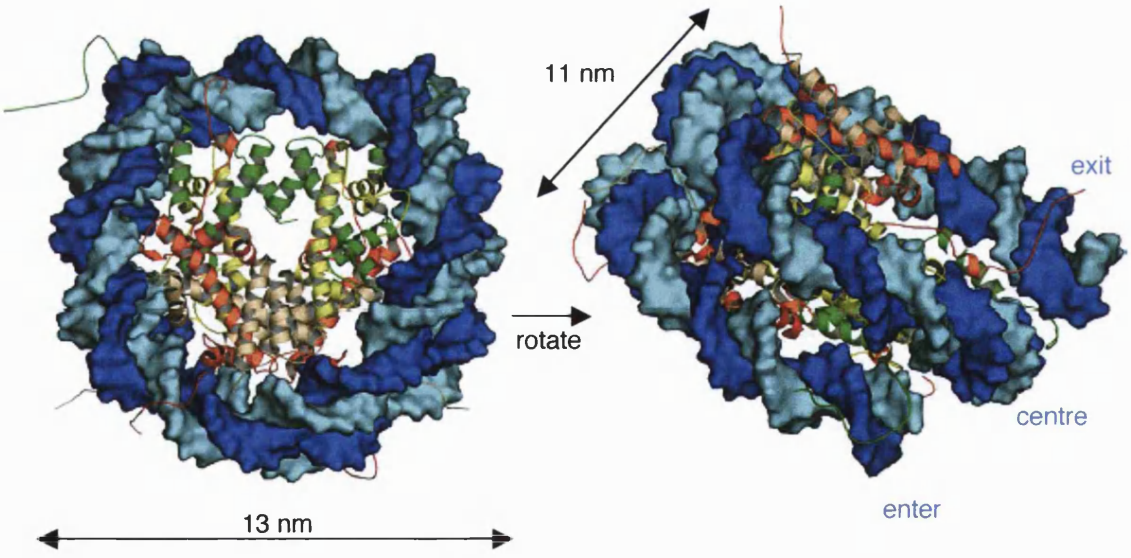

Figure 1.6 The structure of the nucleosome core particle
The DNA makes 1.65 turns around the histone octamer to form an overall particle with a disk-like structure. Each strand of DNA is shown in different shade of blue. Histones H3 are in green, H4 in yellow, H2A in red and H2B in peach. The histone tails protrude outside the core particle. This figure was taken from (Khorasanizadeh, 2004).

During DNA replication, the advancing replication fork triggers a rapid and local disassembly of higher-order chromatin structure allowing the replication machinery access to the nucleosomal DNA (Gasser et al., 1996; Smerdon, 1991; Smith et al., 1984; Sogo et al., 1986). Once enough DNA has been replicated (150-400 bp), it is quickly assembled into nucleosomes (Gasser et al., 1996; Sogo et al., 1986). Half of the nucleosomes are formed by redistribution of parental core histones onto the two nascent chromatids without complete histone dissociation from the DNA (Krude, 1999). This process, known as 'parental histone segregation', probably facilitates replication fork progression (Formosa, 2003).

The other half of the nucleosome complement is formed from newly synthesised and acetylated histones in a pathway known as '*de novo* nucleosome assembly' (Krude and Keller, 2001; Verreault, 2000). This process occurs through a stepwise mechanism whereby two dimers of histones H3/H4 are deposited first and two H2A/H2B dimers are added subsequently (Smith and Stillman, 1991b; Tagami et al., 2004). Both pre-existing and newly synthesised H2A/H2B dimers can co-exist in the same nucleosome (Jackson, 1990).

Following this, a number of steps including nucleosome spacing (Corona and Tamkun, 2004) and incorporation of histone H1 and non-histone chromosomal proteins lead to the formation of mature chromatin (Adkins et al., 2004; Brown, 2003). Nucleosome assembly is essential for viability and long delays between DNA replication and histone deposition are fatal to the cell (Han et al., 1987; Kim et al., 1988). Even subtle defects in nucleosome assembly lead to genome instability (Myung et al., 2003) and sensitivity to DNA damaging agents (Emili et al., 2001; Game and Kaufman, 1999; Tyler et al., 1999). Chromatin assembly events are also associated with DNA repair (Green and Almouzni, 2002), recombination (Lichten and Goldman, 1995) and transcription (Maldonado et al., 1999; Tyler and Kadonaga, 1999).

1.4.4.1 Following the histones

In proliferating cells, the bulk of histone synthesis occurs during S phase (Osley, 1991). Shortly after their synthesis, newly synthesised histones are acetylated at specific lysine residues within their N-terminal domains. The exact function of this modification is not known, but a role in the nuclear import of newly synthesised histones has been suggested (Mosammaparast et al., 2002a and 2002b). This reaction is carried out by B-type histone acetyltransferases (HATs). Unlike A-type HATs that modify chromosomal histones (reviewed in Roth et al., 2001), B-type HATs specifically acetylate newly synthesised histones prior to their incorporation into chromatin. The only known B-type HAT is a dimeric enzyme that consists of a catalytic subunit, Hat1, and a core histone-binding subunit Hat2 (RbAp46 in human cells Kleff et al., 1995; Parthun et al., 1996).

HAT1 acetylates histone H4 on lysines 5 and 12, two sites that have long been recognised as the hallmark of newly synthesised histone H4 (Chicoine et al., 1986; Parthun et al., 1996; Sobel et al., 1994; Sobel et al., 1995; Verreault et al., 1996; Verreault et al., 1998). However, a number of redundant acetylation sites exist in both newly synthesised H3 and H4 (Ma et al., 1998). Consequently, *hat1* mutants, or mutations in either H3 or H4 acetylation sites do not result in severe defects in nucleosome assembly (Kelly et al., 2000; Ma et al., 1998). However, when combined with mutations that compromise acetylation of lysine residues in the H3 tail, *hat1* and *hat2* mutations result in telomeric silencing defects and DNA damage sensitivity (Kelly et al., 2000; Qin and Parthun, 2002). Newly synthesised and acetylated forms of H3/H4 associate with nuclear import factors of the importin b-family known as Kap121 and Kap123 in *S. cerevisiae* (Mosammaparast et al., 2002). However, little is known about the events that immediately follow the entry of histones in the nucleus.

Newly synthesised histones are bound by a number of chaperones, which target them to sites of DNA synthesis (reviewed in Loyola and Almouzni, 2004; Mello and Almouzni, 2001). Their association with chaperones minimises non-specific interaction between the highly basic histones and DNA, which could

potentially interfere with many aspects of cell physiology. The stoichiometry between histone pairs also needs to be carefully controlled. In *S. cerevisiae*, over-expression of either H2A/H2B or H3/H4 pairs leads to a high incidence of mitotic chromosome loss (Meeks-Wagner and Hartwell, 1986).

1.4.4.2 Asf1

In *Drosophila* embryo extracts, the protein Anti-Silencing Function 1 (Asf1) was found associated with newly synthesised and acetylated forms of H3 and H4 in a complex named 'Replication-Coupling Assembly Factor' (RCAF; Tyler et al., 1999). This complex was purified based upon its ability to synergise with Chromatin Assembly Factor 1 (CAF1) to promote nucleosome assembly during DNA replication *in vitro*, under conditions where CAF1 levels were limiting. In contrast with CAF1 (see below), Asf1 is unable to promote nucleosome deposition coupled to DNA synthesis by itself (Tyler et al., 1999), and it is believed to function by transferring histones H3/H4 to downstream chaperones, CAF1 and Histone Gene Regulator (Hir) proteins, with which it interacts (Sharp et al., 2001). The two human homologues of Asf1 (Asf1a and b) can stimulate histone deposition by CAF1 during DNA synthesis coupled to DNA repair (Mello et al., 2002; Munakata et al., 2000).

In *S. cerevisiae*, Asf1 was originally identified in two independent screens for genes whose overexpression interfered with telomeric and mating type silencing (Le et al., 1997; Singer et al., 1998). However, cells lacking Asf1 are fertile and only exhibit very mild silencing defects at telomeres and the mating type. Thus, the name Anti-Silencing Function 1 only refers to overexpression of the protein and is somewhat misleading. Cells lacking Asf1 have an increased doubling time as a result of delayed progression through G2 /M phase of the cell cycle (Le et al., 1997; Tyler et al., 1999), and exhibit sensitivity to a broad range of DNA damaging agents (Emili et al., 2001; Gavin et al., 2002; Gunjan and Verreault, 2003; Ho et al., 2002; Hu et al., 2001; Le et al., 1997; Schwartz et al., 2003; Tyler et al., 1999).

1.4.4.3 CAF1

CAF1 was originally purified as a factor necessary for nucleosome assembly during replication of plasmids containing the SV40 origin in human cell extracts (Smith and Stillman, 1989). CAF1 consists of three evolutionary conserved polypeptide subunits known as p150, p60 and p48 (RbAp48) in human cells or Cac1, Cac2 and Cac3 in *S. cerevisiae* (Bulger et al., 1995; Gaillard et al., 1996; Kamakaka et al., 1996; Kaufman et al., 1995; Kaufman et al., 1997; Murzina et al., 1999; Quivy et al., 2001). The ability of CAF1 to promote preferential assembly of nucleosomes onto newly synthesised DNA is thus far unique among histone chaperones.

Unlike in yeast, CAF1 is essential for viability in human cells (Hoek and Stillman, 2003; Nabatiyan and Krude, 2004), and is not redundant with Hir proteins (see below). Consistent with this, CAF1 targets replication foci throughout S phase and deposits histones H3/H4 behind the replication fork in both eu- and heterochromatin (Krude, 1995; Marheineke and Krude, 1998; Smith and Stillman, 1989; Taddei et al., 1999; Verreault et al., 1996).

The three subunits of CAF1 bind directly to core histones (Shibahara et al., 2000; Verreault et al., 1998). The small subunit p48 (RbAp48) and the highly related protein, RbAp46, both bind to the first a-helix of the histone-fold in core histones H2A or H4 (Verreault et al., 1998). This helix binds directly to DNA and is not accessible for interaction with other proteins when the histones are assembled into nucleosomes (Luger et al., 1997). Consistent with its role as a *de novo* nucleosome assembly factor, CAF1 can be isolated from human cell nuclei as a larger protein complex termed 'Chromatin Assembly Complex' (CAC; Verreault et al., 1996), which contains CAF1 bound to histones H3 and H4. Similarly to ASF1 (Tyler et al., 1999), a fraction of the H4 molecules associated with CAF1 are acetylated on lysines 5, 8, and 12 (Verreault et al., 1996). Although they are redundant with each other and with acetylation of the H3 tail, these modifications are essential for maintaining nucleosome assembly and viability in *S. cerevisiae* (Ma et al., 1998). However, CAF1 binding to H3/H4 does not require acetylation of the N-terminal domain of either histone.

In addition, complexes of CAF1 with histones lacking the N-terminal tails of both H3 and H4 are just as active in replication dependent nucleosome assembly *in vitro* as complexes containing intact histones (Shibahara et al., 2000). Therefore, the exact function of these post-translational modifications in the context of nucleosome assembly remains unknown.

The targeting of CAF1 to sites of DNA synthesis is achieved through direct binding of p150 to PCNA during both DNA replication and repair (Green and Almouzni, 2003; Krawitz et al., 2002; Moggs et al., 2000; Sharp et al., 2001; Sharp et al., 2002; Shibahara and Stillman, 1999; Zhang et al., 2000b). In fact, CAF1 dependent nucleosome assembly can be uncoupled from ongoing DNA synthesis, as long as PCNA remains bound to the template DNA (Kamakaka et al., 1996). Unloading of PCNA from the DNA template by RFC, or incubation with antibodies against PCNA can inhibit subsequent nucleosome assembly by CAF1 (Shibahara and Stillman, 1999). Chapter 3 in this work concentrates on characterising further the interaction between CAF1 and PCNA.

The human p150 protein has several identified domains, as illustrated in Figure 1.7. These include domains rich in charged residues (KER and ED), a PEST domain that may participate in CAF1 turnover, and a PXVXL motif (X being any amino acid) at the N-terminus of mammalian p150. This motif is involved in CAF1 interaction with the heterochromatin protein HP1 (Murzina et al., 1999; Thiru et al., 2004). In yeast, where there is no HP1, Cac1 also interacts with heterochromatin related proteins Silent Information Regulator 1 (Sir1; Sharp et al., 2003) and Something About Silencing 2 (Sas2; Meijsing and Ehrenhofer-Murray, 2001).
However, the first 296 residues of human p150, which constitute the least conserved segment of this protein, are dispensable for PCNA-mediated

nucleosome assembly coupled to SV40 DNA replication *in vitro* (Kaufman et al., 1995). The C-terminal region is important for binding to the p60 subunit, and deletion of this p60 binding domain in p150 prevents nucleosome assembly during SV40 DNA replication (Kaufman et al., 1995). Chapter 4 in this work presents an attempt to identify other CAF1 associated factors by co-immunoprecipitation.

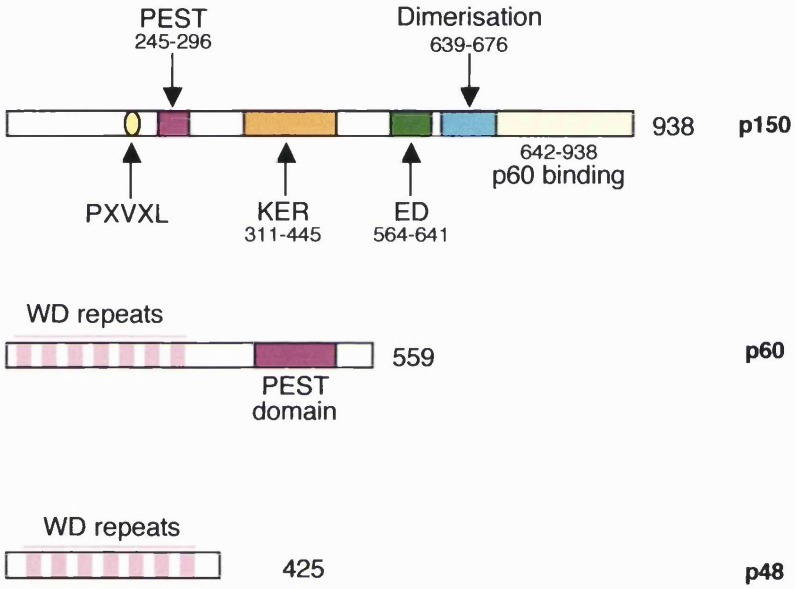

Figure 1.7: CAF1 is composed of three subunits
The three subunits of CAF1 are schematically represented. Known sequence elements are highlighted in the figure. PXVXL – a consensus motif for binding to HP1. PEST domains are thought to be important for protein turnover. KER and ED are domains rich in charged residues. p150 can dimerise through residues 639-676, and binds p60 through residues 642-938. Both p60 and p48 have WD40 repeats.

In higher eukaryotes, the p150 subunit forms dimers and expression of human CAF1 p150 acts as a dominant negative inhibitor of CAF1 activity in *Xenopus* embryos. Expression of human p150 during the rapid cleavage stages of early *Xenopus* development results in a severe loss of cell viability that is abolished when p150 carries a mutation that prevents its dimerisation with the *Xenopus* protein (Quivy et al., 2001). In *Arabidopsis* the p150 and p60 counterparts are needed to maintain the cellular organisation of apical meristems during post embryonic development. They were suggested to function by facilitating stable maintenance of gene expression states (Kaya et al., 2001). Recently,

expression of a dominant negative form of p150 in human cells has been shown to cause inhibition of DNA synthesis in S phase with induction of DNA damage and activation of the S phase checkpoint (Ye et al., 2003). Similar results were obtained by treating human cells with siRNA to deplete p150 (Hoek and Stillman, 2003). Depletion of p60 resulted in programmed cell death in proliferating, but not quiescent cells (Nabatiyan and Krude, 2004). These results further emphasise the importance of chromatin assembly by CAF1 in higher eukaryotes both for normal progression through S phase and for cell viability.

The human p60 subunit also has several distinct structural features. Like p150, p60 has a PEST domain. In addition, p60 contains a conserved WD-repeat region consisting of seven WD repeats (Figure 1.7; Kaufman et al., 1998; Kaufman et al., 1997; Smith et al., 1999b), and interacts with Asf1 (Tyler et al., 2001; Mello et al., 2002).

Significantly, both p60 and p150 have several phosphorylation sites (Keller and Krude, 2000; Marheineke and Krude, 1998; Smith and Stillman, 1991a). During mitosis, p60 is hyperphosphorylated and dissociates from chromatin. CAF1 purified from mitotic cells is inactive for *in vitro* nucleosome assembly (Marheineke and Krude, 1998), but can be reactivated by treatment with phosphatase (Keller and Krude, 2000). This hyperphosphorylated form does not appear to be present in interphase cells, although a variety of other phosphorylated forms (possibly at distinct sites) can be detected. Both p150 and p60 are phosphorylated by CDK2, and are dephosphorylated by a PP1 family member. Experiments with drugs that inhibit either CDKs or protein phosphatases suggest that a continuous cycle of phosphorylation and dephosphorylation is important for full CAF1 activity *in vitro* (Keller and Krude, 2000). Thus, in contrast to the inhibitory hyperphosphorylation of p60 during mitosis, moderate levels of p60 and, possibly, p150 phosphorylation seem to stimulate CAF1 activity during replication.

Like p60, the p48 subunit of CAF1 is a WD repeat protein (Figure 1.7; Verreault et al., 1996), suggesting that they are able to accommodate multiple interactions with different proteins. Both p48 and a highly related protein known as p46 were initially discovered as Retinoblastoma (Rb) binding proteins (Qian and Lee, 1995; Qian et al., 1993). They are therefore often referred to as RbAp46 and RbAp48. p46 and p48 are evolutionarily conserved and indeed exist as components of many distinct proteins. For instance, in yeast and human cells, RbAp46 and p48 (Cac3 or Msi1 in yeast) are respectively part of Hat1 (Parthun et al., 1996; Verreault et al., 1998) and CAF1 (Kaufman et al., 1997; Verreault et al., 1996). Both RbAp46 and p48 are also found in large histone deacetylase complexes (HDACs) that contain HDAC1 and HDAC2 as catalytic subunits. These include the Sin3 complex, the NuRD complex (Nucleosome Remodelling and Deacetylase) and the Polycomb group (PcG) complex, PRC2 (Cao et al., 2002; Taunton et al., 1996; Zhang et al., 1997; Zhang et al., 1999). The Rb tumour suppressor also represses transcription, at least in part by recruiting HDACs that include RbAp48 (Nicolas et al., 2001; Nicolas et al., 2000). Curiously, only one family member has been reported in *Drosophila* and *Xenopus*, although it is clearly part of multiple distinct proteins such as CAF1, Hat1, HDACs and even the ATP-dependent Nucleosome Remodelling Factor, NuRF (Imhof and Wolffe, 1999; Martinez-Balbas et al., 1998; Tyler et al., 1996; Vermaak et al., 1999). Since all these factors have histones as their substrates, RbAp46 and p48 may simply function as histone binding subunits in each of these multiprotein complexes.

A knockout of *Arabidopsis* MSI1, which is most similar to RbAp46, disrupts many developmental aspects. This pleiotropic phenotype can be explained by the participation of MSI1 in several distinct complexes (Hennig et al., 2003). In contrast, *S. cerevisiae* strains that lack any or all three CAF1 subunits are viable and healthy. Unlike in higher eukaryotes, Cac3 was not found as part of HDACs or ATP-dependent nucleosome remodelling factors in *S. cerevisiae*, though it functions as a multicopy suppressor of the *RAS*/cyclic AMP signal transduction pathway independently of Cac1 and Cac2 (Johnston et al., 2001).

Sensitive assays using reporter genes integrated in sub-telomeric chromosomal regions, the silent mating type loci (*HMLα* and *HMRa*) or the rDNA locus (*RDN1*) reveal that, like *asf1* mutants, cells lacking CAF1 have subtle defects in heterochromatin-mediated transcriptional silencing (Enomoto and Berman, 1998; Enomoto et al., 1997; Kaufman et al., 1997; Smith et al., 1999a). Importantly, these mild silencing defects are not due to pronounced changes in chromatin structure as reporter genes integrated next to telomeres remain packaged into nucleosomes in the absence of CAF1 (Kaufman et al., 1998), and no obvious difference in histone H4 acetylation of telomere-proximal genes has been found between wild type and CAF1 mutant cells (Monson et al., 1997). However, Rap1, a protein involved in both telomeric and mating type silencing, is mis-localised in CAF1 mutants. In wild type cells, a major fraction of Rap1 is associated with clusters of telomeres at the periphery of the cell nucleus. In CAF1 mutants, telomeric DNA clustering at the periphery of the nucleus is maintained, but the Rap1 foci are more numerous and more diffuse throughout the nucleus (Enomoto et al., 1997).

Importantly, yeast cells lacking both CAF1 and Asf1 display more pronounced growth and silencing defects than either single mutant (Le et al., 1997; Singer et al., 1998; Tyler et al., 1999). Moreover, mutations in the yeast Cac1 protein that impair its binding to PCNA cause subtle telomeric silencing defects and render the residual silencing strongly dependent upon the Asf1 and Hir proteins, which are all redundant with CAF1 (Krawitz et al., 2002).

1.4.4.4 CAF1 in DNA repair

Chromatin structural alterations clearly occur at sites of DNA damage (Gontijo et al., 2003; Green and Almouzni, 2002; Moggs and Almouzni, 1999). Both *in vitro* and *in vivo* experiments have implicated CAF1 in nucleosome assembly at sites of DNA repair during NER and Single Strand Break (SSB) repair (Gaillard et al., 1996; Green and Almouzni, 2003; Martini et al., 1998; Okano et al., 2003). Following ultraviolet (UV) irradiation of cells outside of S phase, p60 is phosphorylated and CAF1 is recruited to sites of DNA repair (Martini et al.,

1998). *In vitro*, CAF1 nucleosome assembly is coupled to PCNA-dependent DNA synthesis during NER and the repair of nicked DNA (Gaillard et al., 1997; Moggs et al., 2000).

In yeast, deletion of *CAC1*, *CAC2* or *CAC3* results in mild sensitivity to UV, but not ionising radiation (Enomoto and Berman, 1998; Enomoto et al., 1997; Game and Kaufman, 1999; Kaufman et al., 1997; Monson et al., 1997). Significantly, CAF1 mutations enhance the UV sensitivity of both NER and recombination-mediated repair mutants, but do not increase the UV-sensitive phenotype of *rad6Δ* or *rad18Δ* strains (Game and Kaufman, 1999). Rad6 and Rad18 are involved in DNA damage tolerance through the PCNA dependent DNA polymerases that bypass UV lesions (Torres-Ramos et al., 1996). These genetic studies argue that the UV-sensitive phenotype of CAF1 mutants in yeast is primarily the result of a defect in Rad6/Rad18-dependent DNA lesion bypass mechanisms. Thus, at least in *S. cerevisiae*, the role of CAF1 in UV damage tolerance may be to promote rapid nucleosome assembly during DNA lesion bypass.

As with silencing defects, *asf1cac1* double mutants are much more sensitive to a variety of DNA damaging agents than either single mutant, suggesting that they have overlapping functions in promoting nucleosome assembly during DNA repair (Tyler et al., 1999). Interestingly, mutations in Cac1 or Asf1 induce gross chromosomal rearrangement (Myung et al., 2003). These rearrangements are likely triggered by spontaneous DNA damage that occurs more frequently in cells lacking either CAF1 or Asf1. Cells lacking both CAF1 and Asf1 exhibit a delay in G2/M progression but remain viable. Because nucleosome assembly is essential for viability (Ma et al., 1998), this indicates that there are other unidentified nucleosome assembly factors in yeast. The work presented in chapter 5 describes a micro-array pilot screen in search for novel chromatin assembly factors in yeast, and introduces a potential novel factor in the existing pathway.

1.4.4.5 The Hir proteins

The Hir proteins form a group of four functionally related proteins in *S. cerevisiae* (Hir1, Hir2, Hir3 and Hpc2) that play a dual role in the nucleosome assembly pathway. They contribute to histone gene regulation during normal cell cycle progression by repressing transcription of three of the four histone gene pairs, except in late G1 and early S phase when the demand for histone synthesis is maximal (Osley and Lycan, 1987). In addition, Hir proteins are necessary to repress transcription from the HTA1–HTB1 locus (one of the two gene pairs encoding histones H2A/H2B) in response to inhibition of DNA replication or the presence of multiple copies of the HTA and HTB (Moran et al., 1990; Osley and Lycan, 1987; Recht et al., 1996; Sherwood and Osley, 1991; Sherwood et al., 1993).

Like CAF1, the Hir proteins also bind to newly synthesised H3/H4 and promote their assembly into nucleosomes (Gunjan and Verreault, 2003; Kaufman et al., 1998). In yeast, CAF1 and Hir proteins are largely redundant for nucleosome assembly during S phase (Kaufman et al., 1998; Sharp et al., 2001). Cells lacking any or all four Hir proteins have no striking phenotype (Enomoto et al., 1997; Kaufman et al., 1997) and the chromatin structure of *hir* mutants is essentially normal (Kaufman et al., 1998). This implies that the transcription of histone genes that occurs outside of S phase in *hir* mutants does not give rise to any severe phenotypes (Sherwood et al., 1993). However, cells lacking both Hir proteins and CAF1 exhibit defects in chromatin structure at a number of chromosomal loci, and a prolonged delay in progression through G2/M phase of the cell cycle (Kaufman et al., 1998; Sharp et al., 2002). This delay arises from alterations in pericentric chromatin structure that interfere with chromosome attachment to the mitotic spindle, thereby activating the spindle checkpoint. Even though the spindle checkpoint functions to minimise mis-segregation in *caf1hir* double mutants, these mutants still exhibit a high incidence of mitotic chromosome loss (Sharp et al., 2002). These cells also have severe silencing defects, elevated rates of Ty1 retrotransposition, increased sensitivity to the DNA alkylating agent methyl methane sulfonate (MMS) and pronounced defects in cell cycle progression (Kaufman et al.,

1998; Qian et al., 1998). The MMS sensitivity and cell cycle defects are consistent with a global role for CAF1 and Hir proteins in promoting nucleosome assembly throughout the genome.

The synergistic effect of mutating both Hir proteins and CAF1 demonstrates that in yeast, they are genetically redundant. Curiously, the contribution of Hir proteins to nucleosome assembly can be blocked by specific mutations in PCNA (Sharp et al., 2001; Zhang et al., 2000a). This is surprising because none of Hir proteins contains any obvious PBM (Sharp et al., 2001; Sharp et al., 2002; Zhang et al., 2000b). However, the role of Hir proteins in replication-dependent nucleosome assembly is not conserved in human cells.

In higher eukaryotes, the Hir proteins homologue HIRA, unlike CAF1, does not localise to DNA replication foci and has replication-independent nucleosome assembly activity in *Xenopus* extracts (Ray-Gallet et al., 2002). The mammalian HIRA is essential for proper embryonic development, particularly during mesoderm differentiation (Roberts et al., 2002). Overexpression of HIRA leads to transcriptional repression of the histone genes (Nelson et al., 2002). In human cells, HIRA is a nuclear protein that can be phosphorylated by cyclin-cdk2 (Hall et al., 2001), and binds directly to core histones (Lorain et al., 1998). *In vivo*, HIRA is associated with histone H3/H4 dimers that exclusively contain the replication-independent variant H3.3 (Tagami et al., 2004), arguing that HIRA may not function in nucleosome assembly during S phase. Deposition of H3.3 is thought to be restricted to transcriptionally active genes, perhaps as a mechanism to replenish histones displaced during transcription (Ahmad and Henikoff, 2002a; Ahmad and Henikoff, 2002b; Ahmad and Henikoff, 2002c; McKittrick et al., 2004; Ray-Gallet et al., 2002; Tagami et al., 2004). In addition, it has been proposed that H3.3 may serve to activate gene expression by replacing K9-methylated histone H3, a modification that is otherwise metabolically stable (Bannister et al., 2002) and promotes heterochromatin formation and gene repression (Ahmad and Henikoff, 2002b; Ahmad and Henikoff, 2002c).

Taken together, these results imply that in *S. cerevisiae*, where only one form of histone H3 exists, both CAF1 and Hir proteins function in replication dependent nucleosome assembly. In higher eukaryotes, the functions of CAF1 and HIRA have diverged; while CAF1 remains dedicated to replication dependent nucleosome assembly, HIRA has become specialised in replication independent assembly of nucleosomes containing the H3.3 variant. Such specialisation would lead to loss of redundancy, consistent with the severe phenotypes observed due to mutations in chromatin assembly factors in higher eukaryotes (Hoek and Stillman, 2003; Kaya et al., 2001 Quivy et al., 2001; Roberts et al., 2002; Ye et al., 2003).

1.4.4.6 Other histone chaperons

As is the case for H3/H4 tetramers, deposition of H2A/H2B dimers into nucleosomes most likely requires the participation of assembly factors. Nucleosome assembly protein 1 (NAP1) is an evolutionarily conserved histone chaperone that is associated with H2A/H2B both in human cells (Chang et al., 1997) and in *Drosophila* embryo extracts (Ito et al., 1996a), and has been suggested to play this role (reviewed in Loyola and Almouzni, 2004). However, other H2A/H2B chaperones may also exist.

The histone chaperones nucleoplasmin 1 and N1/N2 are associated with the large maternal pools of H2A/H2B and H3/H4 complexes respectively that are stored in oocytes and utilised for nucleosome assembly during early embryogenesis in *Xenopus* and *Drosophila* (Dilworth and Dingwall, 1988; Ito et al., 1996b; Philpott et al., 2000). They are believed to function specifically to sustain nucleosome assembly during early embryogenesis (reviewed in Loyola and Almouzni, 2004).

1.4.5 Replication related chromatin remodelling

To fully restore the chromatin structure onto the nascent DNA, nucleosome assembly by histone chaperones alone may be insufficient as their activity *in vitro* results in an irregular nucleosomal array. In crude chromatin assembly extracts from *Drosophila* or *Xenopus*, the appearance of regular nucleosome spacing, such as those found in eukaryotic chromosomes, is an ATP-dependent process (Glikin et al., 1984; Kamakaka and Kadonaga, 1993), carried out by chromatin remodelling factors.

Chromatin remodelling factors are conserved large multiprotein complexes that have been identified mostly as transcriptional regulators but have since been implicated in other DNA related activities, from DNA replication and repair to mitotic chromosome condensation (reviewed in Becker and Horz, 2002). Among the four major subfamilies of chromatin remodelers, complexes that contain the ATPase subunit of the Imitation SWItch (ISWI) subfamily (also known as the SNF2L subfamily) such as ACF (ATP-utilizing Chromatin assembly and remodeling Factor; Ito et al., 1997) and CHRACH (Chromatin Accessibility Complex; Alexiadis et al., 1998), are most likely to be involved in replication relate chromatin remodelling (Haushalter and Kadonaga, 2003; Corona and Tamkun, 2004).

Recently, two ISWI chromatin remodelling complexes, WICH (for WSTF-ISWI chromatin remodelling complex) and ACF, were found to localise and function specifically at late- but not early-replication foci in mammalian cells (Bozhenok et al., 2002; Collins et al., 2002), suggesting that they may be involved in the formation or disruption of specialised heterochromatin structure in S phase. *In vivo* analysis of *Drosophila* Acf1 null mutants support the function of ACF in heterochromatin formation (Fyodorov et al., 2004).

1.5 THE ASSEMBLY OF SPECIALISED CHROMATIN STRUCTURES

1.5.1 Functionally specialised chromatin structures and epigenetic marks

The primary function of chromatin is to package DNA within the cell nucleus. However, several regions of the genome need to be packaged into specialised chromatin structures that perform specific functions. For instance, pericentric heterochromatin serves to package repetitive DNA elements that surround each centromere and plays an important role in kinetochore function and chromosome segregation (Bernard et al., 2001). Many different factors contribute to the establishment of specialised chromatin structures. These include histone variants (Ahmad and Henikoff, 2002), non-coding RNAs (Grewal and Rice, 2004), DNA methylation and methylated DNA binding proteins (Bird, 2002; El-Osta, 2003) and a bewildering diversity of histone post-translational modifications (Fischle et al., 2003). Some histone modifications, such as acetylation, remove the positive charge of lysine residues and potentially disrupt histone-DNA interactions or the folding of nucleosome arrays into chromatin higher-order structures (Wolffe and Hayes, 1999). However, other modifications such as lysine or arginine methylation do not affect the charge of the modified lysine residues and exert their influence on chromatin structure through their recognition by non-histone chromosomal proteins. Several effector proteins that recognise specific histone modifications are already known. These include bromodomain proteins that bind acetylated histones (Owen et al., 2002) and chromodomain proteins that recognise histones which are methylated at specific lysine residues (Jacobs and Khorasanizadeh, 2002; Nielsen et al., 2002; Fischle et al., 2003). Histone post-translational modifications clearly constitute a form of epigenetic information because, either directly or indirectly, they can alter the expression or affect the function of the underlying DNA sequence. In addition, like DNA methylation, histone modifications and the specialised chromatin structures that they create can be propagated stably through mitotic and meiotic cell divisions (Grewal and Klar, 1996; Ekwall et al., 1997; Cavalli and Paro, 1999).

1.5.2 Propagation of histone post-translational modifications in proliferating cells

In proliferating cells, the faithful maintenance of patterns of histone post-translational modifications that are restricted to specific chromosomal loci poses a problem. This is because a significant fraction of newly synthesised histones are acetylated at a number of distinct residues within their amino-terminal tails (Sobel et al., 1995; Kuo et al., 1996). In addition, other important histone modifications, such as lysine methylation (see below), are not known to occur before newly synthesised histones are packaged into chromatin. Thus, each passage through S phase results in incorporation of a wave of newly synthesised and acetylated histones throughout the genome, but these histones are otherwise devoid of other histone modifications. Histone acetylation is generally associated with transcriptionally active chromatin and is largely absent from telomeric or pericentric heterochromatin (Ekwall et al., 1996; Suka et al., 2001). Therefore, the newly synthesised histones deposited during the replication of pericentric heterochromatin are initially acetylated (Taddei et al., 1999), and this acetylation is removed before the onset of mitosis via a multiprotein histone deacetylase complex containing Sin3 (David et al., 2003). Defects in this deacetylation disrupt the structure of pericentric heterochromatin and result in aberrant mitotic chromosome segregation (Taddei et al., 2001; David et al., 2003). The fact that CAF1 remains associated with the sites of heterochromatin replication during the period when deacetylation takes place has led to the suggestion that CAF1 may help to coordinate histone deposition during pericentric heterochromatin replication with their deacetylation. One possible link between CAF1 and the Sin3 histone deacetylase complex is that they share the RbAp48 histone binding subunit (Verreault et al., 1996; Zhang et al., 1997).

There are several other examples of histone modifications that are targeted to specific loci. For instance, histone H3 lysine 4 (K4) methylation is excluded from heterochromatic loci and correlates with chromosomal domains that are potentially active in transcription (Litt et al., 2001; Noma et al., 2001). In contrast, histone H3 K9 methylation is recognised by HP1 protein and is

present in chromosomal regions that are devoid of histone H3 K4 methylation, such as the pericentric heterochromatin and other loci dispersed along the chromosome arms (Peters et al., 2003). Histone H3 K27 methylation, which is recognised by Polycomb proteins (Fischle et al., 2003), is involved in the epigenetic silencing of homeotic genes and the inactive X chromosome (Cao et al., 2002; Plath et al., 2003). In female mouse cells, both histone H3 K9 and K27 methylation are present along the inactive X chromosome, but absent from the active X (Peters et al., 2002; Plath et al., 2003; Rougeulle et al., 2004). X chromosome inactivation is a clear epigenetic phenomenon as, even though the two X chromosomes have the same DNA sequence, only one of them is packaged into silent chromatin while the other is transcriptionally active. In addition to the presence of histone H3 K9/K27 methylation, the inactive X chromosome is generally hypoacetylated (Jeppesen and Turner, 1993), extensively DNA methylated (Riggs and Pfeifer, 1992) and coated with a non-coding RNA, known as Xist, which plays a critical role in X-chromosome inactivation (Penny et al., 1996). The patterns of DNA methylation are propagated by the maintenance DNA methyltransferase DNMT1 (Li et al., 1992), which uses the modification of the parental DNA as a template to guide the methylation of the nascent DNA, but how the other chromatin features that distinguish the two X chromosomes are stably maintained in proliferating cells is not known. One mechanism that has been invoked to explain the packaging of the two X chromosomes into two distinct chromatin structures is their different replication timing during S phase. As has been observed with many transcriptionally silenced autosomal genes, the inactive X chromosome replicates later than the active X (Riggs and Pfeifer, 1992; Goren and Cedar, 2003). In principle, this could provide a mechanism to ensure that transcriptionally repressed genes only replicate during a portion of S phase when the enzymes that carry out histone modifications involved in gene repression are active. However, there is currently no evidence that the enzymes that methylate K9 and K27 of histone H3 are regulated during the progression from early to late S phase. In addition, studies of genes that are subject to heritable transcriptional silencing in human lymphocytes have revealed that these genes do not always exhibit late replication, even when

they are located in close proximity to late-replicating pericentric heterochromatin (Azuara et al., 2003). Instead of delayed replication, the stably silenced genes exhibited a delay in sister chromatid separation (Azuara et al., 2003). During replication, the pre-existing histone H3/H4 tetramers do not appear to be completely displaced from the DNA and segregate onto both the leading and lagging strands (Sogo et al., 1986; Jackson, 1988). Therefore, sister chromatid cohesion could facilitate the copying of patterns of parental histone modifications onto the newly synthesised histones.

The transient disruption of chromatin structure that occurs during replication provides a unique window of opportunity for cells to modify or maintain patterns of histone modifications (Kass and Wolffe, 1998). Consistent with this, several genetic links exist between DNA replication, nucleosome assembly, and the propagation of specialised chromatin structures (McNairn and Gilbert, 2003). For instance, mutations in several different replication proteins reduce epigenetic silencing of reporter genes without affecting DNA replication (Ehrenhofer-Murray et al., 1999). One particularly interesting class of mutations that affect heterochromatin-mediated silencing in both *S. cerevisiae* and higher eukaryotes are those that affect the DNA polymerase processivity factor PCNA (Ehrenhofer-Murray et al., 1999; Henderson et al., 1994; Zhang, Shibahara and Stillman, 2000; Sharp et al., 2001). This is because PCNA binds directly to nucleosome assembly factors such as CAF1 (Shibahara and Stillman, 1999), which is itself required for heterochromatin-mediated silencing in both yeast and higher eukaryotes (Kaufman et al., 1997; Kaya et al., 2001). Surprisingly, the potential role of PCNA in the propagation of epigenetic marks, such as histone post-translational modifications, has not been explored. In Chapter 6, I have attempted to determine whether PCNA may directly contribute to the methylation of newly synthesised histone H3 at K4 by attracting the Set1 methyltransferase to sites of DNA replication.

CHAPTER 2 – MATERIALS AND METHODS

All materials were purchased from Sigma and were of the highest purity grade available, unless otherwise stated. All solutions were made with distilled water (dH_2O) and sterilised by autoclave or filtration. Radiolabelled reagents were from either Amersham Pharmacia Biotech [^{32}P] or ICN [^{35}S]. Radioactive and hazardous substances were disposed of according to the safety regulations in Clare-Hall.

Most methods in this work, were taken or adapted from Sambrook (1989).

2.1 BUFFERS

6 x Agarose loading buffer (ALB): 0.25% Bromophenol blue, 0.25% Xylene cyanol FF, 30% Glycerol in dH_2O.

Buffer A: 25 mM Tris-Cl pH 7.5, 0.1% NP40, 10% Glycerol, 1 mM DTT, 1x Protease Inhibitors (PI). NaCl concentration was 0-1000 mM as indicated in the text (for example buffer A400: buffer A with 400 mM NaCl).

Chromatin extract buffer B: 50 mM Tris-Cl pH 8, 5 mM $MgCl_2$, 0.5 mM Na_2EDTA, 25% Glycerol, 5 mM DTT, 1x PI.

10x CDK2 phosphorylation buffer: 100 mM HEPES pH 7.5, 1 μM KCl, 500 nM Na-β-Glycerophosphate, 50 nM NaF, 30 mM EDTA, 10 mM DTT.

Coomassie staining buffer: 45% Methanol, 10% Glacial Acetic acid, 0.1% Coomassie brilliant blue R in dH_2O.

Coomassie staining buffer for mass-spectrometry: 0.05% Coomassie brilliant blue G-250, 10% methanol, 5% acetic acid in dH_2O.

Destain buffer for mass-spectrometry: 10% Methanol, 5% Acetic acid in dH_2O.

Fixation (destain) buffer: 10% Methanol, 10% Acetic acid in dH_2O.

Grace's Insect Medium: For 1 litre, 1 kg Grace's insect medium powder, 3.3 g Lactalbumin hydro slate, 3.3 g Yeastolate, 0.35 g Sodium bicarbonate, pH to 6.2 with NaOH. 10 ml of Pen Strep added per litre.

GST elution buffer (GEB): 50 mM Tris-Cl pHd 8.7, 100 mM NaCl, 1 mM EDTA, 0.02% NP-40, 10% Glycerol, 1 mM DTT, 1x PI and 10 mM fresh Glutathione.

GST lysis buffer (GLB): 50 mM Tris-Cl pH 8, 120 mM NaCl, 1 mM EDTA, 0.02% NP-40, 10% Glycerol, 1 mM DTT, 1x PI.

His lysis buffer (HLB): 50 mM $NaPO_4$ pH 8, 20 mM Imidazole, 10% Glycerol, 0.02% NP-40, 5 mM βME, 1x PI. NaCl concentration was adjusted to each protein, for example 150 mM and 300 mM NaCl were used for purification of C-His PCNA and C-His hp150 respectively.

Hypotonic buffer: 20 mM HEPES-KOH pH 8.0, 5 mM KCl, 1.5 mM $MgCl_2$, 0.1 mM DTT. Na butyrate was added just before use to a final concentration of 5 mM.

5x Laemmli sample buffer: 50% Glycerol, 5% SDS, 250 mM Tris-Cl pH 6.8, 0.01% Bromophenol blue, 715 mM βME. When eluting from antibody beads, Laemmli buffer without βME was used to minimise elution of the antibodies.

LB: For 1 litre, 10g bacto-tryptone, 5g bacto-yeast extract, 10g NaCl in 1litre dH_2O, pH to 7.0 with NaOH. Sterilise by auotclaving.

LB/Amp: LB with 100 μg / ml Ampicillin.

LB/Kan: LB with 50 μg / ml Kanamycin.

LB/CM: LB with 34 μg / ml Chloramphenicol.

LB agar: 1 litre LB, 15 g agarose.

λPPase reaction buffer: 50 mM Tris-Cl pH 7.5, 0.1 mM Na_2EDTA, 5 mM DTT, 0.01% BRIJ 35, 2 mM $MnCl_2$.

Mammalian lysis buffer (MLB): 20 mM HEPES pH 7.5, 100 mM NaCl, 40 mM KCl, 1.5 mM $MaCl_2$, 10% Glycerol, 1 mM EGTA, 0.5% NP40, 1x PI.

Mowiol mounting media: 6 g Glycerol, 2.4 g Mowiol 4-88 (Calbiochem) were stirred thoroughly, added to 6 ml dH_2O and left for 2 h at room temperature, 12 ml 0.2 M Tris-Cl pH 8.5 added and solution was incubated at 53˚C until Mowiol has dissolved, then centrifuged to clarify for 20 min at 5000 rpm and store at –20˚C.

NaOH β-ME: Prepared fresh before use by adding 80 μl βME to 1 ml 1 M NaOH.

Oligo Buffer: 0.3 M $NaCH_3CO_2$, 10 mM $MgCl_2$.

PBS: For 1 litre, 8 g NaCl, 0.2 g KCl, 1.44 g Na_2HPO_4, 0.24 g KH_2PO_4 in 1 litre dH_2O, pH to 7.4 with HCl.

PBS-T: PBS with 0.2% Tween 20.

PBS-TB: PBS-T with 5% (w/v) BSA.

PBS-TM: PBS-T with 5% (w/v) low fat milk.

Pen Strep: 1.567 g Pen (1647 U/mg), 5 g Strep (767 U/mg), dH_2O to 500 ml.

Pol α / primase dilution buffer: 20 mM Tris-Cl pH 8.3, 1 mM Na_2EDTA, 10% Glycerol, 0.35 M KCl, 0.1 mM DTT, 1x PI.

Pol α / primase eiution buffer: 20 mM Tris-Cl pH 8.3, 1 mM Na_2EDTA, 10% Gycerol, 0.5 M NaCl, 50% ethylen glycol 1x PI.

Ponceau S staining: For 500 ml, 1 g Ponceau S, 15 g Trichloroacetic acid, 15 g Sulphosalicylic acid.

200x Protease Inhibitors cocktaii (Pi): 0.1 mg/ml Aprotinin (Roche), 200 mM Benzamidine, 40 μg/ml Chymostatin (from stock dissolved in DMSO), 0.1 mg/ml Leupeptin (Boehringer Mannheim), 0.2 mg/ml Pepstatin A (from stock dissolved in methanol), 20 mM Pefabloc (Roche).

5x replication reaction mix: 200 mM HEPES (optimised pH determined by titration, normally pH 7.6 - 8), 15 mM ATP, 1 mM UTP/CTP/GTP each, 125 μM dATP, 0.5 mM dTTP/dCTP/dGTP each, 200 mM CPi, 2.5 mM DTT, 20 mM $MgCl_2$.

5x replication stop solution: 50 mM Na_2EDTA pH 8, 2.5% SDS.

4x SDS-PAGE separating buffer: 1.5 M Tris-Cl pH 8.8, 0.4% SDS.

4x SDS-PAGE stacking buffer: 0.5 M Tris-Cl pH 6.8, 0.4% SDS.

10x SDS-PAGE running buffer: 0.1 M Tris, 0.768 M Glycine, 1% SDS.

5x SDS-PAGE running buffer for histones: 60 g Tris base, 280 g Glycine, 50 ml 20% SDS, dH_2O to 2 lit.

Silver staining blocking buffer: 4% Tris base and 2% Acedtic acid.

Silver staining developing buffer: 4% (w/v) K_2CO3, 0.025% (v/v) Formalin, 0.025% Sodium dodecyl solphate (STS).

S100 buffer: 50 mM HEPES pH 7.6, 150 mM NaCl, 10% Glycerol, 0.02% NP-40, 5 mM βME (or 1 mM DTT),1 x PI.

T Ag buffer TD: 25 mM Tris-Cl pH 7.4, 136 mM NaCl, 5.7 mM KCl, 0.7 mM Na_2HPO_4.

T Ag buffer B: 50 mM Tris-Cl pH 8.0, 150 mM NaCl, 1 mM Na_2EDTA, 10% (v/v) Glycerol, 1x PI.

T Ag buffer C: 50 mM Tris-Cl pH 8.0, 0.5 M LiCl, 1 mM Na_2EDTA, 10% (v/v) Glycerol, 1x PI.

T Ag buffer D: 10 mM Pipes pH 7.4, 5 mM NaCl, 1 mM Na_2EDTA, 10% Glycerol, 1x PI.

T Ag buffer E: 56.5 g Triethylamine, 10% Glycerol in final volume of 20 ml (pH 10.8), prepared fresh before use.

T Ag dialysis buffer: 10 mM Pipes pH 7, 1 mM DTT, 0.1 mM Na_2EDTA, 5 mM NaCl, 10% Glycerol, 1x PI.

50x TAE: For 1 litre, 242 g Tris base, 57.1 ml Glacial Acetic acid, 100 ml 0.5 M EDTA pH 8.

TE buffer: 10mM Tris-Cl (pH 8.0), 1 mM Na_2EDTA (pH 8.0).

TEV cleavage buffer: 10 mM Tris-Cl pH 8, 150 mM NaCl, 0.1% NP40, 0.5 mM Na_2EDTA, 1 mM DTT.

40x Transfer buffer (protein - Sodium carbonate): 250 mM $NaHCO_3$, 173 mM Na_2CO_3 pH to 9.5 with HCl. For use, dilute to 1x in 20% Methanol.

5x Transfer buffer (histone - Tompson): 0.5 M CAPS. For use, dilute to 1x in 20% Methanol.

Tricine gel buffer: 3 M Tris-Cl pH 8.45, 0.3% SDS.

Tricine SDS-PAGE anode buffer: 0.2 M Tris-Cl pH 8.9.

Tricine SDS-PAGE cathode buffer: 0.1 M Tricine, 0.1% SDS, 0.1 M Tris base.

Triton extraction buffer: 0.3 M Sucrose, 3 mM $MgCl_2$, 1% Normal Goat Serum (NGS -Invitrogen), 0.2% Triton-x 100 in PBS.

TSS (Transformation and storage solution): 85% LB, 10% (w/v) PEG MW 8060, 5% (v/v) DMSO, 50 mM $MgCl_2$, pH 6.5.

Yeast lysis buffer: 20 mM HEPES-KOH pH 7.5, 110 mM KAc pH 7.5, 10% Glycerol, 0.1% Tween 20, 1 mM NaOrtovanadate, 50 mM NaF, 10mM NaButyrate, 10 mM βME, 1x PI.

YNB: 0.67% Yeast nitrogen base without amino acids (Difco), 2% Glucose, appropriate amino acids at 40μg/l final concentration.

YPD: 1% Yeast extract, 2% Peptone, 2% Glucose.

2D gel strip rehydration buffer: 0.5% Immobilised pH Gradient (IPG) buffer range 3-10 (Amersham Pharmacia Biotech), 8M Urea, 2% (w/v) CHAPS, trace of Bromophenol blue, 20-100 mM DTT.

2D gel SDS equilibration buffer: 50 mM Tris-Cl pH 8.8, 6 M Urea, 30% (v/v) Glycerol, 2% SDS (w/v) and a trace of Bromophenol blue.

2.2 BASIC DNA METHODS

All procedures were performed at room temperature (RT) unless stated otherwise.

DNA preparation

DNA preparations were done using DNA QIAprep kits (QIAGEN), following manufacturers instructions. *E. coli* cells were pelleted using Beckman Allegra™ 6KR centrifuge or a Sorvall RC-53 centrifuge for larger cultures. Samples were microfuged using Eppendorf desktop micro-centrifuge.

Enzymatic reactions

Restriction digests, ligations and dephosphorylations were performed with buffers and protocol supplied by the manufacturer. Restriction enzymes and calf intestinal alkaline phosphatase were from New England Biolabs (NEB). Ligations were carried out using T4 DNA ligase from Roche or a DNA ligation Kit (Version 2.0, Takara Biomedical). Enzymes and small DNA fragments were removed after reactions using Qiaquik Nucleotide Removal Kit (Qiagen) according to manufacturers instructions.

Oligonucleotide preparation

Oligonucleotides were obtained from the Cancer Research UK oligonucleotide synthesis facility. The pellet was dissolved in 200 μl oligo buffer and 600 μl cold ethanol was added. The solution was placed on ice for 15 min and centrifuged at 14k rpm for 20 minutes at 4°C. The pellet was washed in 80% ethanol and dried in a speed-vac, then dissolved in 10 mM Tris-Cl pH 8 to a final concentration of 1 mg/ml.

Ethanol precipitation

DNA sample volume was adjusted to ≥50 μl with dH_2O, and NaAc (pH 5.2, or pH 7 for samples with EDTA or EGTA) was added to final concentration of 0.3 M. 10 μg of Glycogen and 2 volumes of cold ethanol were added. Samples were placed at –20°C for at least 15 min, and microfuged at full speed for 10 min at RT. The pellet was rinsed with 70% ethanol, microfuged and dried.

Polymerase chain reaction (PCR)

Pfu and *Pfu turbo* enzymes (Stratagene) were used for cloning purposes. A typical PCR reaction contained 200 μM dATP, dCTP, dGTP and dTTP, 10x Pfu reaction buffer (1.5mM $MgCl_2$, 10mM Tris.HCl pH 8.4, 50mM KCl), 10-20 pmol of each primer and 2.5 - 5 units *Pfu* polymerase in 50 μl final volume. 10–50 ng plasmid DNA were used as template. Reactions were incubated in a MJ Research PTC-200 Peltier thermal cycler, a typical programme is as follows:

4 min @ 95°C,
30 sec @ 95°C, 1 min @ 55°C, 2 min/kb @ 68°C – 25x,
10 min @ 72°C,
cool to 4°C and END.

Programmes varied depending on Tm of primers used. Additionally, when the desired amplification was not obtained, conditions such as annealing temperature, plasmid/$MgCl_2$/primer concentration were altered. DMSO was also added to optimise reactions. The sequences of oligonucleotides used in this work are given in Appendix I.I. If the PCR products were to be cloned, primers were designed with non-complimentary tails containing the required restriction sites for direct cloning into the target vector. For such primers, additional 5 cycles using a lower annealing temperature were included prior to the main chain reaction cycle. The PCR products were purified on agarose gels before cloning.

Site directed mutagenesis by PCR

Site directed mutagenesis was carried out using the Quick-change site directed mutagenesis kit (Stratagene), following the manufacturers instructions.

DNA sequencing

PCR reactions for DNA sequencing were carried out using the ABI PRISM™ dRhodamine Terminator Cycle Sequencing Ready Reaction Kit (PE – Applied Biosystems) according to manufacturers protocol. After precipitation of the labelled products the reactions were loaded onto the automated sequencer by the Cancer Research UK sequencing facility. Sequences were read and analysed using EditView 1.0.1 software (Perkin-Elmer).

DNA extraction

DNA was extracted from cell lysates, replication and other reactions using the QIAquick Nucleotide Removal Kit (QIAGEN) according to the manufacturers instructions with the following alterations: DNA from replication reactions was bound to the mini-columns by passing the reactions through the columns twice. The columns were then washed once with 500 μl PE buffer, and spun three times to remove residual ethanol before eluting with 1x ALB.

DNA extraction from gels was preformed using the QIAquick Gel Extraction kit (QIAGEN), as specified by the manufacturer.

Agarose gels

Agarose gels of 0.7-2% (Gibco BRL) were prepared and run in 1x TAE buffer. Ethidium bromide, 0.5 μg/ml, was added unless otherwise stated. Samples were loaded with 1x ALB. Markers used were: DNA hyper ladder I (as 1 kb ladder) and IV (as a 0.1-1kb ladder), as specified by the manufacturer (BIOLINE). Gels were run using Scotlab apparatus and visualised on a transilluminator (Ultra Violet Products).

Supercoiling assay agarose gels: 1.25% agarose, 1 mM $MgCl_2$ in 1x TAE.

Plasmid stock storage

Plasmids were kept in 10 mM Tris-Cl pH 8 at –20°C. Glycerol stocks of XL1-blue, DH5α or Gold™ (Stratagene) *E. coli* transformed with the relevant plasmids were stored at –80°C.

Plasmids and sub-cloning used for this work

The plasmids used in this work are listed in Appendix I.II, including both plasmids that have been published previously and plasmids constructed specifically for this work.

2.3 RNA METHODS

For all RNA work, RNase free reagents and tubes (Ambion) were used. Work surfaces and all equipments were thoroughly cleaned with detergent and Zap (Ambion) before use.

RNA preparation from yeast

Total RNA was purified from yeast cells using the RNeasy mini kit (QIAGEN), following manufacturers protocols.

Micro-array analysis

Total RNA was purified from the different yeast strains as described above. RNA concentration and purity were determined by values of OD_{260nm} and OD_{280nm} of samples using spectrophotometer (Shimadzu). The RNA was then used to synthesise double stranded cDNA using a Custom SuperScript ds-cDNA synthesis kit (Invitrogen), as directed by the manufacturer. The double stranded cDNA was cleaned up by extraction with 1x volume of Phenol:Chloroform:Isoamyl alcohol (25:24:1) and ethanol precipitation. cDNA was then used to transcribe biotin-labelled cRNA with the T7 BioArray HighYield RNA Transcript labelling kit (ENZO) following manufacturers instructions. Transcripts were purified using the RNeasy miniprep kit (QIAGEN) as instructed by the manufacturer.

The biotin labelled RNA and the original RNA purified from cells were sent to HMGC for hybridisation on Affymetrix Yeast S98 chips and for total RNA integrity assay, respectively.

2.4 BASIC PROTEIN METHODS

All procedures were performed at 4°C or on ice unless stated otherwise.

Determination of protein concentration

Bradford assay: 1μl sample was added to 800 μl dH_2O and mixed by vortexing. Bradford protein assay reagent, 200 μl (BioRad), was then added and mixed. The samples absorbance at 595 nm were determined using a Pharmacia Biotech Ultraspec 200 spectrophotometer. A standard curve was prepared using known concentrations of bovine serum albumin (BSA). Sample protein concentration was determined using the standard curve (Figure 2.1).

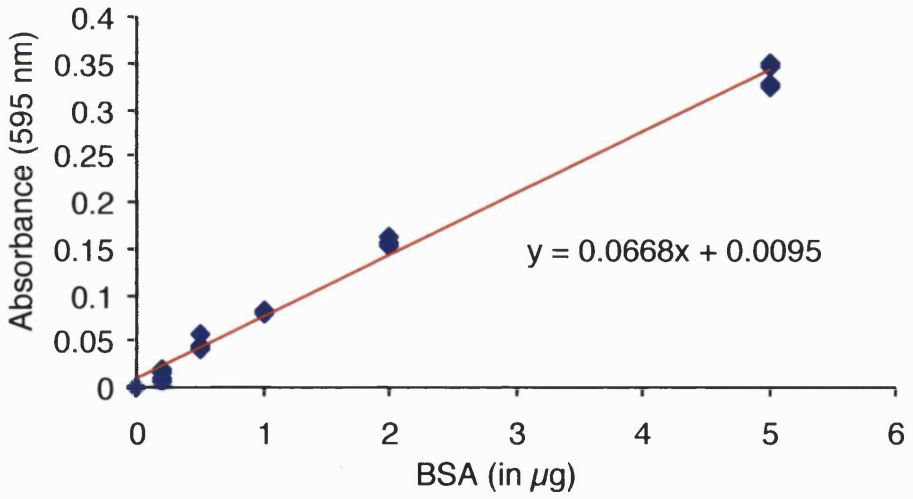

Figure 2.1: Standard curve from Bradford protein reagent with BSA
The samples were prepared as described above. A titration of 0.2, 0.5, 1, 2 and 5 μg BSA was read twice, and a graph was plotted using Excel.

Elman reagent: Protocol was as described by manufacturer (Pierce). Briefly, 2 μl of peptide was incubated for 15 min at RT with 398 μl 80 mM NaPhosphate pH 8, 1 mM Na_2EDTA and 13.3 μl Ellman reagent solution (4 mg/ml 5,5'-Dithio-bis-[2-nitrovenzoic acid] in 100 mM NaPhosphate pH 8, Pierce). The absorbance at 410 nm was determined (using a quartz cuvette) and the free –SH concentration was calculated: $\varepsilon = 14150\ M^{-1}\ cm^{-1}$.

TCA precipitation

0.1-0.2% volume of 100 mg/ml NaDeoxycholate (pH>8.0) was added to each protein sample, mixed and incubated on ice for 30 min. 100% TCA (trichloroacetic acid) was then added to a final concentration of 6%, and incubated on ice for another 30 min. Samples were then microfuged at maximum speed for 10 min at 4˚C. Pellets were rinsed with 0.1 M HCl in acetone followed by acetone, air-dried and resuspended in the appropriate sample buffer.

SDS-PAGE (protein gels)

Protein gels were run on mini and midi gel apparatuses (CBS). The tables below give recipes for common gels used (Tables 2.1 - 2.3). Protein samples were diluted in 5x Laemmli buffer and then incubated for 3-5 min at 100°C. When whole cells were used, samples were sonicated before boiling. The gels were run at 150V for 1.25 h (mini, long) or 200V for 2 h (maxi) in the appropriate 1x gel running buffer. Pre-stained protein markers (Invitrogen) were used, and gels were either stained with Coomassie blue, silver or transferred to nitrocellulose membrane.

Table 2.1: Commonly used Protein gels

Reagents	6%	7.8%	10%	12%	Stacking
dH_2O	3 ml	2.775 ml	2.5 ml	2.25 ml	3.25 ml
4 x separating buffer	1.25 ml	1.25 ml	1.25 ml	1.25 ml	-
4 x stacking buffer	-	-	-	-	1.25 ml
40% Acrylamide : Bis (37.5:1)	0.75 ml	0.975 ml	1.25 ml	1.5 ml	0.5 ml
10% APS	30 µl	30 µl	30 µl	30 µl	30 µl
TEMED	10 µl	10 µl	10 µl	10 µl	10 µl

Table 2.2: Histone gels

Reagents	Separating gel	Stacking gel
40% Acrylamide	9 ml	0.75 ml
2% N, N'-Bis Acrylamide	0.9 ml	0.75 ml
3 M Tris-Cl pH 8.8	5 ml	-
1 M Tris-Cl pH 6.8	-	1.2 ml
10% SDS	0.2 ml	0.1 ml
dH_2O	4.7 ml	7.09 ml
10% APS	200 µl	100 µl
TEMED	4 µl	10 µl

Table 2.3: Tricine gels*

Reagents / gels	Separating gel	Stacking gel
Acrylamide: Bis (40:3)	7.953 ml	1.2 ml
Tricine gel buffer	6.667 ml	3.1 ml
Glycerol	2.115 ml	-
dH_2O	3.15 ml	8.09 ml
10% APS	100 µl	100 µl
TEMED	15 µl	10 µl

*Used to visualise peptides (Schagger and von Jagow, 1987)

2D protein gels

All the equipment for 2D gel analysis was from Amersham Pharmacia Biotech. To ensure the cleanest results for mass-spectrometry all solutions were prepared freshly immediately before use, and all surfaces and equipment used were washed with detergent and double distilled water.

First dimension separation was done using 18 cm precast immobilised pH gradient (IPG) polyacrylamide gel strips (Imobiline® DryStrip gels) with a 3-10 linear gradient on IPGphor™ Isoelectric Focusing System. Second dimension separation was using Hoefer® DALT (large format vertical) 24 x 19 cm gels.

In order to concentrate protein samples and to remove salts and other charged small molecules that interfere with the electrophoresis and IsoElectric Focusing (IEF) processes, samples of calculated 20-100 μg protein were TCA precipitated and resuspended in 350 μl of freshly prepared rehydration buffer. Samples were left to solubilise for at least 1 h and then spun down to pellet any aggregates or precipitates. IPG strips were placed over the sample containing solution. Rehydration and IEF were carried out overnight (ON), as specified by the manufacturers. Strips were then equilibrated in SDS equilibration buffer and applied to the freshly cast second dimension gel together with a protein size marker and purified CAF1. Gels were run according to manufacturers instructions, and stained with either Coomassie or silver.

Staining protein gels

Coomassie: The gel was transferred to a clean plastic box and sufficient amounts of Coomassie stain was added to cover the gel, and incubated for 30 min at RT with constant agitation. The stain was removed by three 30 minute washes in destain solution. Once the stain was sufficiently removed the gel was soaked in 5% glycerol in dH_20 before air-drying between 2 porous cellophane sheets (BioRad).

Silver: All containers used were either new or meticulously cleaned with hot water and detergent. All solutions were made with fresh distilled water that had been filtered through 0.2 μm cellulose nitrate filters. The gel was handled as little as possible, and only with low protein, powder free gloves. Gels were

fixed with 10% each (v/v) Methanol and Acetic acid, and then washed 2 x 10 min with dH_20. To increase staining sensitivity, the gels were incubated in 200 ml 0.02% (w/v) STS for 1 min, and rinsed twice for 1 min each with dH_20. Following this, gels were incubated at 4°C in total darkness with 200 ml 12 mM $AgNO_3$ for 90 min, rinsed in dH_20 for 10 sec and developed in 400 ml of developing solution for up to 30 min. Developing was stopped by incubation with blocking solution for 30-60 min, and rinsing with dH_20.

Transfer of protein gels to nitrocellulose membrane

The SDS-PAGE gel was rinsed with transfer buffer and placed onto cut to size Protran® nitrocelulose membrane (Scleicher & Schuell) which had been previously soaked in transfer buffer. This was sandwiched between three sheets of blotting paper (Schleicher & Schuell) soaked in transfer buffer and placed between two sponges. The entire sandwich was then enclosed inside a plastic cassette and placed in a BioRad Criterion Blotter pre-filled with cold transfer buffer such that the membrane was closest to the anode.

Transfer in carbonate buffer was at 400 mAmp for 1.5-2 h whereas histone gels were transfered at 70 V for 2 h. The efficiency of transfer was qualitatively determined by comparing the amount of prestained markers remaining in the gel to the amount transferred. To obtain an approximate loading control, and as transfer quality control, the membrane was stained in Ponceau S solution for 1 min and rinsed dH_2O, then removed by washing in PBS-T.

Western blotting

The conditions were optimised for each primary antibody and are shown in Table 2.4. The blocking step was generally performed using PBS-TM, or according to manufacturers protocol at RT with constant agitation for at least 1 h (unless otherwise stated). Primary antibody incubation followed in the same buffer for a minimum of 30 min to ON, at room RT with constant agitation. After removal of the primary antibody with at least 3 washes in PBS-T, the membrane was incubated with secondary antibody (anti-mouse and anti-rabbit Ig, horseradish peroxidase linked whole antibody - Amersham Pharmacia). A dilution of 1:10000 in PBS-T was used for at least 30 minutes at RT with

constant agitation. The membrane was washed 3 times with PBS-T and further 2 times with PBS. Following washes, the membrane was exposed to ECL reaction using the various SuperSignal® kits (Pierce), depending on the expected signal intensity, and according to the manufacturers protocol. The membrane was exposed to Kodak BioMax Light film for 1 sec to 20 min and the films were processed in a Compact$_2$ developer (IGP).

Conjugating antibodies to HRP

In some immunoprecipitation experiments, detection of immunoprecipitated or co-immunoprecipitated proteins was hampered by cross-reaction of the secondary antibody with antibodies eluted from the beads. In certain cases this could be overcome by directly cross-linking the primary antibody to Horse-Radish Peroxidase (HRP) using EZ-Link™ Plus activated peroxidase and kit (Pierce), following manufacturers instructions. Membranes incubated with HRP cross-linked primary antibodies were washed and then exposed to the ECL reaction thereby avoiding secondary antibody cross-reacting with antibodies from the beads. This procedure was successful for some antibodies (such as: SS1, PC10, 9E10, M2) but not others (such as: SS24 and αscPCNA).

Detection of [^{35}S] labelled proteins

Protein samples were separated by SDS-PAGE and if necessary, gels were stained with Coomassie and destained. Following this, gels were fixed by incubating with fixation buffer, 3 x 10 min, each at RT and the signal was amplified by incubation in NAMP100 (Amersham Pharmacia) for 30 min at RT. Gels were then dried in a BioRad gel drier (model 583) and exposed to BioMax MS film (Kodak®), in an X-ray cassette ON.

Detection of [^{32}P] phosphorylated proteins

Protein samples were separated by SDS-PAGE and if necessary, gels were stained with Coomassie and destained. The gels were then dried in a BioRad drier and exposed to a BioMax AR film (Kodak®) in an X-ray cassette for 1 h-ON, or to a phosphoimager cassette for 1 to 3 h, scanned and analysed by phosphoimager (Molecular dynamics).

Table 2.4: Primary antibodies used for Western blot analysis

Antibody	Type	Epitope	Incubation conditions	Ref / source
12CA5	mAb	HA (YPYDVPDYA)	1:500 in PBS-TM	(Niman et al., 1983)
9E10	mAb	Myc (AEEQKLISEEDL)	1:500 in PBS-TM	(Kari et al., 1986)
M2	mAb	FLAG (DYKDDDDK)	1:20000 in PBS-TM	Sigma
SS1	mAb	N-terminus (1-296) of hp150	1:1000 in PBS-TM	(Smith and Stillman, 1991)
SS24	mAb	hp60	1:1000 in PBS-TM	Ibid.
SS53	mAb	hp60	1:1000 in PBS-TM	Ibid.
SS75	mAb	hp60	1:1000 in PBS-TM	Ibid.
15G12	mAb	hp48	1:200 in PBS-T	(Qian and Lee, 1995)
PC10	mAb	hPCNA (111-125)	1:1000 in PBS-TM	(Waseem and Lane, 1990)
419	mAb	T Ag	1:1000 in PBS-TM	(Lanford, 1988)
1MOD 1A9	mAb	HP1ß	1:1000 in PBS-TM	Euromedix
7A12	mAb	hLig I	1:1000 in PBS-TM	(Prigent et al., 1994)
αscPCNA	pAb	scPCNA	1:10000 in PBS-TM	(Hoege et al., 2002)
αSET1	mAb	scSET1	1:5000 in PBS-TM	(Nagy et al., 2002)
H3C	pAb	CIQLARRIRGERA	1:2000 in PBS-TM	Developed in our lab
αH3 K14 Ac	pAb	KSTGG$_{Ac}$KAPRK-C	1:1000 in PBS-TM	Upstate
αH3 K4 Me1	pAb	ARTK$_{Me1}$QTAR-GGC	1:500 in PBS-TB	Abcam
αH3 K4 Me2	pAb	ARTK$_{Me2}$QTAR-GC	1:1000 in PBS-TB	Upstate
αH3 K4 Me3	pAb	ARTK$_{Me3}$QTAR-GGC	1:1000 in PBS-TB	Abcam
αH3 K75 Me1	pAb	IAQDFK$_{Me2}$TDLRF	1:1000 in PBS-TB	(Feng et al., 2002)

Coupling antibodies to protein G beads

The method used was a modification of those described in (Schneider et al., 1982) and in (Harlow E and D., 1988). 0.5 ml of 50% protein G slurry (Pharmacia) pre-equilibrated with PBS were incubated with purified antibodies at a final ratio of 5-10 mg antibody/ml of beads. Binding was allowed to occur at 4°C with constant agitation for at least 1 h. After centrifugation at 3000 rpm, the supernatant was discarded and the beads were washed twice in 15 ml 0.2 M NaBorate pH 9.0. Beads were then resuspended in 0.2 M NaBorate pH 9.0, and di-Methylpimelimidate (stored dessicated at –20°C) was added to a final concentration of 20 mM. Coupling was allowed to occur for 40 min at RT on a rotating wheel. The beads were then spun down, the supernatant removed and the reaction washed and blocked by incubation at RT with 0.2 M Ethanolamine pH 8 for 2 h. To ensure that only a minimal amount of antibodies will dissociate with purified proteins upon elution, the beads were washed and incubated with elution buffer, then washed twice in PBS, and stored at 4°C in 0.02% NaAzide. Antibodies used for immunoprecipitation in this work were: SS1, SS24, PC3, PC10, 9E11, 419, CRL1645/SZK-237-71 (anti-pol α p180), M2 (Sigma) and 12CA5.

Peptide synthesis

Peptides were synthesised by the Peptide Synthesis Facility, Cancer Research UK. Table 2.5 lists all the peptides used in this work.

PBM peptides used for DNA replication inhibition assays were HPLC purified.

Table 2.5: Peptides used in this work

Peptide name	Sequence	Other
p21 PBM WT (p21 peptide 10)	CKRRQTSMTDFYHSKRRLIFS	Native + Bio
p21 PBM mut	CKRRQTSMTDAAHSKRRLIFS	Native + Bio
p150 PBM1 WT	CKDRPAFPVKKLIQARLPFKR	Native + Bio
p150 PBM1 mut	CKDRPAFPVKKAAQARLPFKR	Native + Bio
p150 PBM2 WT	CIKAEKAEITRFFQKPKTPQA	Native + Bio
p150 PBM2 mut	CIKAEKAEITRAAQKPKTPQA	Native + Bio
p150 PBM1a WT	CKDRPAFPVKKLIQARLPFKRLNLVPK	Native + Bio
p150 PBM1 mutb	CKDRPAFPVKKLIQARLAAKR	Native + Bio
p150 PBM1b WT	CPVKKLIQARLPFKRLNLVPK	Native + Bio
p150 PBM1b mut	CPVKKLIQARLAAKRLNLVPK	Native + Bio
p60 PBM WT	CRMFHDDSMKSFFRRLSFTPD	Native + Bio
p60 PBM mut	CRMFHDDSMKSAARRLSFTPD	Native + Bio
p21 peptide 5	GDFAWERVRGLGLPKLYLPT	
FLAG	DYKDDDDK	

Mass-spectrometry

The preparatory gel was Coomassie-stained and destained (see above), protein bands were excised, washed three times in 50% methanol, and dried in a speedvac. Identification was done at Dr. Nick Totty mass-spectrometry lab, Cancer Research UK.

Molecular size analysis by gel filtration chromatography

All gel filtration analysis was performed using a Superdex™ 200 HR 10/30 column connected to AKTA FPLC chromatography system or a Superdex 200 PC 3.2/30 column connected to a SMART chromatography system (Amersham Pharmacia Biotech). Up to 0.5 ml or 50 μl of samples were loaded onto each column respectively, and S100 buffer was used as running buffer at a constant flow rate of 100 μl/min or 40 μl/min and fractions of 500 μl or 100 μl were collected (Figure 2.2a). Fractions containing proteins were analysed by Western blotting (Figures 2.2b, 2.5c and 2.6a and b). Size markers (gel filtration standard - BioRad) dissolved in S100 buffer were analysed under the same conditions immediately before the actual sample.

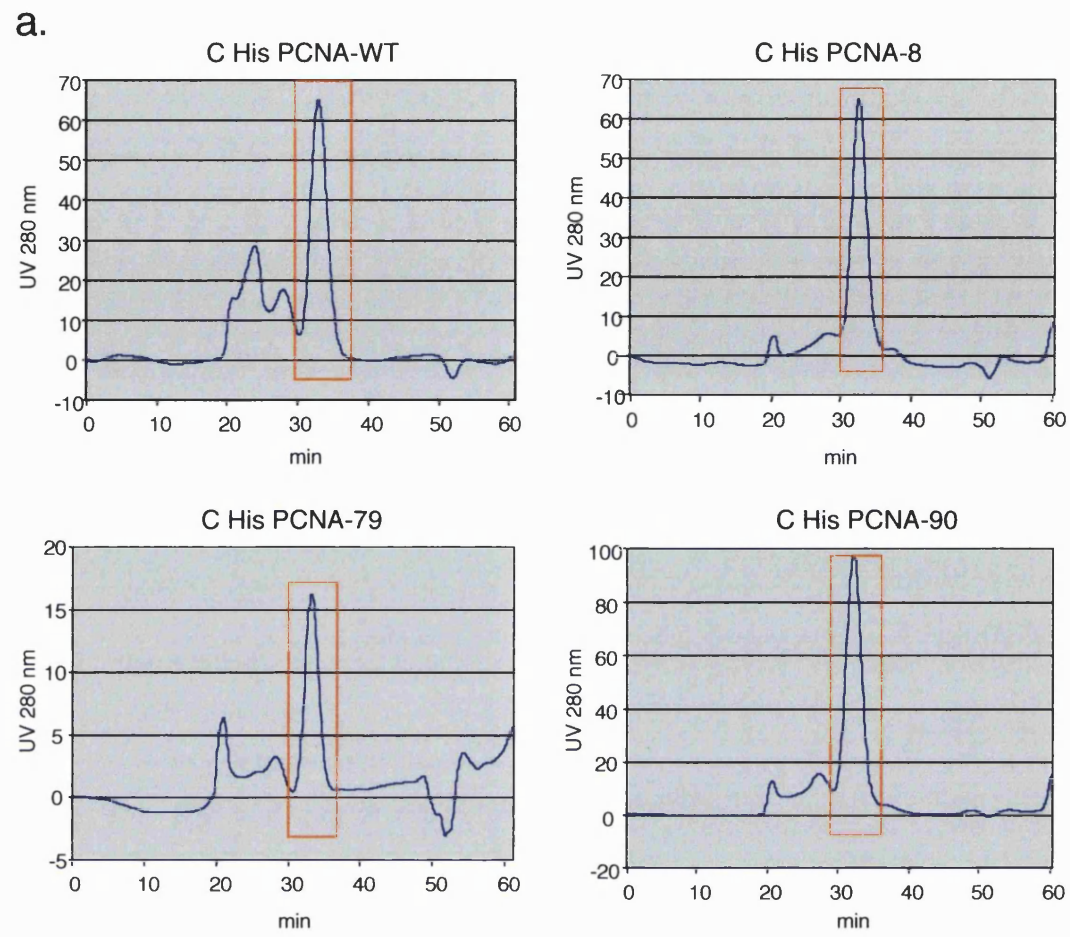

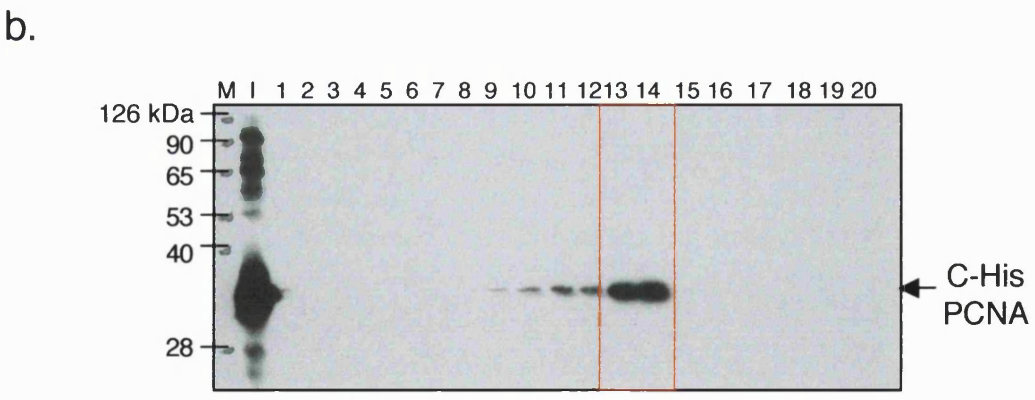

Figure 2.2: Purification of C-His PCNA by gel filtration

a. His-tagged PCNA affinity-purified from *E. coli* was further purified over a Superdex 200 HR 10/30 column placed in an ACTA FPLC. Although purification profiles varied, the major peak was similar in all preps, and ran immediately after Aldolase (data not shown). The UV280 curve of C-His PCNA samples is shown, the red-square highlights fractions used in assays. As is revealed from the scale on the Y-axis, PCNA-79 was expressed poorly in comparison to wild type PCNA, yet did purify with a similar pattern.

b. An example of Western blot analysis of C-His PCNA WT fractionated over Superdex 200. (M) protein marker. (I) 10 μl input wild type C-His PCNA. (1) 10 μl fractions 1-20. PCNA was detected with PC10 as primary antibody. Fractions used for assays are highlighted by the red-square.

2.5 *E. coli* METHODS

E. coli strains used

For DNA extraction XL1-Blue, DH5α or Gold™ (Stratagene) were used. After comparison with several different strains, Epicurian coli® BL21-CodonPlus™ (Stratagene) were used for protein expression.

E. coli cultures

E. coli suspension cultures were normally grown at 37˚C in New Brunswick Scientific shakers. However, for expression of certain proteins, the temperature was reduced to 30/24/16˚C after induction and cultures were transferred to InnOva 4230 (New Brunswick Scientific) shakers. *E. coli* plates were incubated ON at 37˚C in Heraeus incubators.

Preparation and transformation of competent *E. coli* cells

100 ml of LB was inoculated with 1 ml of ON *E. coli* culture and incubated with shaking (200 rpm) at 37°C until OD_{600nm}=0.5. Cells were chilled on ice for 20 min, then centrifuged at 5k rpm for 5 min at 4°C. Pellet was resuspended in 10 ml TSS divided into 50 µl aliquots by snap-freezing on dry ice and stored at -80°C for up to two months.

Transformation was carried out by adding DNA sample to cells thawed on ice and incubating for 5-30 min on ice. Cells were then heat-shocked for 30 sec at 42°C and placed on ice for 5 min. 1 ml of LB was then added and cells were allowed to recover by incubation with shaking at 37°C for 1 h before plating.

Preparation and electroporation of electro-competent *E. coli* cells

50 ml of ON *E. coli* culture was inoculated into 1 litter of pre-aerated LB. Cells were incubated with shaking at 37°C until OD_{600nm}=0.6-0.7. The cells were then incubated on ice in pre-chilled centrifuge bottles for 20 min, followed by centrifugation at 8k rpm for 15 min at 4°C. The cell pellet was resuspended in 1x original volume cold dH_2O and re-centrifuged as above. This procedure was repeated with 0.5x original volume cold dH_2O followed by 0.08x original volume cold 10% glycerol solution. The final cell pellet was resuspended in 2

ml cold 10% glycerol and divided into 50 μl aliquots by snap-freezing on dry ice and stored at -80°C for up to three months. Electroporation was carried out by adding DNA sample (up to 2 μl of ligation mixture) to cells on ice. The mixture was then transferred into a chilled cuvette, placed in the electroporator (BioRad) and a single pulse of 600Ω, 25 μF and 1.8-2 kV (depending on the *E. coli* strain) was applied. 1 ml of LB was then added and cells were allowed to recover by incubation with shaking at 37°C for 1 h, before plating.

Storage of *E. coli* stocks

Cultures grown ON at 37°C in LB with the relevant antibiotics were diluted 1:1 in 60% Glycerol in dH_2O, snap-frozen on dry ice and stored at -80°C.

2.6 BACULOVIRUSES AND INSECT SF9 CELLS

All baculovirus and insect SF9 cells (Smith et al., 1985) methods were taken and adapted from (O'Reilly et al., 1994).

SF9 cell cultures

Storage and growing large scales of cells were carried out at the tissue culture facilities of Cancer Research UK. All cell manipulations were done under stringent conditions in a Medical Air Technology, BioMAT^2 hood to avoid contamination. Cells were grown in Grace media with Pen Strep and 10% foetal bovine serum (FBS) and incubated at 27°C.

Amplifying viral stocks

750 μl of original viral stock (or multiplicity-of-infection (MOI) of about 0.1 virus per cell) were used to infect 600 ml of 1 x 10^6 SF9 cells/ml by incubation at 27°C for 1 week with constant agitation. The cells morphology was monitored and at the end of the incubation period, the cells were spun down, supernatant filtered and used as new viral stock. This stock was stored at 4°C wrapped in aluminium foil to protect it from light (as virus particles are sensitive to UV). Potency of each stock was tested by small-scale titration followed by Western blot analysis.

Protein expression by baculovirus infection of SF9 cells

Virus titration: In order to determine and optimise protein expression conditions of fresh viral stocks, a 6 well microtiter plate containing 2ml of 1 x 10^6 SF9 cells/ml in each well was infected with increasing amounts of the relevant virus. Alternatively, 5 ml suspension cultures were infected. Infection was allowed to occur for 48 h, after which cells were harvested, lysed in Laemmli sample buffer by sonication and analysed by Western blotting (Figure 2.3). The concentration of virus stock that produced the highest protein expression level was used for larger scale expression. When the protein to be purified was comprised of several subunits and expressed by separate viruses (such as CAF1 and RFC), titration of each virus was carried out similarly, and the choice of titre used for expression was adjusted to the least expressed subunit.

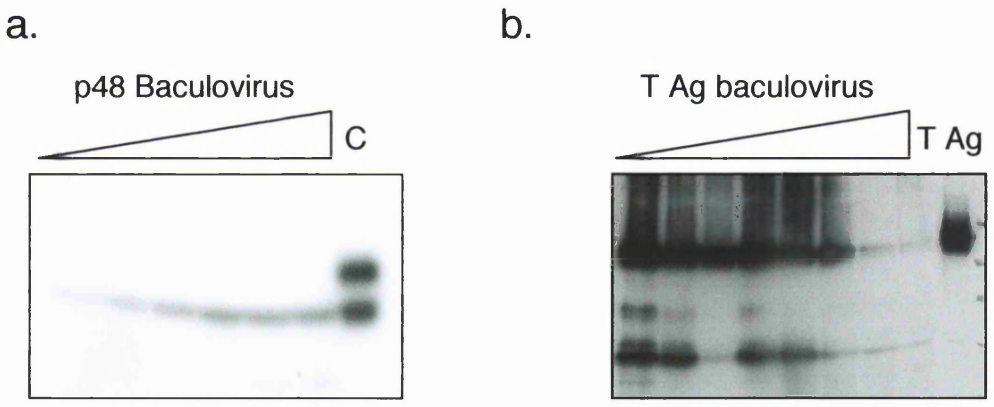

Figure 2.3: Titration of baculovirus to SF9 cells for protein expression
a. A small scale titration of a fresh stock of p48 expressing baculovirus. 1/2/5/10/20/50 µl of stock were titrated to 2 ml cultures at 10^6 SF9 insect cells/ml. After 48h, cells were harvested, lysed in 100 µl 1x Laemmli buffer, and 10 µl of each sample was analysed by SDS-PAGE and Western blotting. 5 µl of recombinant CAF1 were loaded as a control (C). p48 was detected with 15G12 as primary antibody.
b. A small scale titration of a fresh stock of T Ag expressing baculovirus. Procedure and samples are as in Figure a. 0.5 µl of previously purified T Ag was loaded as a control (T Ag). T Ag was detected with 419 as primary antibody.

Protein expression: Large scale baculovirus infections were carried out similarly to the smaller scale. To express heterocomplexes, each culture was co-infected with all the relevant baculoviruses. Infected cells were grown at 27°C in T-flasks and harvested after 48 h.

2.7 EXPRESSION AND PURIFICATION OF RECOMBINANT PROTEINS

Protein expression and purification from *E. coli*

I found that protein expression was more efficient, avoiding accumulation of truncated products, using the CodonPlus™ (Stratagene) *E. coli* strains rather then the parental BL21 (DE3) or B384 strains, in all cases tested (Figure 2.4). Therefore, all protein expression was performed in CodonPlus™.

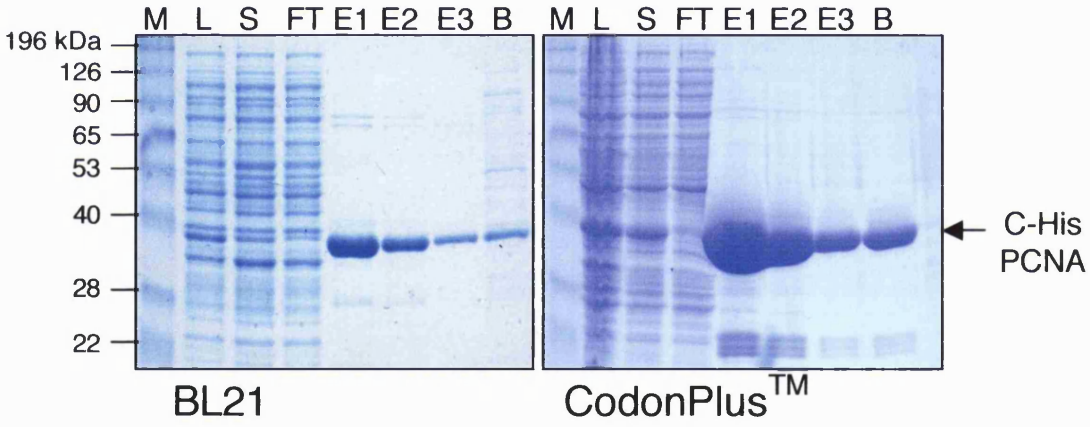

Figure 2.4: Comparing expression of C-His PCNA in BL21 and in CodonPlus™
Expression and purification gel of C-His PCNA from BL21 *E. coli* strain (left panel) compared to expression and purification gel of C-His PCNA from CodonPlus™ *E. coli* strain (right panel). Similar volumes of extracts, eluates and beads were loaded and both gels were stained with Coomassie blue. (M) Protein marker. (L) *E. coli* extract prior to sonication. (S) Supernatant after sonication and centrifugation. (FT) Flow through from Ni-NTA (QIAGEN) beads. (E) Elutions 1-3 in lysis buffer plus increasing concentration of Imidazole. (B) Beads after elution.

Table 2.6: Protein expression in *E. coli* and purification procedures

Plasmid	Antibiotics	Expression induction			Tag	Lysis buffer	Elution buffer	Other steps
		IPTG	Temp.	Time				
pET23 C-His PCNA*	Amp	1 mM	37˚c	2 h	6-His	HLB / 150 mM NaCl	Lysis buffer + 250 / 500 mM Imidazole	Gel filtration
PET30a+ N-His PCNA	Amp	1 mM	37˚c	2 h	6-His	Same	Same	Dialysis
pET28 hp150 1-296*	Kan	0.5 mM	37˚c	2 h	6-His	HLB / 300 mM NaCl	Same	Dialysis
pET28 hp150 1-462*	Kan	0.5 mM	24˚c	4 h	6-His	Same	Same	Gel filtration
pET28 hp150 full length*	Kan	0.5 mM	24˚c / 18˚c	4 h / 6 h	6-His	Same	Same	Gel filtration
His-Lig1 (and pET16b p150 (1-32) Lig I (20-919))	Amp	0.5 mM	24˚c	2 h	6-His	Same	Same	Gel-filtration
pGEXKG MOD1	Amp	1 mM	37˚c	2 h	GST	GLB	-	-
pGEXKG MOD2	Amp	1 mM	37˚c	2 h	GST	Same	-	-
pGEXKG HP1a	Amp	1 mM	37˚c	2 h	GST	Same	-	-
pGEX2TL hH3	Amp	1 mM	37˚c	2 h	GST	Same	-	-
pGEX2TL hH4	Amp	1 mM	37˚c	2 h	GST	Same	-	-
pGEXKG CAC1 PBM1*		1 mM	37˚c	2h	GST	Same	-	-

* Expression and purification procedure were similar to wild type and mutant proteins.

a.

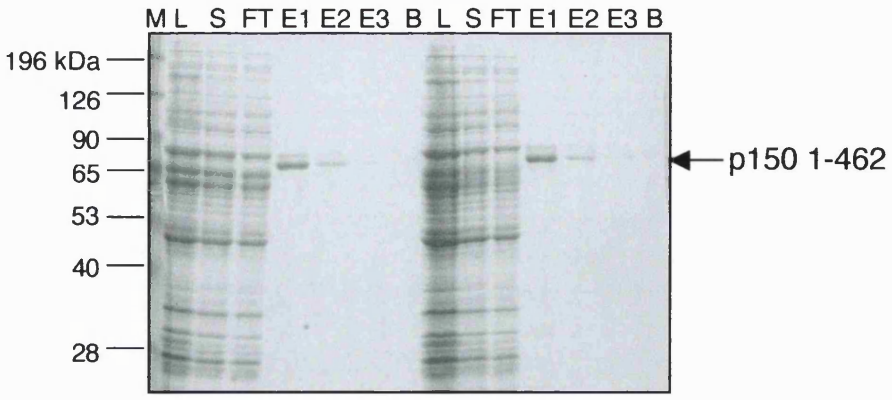

b.

c.

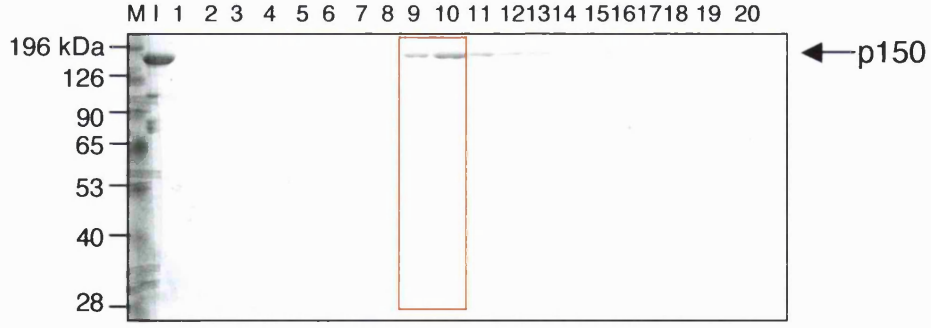

Figure 2.5: Purification of C-His p150

a. The purification of wild type and mutants C-His p150 1-462 was as described in the text, here samples from the purification procedure of C-His p150 wt and ΔPBM1 are shown. (M) Protein marker. (L) *E. coli* extract prior to sonication. (S) Supernatant after sonication and centrifugation. (FT) Flow through from Ni-NTA (QIAGEN) beads. (E) Elutions in lysis buffer plus increasing concentration of Imidazole. (B) Beads after elution.

b. The purification of full length C-His p150, here ΔPBM2 and ΔPBM1+2 are shown. (C) SF9 expressed recombinant CAF1, other samples are as in Figure a.

c. Further purification of wild type C-His p150 over a Superdex 200 HR 10/30 column. (M) Protein marker. (I) 1% of input. (1-20) fractions eluted from the column. Proteins were detected by Coomassie staining. Fraction used in binding and chromatin assembly assays are highlighted by the red-square.

a.

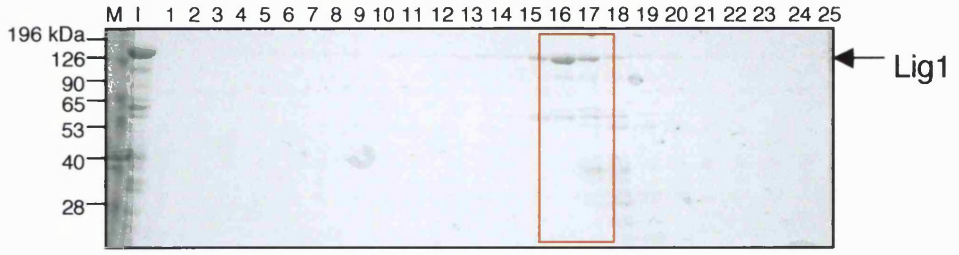

b.

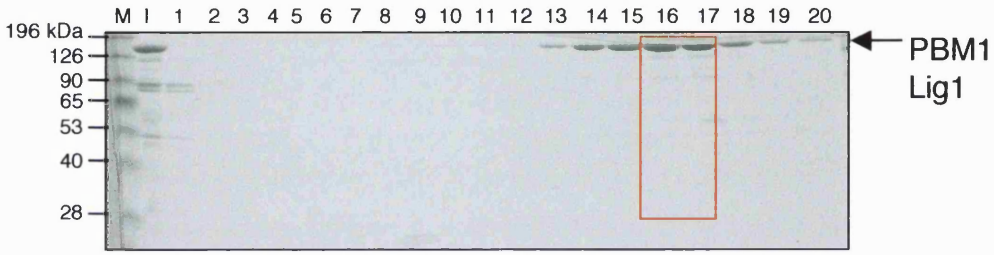

c.

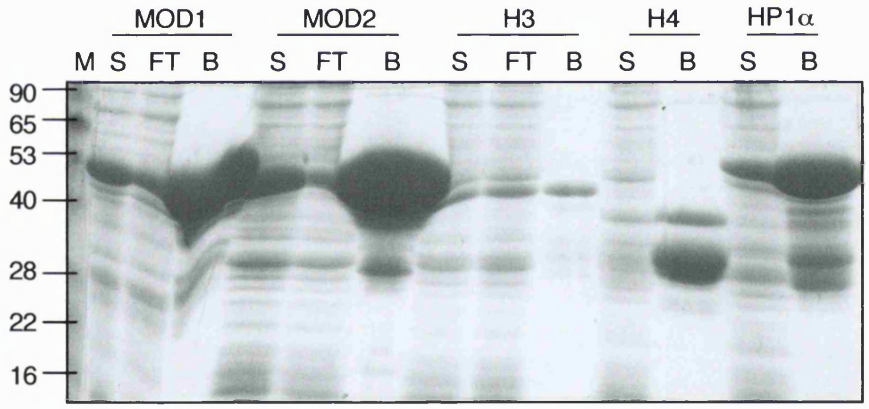

Figure 2.6: Purification of N-His Lig1 and PBM1-Lig1 and of GST-tagged proteins

a. The last step of purification of N-His Lig1 over a Superdex 200 HR 10/30 column. (M) Protein marker. (I) 1% of input. (1-25) fractions eluted from the column. Proteins were detected by Coomassie blue staining. Fraction used in binding and DNA replication and chromatin assembly assays are highlighted by the red-square.

b. The last step of purification of N-His PBM1-Lig1 over a Superdex 200 HR 10/30 column. Proteins were detected by Coomassie blue staining. Symbols are as in a.

c. Expression and purification of GST-tagged MOD1, MOD2, H3, H4 and HP1α. (M) Protein marker. (S) *E. coli* supernatant after sonication and centrifugation. (FT) Flow through from Glutathione Sepharose beads (Amersham Pharmacia). (B) Proteins bound to beads after washes. Samples were not eluted but directly used for binding assays.

Expression and purification conditions for each recombinant protein are given in Table 2.6. All purification steps were carried out at 4°C or on ice. *E. coli* cell pellet from 1 litre culture was resuspended in 20 ml of the relevant lysis buffer (*i.e.* HLB or GLB) and sonicated on ice by 8 x 15 sec pulses at level 5 (Branson Sonifier 250). The extract was then spun down at 16k rpm for 30 min (Sorvall SS34) and the supernatant was incubated with 0.2-0.5 ml of the relevant pre-equilibrated beads for 2 h–ON. All His-tagged proteins were purified over Ni-NTA beads (QIAGEN) and all GST-tagged proteins were purified over Glutathione Sepharose™ (Amersham Pharmacia). Beads were then washed 4 x 50 ml with the respective lysis buffer. If necessary, the beads were equilibrated in elution buffer and eluted in two steps with 2x bead volume. Eluates were dialysed against S100 buffer or further purified by gel filtration in S100 buffer. Figures 2.5–2.6 show the purification profiles of some of the *E. coli* expressed and purified proteins used in this work.

Protein expression and purification from SF9 cells

CAF1: Ten flasks (2 x 10^7 cells per flask in 25 ml Grace medium with 10% FBS and antibiotics) were infected with optimised amounts of the three recombinant viruses for expression of the CAF1 subunits (rCAF1 p48, p60 and p150 viruses – Kaufman et al., 1995; Verreault et al., 1996) and incubated at 27°C for 48 h. Cells were scraped and spun down at 2k rpm for 5 min at 4°c, and washed in chilled PBS. Cells were washed further with 12.5 ml hypotonic buffer, resuspended in 6.25 ml hypotonic buffer and incubated on ice for 20 min. The cells were subjected to Dounce homogenisation using a loose pestle, and spun at 10k rpm for 10 min at 4°C (Sorvall SS34 rotor). The supernatant fraction (cytosolic extract) contains some p60 and p48 protein. The pellet was resuspended in 15 ml buffer A400, mixed for 20 min at 4°C to extract CAF1 from nuclei and then spun at 10k rpm for 20 min at 4°C. The resulting supernatant fraction (nuclear extract) was pre-cleared by incubation with 1 ml of mAb 419-protein G-Sepharose beads for 1 h at 4°C. As p150 was the least abundant CAF1 subunit, the pre-cleared extract was incubated ON at 4°C with SS1 antibody beads, with constant agitation, to bind CAF1 complexes. The beads were then spun down and the supernatant used for purification of

p60/p48 complexes using mAb p60-24-protein G-Sepharose beads. The SS1 antibody beads were then washed four times with 50 ml buffer A400 and incubated with constant agitation for 30 min at 4˚C with 5M LiCl in buffer A0 to elute recombinant CAF1. Elution was repeated once more, and the eluates were dialysed against two changes of buffer A25 or buffer S100, aliquoted and stored at –80˚C. Purification of p60/p48 followed similar steps, except that elution was carried out with 3.5 M $MgCl_2$. A typical example of rCAF1 purification in shown in Figure 2.7a.

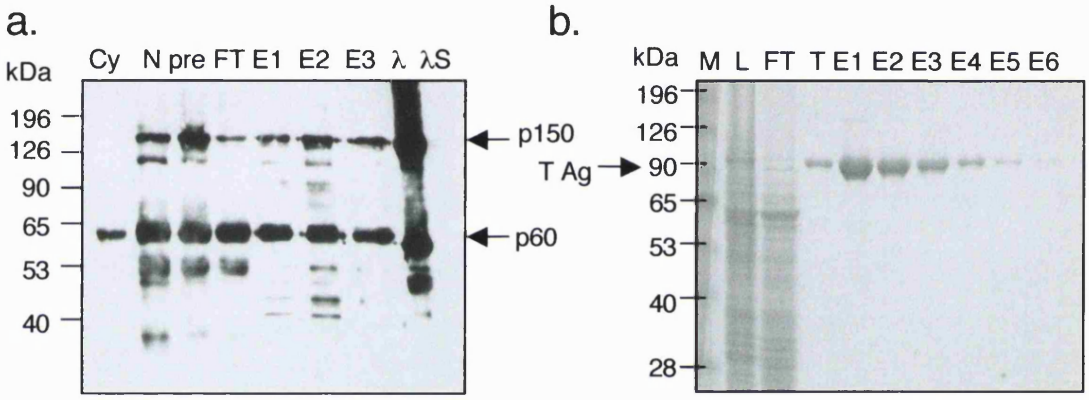

Figure 2.7: Purification of recombinant CAF1 and T Antigen from SF9 cells
a. Purification of recombinant CAF1 complex from SF9 cells was as described in the text. Purification was analysed by Western blotting with SS1 and SS24 antibodies for detection of p150 and p60 respectively. (M) Protein marker. (Cy) Cytosolic extract. (N) Nuclear extract. (Pre) Pre-cleared (FT). Flow trough from SS1 beads. (E) Elutions. (λ) CAF1 after treatment with λ PPase on beads. (λS) Supernatant of λPPase. p60 but not p150 is present in the cytosolic extract. Note the band shift of p60 after treatment with λ PPase.
b. The lowest concentration used in Figure 2.3b was scaled up to infect 1.2 lit of SF9 cells in suspension. After 48 h the cells were harvested and T Ag purified as described in the text. T – purified TAg from a previous prep, other samples are as in Figure a. Proteins were detected by Coomassie staining.

T Ag: 1.2 litre of SF9 cells ($2x10^6$/ml) were infected with T Ag expression virus (Lanford et al., 1988), and harvested after 48 h by scraping. Cells were spun down, resuspended in 25 ml, respun and resuspended in 30 ml buffer B. NP40 was added to a final concentration of 0.5%, and samples were placed on ice for 30 min, mixed every 10 min. Samples were spun down at 10k rpm for 10 min at 4˚C and the supernatant was pre-cleared over a pre-equilibrated protein A sepharose (PAS) column.

The flow through fraction was incubated with PAS-419 (anti T Ag antibodies) ON at 4°C with constant agitation. Beads were collected into a 30 ml disposable column and washed with 200ml buffer C, followed by 100 ml buffer D, then incubated for 10 min with buffer E and eluted in 0.5 ml fraction. Elutions were immediately neutralised with 25 µl of 1.0 M Pipes pH 7.0 and placed on ice. 2 µl of each elution were used for SDS-PAGE (Figure 2.7b) and for determination of protein concentration by Bradford assay. T Ag containing eluates were dialysed in T Ag dialysis buffer and stored at –80°C.

Protein expression *in vitro*

In vitro protein expression was carried out using TNT™ or Gold™ Quick coupled transcription translation (T7) kits (Promega) as specified by the manufacturer. Figure 2.8 shows an example of [^{35}S]-labelled *in vitro* translated p150.

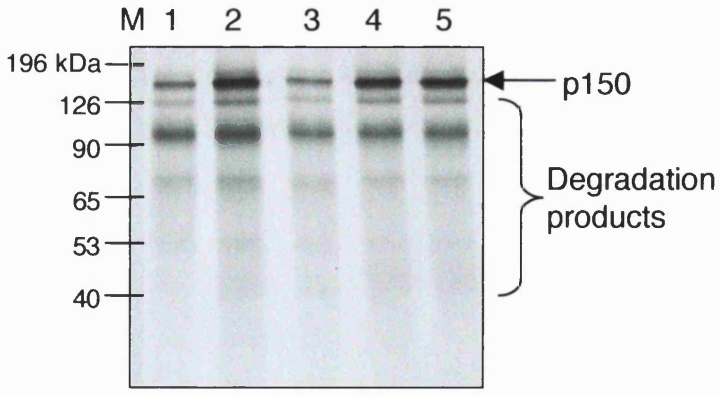

Figure 2.8: p150 expression *in vitro*
Wild type and mutant p150 were expressed by *in vitro* translation in the presence of [^{35}S] methionine as described in the text. Samples were analysed by SDS-PAGE and autoradiography.

2.8 PROTEIN-PROTEIN INTERACTION ASSAYS

Pull down assays with recombinant proteins

Generally, for small-scale pull down and co-immunoprecipitation experiments, up to 10 μg of purified proteins or 200 pmol peptides were incubated with 200 μl S100 buffer and 20 μl pre-equilibrated Sepharose or agarose bead slurry, or with 10 μl DYNA bead slurry. Binding was allowed to occur by incubation at 4˚C (unless otherwise stated) for 2 h–ON with constant agitation. Beads were washed 4 x 1.5 ml with S100 buffer, eluted in Laemmli sample buffer and analysed by SDS-PAGE and Western blotting. In some cases, Western blot analysis of immunoprecipitation experiments was hampered by antibody cross-reaction. This was minimised by eluting beads with Laemmli sample buffer without βME, and adding the reducing agent to the eluates separately.

BIAcore experiments

BIAcore experiments were performed as directed by the manufacturer using CM5 sensor chip. Manufacturers priming and running buffer (HBS) was used. Original protein samples (0.6 mg/ml PCNA and 0.3 mg/ml CAF1) were diluted to the recommended concentration in HBS buffer. Surface generation was obtained by continuous flow of running buffer with up to 2 M NaCl.

2.9 YEAST

Most methods were taken or adapted from Adams et al. (1997). Appendix I.III lists all the yeast strains used in this work.

Yeast cultures

S. cerevisiae suspension cultures were normally grown at 30˚C in New Brunswick Scientific shakers. Yeast plates were grown at 30˚C in Heraus incubators.

Normal culture conditions: Yeast cultures were grown in conical flasks in YPD liquid medium at 30°C, with agitation at approximately 200 rpm. To ensure adequate aeration, the culture volume did not exceed one quarter of the nominal flask volume. Yeast plates were made with YPD plus 2% agar and allowed to set for 24 h at RT before use. Diluted liquid yeast cultures were

plated to recover single colonies using 5 to 10 sterile 4mm glass balls (Fisher) per plate. For replating, yeast colonies were streaked out to give single colonies using sterile, sealed 50 μl glass capillaries. Plates were incubated at 30°C in the dark, colonies were approximately 1mm diameter after 40 hours.

Selective media: Solid selective media was YNB with 2% agar and the required amino acids (W303 requires histidine, leucine, tryptophan and uracil as well as adenine). The carbon source was normally 2% glucose. If galactose based media was required, 2% sucrose was added in addition to 2% galactose in order to increase cell growth rate.

Arresting yeast cultures in G1 or S phase

To arrest cells in G1 phase, α-factor was added to the growth medium at 10 μg/ml, for at least 2 h. Arrest was confirmed by microscopy; a fully arrested culture contained at least 95% unbudded cells. For S-phase arrest, cells were first arrested in G1 as above, then the α-factor containing medium was washed off and replaced with medium containing 0.2 M Hydroxyurea (HU). This was maintained for another hour, resulting in an uniform arrest in early S phase. Arrest was confirmed by microscopy; a fully arrested culture contained at least 90% budded cells.

Treatment with DNA damaging agents

MMS treatment: MMS treatment was performed by the addition of MMS to mid logarithmic cultures at a final concentration of 0.05-0.2%. Cells were incubated for up to 1 h with the chemical and then harvested for analysis. All media solutions containing MMS and contaminated glassware was treated with concentrated NaOH solution to inactivate the MMS before disposal.

UV irradiation: Cultures were harvested, washed into saline and irradiated using a prewarmed Philips 254 nm UV-C lamp (Ultra Violet Products). The distance from the lamp was adjusted to give a fluence rate of 100 J/m^2/s, measured on a UVP dosimeter. The cells were irradiated in large surface area containers, at a cell density of no more than 1x10^7 cells/ml. 10 cm square petri dishes were used to irradiate up to 20 ml samples. After treatment, the cells

were pelleted by centrifugation and resuspended in YPD. The cells were recovered for 30 min at 30°C before harvesting for analysis.

Storage of yeast stocks

Cultures grown ON at 30°C in YPD were diluted 1:1 in 60% Glycerol in dH_2O, snap-frozen on dry ice and stored at -80°C.

Genetic manipulations

Transformation: The yeast strain was grown at 30°C in YPD to cell density of 2 X 10^7 cells/ml as determined using a Coulter multisizer II (Coulter). Allowing 5 ml of cultured cells per transformation, cells were harvested at 3k rpm for 5 min, washed once in 0.5 volume dH_2O and resuspended in 0.02 of original volume 0.1 M LiAc. Cells were re-pelleted by microfuging at top speed for 5 sec, the supernatant was removed and the cell pellet resuspended to a final concentration of 2 X 10^9 cells/ml in 0.1 M LiAc. Cells were divided to 50 µl samples, spun down and supernatant was removed. To the cell pellet, the transformation mix reagents were added in the following order: 240 µl PEG 3350, 36 µl 1 M LiAc, 25 µl single stranded carrier DNA (2mg/ml herring testes DNA in TE pH 8, pre-boiled and kept on ice), 50 µl of DNA to be transformed in dH_2O (0.1-10 µg). Tubes were vortexed to homogeneity and incubated at 30°C for 30 min, and cells were heat-shocked at 42°C for 20-25 min. Cells were then pelleted, resuspended in dH_2O and plated immediately on selective plates.

Plasmid shuffling: Shuffling of *pol30* carrying plasmid was performed essentially as described by Ayagarri (1995). Briefly, cells were transformed with pBL230 plasmids as described above, and plated on the appropriate selective media (-Trp), corresponding to the Trp1 marker on the plasmid. To shuffle out the original URA3-*POL30* carrying plasmid, cells were plated on plates containing all amino acids plus 0.1% (w/v) 5-Fluoro-orotic Acid (5-FOA – Boeke el al., 1984). As *POL30* is an essential gene, cells growing on 5-FOA will have most likely lost the original plasmid and therefore relied on the second plasmid as a sole source of PCNA. Colonies from these plates were

replated on 5-FOA –Trp plates to confirm that plasmid shuffling has occurred, and colonies grown on these plates were used for further experiments.

Chromosome loss assays: Partial disomic strains carrying an extra chromosome fragment consisting of the left arm of chromosome III were constructed as in Spencer et al. (1990). At least three Ura^+ colonies for each strain were grown ON in minimal media -Ura to select for the extra chromosome fragment. Cells were diluted down to 200 cells/ml in rich medium (YPD) and grown for an additional 24 h in the absence of selection for the extra chromosome. Cells were counted and 1000 cells were plated in duplicate on minimal media plates containing low levels of adenine and uracil. The plates were incubated for 5 days at 30°C, and colonies that were >50% red were scored as those that had lost the extra chromosome fragment. The frequency of chromosome loss was calculated after accounting for the number of cell divisions in the absence of selection for the extra chromosome.

Yeast whole cell extracts

Sodium-hydroxide β-mercaptoethanol (denatured extract): 2 x 10^7 yeast cells were spun down and resuspended in 1 ml dH_2O, to which 150 µl of freshly prepared NaOH -βME solution was added. Samples were vortexed and incubated on ice for 10 min, then microfuged for 1 min at maximum speed. Pellet was resuspended in 50 µl 1x Laemmli sample buffer, neutralised if necessary with Tris-Cl pH 8.5, boiled for 5 min, spun down for 1 min and 5-10 µl supernatant were loaded on SDS-PAGE.

Small scale native extract: After harvesting, yeast were resuspended in 0.5-1 ml of lysis buffer per 1 g of cell pellet, then aliquoted to 0.6 ml added to ~0.6 ml of glass beads (0.5 mm in diameter). Samples were lysed on a ribolyzer (Hybaid), by mixing 6 x 15 sec at setting 4 with 1 min intervals on ice. Extracts were collected by puncturing a hole at the bottom of the tubes, placing them in collection tubes and spinning at full speed for 2 min. The flow through was further centrifuged at full speed for 10 min and the supernatant was used for further analysis.

Large scale native extract: Yeast pellets were resuspended in 0.02 x of the original culture volume or in 1 ml yeast lysis buffer/1.5 g culture pellet, then

lysed by passing through a French-press at 20 kpsi 4 times or by using a freezer mill (Spex). Extracts were spun down for 30 min at 16k rpm at 4°C. In order to remove RNA, the supernatant was treated with 100 μg/ml RNase A for 30 min on ice. To remove chromatin, supernatant was incubated with 50 μg/ml ethidium bromide for 30 min at 4°C with constant agitation. Samples were spun-down at 35k rpm for 1 h at 4°C, and the supernatant was used for biochemical experiments.

Purification of proteins from yeast extracts

FLAG tag purification: 20-50 ml yeast extracts were incubated ON with 250 μl pre-equilibrated M2 beads. Beads were then washed 4 x 50 ml yeast lysis buffer and eluted by resuspending in 1x Laemmli sample buffer (-βME) and incubation for 5 min at 37°C. 143 mM βME were then added to the supernatant and samples were boiled and analysed by SDS-PAGE and Western blotting. Alternatively, beads were eluted by incubation for 10 min in 2x bead volume yeast lysis buffer with increasing concentration of FLAG peptide.

2.10 MAMMALIAN CELLS

Most methods were taken or adapted from Spector et al. (1997). All cell lines were provided by Research Cell Services at Cancer Research UK (Table 2.7). All cell manipulations were done under stringent conditions in a Medical Air Technology BioMAT^2 hood to avoid culture contamination. Cells were grown in Dulbeco Modified Eagle (E4/DMEM – Life Technologies) media containing antimycin and Penn/Strep with 10% FBS or 10% bovine serum for L cells, at 37°C with 5% or 10% CO_2 in Sanyo CO_2 incubators. Cultured cells were split by trypsine/versene treatment and visualised on a Leitz diavert microscope.

Mammalian cells extracts

Small scale total cell extract: Cells from one 90 mm plate were collected using a cell scraper and washed in PBS. Cells were lysed in 1 ml MLB by rocking at 4°C for 20 min and then passed through a 21-gauge needle five times. In order to solubilise the HP1 complex in extracts, the lysate was sonicated on ice

briefly. Sample was then microfuged at maximum speed for 10 min at 4°C and the supernatant was treated with Benzonase® nuclease (Novagen) as described by the manufacturer, and used for further analysis.

Large scale cytosolic extract – S100: extracts were prepared essentially as described in (Stilman and Gluzman, 1985). All steps were carried out on ice. 16-100 litre of 293 or HeLa cells at 6 x 10^5 cells/ml were harvested by centrifugation at 2.5k rpm, 4°C for 10 min. Cell pellet was resuspended in PBS, transferred to 50 ml Falcon tubes on ice, centrifuged at 2.5k rpm at 4°C for 3 min and the resulting supernatant was removed. 20 ml of chilled PBS was added to each tube and the cell pellet was resuspended by gentle pipetting with a 25 ml glass pipette. Cells were pelleted as before and the supernatant removed. The volume of packed cells in each tube was noteded and each cell pellet was resuspended by gentle pipetting in 20 ml of chilled Hypo buffer. Cells were spun down for 5 min and the supernatant removed using a pipette. Cells were resuspended in 1 ml Hypo buffer for each ml of packed cell volume (as estimated previously), by gentle pipetting and kept on ice for 10 min. PI were added to 1x, and cells were subjected to Dounce homogenisation (Sigma) using a loose pestle until most cells were lysed. Samples were transferred to 30 ml corex tubes, kept on ice for 30 min and spun at 16k rpm at 4°C for 10 min. The pellet was kept for nuclear extracts preparation (see below). To the supernatant, 0.1 M NaCl was added, mixed gently, and centrifuged in a pre-chilled Ti60 ultra centrifuge rotor head at 31k rpm (100k g), at 4°C for 60 min. Supernatant was snap frozen in liquid nitrogen and stored at –80°C to be used for immunoprecipitation and DNA replication assays.

Large scale nuclear extract (NE - Smith and Stilman, 1989): Nuclear and organelle pellet from S100 preparation of was resuspended in 1 ml A400 buffer for each ml of previously estimated packed cell volume. For immunoprecipitation experiments, phosphatase inhibitors were also added (50 mM Na-β-Glycerophosphate, 50 mM NaF, 1 mM NaOrthovanadate). The extract was incubated for 20 min at 4°C with constant agitation and then centrifuged at 16k rpm for 20 min. The supernatant was stored as nuclear extract at –80°C and the pellet was used to prepare chromatin extract.

Table 2.7: Mammalian cells used in this work

Cell line	Cell type	Growth scale	Use in this work	Ref.
HeLa S3	Human epithelial cells	4-5 litre in suspension	Large scale extracts	(Scherer and Hoogasian, 1954)
HeLa Ohio	Human epithelial cells	90 mm plates and coverslips	Immunostaining,	(Roder and Punter 1977)
293	Human fibroblasts	100 ml or 4-5 litre in suspension	Large scale extracts	(Graham et al., 1997; Harrison et al. 1977)
HT1080	Human epithelial cells	90 mm plates	Transformation and small scale IP	(Rasheed et al., 1974)
L	Mouse epithelial cells	90 mm plates and coverslips	Immunostaining	(Scherer and Hoogasian, 1954)
NIH 3T3	Mouse fibroblasts	90 mm plates and coverslips	Immunostaining	(Andersson et al., 1979)

Large scale mammalian chromatin extraction by Ammonium Sulphate: Pellet from nuclear extract preparation was resuspended in buffer B at 36 ml/10^{10} cells of original culture, by constant agitation at 4°C and the subjected to Dounce homogenisation with a loose pestle on ice. The extract volume was measured and carefully added to $(NH_4)_2SO_4$ to give a final concentration of 0.3 M with constant agitation. This caused proteins to dissociate from the DNA, making the solution highly viscous. This was relieved by controlled sonication on ice until solution was liquid again and then ultra-centrifuged at 40k rpm for 1 h. Supernatant was kept and diluted to a final concentration of 0.1 M $(NH_4)_2SO_4$ with buffer B. In order to remove genomic DNA in the extract and to avoid non-specific binding in immunoprecipitation experiments, extracts were incubated with 0.05% (w/v) Polyethylneneimine (PEI) at 4°C for 30 min with constant agitation and ultra-centrifuged at 32k rpm at 4°C for 1 hour. The resulting supernatant was stored as chromatin extract at –80°C.

Depleting S100 from PCNA: 80 µl SS1 antibody beads, preincubated with p150 1-296 wt to saturation, were equilibrated and incubated ON with 1 ml of S100 at 4°C with constant agitation. The beads were pelleted and the supernatant used for Western blot analysis and for *in vitro* DNA replication reactions. The same procedure was followed with 200 µl streptavidine coated DYNA beads (Dynal), preincubated with biotinylated p21 PBM peptide to saturation. However, PCNA was not depleted in this case even after several rounds of further incubation with fresh p21 PBM beads (see chapter 3).

Purification of proteins from mammalian extracts

DNA polymerase α/primase: To S100 extract, 20 mM Tris-Cl pH 8.9 and 250 mM KCl were added. This was then mixed 1:1 with dilution buffer and spun at 9k rpm for 20 min. The supernatant was then pre-cleared with protein G sepharose, and incubated ON with pre-equilibrated CRL1645/SZK-237-71 (α p180; Tanaka et al., 1982) beads at 4°C with constant agitation. After 3 washes with dilution buffer, Pol α/primase were eluted with elution buffer and dialysed against S100 buffer.

Co-immunoprecipitation from extracts

For large scale experiments up to 150 ml extract were incubated with 0.5–1 ml antibody beads against the relevant antigen. For small scale experiments up to 1 ml of extract was incubated with 20 μl antibody beads. Samples were incubated ON at 4˚C with constant agitation, washed 4-6 times with lysis buffer and eluted with Laemmli sample buffer (without βME) or by specific elution conditions (i.e. 5 M LiCl for SS1, 3.5 M $MgCl_2$ for SS24 etc.).

2.11 FLUORESCENCE AND IMMUNOFLUORESCENCE MICROSCOPY

Pulse labelling with BrDu

Cells were pulse labelled with 1:1000 BrDu solution (Amersham biosciences) in culture media and incubation for 10 min, followed by washes with PBS. BrDu immunostaining was done using Anti-Bromodeoxyuridine + Nuclease kit (Amersham Biosciences) following manufacturers instructions.

Preparing mammalian cells for microscopy and fluorescence analysis

Cells were seeded on coverslips coated with Poly-L-lysine and left to adhere for 4 h-ON in 6 well microtiter plates. When cells reached confluency of 20-60%, they were transfected with the appropriate DNA using SuperFect® transfection reagent (QIAGEN) according to manufacturers protocol. After 24-48 h, transfection efficiency was estimated under Axiovert10 inverted fluorescence microscope (Zeiss), using AttoArc UV light source (Zeiss) and filters sets 10 and 15 for detection of GFP and RFP, respectively. Cells were washed 3 x 2 ml for 2 min each with PBS. If triton extraction was carried out before fixation, cells were kept on ice and chilled PBS was used. Cells were extracted with triton extraction buffer on ice for 5 min, washed 3 x 2 ml for 2 min with chilled PBS, fixed for 5 min at RT with 4% paraformaldehyde diluted from a 16% stock (Electron microscopy sciences) in PBS, and then washed 3 x 2 ml for 2 min each in PBS. If cells were not treated with triton prior to fixation, extraction was carried out as described above, only at RT. For immunostaining with PC10 antibodies, cells were incubated with cold (-20˚C) Methanol for 10 min at –20˚C, to expose the epitope recognised by the antibody. Cells to be immunostained were washed 4 x 2 ml for 3 min in PBS +

1% NGS and incubated with 40 μl of primary antibody in PBS + 1% NGS for 30 min – 1 h by inverting the coverslip over the solution on a sheet of parafilm. Concentrations of primary antibodies used are as listed in Table 2.8.

Table 2.8: Primary antibodies used for immunostaining

Antibody	Source	Incubation conditions
SS1	(Smith and Stillman, 1991)	1:1000 of purified antibody at 0.6 mg/ml
Anti BrDu	Amersham Pharmacia	1:100 in nuclease solution
PC10	(Waseem and Lane, 1990)	1:100 of hybradoma supernatant

Coverslips were then returned to the 6 well microtiter plates and washed 4 x 2 ml PBS + 1% NGS for 3 min each and then incubated with secondary antibodies. Texas Red or Fitci sheep-anti-mouse (ICN) were used at 1:100-200, Alexia dye Secondary antibodies (Molecular Probes) were used at 1:5000. Coverslips were washed 2 x 2 ml for 3 min in PBS, incubated for 1 min with 0.1 μg/ml Hoechst 33258, washed again twice in PBS, rinsed with dH_2O, dried on a piece of tissue paper and then mounted over a drop of Mowiol mounting media on a microscope slide. Slides were left to dry at RT, coverslips were sealed with nail polish, and kept at 4°C.

Fluorescence microscopy

A Zeiss Axioplan microscope was used to view cells under phase 100x lens, using Zeiss AttoAre UV light source, Zeiss filter set 01 for detection of Hoechst staining, filter set 15 for detection of RFP and Texas-Red and filter set 10 for Fitci detection. Chroma 41001 filter was used for GFP detection. Photos were taken with a Hamamatsu camera and the images were stored and processed with OpenLab software (Improvision).

Confocal microscopy

A LSM510 laser scanning microscope (Zeiss) was used to take focal plain images of cells using. Images were stored and processed with accompanying software.

2.12 SV40 DNA REPLICATION AND CHROMATIN ASSEMBLY ASSAY

SV40 DNA replication and chromatin assembly reactions were prepared as shown in Table 2.9. Exact quantities of enzymes, extract and $MgCl_2$ were determined by titration with each new preparation.

Table 2.9: SV40 DNA replication and chromatin assembly reaction

Reagent	12.5 µl reaction
5 x RM (reaction mix)	2.5 µl
PSV011+	100 ng
1.2 u/µl Creatine phosphokinase	0.04 µl
[α-^{32}P] dATP	0.5-1 µCi
S100 extract	As determined by titration 3.5-6 µl
Topoisomerase I (5-15 u/µl – invitrogene)	As determined by titration 0.04-0.2 µl
$MgCl_2$	As determined by titration 0-10 mM
T Antigen	As determined by titration
rCAF1 or p150	As determined by titration
Others (such as peptides, inhibitors etc)	As determined by titration
Nuclease free dH_2O	Up to 12.5 µl

All master mix solutions and reactions were prepared on ice. The 12.5 µl reactions were incubated at 37°c for 45 min, spun down and 100 ng of H2A/H2B purified from human cells were added to each reaction which were then incubated further for 30 min at 37°C. In certain experiments, DNA replication efficiency was determined by scintillation counting 1 µl of each reaction (see below). RNA was digested by incubation with stop solution (final concentration 1x) and 1 µg boiled RNase A in a final volume of 50 µl for 15 min at 37°C. This was followed by pronase digestion (50 µg self treated pronase per reaction) for 1 h at 37°C.

DNA was extracted using QIAquick nucleotide removal kit (QIAGEN) as follows: 300 µl buffer PN was added to each reaction and transferred to a mini column. The columns were centrifuged for 1 min at 6k rpm, and the flow through was passed through the mini columns again and carefully discarded. The columns were washed with 500 µl buffer PE by centrifugation at 6k rpm for 1 min, and then centrifuged twice at 14k rpm for 2 min each, to remove residual ethanol. 35 µl of 1x ALB was pipetted to the centre of each column,

incubated at RT for 10 min and centrifuged for 2 min at 14k rpm. The eluates were analysed on a supercoiling assay agarose gel. Gels were generally run ON at 20-40 Volts, followed by incubation with 0.1 μg/ml Ethidium bromide in TAE to visualise total DNA. The gels were rinsed in dH_2O, fixed for 30 min in fixing solution and dried using a BioRad gel drier at RT for 30 min followed by 1 h at 80°C. The dried gels were either exposed to film or to a phospho-cassette.

Determination of DNA replication efficiency: prior to adding the stop solution, 1 μl of each reaction was dotted on a DE81 paper (Whatman). The paper was washed 3 x 3 min with excess of 0.5 M Na_2HPO_4, rinsed twice with dH_2O followed by a brief rinse with 95% ethanol. The paper was left to dry at RT, placed in a scintillation bottle containing 10 ml EcoScint A scintillation fluid (National Diagnistics), and the [^{32}P] count was determined using a Beckman LS6000IC scintillation counter.

2.13 ENZYMATIC REACTIONS

Phosphorylation by CDK2/cyclin A3

Recombinant CDK2/A3 complexes were a generous gift from the laboratory of Tim Hunt (Duncan, 2001). Reactions conditions were optimised (Figure 2.9), and are as follows: all reactions were prepared on ice,

5 μl freshly prepared 10 X CDK2 phosphorylation buffer

3 μg of purified protein

0.75 μl $MgCl_2$ (15 mM final)

0.5 μl 10 mM ATP

1 μl [$\partial^{32}P$] ATP (= 10 μCi)

Up to 49 μl with dH_2O

To this 1 μl of 12.5 ng/μl CDK2/A3 complex was added and reactions incubated at 30°C for 1 h.

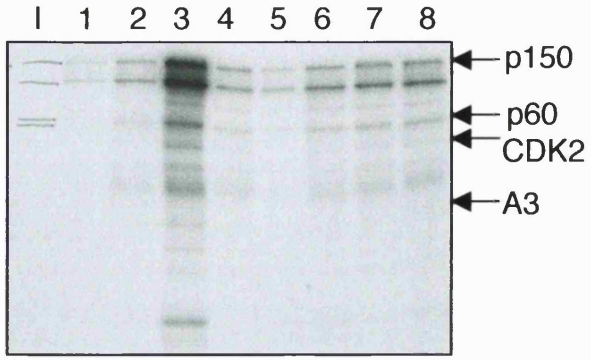

Figure 2.9: Phosphorylation of CAF1 by CDK2/A3
Optimising the phosphorylation of rCAF1 by CDK2/A3. CDK2/A3 was titrated to reactions in two different reaction buffers (1-4) and (5-8). The conditions giving best results (lane 3) are detailed in the text. Samples were detected by SDS-PAGE and autoradiography. (I) Input dephosphorylated rCAF1 and CDK2/A3 were detected by Coomassie staining prior to drying the gel, their positions on the gel are marked.

Dephosphorylation by λ protein posphatase (λ PPase)

Reactions were carried out following manufacturers protocol (Sigma). When dephosphorylating rCAF1 on beads, beads were equilibrated in the reaction buffer and the reactions performed in 2x bead volume buffer at 30°C with constant agitation (see Figure 2.7a).

2.14 WORD AND IMAGE PROCESSING AND MOLECULAR BIOLOGY COMPUTER PROGRAMMES

This thesis was created on an Apple Macintosh G3 desktop computer.

Abode photoshop: used to process figures and images.

Clustalx: used for Alignment of DNA and protein sequences.

EditView 1.0.1 (Perkin-Elmer): used for viewing DNA sequencing analysis.

Endnote 3.1: used to create a citation library.

GeneSpring 6.0 (Silicon Genetics): used to analyse micro-array data.

Microsoft excel 98: used for numerical analysis and graph production.

Microsoft powerpoint 98: used to create Figures.

Microsoft word 98: used for writing this document.

Open lab: used for creating digital microscopy images.

Strider 3.1: used for storing DNA and protein sequences.

Unicorn V3.10: used to run AKTA FPLC and analyse results.

3D Molecular Graphics: Cn3D was used for 3D illustration of PCNA.

2.15 WWW USEFUL SITES

BMERC-www.bu.edu/wdrepeat – a site dedicated to WD repeat proteins.

http://genome-www.stanford.edu/Saccharomyces/ - The *Saccharomyces* Genome Project sequence database.

http://www.affymetrix.com – The Affymetrix web site, with micro-array analysis tools.

http://www.geneontology.org/doc/GO.doc.html – General gene ontology web site.

http://www.google.com/ - A meta search engine.

http://www.ncbi.nlm.nih.gov/PubMed/ - A search site for the NCBI PubMed database of scientific publications.

http://us.expasy.org/ - proteomic server dedicated to the analysis of protein sequence and structure calculated mass as pI as well as 2D PAGE.

CHAPTER 3 – CHARACTERISATION OF THE INTERACTION BETWEEN CAF1 AND PCNA AND ITS IMPLICATIONS

3.1 INTRODUCTION

Shortly before initiating this work, CAF1 was shown to interact with PCNA using recombinant proteins (Shibahara and Stillman, 1999). The authors suggested that this interaction serves as the mechanism by which CAF1 dependent nucleosome assembly is targeted to newly synthesised DNA. To understand further the mechanism of nucleosome assembly by CAF1, I decided to characterise its interaction with PCNA in detail and determine its relevance for CAF1 function *in vivo*.

The involvement of PCNA in epigenetic inheritance was recognised initially through genetic data. A mutation of the *mus209* gene encoding PCNA in *Drosophila* causes pleiotropy of temperature-sensitive lethality, hypersensitivity to DNA damage and importantly, suppression of PEV (Henderson et al., 1994). Genetic studies in *S. cerevisiae* describe several other PCNA mutations that affect silencing at telomeres and at mating-type loci (Sharp et al., 2001; Zhang et al., 2000).

As highlighted throughout the introduction, published work in recent years has uncovered an overwhelming number of PCNA binding proteins (PBPs - see Table 3.1; Maga and Hubscher, 2003). Identification of the minimal requirement for a functional PCNA Binding Motif (PBM - see below) and the finding of an additional PCNA binding motif named the KA-box (Xu et al., 2001), alongside utilisation of proteomics (Ohta et al., 2002) suggest that more PBPs will surely be discovered in the near future.

Table 3.1: PCNA binding proteins

PBP	Function	PBM*	Main ref**
DNA replication factors			
RFC1	Large subunit of PCNA loading complex	1or 2 h $_{1}$MDIRK**FF**$_{7}$ May have non PBM PCNA binding domain (481-728) or additional PBM h $_{695}$NTSIKG**FY**$_{702}$	(Fotedar et al., 1996; Montecucco et al., 1998)
RFC2-5	Small subunits of several Clamp loading complexes	non-PBM PCNA binding domains	(Cai et al., 1997; Pan et al., 1993; Schmidt et al., 2001)
Pol δ	Main DNA replication polymerase, also functions in DNA repair	up to 3 hp125 N2: $_{129}$GVTDEGFSVCCHIHGFAPYFY$_{149}$ hp50 $_{60}$**Q**MRP**FL**$_{65}$ hp66 $_{455}$**Q**VSITG**FF**$_{462}$ contains also a KA box (N4)	(Brown and Campbell, 1993; Eissenberg et al., 1997; Tan et al., 1986; Zhang et al., 1995) (Lu et al., 2002); (Ducoux et al., 2001; Gerik et al., 1998) (Xu et al., 2001)
PDPI1	Pol δ interacting protein, stimulates polymerase activity in PCNA dependent manner. May link between cytokine activation and DNA replication	1 h $_{249}$**Q**TKVEF**P**$_{255}$	(He et al., 2001)
Pol ε	Possible DNA replication polymerase; involved in DNA repair and damage check-point	1 PBM on p59	(Eissenberg et al., 1997; Fuss and Linn, 2002; Lee et al., 1991; Maga et al., 1999)
FEN1	5'-3' exo/endonuclease, cleaves flap structures in Okazaki fragment maturation	1 h $_{337}$**Q**GRLDD**FF**$_{344}$	(Chen et al., 1996; Gomes and Burgers, 2000; Li et al., 1995; Warbrick et al., 1997)
LIG1	Ligates nicked DNA, functions in Okazaki fragment maturation and DNA repair	1 h $_{2}$**Q**RSIMS**FF**$_{9}$	(Levin et al., 1997) (Montecucco et al., 1998)

WRN/WS	A member of the RecQ family of DNA helicases, has helicase and exonuclease activities	1 (?) h $_{144}$QWKLSRDFDVK$_{154}$	(Lebel et al., 1999)
RRM3	5'-3' DNA helicase	sc $_{35}$**Q**QT**L**SS**FF**$_{42}$	(Schmidt et al., 2002)
DNA repair polymerases			
Pol ß	DNA polymerase (BER)	up to 3 h $_{136}$**Q**RIG**L**K**YF**$_{143}$ h $_{217}$**Q**LQK**V**H**F**$_{223}$ h $_{264}$**Q**YYCG**V**L**YF**$_{272}$	(Kedar et al., 2002)
Pol η	Lesion bypass DNA polymerase, functions at the replication fork and after UV irradiation	1 h $_{702}$**Q**T**L**ES**FF**$_{708}$	(Haracska et al., 2001a; Haracska et al., 2001c; Kannouche et al., 2004)
Pol ι	Lesion bypass DNA polymerase, functions at the replication fork and after UV irradiation	1 (?) h $_{540}$S**R**G**V**LS**FF**$_{547}$	(Haracska et al., 2001b; Kannouche et al., 2003)
Pol κ	Lesion bypass DNA polymerase, functions at the replication fork	1 h $_{863}$**K**HT**L**DIFFK$_{870}$	(Haracska et al., 2002)
DNA repair factors			
XPG	5'-3' exo/endonuclease, cleaves flap structures (NER)	1 h $_{990}$**Q**L**R**IDS**FF**$_{997}$	(Gary et al., 1997)
MSH2	Involved in recognition and repair of all forms of mismatches (MMR)	?	(Umar et al., 1996)
MSH3	Involved in recognition and repair of insertion/deletion mispairs (MMR)	1 h $_{21}$**Q**AV**L**SR**FF**$_{28}$	(Clark et al., 2000)
MSH6	Involved in recognition and repair of base-base mismatches and small insertion/deletion mispairs (MMR)	1 h $_{4}$**Q**ST**L**YS**FF**$_{11}$	(Clark et al., 2000; Lau and Kolodner, 2003)
MLH1	Involved in excision of the error in the newly replicated strand (MMR)	?	(Umar et al., 1996)

Apn2	Exhibits weak AP endonuclease activity, and strong 3'-5' exonuclease and 3'-phosphodiesterase activities. Functions in the repair of DNA strand breaks that have 3'-damaged termini	1 sc $_{427}$NKS**L**DS**FF**$_{434}$	(Unk et al., 2002)
UNG2	Uracil DNA glycosylase, functions at the replication fork (BER)	1 h $_{4}$**Q**KT**L**YS**FF**$_{11}$	(Otterlei et al., 1999)22 (Muller-Weeks and Caradonna, 1996)
hMYH	DNA glycosilase involved in removal of adenines or 2-hydroxyadenines misincorporated with template guanines or 7,8-dihydro-8-oxodeoxyguanines (BER)	1 h $_{512}$**Q**QVL**D**N**FF**$_{519}$	(Parker et al., 2001)
Chromatin related factors			
5-meC DNA glycosylase	Base excision by 5-meC-DNA Glycosylation (DNA demethylation)	?	(Vairapandi et al., 2000b)
DMNT1	CG methylation, functions at the replication fork	1 h $_{164}$**Q**TT**I**TS**HF**$_{172}$	(Chuang et al., 1997)
CAF1	Assembles newly synthesised H3/H4 onto nascent DNA, functions at the replication fork and during DNA repair	2	(Krawitz et al., 2002; Moggs et al., 2000; Shibahara and Stillman, 1999; Zhang et al., 2000)
HDAC1	Deacetylates histones, functions in transcription and at the replication fork	?	(Milutinovic et al., 2002)
P300	Transcription related HAT	1 (?)	(Hasan et al., 2001; Hong and Chakravarti, 2003)
Cramped (CRM)	Polycomb-group gene	?	(Yamamoto et al., 1997)
Cell cycle regulators			
p21	CDK/cyclin inhibitor, functions at the replication fork and in DNA repair	1 h $_{144}$**Q**TS**M**TD**FY**$_{151}$	(Gulbis et al., 1996; Warbrick et al., 1995)
p57	CDK/cyclin inhibitor	1 h $_{269}$GP**L**IS**DFF**$_{276}$	(Watanabe et al., 1998)

Cyclin D	G1 cyclin in mammalian cells	?	(Matsuoka et al., 1994; Xiong et al., 1992)
CDK2	S phase cyclin dependent kinase	?	(Koundrioukoff et al., 2000)
CDC25C	Cdc2 phosphoatase, plays a central role in G2 checkpoint	1 $_{319}$**Q**GLIEK**FY**$_{326}$	(Ando et al., 2001; Kawabe et al., 2002)
GADD45	Required for activation of G2/M checkpoint after treatment with DNA damaging agents	1 (?) C-terminus aa 95-165	(Chen et al., 1995; Vairapandi et al., 2000a)
MyD118	Myeloid-differentiation primary-response, related to GADD45, growth arrest and DNA-damage-inducible protein	? C-terminus aa114-156	(Vairapandi et al., 2000a; Vairapandi et al., 1996)
CR6	Related to GADD45 and MyD118, functions in negative control of cell growth	? C-terminus aa 76-159	(Azam et al., 2000)
CHL12 RFC2-5	Involved in checkpoint response and chromosome cohesion clamp loader	?	(Ohta et al., 2002)
Other			
sc pol ϕ	B type polymerase in budding yeast, may be involved in regulation of rRNA synthesis	1 (?) $_{330}$KMA**V**DES**FF**$_{338}$	(Shimizu et al., 2002)
Rad 6	Ubiquitin-conjugating enzyme (E2)	?	(Hoege et al. 2002)
Rad18	Binds single-stranded DNA and has single-stranded DNA dependent ATPase activity; forms heterodimer with Rad6p	?	(Hoege et al. 2002)
Ubc9	SUMO-conjugating enzyme	?	(Hoege et al. 2002)
Tigger/Pogo	DNA transposon	1 h $_{89}$**Q**TSLLS**YF**$_{96}$ d $_{492}$**Q**KKITD**YF**$_{499}$	(Warbrick et al., 1998)

* - Examples of the core PBM sequence from various organisms are given. Some but not all non-PBM PCNA binding domains are also listed.
? – The interaction between PCNA and the PBPhas not been characterised. h: *Homo sapiens* ; sc: *Saccharomyces cerevisiae*; d: *Drosophila melongaster.*
- Due to the wealth of literature on PCNA binding proteins, only some were quoted in this table.

Through these interactions, PCNA seems to be involved in DNA replication, DNA repair, cell cycle regulation and differentiation as well as epigenetic inheritance and chromatin structure (via interactions with proteins such as DNMT1, HDAC1, p300 and CAF1). PCNA may also be involved in sister chromatid cohesion, necessary to separate sisters precisely into daughter cells during mitosis (Skibbens et al., 1999). Therefore, PCNA seems to serve as a master molecule for chromosome processing.

Remarkably, most of the PBPs contain very similar PBMs that bind to the front side of the PCNA trimeric ring, *i.e.* the side that associates with DNA polymerases (Table 3.1). This consensus sequence is loosely defined as QXXHXXFF (Figure 3.1a) where H is a hydrophobic residue with a long side chain (leucine, isoleucine or methionine) and F is an aromatic residue (phenylalanine, tyrosine or occasionally histidine). This motif is generally followed by a sequence containing several basic residues. On PCNA, this interaction involves various sites including both domains and the Inter-Domain Connector Loop (IDCL), a protruding feature in each PCNA monomer connecting the two domains, as demonstrated by exhaustive mutational analysis as well as the structural dissection of several such interactions (Ayyagari et al., 1995; Chapados et al., 2004; Eissenberg et al., 1997; Gulbis et al., 1996; Lau et al., 2002; Matsumiya et al., 2002). Firstly, The hydrophobic and aromatic residues on PBM fit into a hydrophobic clef under the IDCL, created by the IDCL, several smaller loops, and the C-terminus of PCNA. Secondly, The side chain of the partially conserved Q in PBM, makes hydrogen bonds with residues at the C-terminus of PCNA via both its carbonyl and amino groups, stabilising the base of the C-terminus and the hydrophobic binding pocket (Chapados et al., 2004; Matsumiya et al., 2002). Thirdly, the residues preceding the Q of the PBM core make a series of ionic interactions with the highly charged region at the very C—terminus (residues 256-261) of PCNA (Chapados et al., 2004; Matsumiya et al., 2002). Additionally, in the complex of the p21 PBM peptide with PCNA, the residues immediately C-terminal to the aromatic residues of the PBM form an antiparallel β-strand with the IDCL of PCNA.

a.

hp21	143-	RQTSMTDFYHSKRRLIFSKRKP	-164
hMCMT	163-	RQTTITSHFAKGPAKRKP	-174
hFEN1	335-	TQGRLDDFFKVTGSLSSAKR	-355
hXPG	981-	TQLRIDSFFRLAQQEKEDAKR	-1009
hRFC p140	1-	MDIRKFFGVIPSGKKLVSETVKK	-24
hLigI	1-	MQRSIMSFFHPKKEGKAKK	-20
hp150	7-	PAFPVKKLIQARLPFKRLNLVPKGKA	-32
mp150	21-	PGFPVKRLIQARLPFKRLNLVPKEKV	-46
scCAC1	15-	KKKGILSFFQNTTTVKSNKFLTKEK	-39
hp150	423-	EKAEITRFFQKPKTPQAPKT	-442
mp150	420-	EKAEITRFFQKPKTPQAPKT	-439
xp150	458-	EKAEITRFFQKPKTPQAPKT	-477
scCAC1	226-	AQSRIGNFFKKLSDSNTP	-243
spCAC1	171-	QQLKLNNFFTKGVEKR	-186
hp60	229-	HDDSMKSFFRRLSFTP	-244
mp60	229-	HDDSMKSFFRRLSFT	-243
scCAC2	252-	HNETLPSFFRRCSISP	-267
spCAC2	295-	CNETLVSFFRRPAFSPD	-312

b.

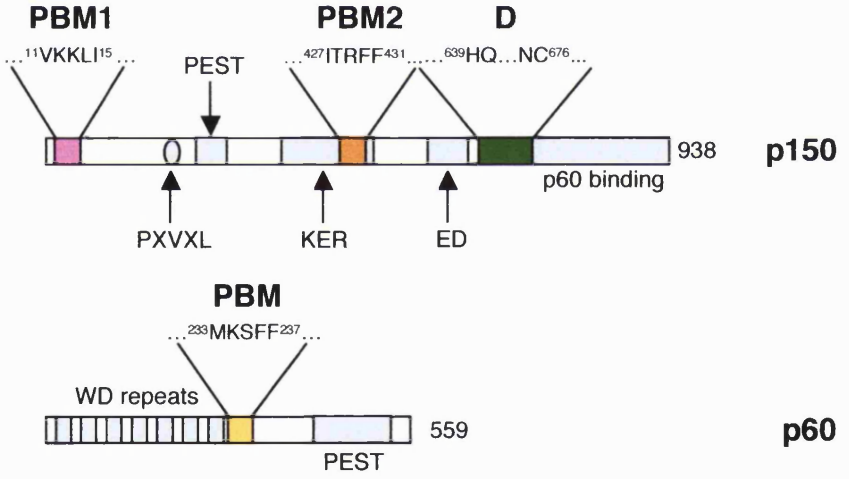

Figure 3.1: CAF1 contains three putative PCNA binding motifs

a. Alignment of PCNA binding motifs (PBMs) in known PCNA-binding proteins with the putative CAF1 PBMs identified in this study. The CAF1 PBMs are evolutionarily conserved. h: *Homo sapiens* ; m: *Mus musculus*; sc: *Saccharomyces cerevisiae*; x: *Xenopus laevis*; sp: *Schizosaccharomyces pombe*. The conserved hydrophobic and aromatic residues are highlighted in yellow, the conserved glutamine is underlined in green, and basic residues following the core PBM are underlined and in red.

b. Location of the putative PBMs in CAF1 p150 and p60 relative to other amino acid sequence motifs (see Figure 1.7).

The hydrophobic residues at the C-terminus of the p21 peptide interact with a second small hydrophobic pocket of PCNA that is formed by a number of PCNA residues, including some derived from the IDCL.

As there is a wide diversity in PBM sequences (Maga and Hubscher, 2003; Xu et al., 2001) and because several PCNA mutations affect the interaction of some but not other PBPs, it seems that the associations of different PBMs with PCNA are overlapping rather than identical.

3.2 CAF1 HAS THREE PUTATIVE PCNA BINDING MOTIFS

A search for the consensus sequence within CAF1 revealed that this complex possesses three putative PBMs, which are at least partially conserved through evolution, as indicated in Figure 3.1a. I considered these sequences as likely candidates that contribute to the interaction between CAF1 and PCNA. As represented schematically in Figure 3.1b, two of these sequences were found in p150, one at the very amino-terminus of the polypeptide (termed PBM1) and a more distal sequence within the so-called KER domain (PBM2). A PBM was also found in p60 (designated p60 PBM). This was unexpected, as the work published by Shibahara and Stillman (1999) found no direct interaction between p60 and PCNA.

3.3 CAF1 BINDS PCNA *IN VITRO*

3.3.1 CAF1 binds PCNA *in vitro* via the first 467 residues in p150

In order to examine the interaction between CAF1 and PCNA, I used a series of deletion mutants of the p150 subunit (Kaufman et al., 1995). A schematic description of these deletion mutants is presented in Figure 3.2a. The three subunits of the CAF1 complex and the p150 deletion mutants were expressed by *in vitro* transcription/translation in rabbit reticulocyte lysates (Kaufman et al., 1995). His-tagged PCNA was expressed and purified from *E. coli* using two different constructs that were generous gifts from Ulrich Hübscher and Paul Fisher. Published work (Jónsson et al., 1998; Zaika et al., 1999) has demonstrated that these tagged PCNA proteins can be used to stimulate the activity of various PBPs (pol δ, Lig1), and are therefore functional.

a.

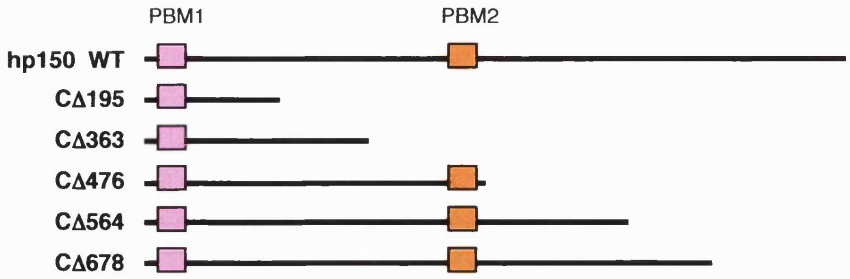

b.

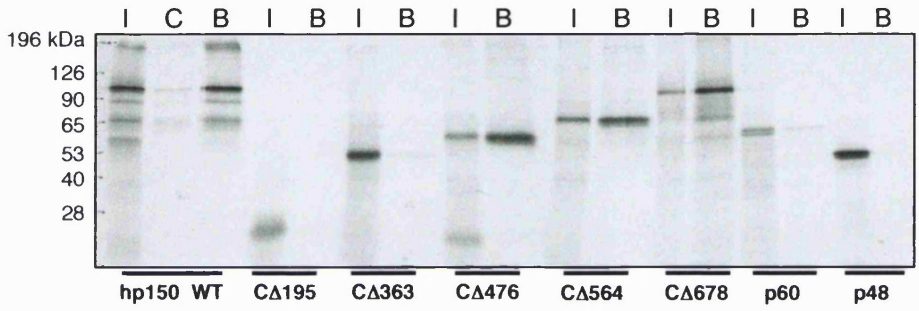

c.

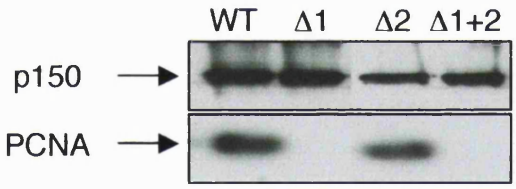

Figure 3.2: p150 binds to PCNA

a. Schematic illustration of p150 truncation mutants used in the binding assay shown in b.

b. Full length and truncated p150 were expressed by *in vitro* translation in the presence of [^{35}S] methionine, then incubated at 4°C with 20 μl Ni-NTA beads and purified C-His-PCNA in PCNA binding buffer for 2 h with constant agitation. Beads were washed and analysed by SDS-PAGE and autoradiography. (I) 50% of input. (B) Proteins bound to PCNA beads. (C) Proteins bound to control beads without PCNA.

c. Binding of p150 PBM mutants to PCNA. Full length wt and PBM mutants of p150 were expressed in *E. coli* and purified. 100 ng of each was bound to 20 μl p150 antibody (SS1) bead slurry. After washes, the beads were incubated with 1μg C-His-PCNA in 200 μl S100 buffer at 4°C for 2 h with constant agitation. Beads were washed and assayed for PCNA binding by SDS-PAGE and Western blotting. Top panel: Bound p150 detected with SS1. Bottom panel: Bound PCNA detected with PC10 antibody. (WT) wild type p150. (Δ1, Δ2, Δ1+2) p150 mutants lacking PBM1, PBM2 or both PBMs, respectively.

Recombinant PCNA bound to nickel beads was incubated with *in vitro* translated CAF1 polypeptides (see Chapter 2.8 for a detailed protocol). The results of the binding assay are presented in Figure 3.2b. In agreement with published data (Shibahara and Stillman, 1999), more than 50% of the full-length p150 bound to PCNA beads. Among the truncated forms of p150, only fragments containing the first 476 amino acids were found to bind to the PCNA beads. However, neither p60 nor p48 bound to the beads in the absence of p150. As both putative p150 PBMs are within the 1-476 fragment, it is likely that these sequences are responsible for the interaction between CAF1 and PCNA.

3.3.2 p150 binds PCNA *in vitro* via PBM1

Eukaryotic proteins expressed in rabbit reticulocyte lysates are often post-translationally modified. In addition, the reticulocyte lysate used for *in vitro* transcription/translation of CAF1 p150 contains a complex mixture of rabbit proteins and some of these proteins may facilitate or compromise the binding of p150 to PCNA. To rule out this possibility, I initially tried to purify tagged p150 from the reticulocyte lysate. However, my attempts to obtain concentrated functional proteins were unsuccessful, probably due to the low level of protein expression in this lysate (at most 200 ng/50 µl reaction according to the manufacturer). Using His-tagged PCNA bound to nickel agarose beads as the binding matrix also proved to be problematic as many proteins bind to nickel agarose beads non-specifically, resulting in unacceptably high background in protein interaction assays.

Proteins expressed in *E. coli* are generally devoid of post-translational modifications. In order to establish a biochemical system to study the interaction between p150 and PCNA, I therefore set out to develop a protocol for expression and purification of human p150 from *E. coli*.

Using *E. coli* for expression of eukaryotic proteins and specifically p150 may be troublesome for two main reasons. First, p150 is a large protein and such proteins are notoriously difficult to express in *E. coli*, often giving rise to many truncation or degradation products. Moreover, many proteins depend on

various modifications for their activity, and these pathways do not exist in bacteria. CAF1 is phosphorylated *in vivo* in a cell cycle regulated manner and in response to DNA damage induced by UV radiation (Marheineke and Krude, 1998; Martini et al., 1998). The phosphorylation of CAF1 that occurs throughout S phase contributes to its nucleosome assembly activity during DNA replication *in vitro* (Keller and Krude, 2000). In spite of this, *E. coli* expressed human p150 has been shown to have some activity *in vitro* (Quivy et al., 2001). I was therefore hopeful that, once expression was optimised, purified p150 expressed in *E. coli* would be active. After trying various strategies and many optimisation steps, a final protocol was developed for purification of p150 from *E. coli* in milligram quantities (Table 2.6).

I mutated the two putative PBMs in human p150 by deleting the five core residues of each PBM, purified the proteins and repeated the binding assay. The purified full-length p150 proteins were bound to p150 monoclonal antibody beads (SS1), which were then used in binding assays with purified His-tagged PCNA. The results of these experiments are shown in Figure 3.2c. The mutant lacking both PBMs did not bind to PCNA at all. Remarkably, deleting PBM2 had no effect on the affinity of p150 for PCNA whereas deleting PBM1 abolished the interaction. This was surprising because in my initial binding assays using p150 truncation mutants, PBM2 was suspected to be more important for PCNA binding, as fragments containing PBM1, but lacking PBM2, did not bind PCNA (Figure 3.2b, mutants CΔ195 and CΔ363).

3.3.3 p150 PBM1, but not PBM2 nor the p60 PBM, binds to PCNA

To test directly which putative PBM binds to PCNA, I used short synthetic peptides containing the different human PBM sequences. In previous studies, PBM peptides proved useful for comparing the properties of individual PBMs in binding and competition assays as well as in replication assays and immunofluorescence experiments (Chen et al., 1995a; Ducoux et al., 2001; Kedar et al., 2002; Rousseau et al., 1999). Table 3.2 lists the peptides used in this chapter. Twenty one aa long peptides (21mers) were produced either with or without a biotin group. The biotin moiety was attached to the N-terminus of the peptide via a 14mer-carbon spacer arm.

Table 3.2: PBM peptides used in this work

peptide	sequence
p21 PBM WT	CKRRQTSMTD**FY**HSKRRLIFS
p21 PBM mut	CKRRQTSMTD**AA**HSKRRLIFS
p150 PBM1 WT	CKDRPAFPVKK**LI**QARLPFKR
p150 PBM1 mut	CKDRPAFPVKK**AA**QARLPFKR
p150 PBM2 WT	CIKAEKAEITR**FF**QKPKTPQA
p150 PBM2 mut	CIKAEKAEITR**AA**QKPKTPQA
p60 PBM WT	CRMFHDDSMKS**FF**RRLSFTPD
p60 PBM mut	CRMFHDDSMKS**AA**RRLSFTPD
p150 PBM1a WT	CKDRPAFPVKK**LI**QARL**PF**KRLNLVPK
p150 PBM1 mutb	CKDRPAFPVKK**LI**QARL**AA**KR
p150 PBM1b WT	CPVKK**LI**QARL**PF**KRLNLVPK
p150 PBM1b mut	CPVKK**LI**QARL**AA**KRLNLVPK

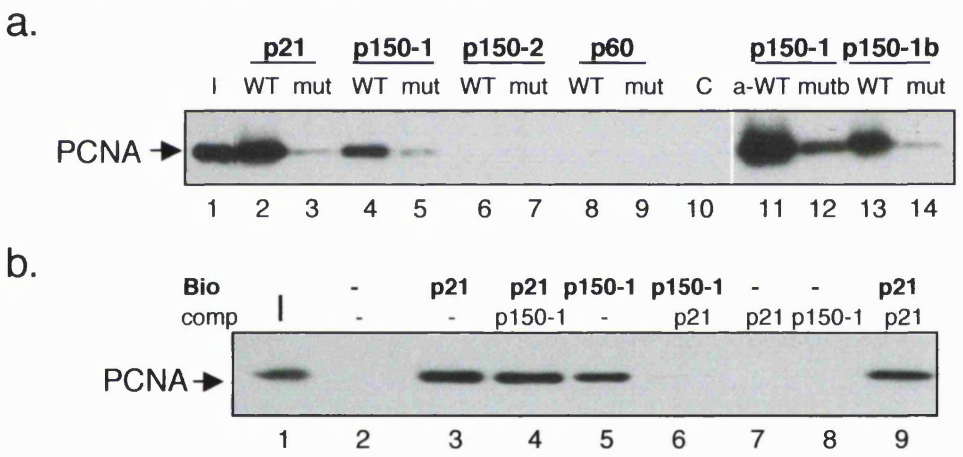

Figure 3.3: Binding of PBMs to PCNA

a. C-His-PCNA and biotinylated peptides were incubated in 200 µl S100 buffer in a 1:1 molar ratio (per PCNA monomers) for 2 h at 4°C with constant agitation. The reactions were then mixed with 10 µl streptavidin magnetic beads and incubated for 1 h. Beads were washed and assayed for PCNA binding by SDS-PAGE and Western blotting, using PC10 as primary antibody. (I) 10% of input PCNA. (p21) Bound to p21 PBM peptides. (p150-1) Bound to p150 PBM1 peptides. (p150-2) Bound to p150 PBM2 peptides. (p60) Bound to p60 PBM peptides. (WT) PCNA bound to the PBM WT peptide. (mut) PCNA bound to mutated PBM peptides (listed in Table 3.2). (C) Protein bound to streptavidin beads without any peptide.

b. p21 PBM WT peptide (p21) and p150 PBM1 WT peptide (p150-1) were used for binding and competition assays using S100 extract as a source of PCNA. Reactions were carried out as in a. The competitor peptides were not biotinylated and therefore did not bind to streptavidin beads and were discarded during the washes together with PCNA bound to them. Samples were analysed by Western blotting for PCNA with PC10 antibody. (1) 1% of input S100 extract. (2) PCNA bound to streptavidin beads in the absence of any PBM peptide. (3) PCNA bound to Bio-p21 PBM WT peptide. (4) PCNA bound to Bio-p21 PBM WT peptide in the presence of a 1:1 molar ratio of p150 PBM1 WT competitor. (5) PCNA bound to Bio-p150 PBM1 WT peptide. (6) PCNA bound to Bio-p150 PBM1 WT peptide in the presence of a 1:1 molar ratio of p21 PBM WT competitor. (7) PCNA bound to streptavidin beads in the presence of only the p21 PBM WT competitor. (8) PCNA bound to streptavidin beads in the presence of only the p150 PBM1 WT competitor. (9) PCNA bound to Bio-p21 PBM WT peptide in the presence of a 1:1 molar ratio of p21 PBM WT competitor.

As controls, I used wild type and mutant p21 peptide (p21 PBM WT, also known as p21 peptide 10, and p21 PBM mut, respectively), which were used in previous studies (Shivji et al., 1998; Warbrick et al., 1995). Biotinylated peptides and purified PCNA were incubated together in solution, and then added to streptavidin coated DYNA beads (see Chapter 2.8). After washing the beads, the bound proteins were analysed by SDS-PAGE and Western blotting, and the results are presented in Figure 3.3a. p21 PBM WT and p150 PBM1 WT both bound to PCNA (lanes 2 and 4). In agreement with published data (Warbrick et al., 1995), the interaction with the p21 peptide was greatly reduced by mutating the two aromatic residues to alanines (lane 3). The same was true for p150 PBM1 mut (lane 5). A previous report suggested that a sequence in p150 adjacent to PBM1 as defined by me was a PCNA binding motif (sequence PBM1b in Table 3.2), but no supporting data was presented (Moggs et al., 2000). To test the relevance of this sequence, the binding assay was repeated with peptides p150 PBM1a WT (a 27mer containing both putative PBMs in the centre), p150 PBM1 mutb (same as PBM1 but the proline and phenylalanine at the C-terminus of the peptide were changed to alanines), p150 PBM1b WT (the adjacent PBM is central) and p150 PBM1b mut (the proline and phenylalanine at the centre of the peptide were changed to alanines). PCNA bound strongly to the longer peptide (compare lane 11 with lane 4), suggesting that the presence of additional residues increased the affinity of the PBM peptide for PCNA. However, short peptides are often disordered in solution; the stronger binding to PCNA observed with the longer peptide may simply reflect the fact that sequences surrounding the PBM in the longer peptide are needed to stabilise the peptide conformation that binds to PCNA. Mutating the proline and phenylalanine at the edge of the peptide did not strongly affect PCNA binding (compare lane 12 with lane 4), whereas mutating them in central position decreased binding significantly (compare lanes 14 and 13). These results suggest that PBM1 is in fact more complex than thought initially, but since the initial mutation greatly reduced the affinity of full-length p150 for PCNA, I continued to work with this PBM1 mutant.

In contrast to p150 PBM1 WT, neither the p150 PBM2 WT nor the p60 PBM WT peptides bound to PCNA under any of the conditions tested (including a

gradient of salt concentration and pH, Figure 3.3a lanes 6-9 and data not shown).

The relative affinity of PBM peptides for PCNA was also tested in competition assays where the biotinylated peptide and recombinant PCNA or S100 extract containing PCNA were incubated with non-biotinylated PBM competitor peptides before adding the streptavidin coated beads. An example of the competition assays is shown in Figure 3.3b. None of the p150 peptides was able to compete PCNA off the p21 peptide (p150 PBM1 WT in lane 4 of Figure 3.3b, and data not shown), but p21 PBM WT peptide could compete PCNA off p150 PBM1 WT peptide (lane 6). Therefore, *in vitro* the affinity of the p21 PBM WT peptide to PCNA is stronger than that of the p150 PBM1 WT peptide. It is important to note that while this result is true for these *in vitro* conditions, p21 affinity to PCNA may not suffice to displace CAF1 (or CAC) from PCNA *in vivo* (see discussion below).

3.4 THE RATIONALE BEHIND PCNA MUTAGENESIS

At this point, I was confident that CAF1 is a *bona fide* PBP, which binds to PCNA via a motif that resembles the consensus PBM. While this work was in progress, a number of studies addressed the role of PCNA in promoting CAF1-dependent functions in *S. cerevisiae* (Krawitz et al., 2002; Sharp et al., 2001; Zhang et al., 2000). Zhang et al. (2000) found that the association of Cac1 with chromatin was impaired by several PCNA mutations: *pol30-6*, *pol30-8* and *pol30-79*. They also showed that these mutant PCNA proteins had reduced affinity for Cac1 *in vitro*. However, the physiological relevance of these assays is questionable because the *pol30-6* and *pol30-79* mutations do not impair the function of CAF1 in telomere silencing (Sharp et al., 2001).

In budding yeast, CAF1 is functionally redundant with both Asf1 and the four Hir proteins for the assembly of telomeric heterochromatin and for telomeric silencing (Kaufman et al., 1998; Krawitz et al., 2002). Interestingly, *pol30-8* specifically blocks the contributions of CAF1 to telomere silencing while *pol30-6* and *pol30-79* block that of Asf1 or the Hir proteins (Sharp et al., 2001). This is surprising because although the *pol30-8* mutation (residues RD 61,63 AA)

has mild sensitivity to DNA damaging agents (Ayyagari et al., 1995; Eissenberg et al., 1997; Gulbis et al., 1996; Matsumiya et al., 2002), it isn't located in a region of PCNA that makes critical contacts with PBM proteins and does not influence the interaction of PCNA with several PBPs. Current solved crystal structures suggest that most PBM proteins recognise the same surfaces of PCNA (see Chapter 3.1) and this is consistent with the fact that PBPs compete with each other *in vitro* for PCNA binding (Chen et al., 1995a; Chen et al., 1996; Jonsson et al., 1998; Warbrick et al., 1997). In my hands, a p21 peptide competed the p150 PBM1 WT off human PCNA (Figure 3.3b lane 6), arguing that both peptides bind to the same surface of PCNA. The *pol30-79* mutation (residues LI 126,128 AA) affects the IDCL of PCNA, a region that plays an important role in binding the PBM protein pol δ in yeast (Eissenberg et al., 1997) and in human cells (Jonsson et al., 1998; Jonsson et al., 1995). It is not clear why the *pol30-79* mutation has no effect on CAF1 function in yeast, but interferes with the role of Hir proteins in silencing (Sharp et al., 2001). None of the four Hir proteins contains a typical PBM and, unlike CAF1, these proteins have never been located to the replication fork. Such a connection between Hir and PCNA is clearly not conserved as the human homologue HIRA has recently been associated in replication independent nucleosome assembly (Ray-Gallet et al., 2002; Tagami et al., 2004).

Three different mutations in human PCNA that were homologous to the yeast *pol30-8*, *pol30-79* and *pol30-90* mutations were generated (Figure 3.4a). To simplify terminology, these mutants were called PCNA-8, PCNA-79 and PCNA-90 respectively. In PCNA-8, two charged residues (arginine and aspartic acid) are changed to alanines (RD 63,65 AA). The mutant PCNA-79 has two hydrophobic residues within the IDCL replaced with alanines (LI 126,128 AA), which disrupts the structure of the primary PCNA hydrophobic pocket that plays a crucial role in binding the aromatic residues of the p21 PBM (Gulbis et al., 1996). Although *pol30-90* has not been tested for silencing defects, this mutation has been demonstrated to affect the PCNA binding of several PBPs, including pol ε (Eissenberg et al., 1997). The C-terminal P252 which together with K253 are replaced by alanines in PCNA-90, is involved in the binding to the conserved PBM Q.

a.

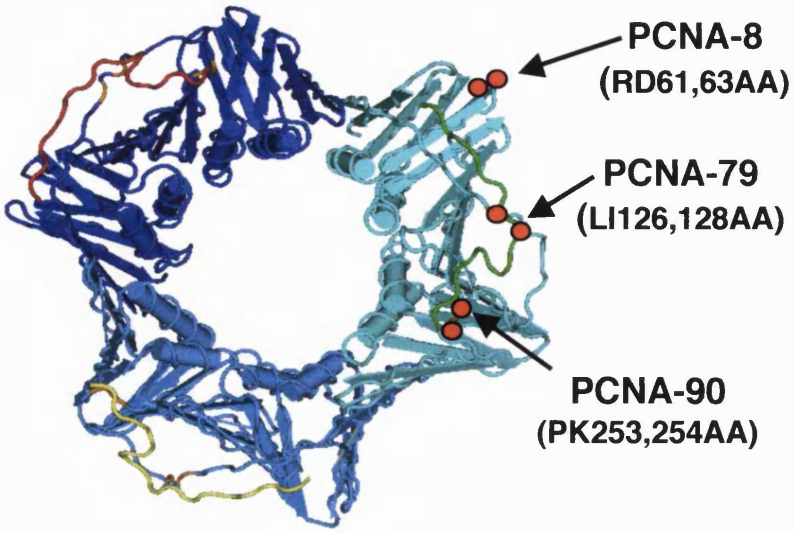
PCNA-8
(RD61,63AA)
PCNA-79
(LI126,128AA)
PCNA-90
(PK253,254AA)

b.

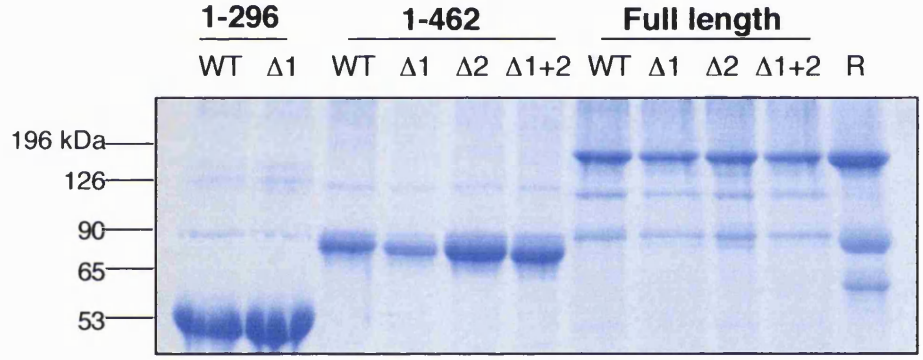
1-296
1-462
Full length
WT Δ1 WT Δ1 Δ2 Δ1+2 WT Δ1 Δ2 Δ1+2 R
196 kDa
126
90
65
53

c.

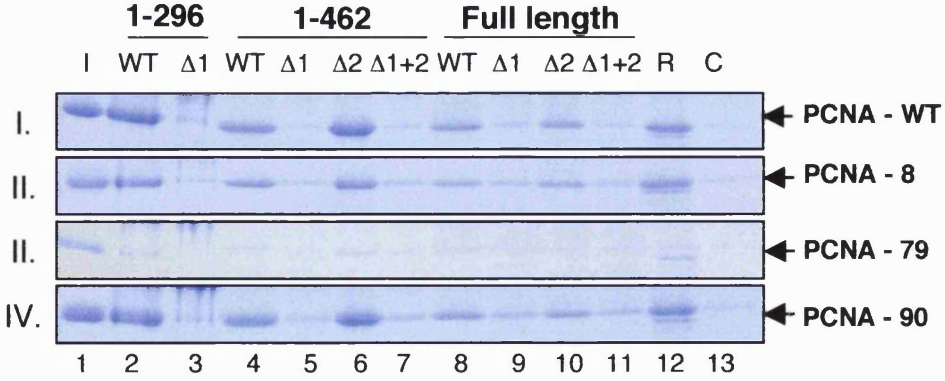
1-296
1-462
Full length
I WT Δ1 WT Δ1 Δ2 Δ1+2 WT Δ1 Δ2 Δ1+2 R C
I.
II.
II.
IV.
PCNA - WT
PCNA - 8
PCNA - 79
PCNA - 90
1 2 3 4 5 6 7 8 9 10 11 12 13

d.

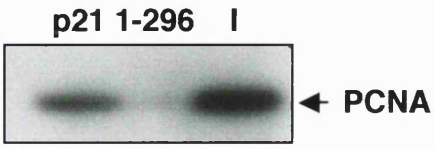
p21 1-296 I
PCNA

Figure 3.4: CAF1 p150 binds to the IDCL of PCNA via PBM1 *In vitro*

a. Sites of PCNA mutations as described in the text. In each mutant, two residues were replaced by alanines. The PCNA structure (in blue) bound by a p21 PBM peptide (in yellow red and green) is based on the coordinates from Gulbis et al. (1996).

b. Full length p150 and truncation mutants were purified from *E. coli* and analysed by SDS-PAGE and stained with Coomassie. (R) Recombinant CAF1 expressed and purified from insect cells. (WT) wild type p150. (Δ1, Δ2, Δ1+2) p150 mutants lacking PBM1, PBM2 or both PBMs, respectively.

c. Full length and fragments of p150 were bound to p150 antibody beads and used in PCNA binding assays as described in Figure 3.2c and Chapter 2.8. Similar amounts of the different PCNA mutants were incubated with the beads, except for PCNA-79 where only 1/3 was used. Samples were analysed by SDS-PAGE and stained with Coomassie. PCNA-WT (panel I), PCNA-8 (panel II), PCNA-90 (panel IV) but not PCNA-79 (panel III) bound to p150. Only p150 with intact PBM1 (lanes 2, 4, 6, 8 and) bound tightly to PCNA. (I) 40% of input PCNA. (C) SS1 beads without p150.

d. An N-terminal fragment of p150 containing PBM1 can deplete PCNA from the S100 extract. (I) input S100 extract. (1-296) Extract after incubation ON with p150 1-296 WT bound to p150 antibody beads. (p21) extract after incubation with similar amounts of p21 PBM WT peptide. PCNA was detected with PC10 antibody.

3.5 CAF1 AND PCNA INTERACT *IN VITRO* VIA PBM1 ON p150 AND HYDROPHOBIC RESIDUES ON THE PCNA IDCL

The PCNA mutants were generated and I repeated the binding assay as described in section 3.3.2 with the purified PCNA mutant proteins. In this set of experiments I included both full-length p150 and truncated forms of p150 expressed in *E. coli*. These were fragments containing either the first 296 amino acids (WT and ΔPBM1) or the first 476 amino acids of p150 (WT, ΔPBM1, ΔPBM2 and ΔPBM1+2). Figure 3.4b shows the different p150 fragments and recombinant CAF1 bound to SS1 beads and Figure 3.4c shows the results of the binding assays. As shown in Figure 3.2c, deleting PBM1 abolished the interaction with WT PCNA (panel I, lanes 3, 5 and 9) and all of the PCNA mutants (panels II-IV). This was true for fragments of p150 containing only the first 296 amino acids (lanes 2-3), the first 462 amino acids (lanes4-7) or the full-length protein (lanes 8-11). Therefore, in contrast to the results I obtained with p150 fragments expressed in rabbit reticulocyte lysates (Figure 3.2b), the first 296 amino acids of human p150 were sufficient for binding to wild type PCNA when p150 was expressed in *E. coli*. Deleting the second PBM alone had no effect on PCNA binding (lanes 6 and 10), whereas the mutant lacking both PBMs did not bind at all to PCNA (lanes 7 and 11). Recombinant CAF1 purified from insect cells was used as a positive control.

As presented in panels II and IV of Figure 3.4c PCNA-8 and PCNA-90 bound to WT p150 and to the different p150 mutants essentially like WT.
PCNA-79 was expressed less efficiently than the other PCNA mutants, but nevertheless, did purify as a ~90kDa complex (Figure 2.2a), consistent with the fact that this portion of the IDCL is not required for PCNA trimer formation (Jonsson et al., 1998). PCNA-79 trimers did not bind to any of the p150 truncations (WT or mutants) nor to the full-length p150 or CAF1 (Figure 3.4c, panel III).

Taken together, these results demonstrate that human CAF1 and PCNA interact *in vitro* via PBM1 in p150 and two hydrophobic residues in the PCNA IDCL involved in the formation of a hydrophobic cleft, which accommodates the PBM aromatic residues. To emphasise further the strong affinity of PBM1 for PCNA, Figure 3.4d demonstrates that beads containing the N-terminal region of p150 can deplete PCNA from S100 extract more efficiently than beads with similar levels of a p21 PBM peptide. p21 PBM WT dissociation constant from PCNA has been estimated between 10 nM (Chen et al., 1996) and 90 nM (Zheleva et al., 2000). This result also suggests that the binding of p150 PBM1 must be carefully regulated *in vivo* to prevent indiscriminate binding to PCNA molecules involved in processes other than nucleosome assembly.

3.6 PBM MUTATIONS DO NOT INTERFERE WITH p150 BINDING TO OTHER PROTEINS

In order to make sure that the p150 PBM mutants were only defective in their ability to bind PCNA, I tested their binding to other known p150 binding proteins, such as p60 (Kaufman et al., 1995), HP1 (α, β and γ; O'Keefe et al., 1992), and histones H3 and H4 (Shibahara et al., 2000).

Some of these results are presented in Figure 3.5. GST tagged HP1α, MOD2 (the mouse orthologue of HP1γ), H3 and H4 were expressed in *E. coli* and purified over glutathione Sepharose beads (Figure 2.6c). These beads were then used for binding assays with recombinant p150 expressed in *E. coli*. The

full-length p150 mutants lacking either or both PBMs bound to all these proteins like WT p150 (Figure 3.5a). This result also shows that post-translational modification of p150 is not necessary for binding to HP1α, MOD2, H3 or H4.

Recombinant p60 expressed in insect cells also bound to both WT and p150 PBM mutants expressed in *E. coli* (Figure 3.5b). Both WT and PBM mutants of p150 expressed in rabbit reticulocyte lysates also bound to recombinant CAF1 complexes on SS24 beads (Figure 3.5c). Because the SF9 expressed CAF1 was first purified using anti-p150 antibodies (Chapter 2.7), this suggests that WT and PBM mutants could dimerise with complexed p150 (Quivy et al., 2001).

3.7 PBM2 IS ESSENTIAL FOR CAF1 DEPENDENT NUCLEOSOME ASSEMBLY *IN VITRO*

In order to determine the relative importance of the two PBMs for CAF1 function, SV40 DNA replication and nucleosome assembly reactions were carried out as described in Chapter 2.12. In these reactions the S100 extract contains both p60 and p48 subunits of CAF1, but has undetectable levels of p150 (Kaufman et al., 1995). Therefore, nucleosome assembly can be achieved by adding p150 alone to the reactions (Figure 3.6b, lanes 2-5). In these assays, each histone octamer deposited onto plasmid DNA creates one negative superhelical turn (Simpson et al., 1985) that is protected from relaxation by DNA topoisomerases present in the S100 extract. Consequently, the degree of nucleosome assembly is assessed by the superhelical state of the radiolabelled DNA replication products after removal of proteins. Efficient nucleosome assembly results in a highly negatively supercoiled plasmid (termed 'form I') that migrates rapidly in a native agarose gel.

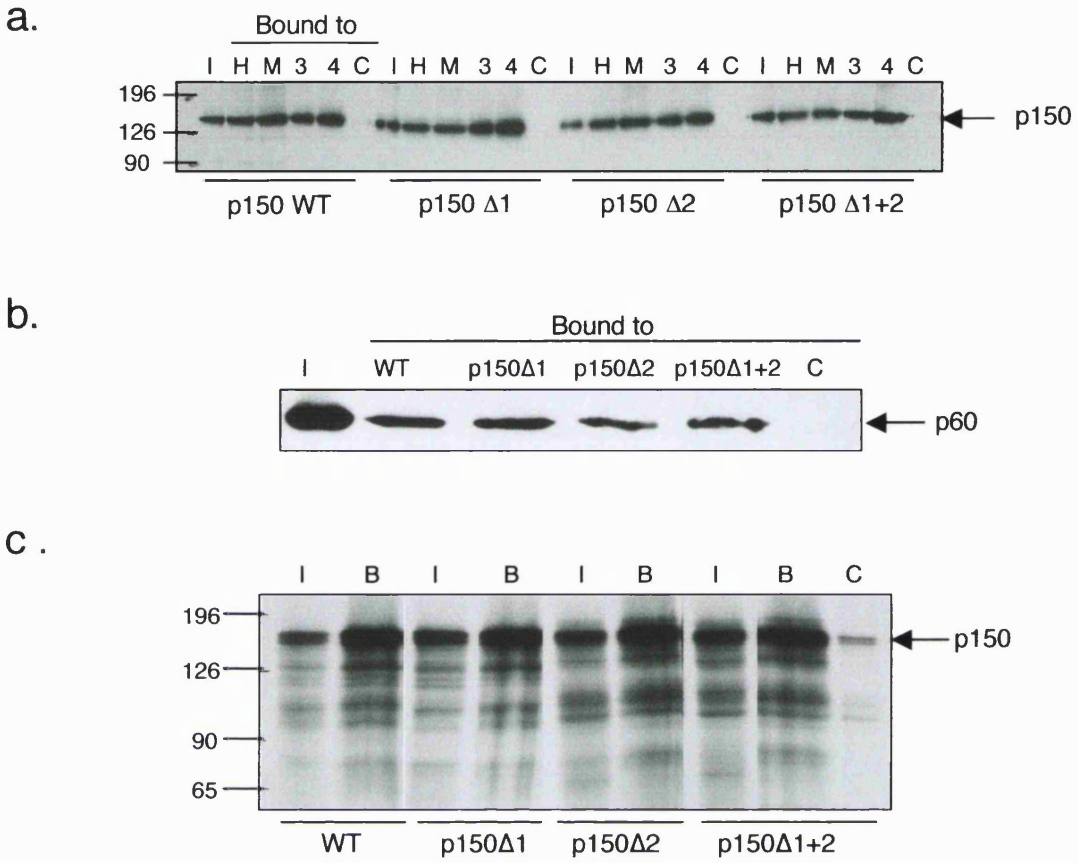

Figure 3.5: PBM mutations do not prevent p150 from interacting with other p150 target proteins

a. 100 ng of full length p150 (wt or PBM mutants) was incubated with 20 μl beads containing GST fusion proteins as shown in Figure 2.6c in 200 μl S100 buffer at 4°C ON with constant agitation. After extensive washes, bound material was analysed by SDS-PAGE and p150 binding was detected with SS1 antibody. (I) 50% input. (H) Bound to GST-HP1α. (M) Bound to GST-MOD1. (3) Bound to GST-H3 (4) Bound to GST-H4. (C) Bound to GST alone as a negative control.

b. 50 ng of recombinant p60 expressed and purified from insect cells was assayed for binding to full length p150 (wt or PBM mutants) as in Figure 3.4c. (I) Input. (C) Bound to control SS1 antibody beads. p60 was detected with SS24 antibody.

c. Full length p150 expressed by *in vitro* translation in the presence of [^{35}S] methionine were incubated with at 4°C with 20 μl SS24 beads bound by recombinant CAF1 in S100 buffer for 2h with constant agitation. Beads were washed and analysed by SDS-PAGE and autoradiography. (I) 10% of input. (B) Proteins bound to CAF1 beads. (C) Proteins bound to control beads without CAF1.

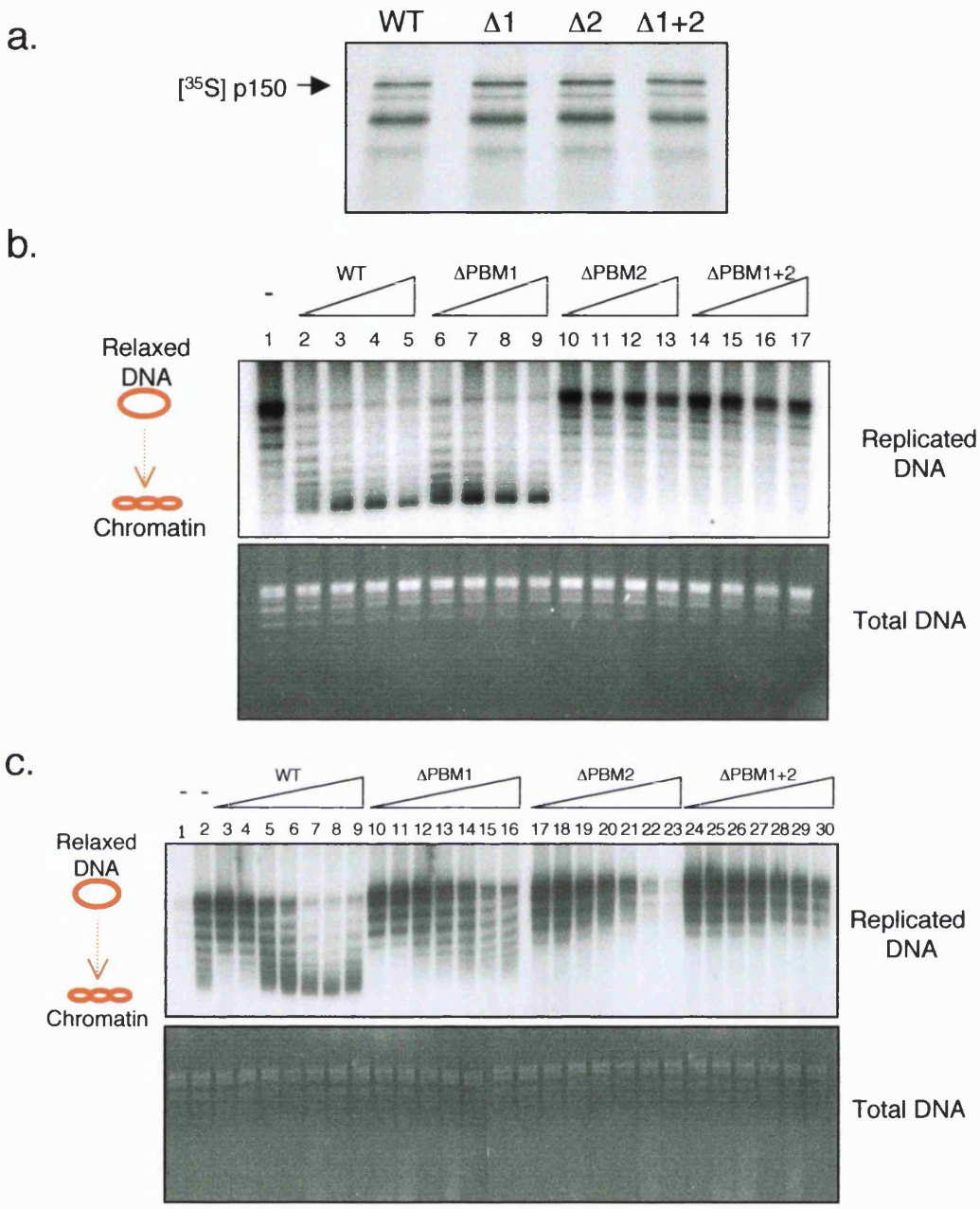

Figure 3.6: PBM2 but not PBM1, is important for nucleosome assembly during SV40 DNA replication *in vitro*

a. Recombinant human p150 (WT and PBM mutants) expressed in rabbit reticulocyte lysates. (WT) wild type p150. (Δ1, Δ2, Δ1+2) p150 mutants lacking PBM1, PBM2 or both PBMs, respectively.

b. Chromatin assembly reactions were carried out using the SV40 replication system as described in Chapter 2.12 and equal amounts of recombinant human p150 (WT and mutants) as shown in panel a. When no recombinant p150 was added to the reaction, replicated DNA remained essentially uncoiled (lane 1). Increasing amounts hp150 WT (lanes 2-5) or ΔPBM1 (lanes 6-9), but not ΔPBM2 (lanes 10-13) nor ΔPBM1+2 (lanes 14-17), efficiently promoted nucleosome assembly onto essentially all the replicated pSV011+ plasmid, but not onto the non-replicated DNA. Compare the upper panel (autoradiogram showing only the replicated DNA) with the lower panel (ethidium bromide stained gel showing all the DNA).

c. Reactions performed as in b with p150 proteins purified from *E. coli*. Incorporation of [^{32}P] dAMP was minimal without the addition of T Ag to the reactions (lane 1 - no T Ag, lane 2 - T Ag added). p150 WT (lanes 3-9), ΔPBM1 (lanes 10-16), ΔPBM2 (lanes 17-23) or ΔPBM1+2 (lanes 24-30) were titrated into the reactions.

3.7.1 p150ΔPBM2 but not p150ΔPBM1 is deficient in nucleosome assembly *in vitro*

To determine the functional importance of PBM1 and PBM2 I used the mutants described previously in SV40 replication and nucleosome assembly assays. Initially, I used human p150 expressed in rabbit reticulocyte lysates (see Figure 3.6a for an autoradiogram of the expressed proteins). Surprisingly, a titration of p150ΔPBM1 indicated that it was as efficient as WT p150 in promoting DNA replication dependent nucleosome assembly *in vitro* (Figure 3.6b lanes 6-9). In fact, this result was not entirely unexpected because deletion of the first 296 amino acids of human p150 did not interfere with its nucleosome assembly activity *in vitro* (Kaufman et al., 1995; and data not shown). It is important to note that WT p150 and p150ΔPBM1 were indistinguishable in terms of their specific activity for nucleosome assembly *in vitro*. Like WT p150, p150ΔPBM1 promoted nucleosome assembly in a replication dependent manner, as judged from the fact that only the radiolabelled DNA was supercoiled, while the bulk of input DNA that was not replicated during the course of the reactions remained topologically relaxed (Figure 3.6b lower panel). Therefore, if replication dependent nucleosome assembly *in vitro* is strictly dependent upon PCNA, the p150ΔPBM1 mutant must retain some ability to bind to PCNA in the S100 extract. In contrast, titrating p150ΔPBM2 or ΔPBM1+2 into the reaction had no effect and replicated DNA plasmids remained in relaxed form (Figure 3.6b lanes 10-17). Similar results were obtained with higher amounts of these mutants (data not shown).

More recently, Krawitz et al. (2002) presented similar data. They demonstrated that recombinant yeast CAF1 in which the PBM2 of Cac1 contained mutations of two phenylalanine residues to alanine and glycine (Cac1-20 mutant) did not support PCNA dependent nucleosome assembly in the human SV40 replication system. Moreover, they showed that in the presence of Asf1 and histone H3/H4 tetramers, Cac1-20 was able to promote replication independent nucleosome assembly. This suggests that the activity of Cac1-20,

and possibly that of p150ΔPBM2, is only impaired due to its inability to promote nucleosome assembly via PCNA, and the protein is otherwise functional.

In a set of experiments (an example of which is presented in Figure 3.6c), I titrated increasing amounts of p150 proteins expressed *E. coli* into the replication reactions (10-800 ng or 0.06-4.8 pmol). Neither p150ΔPBM2 (lanes 17-23) nor ΔPBM1+2 (lanes 24-30) promoted nucleosome assembly. Surprisingly, although the WT protein was quite potent, p150ΔPBM1 was very poor at promoting nucleosome assembly *in vitro* (compare lanes 3-9 with lanes 10-16). p150ΔPBM1 activity was not enhanced by pre-incubation with crude rabbit reticulocyte lysate, by pre-phosphorylation with CDK2 (bound to a derivative of cyclin A – see Chapter 2.13) or by binding to recombinant p60 and p48 prior to adding the complexes to the replication reaction (data not shown). Thus, the cause of the poor activity of the p150ΔPBM1 mutant expressed in *E. coli* is not clear.

3.7.2 p150ΔPBM1 binds weakly to PCNA in S100 extract

My experiments with recombinant proteins purified from *E. coli* suggest that PBM1 was more important than PBM2 for CAF1 p150 binding to PCNA (Figures 3.2c and 3.3b). However, the fact that p150ΔPBM1 did promote replication dependent nucleosome assembly argues that this mutant did retain some capacity to bind PCNA in the S100 extract. In order to test this hypothesis, WT and PBM mutants of p150 expressed in *E. coli* were incubated with S100 extracts at 4°C and the mixtures were added to p150 antibody beads. After further incubation, the beads were washed, and bound proteins were analysed by Western blotting for the presence of PCNA. As observed with purified proteins (Figure 3.2c), similar amounts of PCNA bound to WT p150 and p150ΔPBM2 (compare lanes 1 and 3 in Figure 3.7a). However, under less stringent washing conditions, a small amount of PCNA from the S100 bound to p150ΔPBM1 (lane 2). This binding was reduced compared to the level observed with WT p150 or p150ΔPBM2, and was specific for binding

in S100, since it was not seen with purified recombinant proteins (see Figure 3.2c). However, this low level of PCNA binding was mediated by PBM2 because PCNA did not bind at all to the p150ΔPBM1+2 mutant under the same low stringency washing conditions (compare lane 4 with background binding in lane 5 in Figure 3.7a). Thus, the replication dependent nucleosome assembly activity of p150 appeared to be driven by a low level of PCNA binding mediated by PBM2. Surprisingly, the stronger binding to PCNA observed when PBM1 was intact apparently did not contribute to nucleosome assembly *in vitro*.

These results raise the important issue of why some PCNA binding via p150PBM2 was observed in the S100 extract but not with purified proteins. A trivial explanation may be that the 6-histidine tag present at the C-terminus of recombinant PCNA occluded its binding to p150 via PBM2, while the absence of tag in the PCNA present in the S100 extract allowed some degree of binding. This was unlikely because PCNA with an N-terminal 6-histidine tag also failed to bind p150 via PBM2 (data not shown). In addition, PCNA with a C-terminal 6-histidine tag clearly bound to p150 via PBM1 (Figure 3.4) and has been shown to bind and stimulate the activity of a number of other PBM proteins (Jonsson et al., 1998). Consistent with this, I found that PCNA with a C-terminal 6-histidine tag was able to restore DNA replication to a PCNA-depleted S100 extract (Figure 3.7b). Therefore, it was more likely that a component of the S100 extract, which was absent in the experiments performed with purified proteins, was responsible for a low level PCNA binding to p150 PBM2. One possibility was that the interaction between p150 PBM2 and PCNA was stabilised by the presence of the other subunits of CAF1 in the S100 extract. Although this possibility was not exhaustively examined, pre-binding of purified p60 to p150ΔPBM2 expressed in *E. coli* did not increase binding to purified PCNA. Alternatively, the binding of PCNA to p150ΔPBM1 may be driven by post-translational modification of p150 or PCNA during incubation in the S100 extract or by modification of PCNA prior to incubation. In this case, the low level of PCNA binding via PBM2 would involve a sub-population of the PCNA molecules in the extract. Because phosphorylation of

CAF1 by S phase CDK has been shown to promote nucleosome assembly (Keller and Krude, 2000), this modification was an obvious candidate for stabilising the interaction between CAF1 and PCNA.

a.

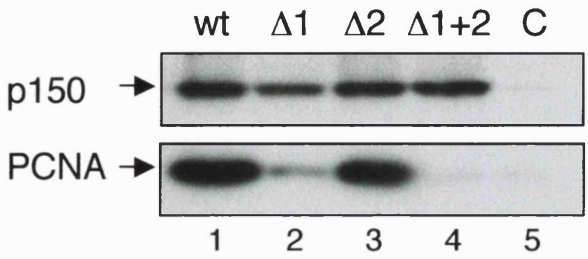

b.

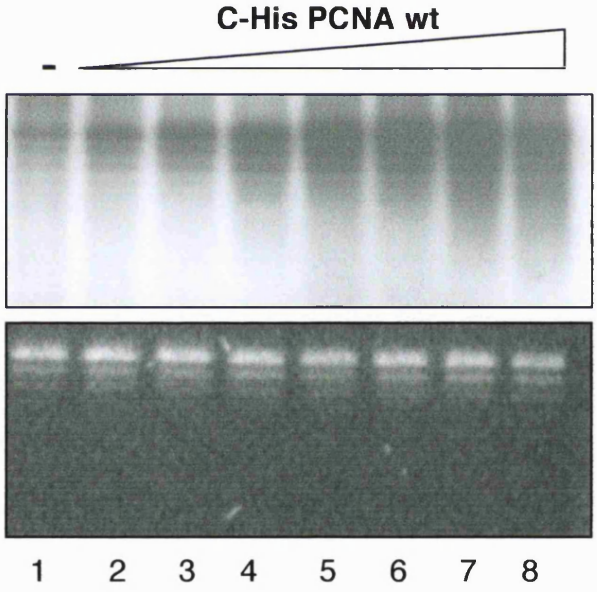

Figure 3.7: PCNA in the S100 extract binds weakly to p150ΔPBM1

a. Binding assays were carried out as in Figure 3.2c, with the exception that instead of recombinant PCNA, beads were incubated with 50 μl S100 extract. Note that there is residual binding of PCNA (as detected by PC10) to p150 ΔPBM1. (C) Control without p150. **b.** S100 extract depleted of PCNA by p150 1-296 WT as in Figure 3.4d, was used for replication reaction, where 5-400 ng C-His-PCNA were titrated into the reactions. the recombinant PCNA could compliment the extract and DNA replication levels increased.

3.8 THE INTERACTION OF P150 WITH PCNA DOES NOT SEEM TO DEPEND UPON ITS PHOSPHORYLATION STATE

Human CAF1 p60 and p150 are both phosphorylated *in vivo* (Smith and Stillman, 1991) and p60 phosphorylation is strongly cell cycle regulated (Marheineke and Krude, 1998). Interestingly, unlike at other stages of the cell cycle, the CAF1 protein is not associated tightly with chromatin in mitosis (Marheineke and Krude, 1998). The mitotic form of CAF1 contains hyperphosphorylated p60 and is inactive in nucleosome assembly *in vitro*, but can be activated by treatment with lambda phosphatase, arguing that mitotic phosphorylation inhibits CAF1 activity (Keller and Krude, 2000). The p60 subunit of CAF1 can be phosphorylated directly by the S phase kinases Cyclin A/CDK2 and Cyclin E/CDK2, but also by the mitotic kinase Cyclin B1/CDK2 (Keller and Krude, 2000). Addition of either the protein phosphatase inhibitor okadaic acid or the CDK inhibitor roscovitine to the replication reactions modulated the degree of p60 phosphorylation and reduced nucleosome assembly by CAF1, arguing that reversible CDK phosphorylation and dephosphorylation are both important for optimal CAF1 activity *in vitro* (Keller and Krude, 2000).

Furthermore, a number of proteins with PBMs undergo phosphorylation by CDKs and possibly other protein kinases (for review see Henneke et al., 2003a; for p21 - Scott et al., 2000; Lig1 - Koundrioukoff et al., 2000; Rossi et al., 1999; FEN1 - Henneke et al., 2003b; RFC - Salles-Passador et al., 2003). Phosphorylation of these proteins generally inhibits their binding to PCNA. In some cases, the sites of phosphorylation are very remote from the PBMs in the primary amino acid sequence (Henneke et al., 2003b; Salles-Passador et al., 2003), suggesting that phosphorylation can inhibit PCNA binding through conformational changes in the target proteins. CDK binding to the C-terminus of PCNA has been proposed to facilitate the phosphorylation of PBM proteins such as Lig1 or RFC (Koundrioukoff et al., 2000).

a.

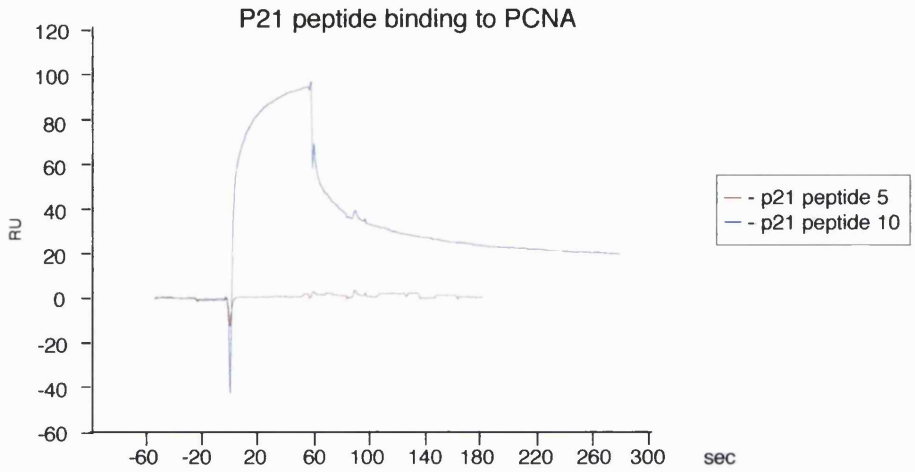
P21 peptide binding to PCNA
RU
120
100
80
60
40
20
0
-20
-40
-60
-60 -20 20 60 100 140 180 220 260 300
sec
- p21 peptide 5
- p21 peptide 10

b.

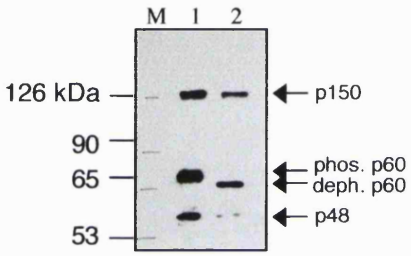
M 1 2
126 kDa
90
65
53
p150
phos. p60
deph. p60
p48

c.

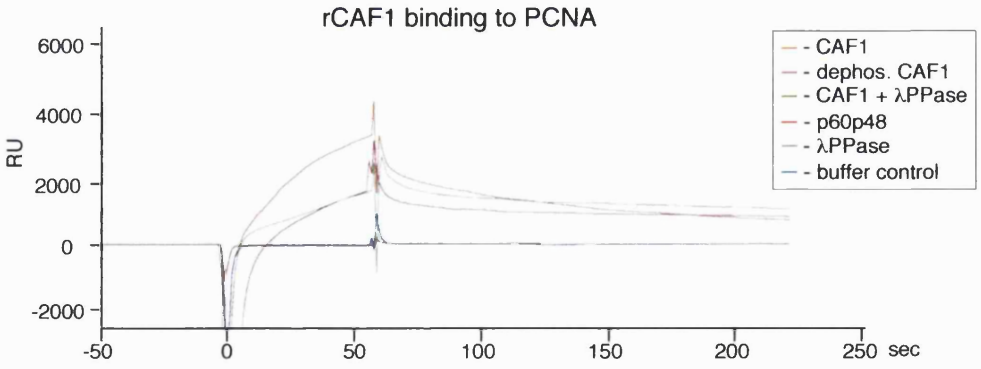
rCAF1 binding to PCNA
RU
6000
4000
2000
0
-2000
-50 0 50 100 150 200 250 sec
- CAF1
- dephos. CAF1
- CAF1 + λPPase
- p60p48
- λPPase
- buffer control

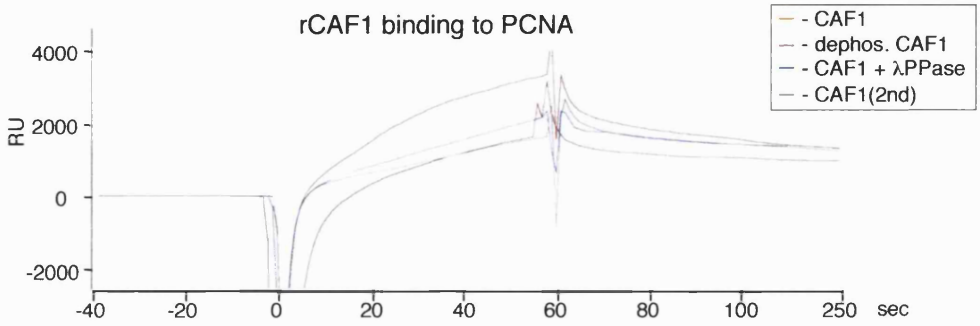
rCAF1 binding to PCNA
RU
4000
2000
0
-2000
-40 -20 0 20 40 60 80 100 250 sec
- CAF1
- dephos. CAF1
- CAF1 + λPPase
- CAF1(2nd)

Figure 3.8: CAF1 phosphorylation does not seem to affect PCNA binding *in vitro*

a. 2000 Reflectance Units (RU) of recombinant PCNA were covalently bound to a CM5 surface plasmon chip. p21 PBM WT peptide (peptide 10) and a peptide of a separate region in p21 (peptide 5 - see table 2.5) were used at 5 μg/ml as positive and negative control analytes for binding to PCNA, respectively. The X-axis shows time in seconds. The Y-axis shows the corrected change in UV absorbance on the chip, represented by RU. Injection was initiated at Time 0, and lasted for 1 min. The graphs between 0 and 60 sec therefore represent a binding curve of injected analyte (peptides) as a function of time whereas the curve following the end of injection shows the dissociation of the analyte with a constant flow of buffer. Almost 100 units of peptide 10 bound to PCNA, 20 of which remained tightly bound to the chip. As expected peptide 5 did not bind PCNA at all. In between runs, the chip was regenerated, in order to wash off any remaining analyte.

b. Recombinant CAF1 was purified from SF9 cells (lane 1) and dephosphorylated (lane 2) as described in Chapter 2.7. Samples were run on a 10% SDS-PAGE and analysed by Western blotting. Detection was with SS1, SS24 and 15G12 for p150, p60 and p48, respectively.

c. Two examples of PCNA-binding experiments using surface plasmon resonance are shown, conditions are as in b. Reactions were carried out as described in a. 10 μg/ml recombinant CAF1 (CAF1) and dephosphorylated CAF1 (dephos. CAF1) were used. The binding reactions were carried out several times and surface plasmon chips were regenerated after each run. The injections were done in an ascending order as shown in the legend box. All the procedures were carried out at 4°C. The lower binding efficiency of this sample (after CAF1 and dephos. CAF1) is due to swelling of the cell surface as it is being used causing a distortion in UV absorption or due to incomplete regeneration of the chip. The binding of CAF1 in a second attempt (at the lower panel) also seems poorer than the first one. Taking this into consideration, both forms of CAF1 appear to bind similarly to the PCNA. p60p48 complexes (purified from SF9 cells), λ PPase or buffer alone did not bind to PCNA on the chip.

To test whether the phosphorylation of CAF1 changes its affinity for PCNA, I initially set up protein-protein interaction assays using a BIAcore system. Recombinant PCNA without a tag (2000 Reflectance Units, RU) was covalently immobilised via amino groups as ligand onto a CarboxyMethylated dextran matrix sensor chip (CM5). Two peptide samples were then used as analytes: p21 peptide 10 (similar to p21 PBM WT), which contains the p21 PBM was used as a positive control for PCNA binding, and p21 peptide 5, which is derived from a different part of p21 was used as negative control (Shivji et al., 1998; Warbrick et al., 1995). As expected the PBM peptide containing the PBM bound to the plasmon surface, whereas the unrelated p21 peptide did not (Figure 3.8a). This procedure was repeated with recombinant CAF1 purified from insect cells as analyte. When expressed in SF9 cells, the p60 subunit of CAF1 is extensively phosphorylated, and treatment of recombinant CAF1 with λ Protein Phosphatase (λ PPase) resulted in CAF1 dephosphorylation as seen by an increase in the mobility of p60 (compare lanes 1 and 2 in Figure 3.8b). By alternating the use of phosphorylated and

dephosphorylated forms of purified CAF1 and regenerating the chip after each analysis, I was able to demonstrate that there was no significant difference in the affinity for PCNA of these two forms of the CAF1 protein. This can be seen in Figure 3.8c, which shows a comparison of the association and dissociation curves for dephosphorylated and untreated recombinant CAF1.

These assays did not rule out the possibility that p150 phosphorylation may influence its binding to PCNA because the treatment with λ PPase did not affect the mobility of p150 (Figure 3.8c). However, further analysis using cyclin A3/CDK2 and radiolabelled ATP prior to dephosphorylation under similar conditions demonstrated that λ PPase treatment removed all traces of *in vitro* phosphorylation (see below). These experiments were performed before I developed an easy method to express p150 in *E. coli* and prior to the demonstration that CAF1 could be phosphorylated *in vitro* by CDK2 (Keller and Krude, 2000).

The sites of CAF1 phosphorylation are not known. Both WT p150 and the PBM mutants were readily phosphorylated by cyclin A3/CDK2 *in vitro* (Figure 3.9a), showing that the PBM sequences were not needed for p150 phosphorylation by CDK. However, due to technical difficulties, I could not check the effect of phosphorylation on their affinity for PCNA *in vitro*. Significantly, adding pre-phosphorylated p150 to the replication reactions did not affect its ability to function in nucleosome assembly (data not shown).

To address this issue indirectly, *E. coli* expressed full-length p150 was incubated with S100 in the presence or absence of 0.5 or 2 mM roscovitine, a cyclin-dependent kinase inhibitor (Keller and Krude, 2000). Reactions were incubated with p150 antibody beads (SS1), the beads were washed and analysed by Western blotting to detect PCNA and p150. These reactions were incubated at 4°C or 37°C prior to adding the beads to determine whether enzymatic activity was needed. Additionally, beads derived from reactions performed in the absence of roscovitine were further incubated at 30°C with λ

PPase in the presence or absence of 2 μM Na-orthovanadate as phosphatase inhibitor. None of the conditions tested resulted in any significant difference in PCNA binding between reactions that were carried out in the presence or absence of roscovitine, nor between reactions incubated at 4°C or 37°C. Binding of PCNA was reduced in reactions that were further incubated with λ PPase, but this was also true of reactions carried out in the presence of Na-orthovanadate (Figure 3.9b for wt and data not shown). This implies that the reduction in PCNA binding was due to the additional incubation and washing steps rather than the dephosphorylation of p150. Controls performed with recombinant CAF1 phosphorylated by CDK2 in the presence of [^{32}P]-labelled ATP, demonstrated that λ PPase was able to dephosphorylate p150 bound to antibody beads and this dephosphorylation was completely inhibited by Na-orthovanadate (Figure 3.9c).

Although my results suggest that phosphorylation does not strongly alter the affinity of p150 for PCNA *in vitro,* I was not able to demonstrate that changes in p150 phosphorylation did take place in the S100 extract under the conditions used. I did not perform these experiments with the CAF1 heterotrimer or with CAC and I have only tested the binding of p150 to PCNA in solution. It is possible that p60 phosphorylation may alter the binding of intact CAF1 to PCNA or that CAF1 phosphorylation only affects its interaction with PCNA loaded onto DNA. A more exhaustive study is needed to rule out these possibilities. These results therefore do not exclude the possibility that phosphorylation of p150 or p60 may modulate the interaction of CAF1 and PCNA *in vivo.*

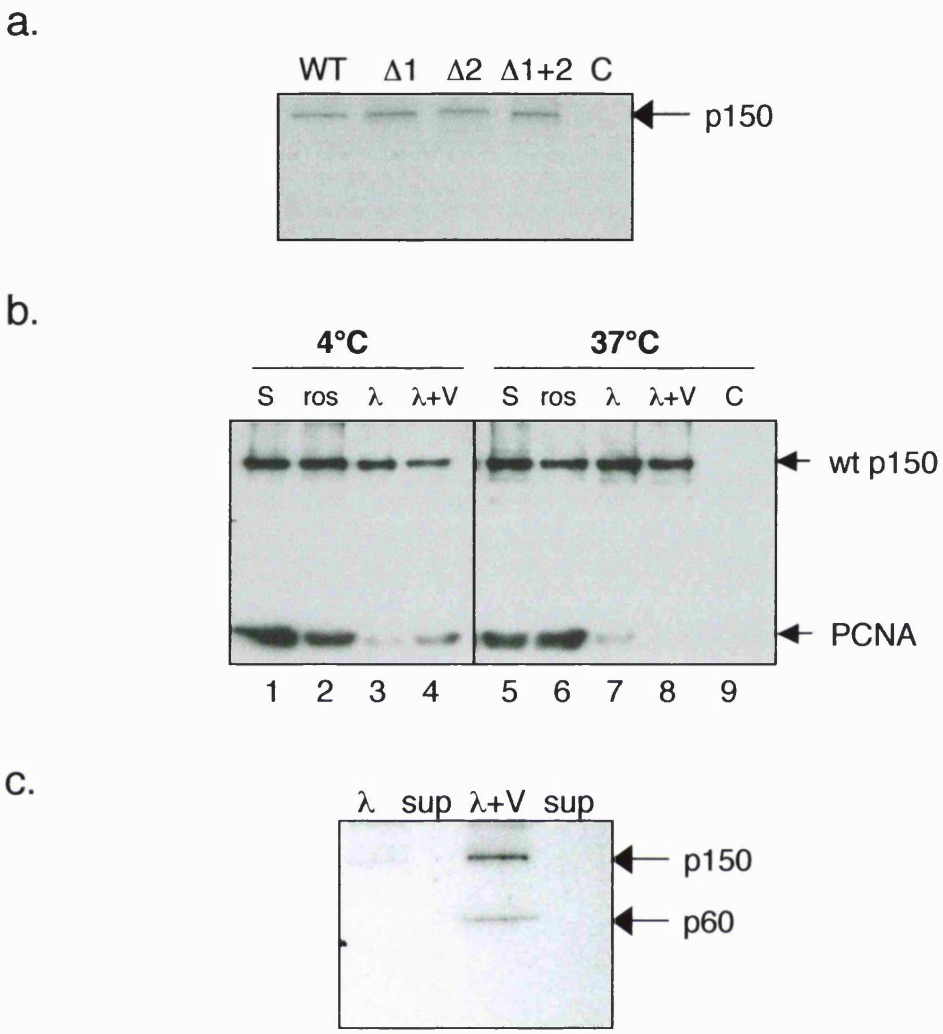

Figure 3.9: Phosphorylation of p150 does not appear to be involved in PCNA binding

a. Wild type and mutants p150 expressed and purified from *E. coli* were phosphorylated by recombinant CDK2/A3 using [^{32}P] labelled ATP (see Chapter 2.13). CDK2/A3 phosphorylated all three PBM mutants to similar level as wild type p150. (WT) wild type p150. (Δ1, Δ2, Δ1+2) p150 mutants lacking PBM1, PBM2 or both PBMs, respectively. (C) control reaction carried out in the presence of 2 mM Roscovitin.

b. Binding of PCNA from S100 extract to wild type p150 at 4°C and 37°C. 50 μl S100 were incubated for 1 h with 100 ng p150 in presence (ros) or absence (S) of roscovitin to identify the possible affect of CKD inhibition on this binding (lanes 1-2 and 5-6). Reactions were then added to SS1 antibody beads and incubated for 2 h at 4°C with constant agitation. Reactions 3-4 and 7-8 were further incubated with λ PPase in the presence (λ + V) or absence (λ) of 2 μM Na-orthovanadate, to test the effect of dephosphorylation on p150 affinity to PCNA. Samples were analysed by SDS-PAGE and Western blotting for the association of p150 and PCNA to antibody beads. SS1 and PC10 were used for detection of p150 and PCNA, respectively. (C) Control assay for binding by excluding p150 from the assay.

c. λ PPase can dephosphorylate p150 bound to SS1 beads. CAF1 was phosphorylated as in Figure a, and bound to SS1 antibody beads. Treatment with λ PPase was as in b. Control in the presence of 2 μM Na-orthovanadate shows that dephosphorylation is inhibited by this substance. Note that both p150 and p60 were phosphorylated in this reaction. In the absence of Na-orthovanadate all radiolabelled phosphate is removed from CAF1. Supernatant of the dephosphorylation reactions (sup) contained no phosphorylated CAF1, demonstrating that loss of radioactive signal was not due to CAF1 dissociation from the beads.

3.9 TARGETING CAF1 TO DNA REPLICATION *IN VIVO*

Two different functions, which are not mutually exclusive, have been proposed for PBMs. The first function is simply to provide a docking mechanism to tether PBM proteins to PCNA. In this way, the PCNA sliding clamp could serve as an auxiliary factor not only for DNA polymerases but also for many other PBM proteins (Maga and Hubscher, 2003). The second proposed function of PBMs is to act as replication factory targeting sequences (Montecucco et al., 1995). Many lines of evidence exist to support both functions. For example, DNA pol δ binding to PCNA via a canonical PBM in its p66 subunit is crucial for processive DNA synthesis *in vitro* (Ducoux et al., 2001; Reynolds et al., 2000) and DNA replication *in vivo* (Reynolds et al., 2000). Similarly, p21 can no longer inhibit DNA replication when the core hydrophobic residues within the PBM are mutated to alanines (Warbrick et al., 1995). Interestingly, the *in vitro* stimulation of the nucleases FEN1 and Apn2 by PCNA is independent of their ability to bind PCNA via their PBMs (Frank et al., 2001; Gomes and Burgers, 2000; Unk et al., 2002). However, a *S. cerevisiae* strain with a mutated FEN1 PBM has similar, but milder phenotypes than those observed in a null mutant strain, showing that the PBM contributes to FEN1 function *in vivo* (Gomes and Burgers, 2000). In addition, short PBM peptides derived from DNMT1 (Chuang et al., 1997), RFC p140 and Lig1 (Cardoso et al., 1997; Montecucco et al., 1995) are all sufficient for targeting heterologous proteins to DNA replication foci when expressed as fusion proteins.

3.9.1 PBM1 and PBM2 synergistically contribute to the targeting of p150 to DNA replication foci *in vivo*

In mammalian cells, CAF1 is targeted to replication foci throughout S phase, showing a staining pattern that coincides with that of PCNA or sites of incorporation of the DNA precursor bromodeoxyuridine (BrDU) (Krude, 1995; Murzina et al., 1999; Shibahara and Stillman, 1999; Taddei et al., 1999; Figure 1.3). To examine whether the PBMs serve as targeting sequences to direct CAF1 to DNA replication foci, I transiently transfected mouse (NIH 3T3 and L) cells with constructs expressing EGFP-mouse p150 fusion proteins from the CMV promoter (as described by Murzina et al., 1999), and followed their

localisation using both conventional and confocal fluorescence microscopy. Identification of replication foci was achieved by immunostaining endogenous PCNA, co-transfecting cells with an RFP-PCNA construct and following the red staining or by pulse labeling with BrDU prior to fixation and immunostaining the incorporated BrDU.

Unlike human cells, mouse cells have extensive T/A rich repetitive DNA that is packaged into pericentric heterochromatin and binds avidly to the flurorescent DNA dyes Hoechst 33258 or DAPI. Because heterochromatin is known to replicate late during S phase (O'Keefe et al., 1992), it is easy to distinguish the different stages of S phase (early-, mid- or late-S phase) using mouse cells.

Outside of S phase, p150 binds to HP1 proteins and is targeted to pericentric heterochromatin via this interaction (Murzina et al., 1999). Curiously, I found that p150 mutants defective in PCNA binding and targeting to replication foci (see below) were concentrated in pericentric heterochromatin, presumably due to their interaction with HP1. Figure 3.11d shows that transfected EGFP-mp150, this time tagged with flag, still binds to HP1 *in vivo*. The implications of this observation will be discussed later. However, this PBM-independent localisation of p150 to heterochromatin makes it impossible to score for mis-localisation of p150 PBM mutants during heterochromatin replication in late-S phase (O'Keefe et al., 1992). At that stage of S phase, CAF1 can be targeted to heterochromatin replication foci via both PBM-dependent and PBM-independent mechanisms. Consequently, I scored for p150 mis-localisation only during early- and mid-S phase, as determined from the immunostaining pattern of PCNA or BrDU.

Examples of immunofluorescence images from these experiments are presented in Figure 3.10. In early- or mid-S phase, wild type GFP-p150 is confined to DNA replication foci and does not localise to pericentric heterochromatin (Murzina et al., 1999). In contrast, cells expressing EGFP-p150 with PBM deletions showed three different phenotypes. Some cells in early- and mid-S phase had staining patterns very similar to that of WT p150, in which the GFP signal co-localised with the immunostaining of PCNA (compare image c with b and a, and image l with k and j in Figure 3.10).

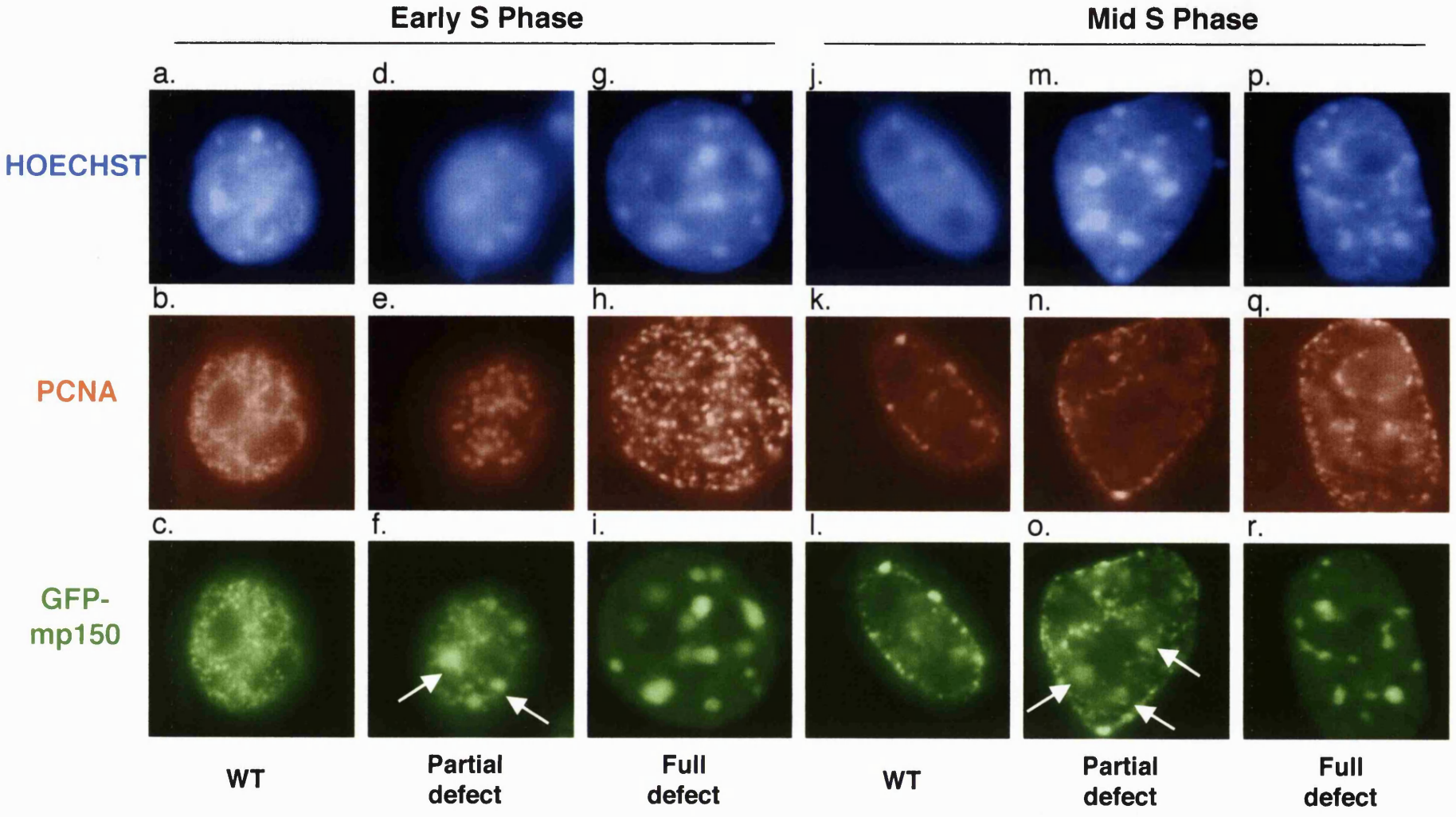
Early S Phase
Mid S Phase
a.
d.
g.
j.
m.
p.
HOECHST
b.
e.
h.
k.
n.
q.
PCNA
c.
f.
i.
l.
o.
r.
GFP-
mp150
WT
Partial
defect
Full
defect
WT
Partial
defect
Full
defect

Figure 3.10: Deletion of PBM1 and PBM2 interferes with localisation of GFP-p150 during early- and mid-S phase

Mouse NIH 3T3 cells were transiently transfected with a plasmid expressing mouse p150 (wild type or mutants) conjugated to EGFP. After 48 h cells were fixed, extracted and stained as described in Chapter 2.11. GFP-wild type p150 localised at replication foci similarly to endogenous p150, during early- (a,b,c) mid- (j,k,l) and late-S phase (data not shown). GFP-p150 mutants localised to replication foci like wild type p150 in some cells, but were mis-targeted at others to pericentric heterochromatin. In some cells mutant GFP-p150 co-localised with both replication foci and heterochromatin in early- (d,e,f) or mid- (m,n,o) S phase. White arrows show GFP-p150 co-localising with heterochromatin. In other cells the mutant GFP-p150 co-localised only with heterochromatin even when the PCNA staining was that of early- (g,h,i) or mid- (p,q,r) S phase. During late S phase both wild type GFP-p150 and the different mutants co-localised with heterochromatin, which is being replicated at this phase (data not shown).

Another fraction of transfected cells exhibited a complex phenotype where some of the EGFP-p150 went to replication foci (as seen by comparison with the PCNA staining - compare image f with e, and o with n), whereas the rest was localised to pericentric heterochromatin (as determined by comparison with the Hoechst staining – white arrows in images f and o). This phenotype represented a partial defect in targeting to replication foci. In a very small subset of cells, the GFP signal co-localised with that of heterochromatin, even though PCNA staining was that of early- or mid-S phase (compare images i with g and h and r with p and q, respectively).

These different phenotypes were not related to the level of expression, since cells with both weak and strong GFP signals showed all three phenotypes. Similar observations were made when cells were extracted with the non-ionic detergent Triton X-100 before formaldehyde fixation. Thus, the GFP-p150 molecules that were localised to both replication foci and heterochromatin were resistant to detergent extraction. Confocal microscopy, in which images of precise focal planes are taken, was used to ensure that GFP-p150 was in fact mis-targeted and that the observed phenotypes were not due to the accumulation of signals derived from different focal planes in the nucleus (Figure 3.11a-c).

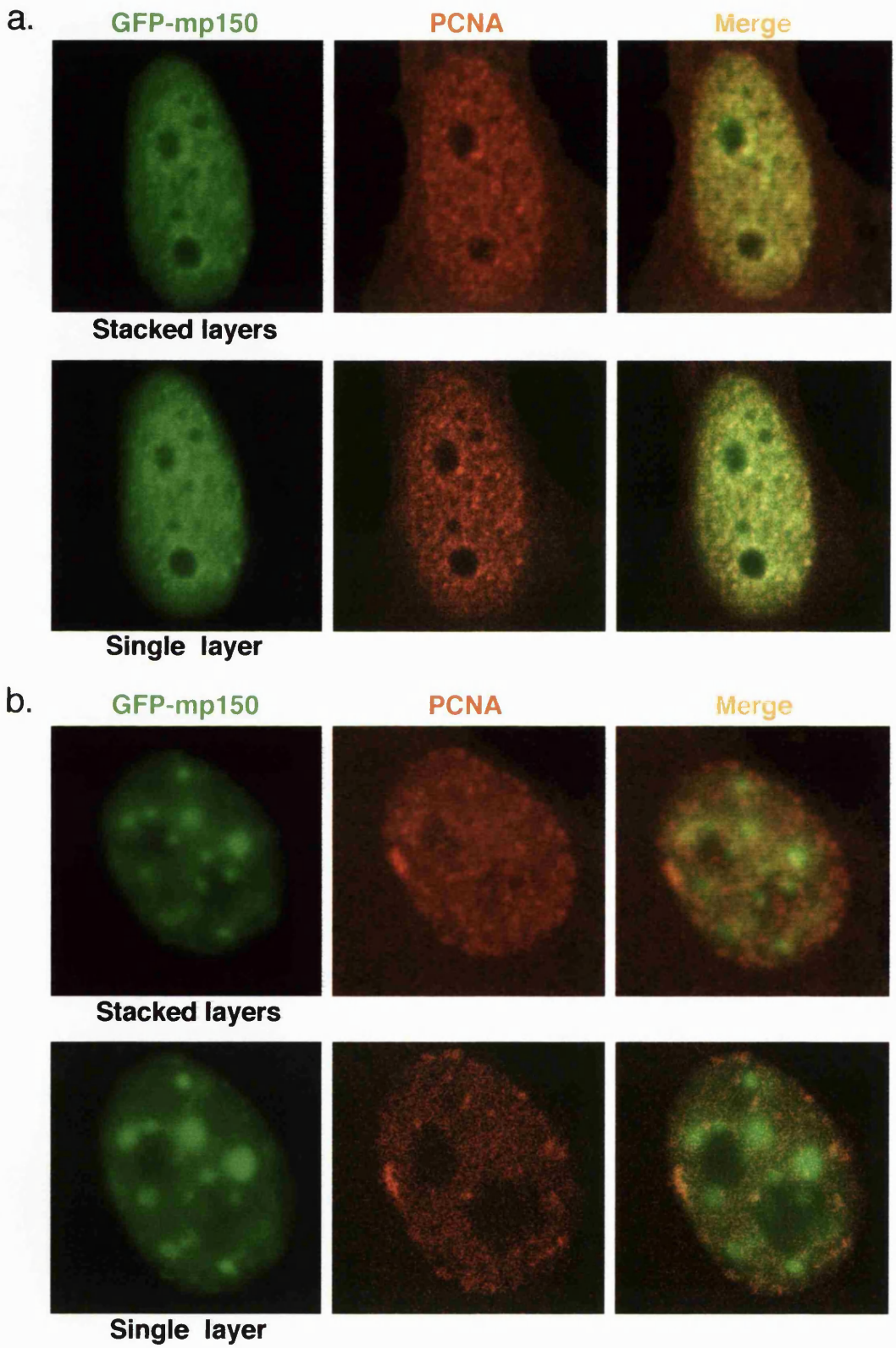
a.
GFP-mp150
PCNA
Merge
Stacked layers
Single layer
b.
GFP-mp150
PCNA
Merge
Stacked layers
Single layer

c.

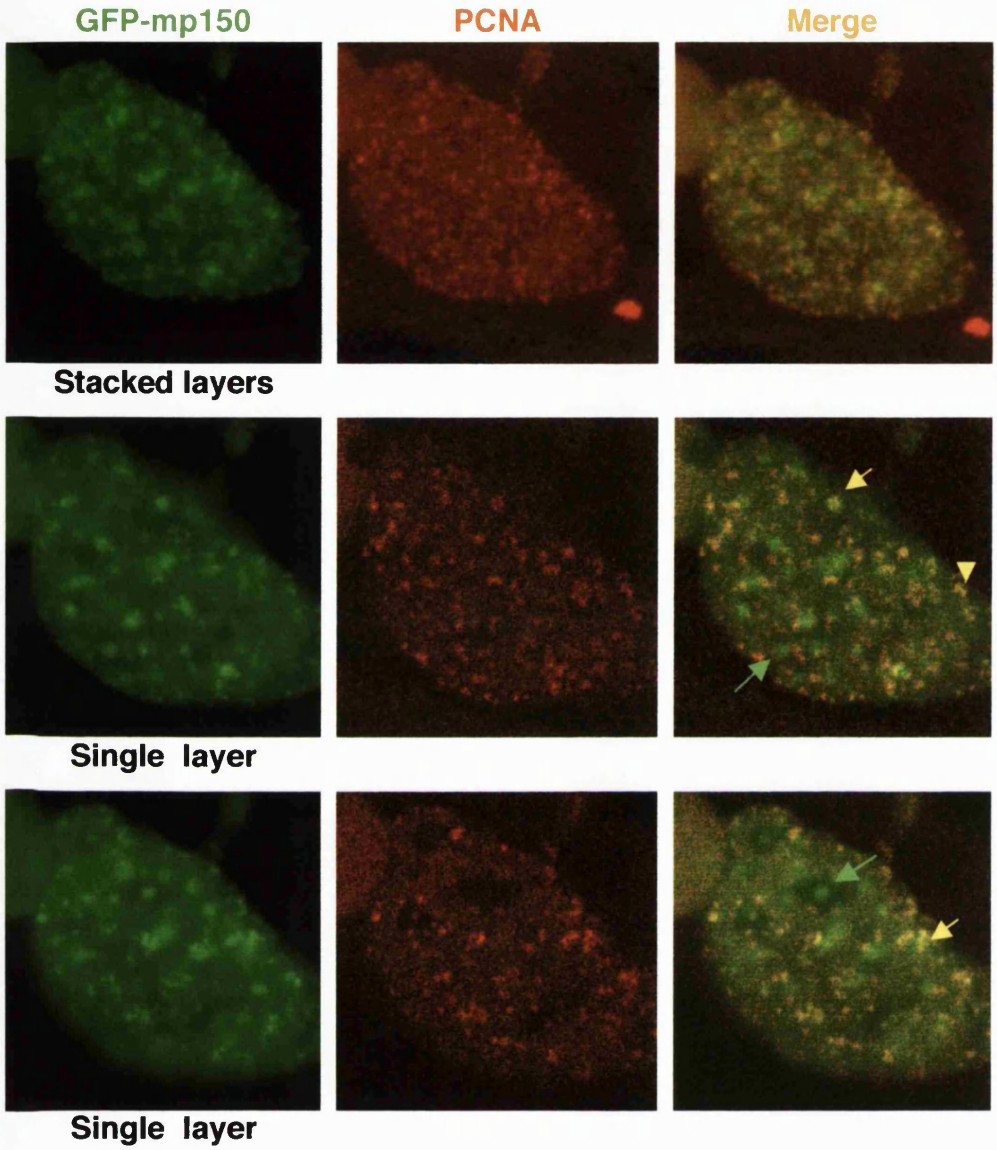
GFP-mp150
PCNA
Merge
Stacked layers
Single layer
Single layer

d.

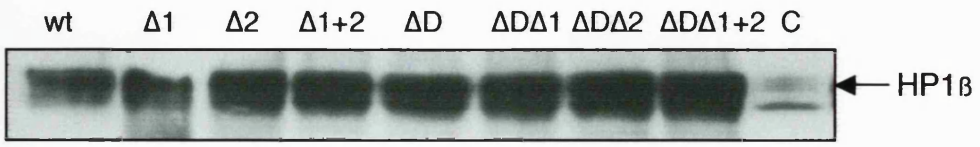
wt
Δ1
Δ2
Δ1+2
ΔD
ΔDΔ1
ΔDΔ2
ΔDΔ1+2
C
HP1ß

Figure 3.11: Confocal microscopy images showing GFP-p150 mis-targeting during S phase due to deletion of PBM1 and PBM2

Mouse NIH3T3 cells were transiently co-transfected with a plasmid expressing mouse p150 (wild type or mutants) conjugated to EGFP and a plasmid expressing human PCNA conjugated to ERFP. After 48 h the cells were extracted, fixes and stained as described in Chapter 2.11. Confocal microscopy images were taken at focal plains with 0.38 micron distribution.

a. The localisation of GFP-p150ΔPBM2 and RFP-PCNA in a cell during early-S phase. The top panels show figures plotted by stacking all the single focal plains. The bottom panels show figures of a single plain. The merged images clearly demonstrate that GFP and PRF staining co-localise.

b. The localisation of GFP-p150ΔPBM1+2 and RFP-PCNA in a cell during early/mid-S phase. Panels are as in (a). In this cell GFP staining mostly does not co-localise with RFP but with HOECHST (not shown).

c. The localisation of GFP-p150ΔPBM2 and RFP-PCNA in a cell during mid-S phase. Panels are as in (a). In this cell some of the GFP staining co-localises with RFP while other foci co-localise with HOECHST staining (not shown).

d. PBM mutations do not affect p150 binding to HP1 *in vivo*. Mouse NIH3T3 cells were transiently co-transfected with a plasmid expressing human p150 (wild type or mutants) conjugated to EGFP. After 48 h nuclear extracts from transfected cells were prepared, and GFP-p150 was immunoprecipitated with SS1 antibody beads. After washes samples were analysed by SDS-PAGE and Western blotting. HP1ß was detected using 1MOD 1A9 mAb (Euromedix) as primary antibody.

In order to estimate the fraction of cells where GFP-p150 showed mis-localisation, one hundred or more NIH 3T3 cells in S phase were analysed for WT p150 and each mutant. A histogram showing the distribution of cells in each phenotypic category is presented in Figure 3.12. Similar results were obtained using transfected mouse L cells. The deletion of each PBM resulted in some mis-targeting of p150 to heterochromatin during early- or mid-S phase. Mutation of both PBMs had a synergistic effect on p150 localisation that was stronger than the sum of the effects conferred by each mutation alone. About 57% of cells expressing the mutant lacking both PBMs showed some mis-localisation of p150 to heterochromatin in early- and mid-S phase, compared with only 13% and 19% for the PBM1 and PBM2 single deletion mutants. However, as many as 43% of the cells transfected with the double PBM deletion mutant showed normal localisation to DNA replication foci with no apparent mis-targeting to heterochromatin. Additionally, it was clear that a substantial fraction of GFP-p150 was targeted properly to replication foci even in cells where mis-localisation to heterochromatin was apparent (*i.e.* in cells with a partial defect phenotype - Figure 3.10 o and f – constituting 55% of all cells). Hence, although these experiments demonstrate that both PBMs are

involved in targeting p150 to replication foci, my results strongly argue that other region/s in p150 contribute to targeting CAF1 to sites of DNA synthesis.

3.9.2 PBM2 and the dimerisation domain are jointly crucial for targeting CAF1 to DNA replication foci *in vivo*

While this work was in progress, experiments with the yeast two-hybrid system and in *Xenopus* revealed the existence of a dimerisation motif in the CAF1 p150 subunit (Quivy et al., 2001; and see Figure 3.1b). This work suggested an interesting hypothesis to explain my results showing that GFP-p150 PBM mutants retained some targeting to DNA replication foci in transfection experiments. In transfected cells, three types of p150 dimers are possible: endogenous p150 homodimers, heterodimers with one endogenous p150 molecule and one GFP-p150 molecule, and GFP-p150 homodimers. Even mutants where GFP-p150 lacks both PBMs may still bind PCNA and target to replication foci through dimerisation with endogenous p150 containing two intact PBMs (see cartoons in Figure 3.12). In contrast, homodimers of mutant GFP-p150 lacking the PBMs would not be targeted to replication foci. The coexistence of both types of dimers in the same transfected cell would explain why only a fraction of GFP-p150 was mis-targeted to heterochromatin while the rest was localised in DNA replication foci.

To test this hypothesis, I repeated the experiments with constructs expressing GFP-p150 with deletions in the dimerisation domain and the PBMs. The patterns of p150 localisation observed with the dimerisation mutants are presented in the right half of Figure 3.12. Deleting the dimerisation domain caused a slight defect in targeting by itself, but this effect was stronger when combined with the deletion of PBM1. Strikingly, GFP-p150ΔDΔPBM2 was completely defective in targeting to replication foci in over 90% of the cells, while the triple mutant (GFP-p150ΔDΔPBM1+2) was mis-targeted to heterochromatin in virtually all the transfected cells.

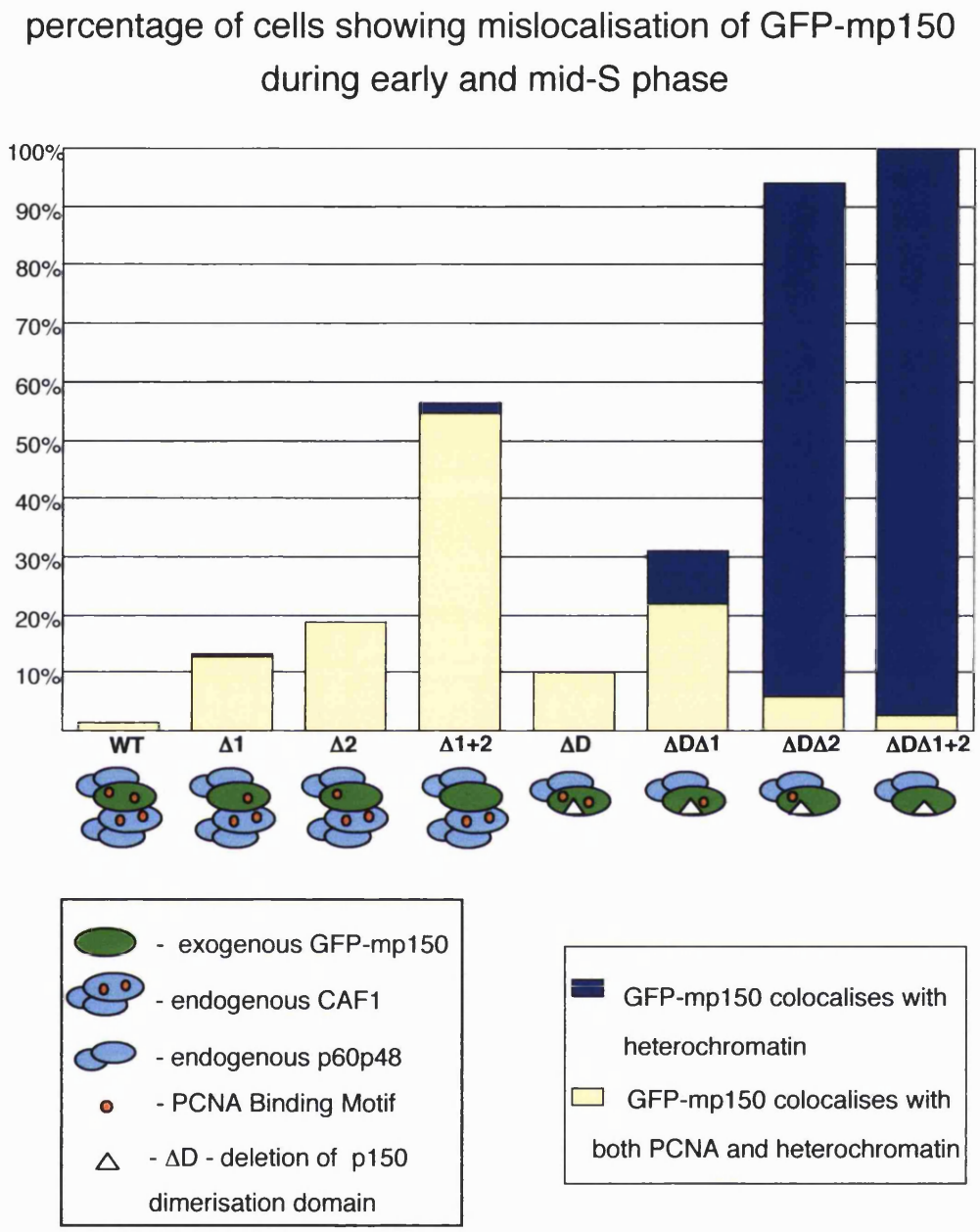

Figure 3.12: Both PBMs in p150 contribute to its localisation at DNA replication foci
The percentage of cells in early- and mid-S phase in which GFP-p150 mislocalised are shown: bars in yellow represent cells in which GFP-p150 colocalised both with PCNA and heterochromatin; bars in blue represent cells in which GFP-p150 colocalised only with heterochromatin. (WT) wild type p150. (Δ1, Δ2, Δ1+2) p150 mutants lacking PBM1, PBM2 or both PBMs, respectively. (D) p150 dimerisation domain. 100-200 cells in early- or mid-S phase were counted for each transfected plasmid. The cartoons at the bottom of the diagram, indicates the maximum number of PBMs in a complex with GFP-p150.

Taken together, these results suggest that p150 is present in replication foci as a dimer. Although mutating the dimerisation domain itself does not strongly influence targeting, when combined with the deletion of PBM2 targeting to replication foci is essentially abolished. Therefore, while both PBMs contribute to targeting p150 to replication foci as discussed in 3.9.1. PBM2 and the dimerisation itself play a more important role than PBM1. These experiments were carried out with PBM1 mutations that did not completely remove the region defined by the PBM1b peptide (Table 3.2). Therefore, I cannot exclude the possibility that a more pronounced effect of deleting PBM1 alone may have resulted from a deletion encompassing the full region included in the PBM1b peptide. However, the fact that the PBM2 deletion was by itself sufficient to compromise p150 targeting to replication foci suggests that even the complete PBM1 is mostly insufficient in targeting CAF1 p150 to sites of DNA replication.

3.10 CAF1 PBM PEPTIDES PREFERENTIALLY INHIBIT NUCLEOSOME ASSEMBLY OVER DNA SYNTHESIS

The fact that CAF1 binds to PCNA in a manner similar to many other PCNA binding proteins raises the question of how these interactions are regulated. Many studies, including my own, use p21 as a point of reference and compare the affinity of specific PBPs for PCNA with that of p21. These studies revealed that p21 has the strongest affinity for PCNA, but only by a few fold (Maga and Hubscher, 2003). Surprisingly, p21 inhibits DNA replication (Waga et al., 1994), but seems to inhibit DNA repair associated DNA synthesis less efficiently (Cooper et al., 1999; Li et al., 1996; Li et al., 1994; Pan et al., 1995; Shivji et al., 1998; Shivji et al., 1994). In spite of the fact that the PCNA trimer contains three distinct surfaces and can potentially accommodate up to three different PBPs, complexes containing both p21 and FEN1 cannot be formed *in vitro* (Warbrick et al., 1997). This suggests that p21 may inhibit DNA replication not only as a result of its higher affinity for PCNA, but also because its binding to PCNA causes a conformational change that prevents other PBPs from associating with PCNA rings simultaneously with p21. Importantly, even during normal DNA replication or PCNA dependent DNA repair there are many functionally distinct proteins that need to bind PCNA without impeding each

other. Because the trimeric PCNA ring has three equivalent docking sites for PBPs, many authors have suggested that each subunit of the trimeric PCNA ring may bind to a distinct PBP, *e.g.* DNA polymerase (DNA polymerase δ or ε), the flap endonuclease (FEN1 in the case of DNA replication) and Lig1. Recently, a tri-functional PCNA ring has been identified in the archaeon *Sulfolobus solfataricus*. In this organism, PCNA is a heterotrimer composed of three different molecules (PCNA1, PCNA2 and PCNA3) that respectively bind to DNA polymerase, DNA ligase and FEN1 (Dionne et al., 2003). However, in most eukaryotes, PCNA is transcribed from a single gene and forms homotrimers. In addition, as mentioned above, attempts to bind two distinct PBPs such as FEN1 and p21 to the same PCNA ring have thus far not been successful (Chen et al., 1996; Jonsson et al., 1998; Warbrick et al., 1997; and data not shown).

In the last few years, the number of identified PBPs has increased considerably (Table 3.1). Many PBPs are present constitutively at the replication fork. Because the PBMs of individual PBPs interact with overlapping surfaces of PCNA, it is clear that a single PCNA ring could not interact with all these factors simultaneously (Kelman, 1997; Kelman and Hurwitz, 1998; Vivona and Kelman, 2003; Warbrick, 2000). In light of this, it seems likely that regulatory mechanisms exist to control the binding of individual PBPs to PCNA. For example, Lig1 should not bind to PCNA before the DNA has been replicated and the RNA-DNA flap removed. Similarly, DNMT1 should not bind to PCNA before the polymerase has replicated the DNA, and should only act on the lagging strand after Okazaki fragment maturation. In addition, CAF1 should promote nucleosome assembly only after the replicated DNA has been sanitised by the uracil DNA glycosylase (Nilsen et al., 2002), proofread by the mismatch repair apparatus (Clark et al., 2000) and possibly modified by DNMT1 (Okuwaki and Verreault, 2004). These processes must be coordinated with remarkable precision given that histones H3/H4 are deposited immediately behind the replication fork (within 150-400 bp) onto both the leading and the lagging strands (Herman et al., 1981; Sogo et al., 1986; Worcel et al., 1978).

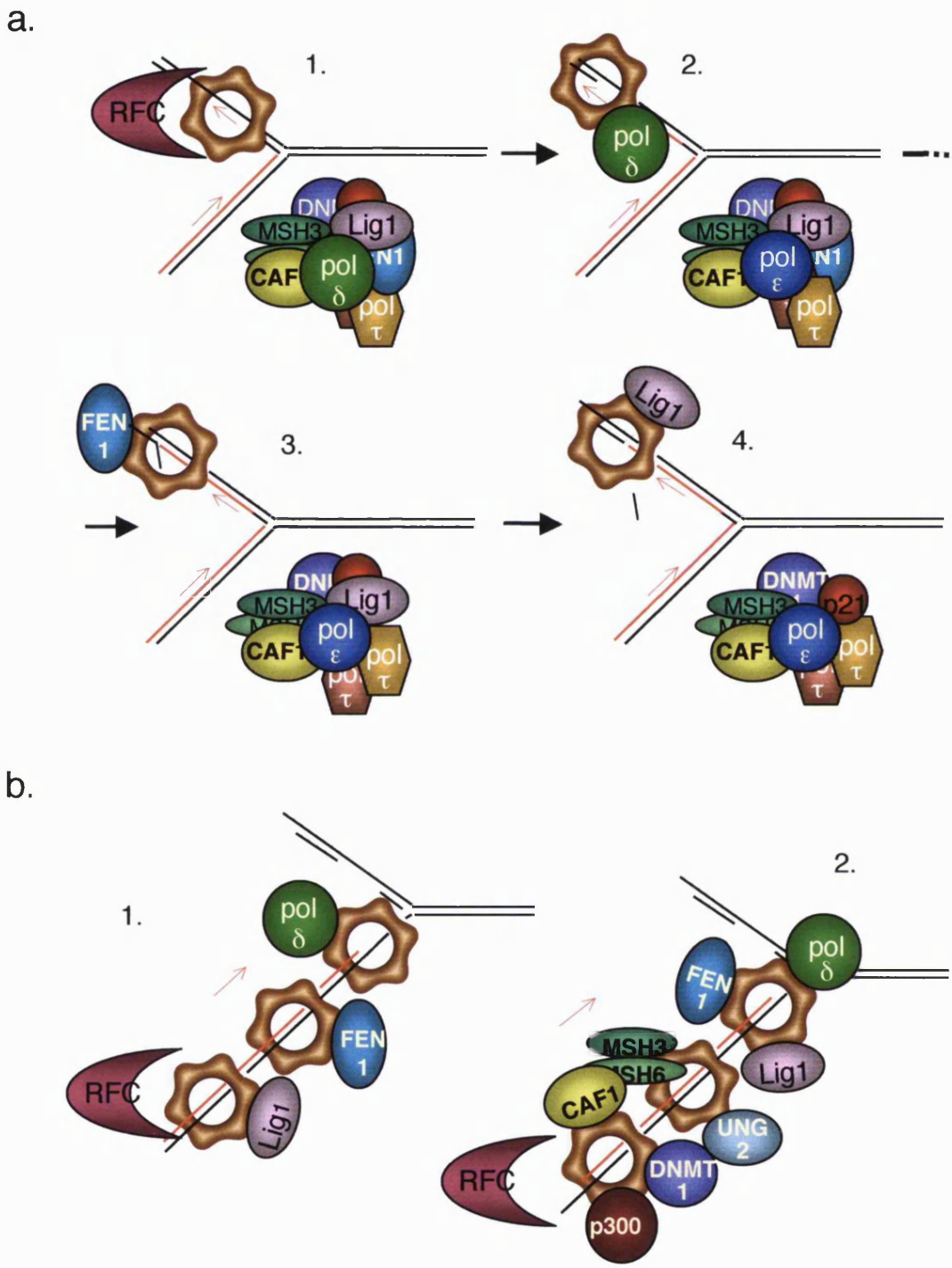

Figure 3.13: Possible models for the sequence of events at the replication fork
Schematic and simplified cartoons to illustrate two possible models.
a. During the replication of a single Okazaki fragment, PCNA is loaded onto DNA by RFC (1), then bound by the DNA polymerase until it reaches the previously synthesised fragment downstream (2). The DNA polymerase is displaced, and FEN1 then binds to PCNA cleaving the flap (displaced strand) DNA (3). After this FEN1 is removed and Lig1 binds to PCNA and ligates the nick remaining on the newly synthesised strand (4).
b. Several PCNA rings are loaded at each replication fork carrying one (1) or several different replication factors (2), ordered according to the sequence of events at each replication fork.

The binding of PBPs to PCNA could be regulated either in a temporal or a spatial fashion. For instance, PBPs may all bind sequentially to a single PCNA trimer, either individually or in groups of three according to a pre-defined temporal sequence (Figure 3.13a). Alternatively, several distinct PCNA rings, each dedicated to a single PBP (or a group of PBPs) may be present at the replication fork (Figure 3.13b).

In previous studies, the addition of PBM peptides to DNA replication reactions simply inhibited replication (Chen et al., 1995b; Ducoux et al., 2001; Kedar et al., 2002). Although both replication and nucleosome assembly are PCNA-dependent processes, these two reactions can be separated and analysed independently from each other in the SV40 system (Kamakaka et al., 1996; Shibahara and Stillman, 1999). This raised the possibility that titration of CAF1 PBM peptides in the SV40 system may differentially affect nucleosome assembly and DNA replication. In these assays, the level of DNA replication was determined by the incorporation of radiolabelled deoxyribonucleotides into nascent DNA, whereas the extent of nucleosome assembly was assayed by the appearance of supercoiled and replicated plasmid DNA in a native agarose gel.

DNA replication-dependent nucleosome assembly reactions were performed with a constant non-saturated concentration of recombinant CAF1 that was sufficient to promote nucleosome assembly on most of the replicated DNA (see Figure 3.14a for titration of CAF1). A number of different PBM peptides (Table 3.2) were titrated into these reactions at concentrations that were within the range used in previously published work (Matsumiya et al., 2002; Warbrick et al., 1995). As CAF1 functions during both T Ag driven replication (Smith and Stillman, 1989) and T Ag independent DNA repair synthesis (Gaillard et al., 1996), the reactions were therefore carried out either in the presence or absence of T Ag. In the absence of T Ag, nucleases present in the extract create nicks in the plasmid that serve as primers for PCNA-dependent DNA synthesis (Moggs et al., 2000).

a.

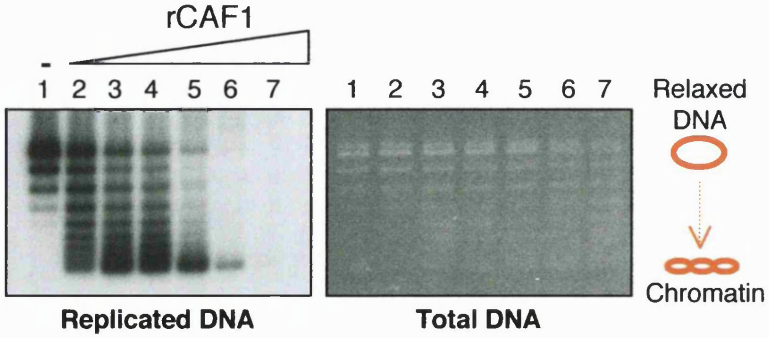
rCAF1
-
1 2 3 4 5 6 7
1 2 3 4 5 6 7
Relaxed DNA
Chromatin
Replicated DNA
Total DNA

b.

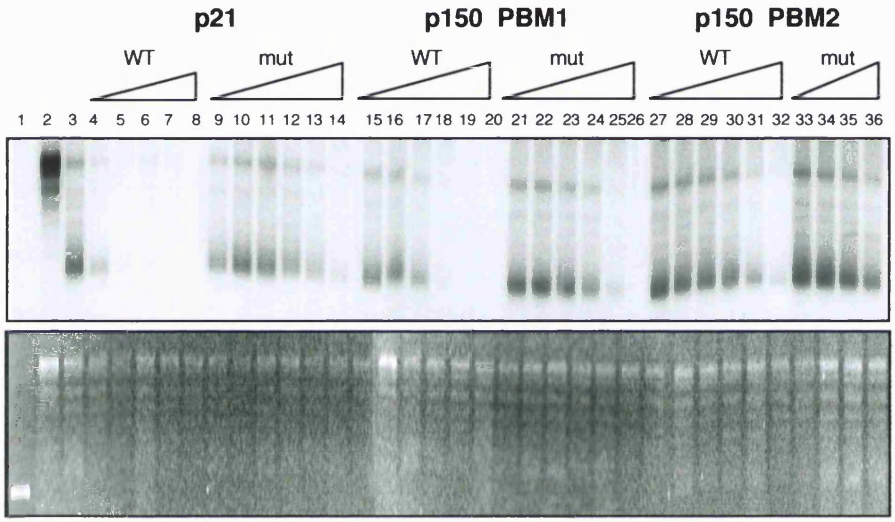
p21
p150 PBM1
p150 PBM2
WT
mut
WT
mut
WT
mut
1 2 3 4 5 6 7 8 9 10 11 12 13 14 15 16 17 18 19 20 21 22 23 24 2526 27 28 29 30 31 32 33 34 35 36

c.

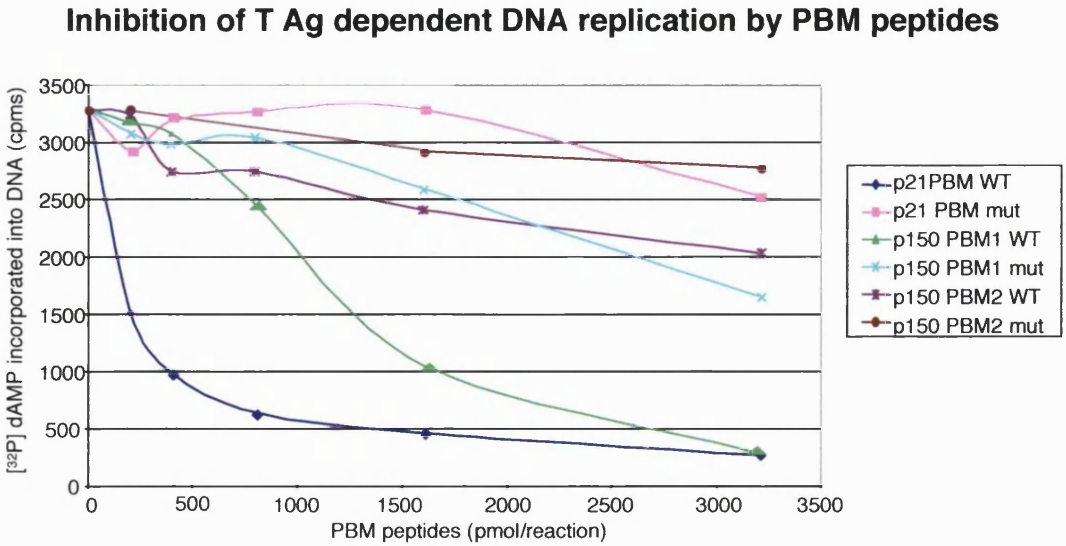
Inhibition of T Ag dependent DNA replication by PBM peptides
[32P] dAMP incorporated into DNA (cpms)
3500
3000
2500
2000
1500
1000
500
0
0
500
1000
1500
2000
2500
3000
3500
PBM peptides (pmol/reaction)
p21PBM WT
p21 PBM mut
p150 PBM1 WT
p150 PBM1 mut
p150 PBM2 WT
p150 PBM2 mut

Figure 3.14: Inhibition of DNA replication by PBM peptides in a T antigen dependent assay
a. CAF1 was titrated (50 ng – 1.6 μg) into SV40 replication reactions to determine a sufficient yet non-saturated levels of CAF1 to specifically promote chromatin assembly onto replicated DNA. The left panel shows autoradiogram of replicated DNA. The right panel shows total DNA stained with ethidium bromide. 0.45 pmol of rCAF1 (lane 3) was used per reaction in the following assays.
b. PBM peptides were titrated into DNA replication and chromatin assembly reactions as indicated at the top of the figure. The top panel shows the autoradiogram of replicated DNA. The bottom panel shows total DNA. Titration was of 0.2 nmol – 3.2 nmol p21 PBM WT and of 0.2 nmol – 6.4 nmol of other peptides (PBM2 mut peptide titration did not include 0.4-0.8 nmol). Whereas p21 PBM WT (lanes 4-8) and p150 PBM1 WT (lanes 15-20) inhibit both DNA replication and chromatin assembly at lower concentrations, p21 PBM mut (lanes 9-14), p150 PBM1 mut (lanes 21-26) and p150 PBM2 WT (lanes 27-32) inhibit both DNA replication and chromatin assembly at higher concentrations. p150 PBM2 mut had little significan effect under conditions used (lanes 33-36).
c. DNA replication inhibition by titration of PBM peptides as determined by scintillation counts of 1μl aliquots of the reactions shown in (b). Inhibition of [^{32}P] dATP incorporation by p21 PBM WT occurred a low peptide concentration. Upon adding 0.2 pmol p21 peptide per reaction incorporation is inhibited by more then half, addition of 0.8 pmol peptide inhibited incorporation close to background levels. By extrapolation from the graph, p150 PBM1 WT would inhibit incorporation by 50% at a concentration of roughly 1.2 nmol per reaction. p150 PBM1 WT cuased full inhibition of replication at 3.2 nmol per reaction. Inhibition by p150 PBM1 mut and PBM2 WT requires much higher peptide concentration. Even at 3.2 nmol, [^{32}P] dAMP incorporation is inhibited by less than half. Inhibition by the p21 PBM mut and p150 PBM2 mut peptides is minimal.

The results are presented in Figures 3.14b and 3.15a. The p21 PBM WT peptide was a relatively potent inhibitor of DNA replication (Figure 3.14b, lanes 3-8). At 200 pmol per 12.5 μl reaction, this peptide reduced replication by more than half and at 800-1600 pmol, replication was completely inhibited (Figure 3.14c). This effect was eliminated or at least greatly reduced when the consensus PBM was mutated (Figure 3.14c). In T antigen dependent DNA replication reactions, p150 PBM1 WT had a similar effect to p21 PBM WT (Figure 3.14b, lanes 15-20 and Figure 3.14c), although higher levels of p150 PBM1 peptide were needed to achieve the same degree of inhibition. As was the case with p21 PBM WT, increasing concentrations of the p150 PBM1 WT or p150 PBM2 WT peptides progressively inhibited replication without any accumulation of partially supercoiled replicated DNA (Figure 3.14b, lanes 15-20 and lanes 27-32), arguing that the CAF1 peptides simply inhibited DNA replication. In striking contrast, in T Ag independent assays, both p150 PBM WT peptides preferentially inhibited nucleosome assembly over DNA synthesis (Figure 3.15a). This was apparent from the fact that low concentrations of p150 PBM WT peptides reduced supercoiling of nascent DNA without any

dramatic inhibition of DNA synthesis (Figure 3.15a, compare lane 12 with lanes 13 and 20). This effect was unique to p150 PBM peptides and was not observed with the p21 PBM WT peptides, which only blocked DNA synthesis (Figure 3.15a, lanes 2-6). However, higher concentrations of the p150 PBM peptides either reduced or completely blocked T Ag independent DNA synthesis (Figure 3.15a, lanes 13-15 and lanes 19-21). Although p150 PBM1 mut was not as potent as the WT peptide, it also affected both nucleosome assembly and DNA synthesis in a similar manner, *i.e.* the lower concentration of peptide tested preferentially inhibited nucleosome assembly over DNA synthesis (compare Figure 3.15a, lanes 13 and 16-17). This suggests that there are other residues within the p150 PBM1 peptide that may compete with CAF1 for PCNA binding, possibly PBM1a (Table 3.2). Thus, as with the PCNA binding assays, PBM1 may still be functional in spite of the LI to AA mutation.

The preferential inhibition of nucleosome assembly only occurs in a very limited range of peptide concentrations, which is not physiologically relevant but is reproducible. However, the higher concentration of peptides needed may merely reflect the fact that most peptide molecules do not assume the correct conformation to bind PCNA. If all the molecules were properly folded, the peptide concentrations needed may well fall within physiological range.

In T Ag independent assays, both p150 PBM2 WT and p60 PBM WT inhibited DNA synthesis (Figure 3.15a, lanes 19-21 and lanes 25-27) and their inhibitory potential was completely eliminated when the core aromatic residues of the PBM were mutated (Figure 3.15a, lanes 22-24 and 28-30). A similar effect was observed with the p150 PBM2 WT peptides in T Ag dependent replication assays (Figure 3.14b, lanes 27-36 and Figure 3.14c). This is surprising given the fact that, unlike p150 PBM1 WT, these peptides did not pull down PCNA from the S100 extract (data not shown), suggesting that even transient interactions between PBM peptides and PCNA are sufficient to inhibit DNA synthesis in the S100 extract. Moreover, while the importance of hp150 PBM2 for CAF1 function is apparent from the immunofluorescence experiments (Figure 3.12) and the nucleosome assembly reactions (Figure 3.6), the result

with the p60 PBM (Figure 3.15a, lanes 25-30) suggests that this motif may also contribute to some aspect of CAF1 activity that has yet to be uncovered.

Preferential inhibition of nucleosome assembly over DNA synthesis in T Ag-independent assays was also observed with an N-terminal fragment of p150 (1-296) purified from *E. coli*. Deletion of the PBM in this fragment of p150 strikingly reduced its ability to interfere with nucleosome assembly (1-296ΔPBM1 – Figure 3.15b, compare lanes 3-7 with 8-12). The p150 (1-296) fragment inhibited nucleosome assembly at much lower concentration (7-70 pmol/reaction) than the synthetic PBM1 peptide (>20 fold), suggesting that the appropriate conformation required for PCNA binding may be stabilised in the longer p150 fragments.

These results suggest that not all PBMs are similar. The core motif itself consists of only 3-4 residues, which are only partially conserved (Xu et al., 2001). Consequently, these PBMs are quite distinct from each other by sequence. The fact that unlike the p21 PBM, CAF1 PBMs preferentially inhibit nucleosome assembly over replication suggests that these PBMs are functionally distinct, and that under appropriate conditions, the interaction of CAF1 with PCNA can be distinguished from that of other PBPs.

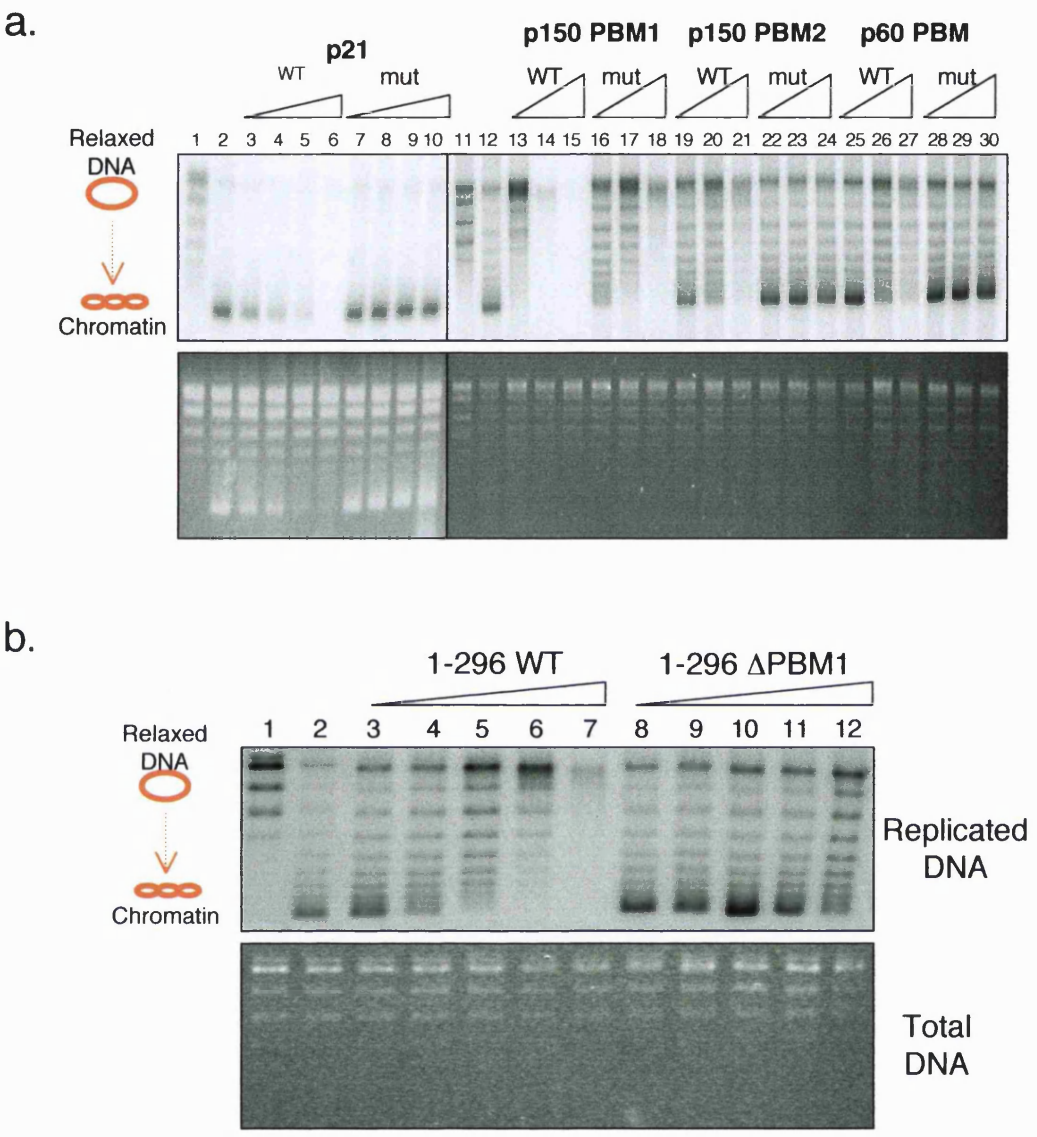

Figure 3.15: p150 PBMs preferentially inhibit chromatin assembly over DNA synthesis in T antigen independent reactions

a. DNA synthesis was allowed to occur in the absence of T Ag (lanes 1 and 11); upon addition of 0.45 pmol of recombinant CAF1 essentially all the plasmids carrying newly synthesised DNA was assembled to chromatin (lanes 2,12), whereas most of the plasmids in the reaction remained relaxed (compare top panels of autoradiogram to the lower panels of ethidium bromide stained gel). Titration of a large excess of p21 PBM WT peptide over CAF1 into the reaction (lanes 3-6 0.2,0.4,0.8 and 1.6 nmol, respectively) inhibited DNA synthesis whereas the p21 PBM mut had no effect (lanes 7-10). Titration of even higher amounts of p150 PBM1 peptide (1.6, 3.2 and 6.4 nmol in lanes 13, 14, and 15, respectively) caused inhibition of chromatin assembly and only at higher concentration inhibited DNA synthesis. p150 PBM1 mut, PBM2 WT and p60 PBM had similar effect upon addition of yet higher peptide concentration (lanes 16-18; 19-21 and 25-27). Finally p150 PBM2 mut and p60 PBM mut peptides had no effect on the reactions under conditions used (lanes 22 -24 and 28-30).

b. Human p150 1-296 WT preferentially inhibits chromatin assembly over T Ag independent DNA synthesis at lower concentration in comparison to the PBM peptides. 7, 14, 35, 70 and 140 pmol of this fragment were added to the reactions in lanes 3-7, respectively. Inhibition of chromatin assembly was detected at the lowest concentration added whereas inhibition of DNA synthesis was only detected at the highest concentration used. This effect was essentially eliminated in hp150 1-296 ΔPBM1 (lanes 8-12).

3.11 CAF1 PBM1 CAN CONVERT DNA LIGASE I INTO A PREFERENTIAL INHIBITOR OF NUCLEOSOME ASSEMBLY

The fact that the form of PCNA involved in nucleosome assembly was preferentially inhibited by CAF1-derived PBM peptides raised the possibility that replacing the natural PBM of a replication protein with that of CAF1 might target the hybrid protein to bind PCNA only behind the replication apparatus. If this were true, then the chimeric protein may preferentially inhibit nucleosome assembly under conditions where the wild type replication protein would only inhibit replication.

The replacement of the PBMs should be as innocuous as possible to avoid disrupting the protein structure. The simplest way of constructing the chimeric protein was to replace the PBM located at either termini of a replication protein by CAF1 p150PBM1. Several replication factors have a PBM at their N- or C-terminus, such as RFC-p140, Lig1 (Montecucco et al., 1998) and FEN1 (Warbrick et al., 1997). We chose Lig1, because Dr. Lindahls laboratory at Clare Hall had previously shown that titration of the N-terminus of this enzyme, containing the PBM inhibited DNA replication in the SV40 system (MacKenney et al., 1997). In addition, they had established conditions to purify active His-tagged human Lig1 from *E. coli* (MacKenney et al., 1997).

The procedures used for the PBM replacement and the expression and purification of the PBM1-Lig1 chimeric protein and WT Lig1 (see Figure 3.16a for a schematic description) are summarised in Tables I.II and 2.6. Equimolar amounts of recombinant PBM1-Lig1 and WT Lig1 were titrated into T Ag independent DNA synthesis reactions (4-128 pmol) supplemented with recombinant CAF1 to promote nucleosome assembly. At the highest concentrations tested, both PBM1-Lig1 and WT Lig1 completely inhibited replication (Figure 3.16b, lanes 7 and 12). However, at lower concentrations PBM1-Lig1 inhibited nucleosome assembly, whereas WT Lig1 had little effect. As in the peptide experiments, the preferential inhibition of nucleosome assembly was only observed in T Ag independent DNA synthesis reactions (Figure 3.16b and data not shown).

a.

```
hLig1 PBM    -      MQRSIMSFFHPKKEGKAKKP
hp150 PBM1   - CKDRPAFPVKKLIQARLPFKRLNLVPKGKA
```

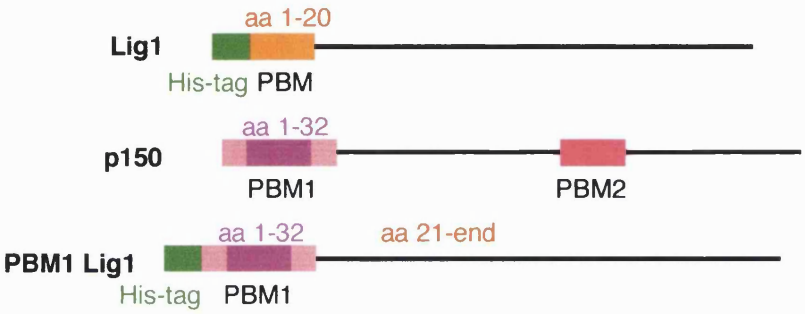

b.

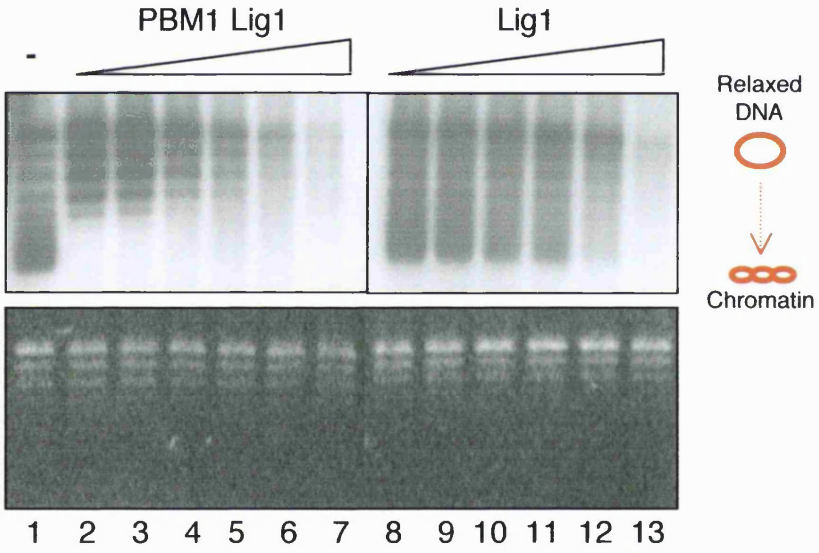

Figure 3.16: PBM1 can convert DNA Ligase I into a preferential inhibitor of chromatin assembly

a. A schematic description of PBM substitution. Using an existing his-tagged DNA ligase I construct, the first 20 residues of the ligase were replaced by the first 32 residues of p150, to create his-tagged PBM1 Lig1 (see Appendix I.II).

b. T antigen independent DNA replication and chromatin assembly reactions were carried out in the presence of increasing levels (0.5-16 μg) of recombinant his-tagged Lig1 (lanes 2-7) or PBM1 Lig1 (lanes 8-13). Both proteins inhibited DNA synthesis at similar concentrations. However, PBM1 Lig1 but not Lig1 preferentially inhibited chromatin assembly at lower concentrations.

3.12 Cac1 BINDING TO PCNA IN YEAST

Work in yeast had suggested that it is PBM2 that is important for PCNA binding (Krawitz et al., 2002), while the N-terminal region of Cac1 did not contribute to this interaction. In order to determine the function of PBM1 *in vivo*, I decided to test directly the importance of PBM1 in *S. cerevisiae*.

3.12.1 PBM1 binding to PCNA is conserved in yeast Cac1 and human p150

Although the N-terminus is the least conserved portion of the p150 subunit, a sequence potentially related to PBM1 is present in the *S. cerevisiae* homologue of p150, Cac1 (Figure 3.1a). To test whether the putative PBM1 contributes to Cac1 binding to *S. cerevisiae* PCNA (ScPCNA), I performed the following pull-down assay. A fragment derived from the N-terminal domain of Cac1 containing either WT PBM1 or a mutation of the two core aromatic residues to alanines (WT or mut – Figure 3.17a) was expressed in *E. coli* as a GST fusion protein and the purified protein was bound to glutathione Sepharose beads. After washing, the beads were incubated with yeast whole cell extracts derived from a strain expressing MYC-tagged ScPCNA (Hoege et al., 2002). As shown in Figure 3.17b, the GST fusion protein containing WT PBM1 (lane 3) bound stably to ScPCNA present in the yeast whereas neither the PBM1 mutant (lane 4) nor GST alone (lane 2) did.

3.12.2 PBM1 is important for Cac1 function *in vivo*

In order to assess the importance of PBM1 *in vivo*, I used a series of yeast strains expressing Cac1 with PBM1 and/or PBM2 mutations. To verify that the PBM mutations did not affect the stability of Cac1, wild type and mutant Cac1 proteins were tagged at their C-termini with a FLAG3 epitope, which does not affect CAF1 function *in vivo* (A. Verreault, personal communication). Western blots of these strains with M2 FLAG antibody showed a single protein that migrated between 75 and 90kDa (Figure 3.17c), as previously reported for Cac1 in *S. cerevisiae* (Sharp et al., 2001). The expression of Cac1-FLAG3 was not affected by mutations in PBM1, PBM2 or both PBMs (Figure 3.17c, lanes 3, 4 and 5, respectively).

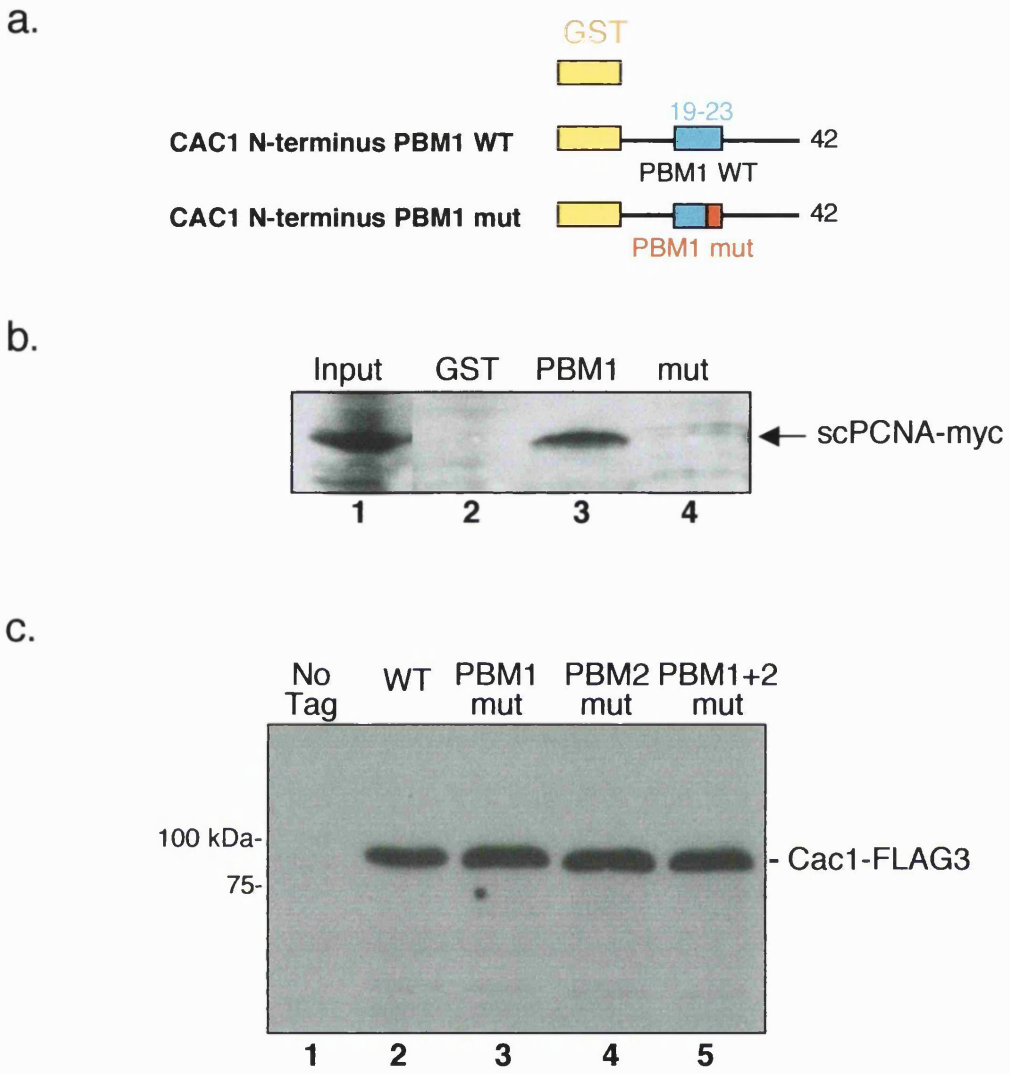

Figure 3.17: The N-terminus of Cac1 can bind PCNA *in vitro* in a PBM1 dependent manner
a. A schematic representation of polypeptides used for pulling down PCNA from yeast extracts. GST-scPBM1 WT (containing the first 42 residues of Cac1) or mut (FF12,13AA) or GST alone were expressed in *E. coli* and bound to glutathione beads.
b. Beads with GST-scPBM1 WT or mut or GST alone were incubated ON at 4°C with PCNA-myc expressing yeast extract. Beads were washed and bound material analysed by SDS-PAGE and Western blotting with 9E10 as primary antibody. Myc-tagged PCNA bound to GST-PBM1 WT but not to GST-PBM1 mut nor to GST alone.
c. PBM mutations do not affect the expression of Cac1 in *S. cerevisiae*. Whole-cell extracts were prepared from cells expressing Cac1-FLAG3 without PBM mutation (WT, strain YAV134, lane 2) or with mutations in PBM1 (FF22,23AA, strain YAV136, lane 3), PBM2 (FF233,234AA, strain YAV135, lane 4) or both PBM1 and PBM2 (strain YAV137, lane 5). Proteins were analysed by SDS-PAGE and Western blotting with FLAG M2 as primary antibody. Lane 1: W303 strain without any FLAG tag as negative control.

3.12.2.1 *cac1 PBM1* mutation in *hirΔ* background confers slow growth

In *S. cerevisiae*, CAF1 and Hir proteins function in a redundant manner to promote the formation of pericentric chromatin. Double mutant cells lacking both CAF1 and Hir proteins, but not single mutants, exhibit a slow growth phenotype, reduced viability and high rates of mitotic chromosome segregation defects due to faults in pericentric chromatin which interfere with the attachment of kinetochores to the microtubule spindle (Sharp et al., 2002). In order to determine whether PBM mutations affect the function of Cac1 *in vivo*, 500 cells of each strain were plated on rich media and allowed to form colonies at either 30°C or 18°C. Growth at low temperature exacerbates the phenotypes of cells that have defects in chromosome attachment to the microtubule spindle (Abruzzi et al., 2002). Consistent with this, *cac1Δhir1Δ* double mutants grow extremely slowly at low temperature (Sharp et al., 2002). In a background where Hir proteins were functional (*HIR1* wt in Figure 3.18), the Cac1 PBM mutations or a *cac1* null mutation had no effect on colony size at 30°C. At 18°C, *HIR1* wt cells with mutations in both PBM1 and PBM2 exhibited a slightly reduced colony size compared with wild type cells or Cac1 single PBM mutations. In addition, the *HIR1* wt *cac1Δ* cells gave rise to a heterogeneous mixture of colony sizes at 18°C (Figure 3.18).

In *hir1Δ* background, the mutation of both PBMs in Cac1 or the *cac1* null mutation resulted in modestly reduced colony sizes at 30°C. In contrast, at 18°C the Cac1 PBM1 mutation in this background gave rise to a slow growth phenotype whereas the PBM2 mutation had no effect on colony size. Furthermore, the mutation of both PBMs did not further reduce the growth of the PBM1 mutant. Nonetheless, the slow growth phenotype of *cac1Δhir1Δ* at 18°C cells was more pronounced than that of the Cac1 PBM mutant in *hir1Δ* cells. The *cac1Δhir1Δ* colonies shown in Figure 3.18 (18°C) were photographed three days later than all the others as they were barely detectable after four days at 18°C. Importantly, the substantial loss of viability observed in *cac1Δhir1Δ* cells at 18°C was not shared by Cac1 PBM mutant *hir1Δ* cells.

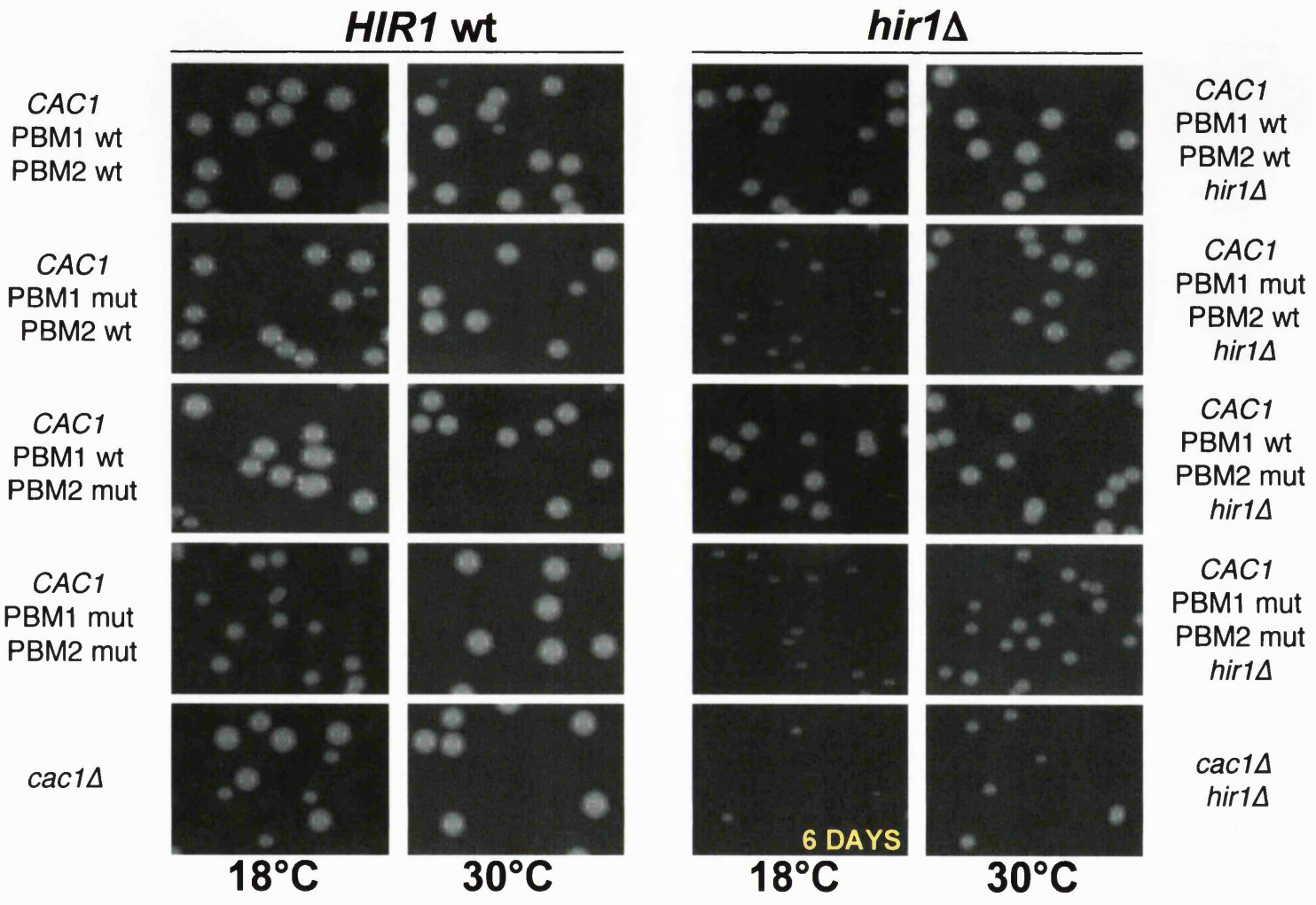
HIR1 wt
hir1Δ
CAC1 PBM1 wt PBM2 wt
CAC1 PBM1 mut PBM2 wt
CAC1 PBM1 wt PBM2 mut
CAC1 PBM1 mut PBM2 mut
cac1Δ
CAC1 PBM1 wt PBM2 wt hir1Δ
CAC1 PBM1 mut PBM2 wt hir1Δ
CAC1 PBM1 wt PBM2 mut hir1Δ
CAC1 PBM1 mut PBM2 mut hir1Δ
cac1Δ hir1Δ
6 DAYS
18°C
30°C
18°C
30°C

Figure 3.18: The Cac1 PBM1 mutation confers a slow growth phenotype at 18°C in cells lacking Hir1 (*hir1Δ*), but not in wild type cells (*HIR1*wt)

Five hundred cells of each genotype were plated onto rich media plates (YPD). Colonies were photographed after 3 days at 18°C or 1.2 days at 30°C, except for *cac1Δ hir1Δ* cells grown at 18°C, which were photographed after 6 days. These colonies were barely visible after 3 days at 18°C. The strains used are as follows: YAV138 (*CAC1* PBM1 wt PBM2 wt); YAV140 (*CAC1* PBM1 mut PBM2 wt); YAV139 (*CAC1* PBM1 wt PBM2 mut); YAV141 (*CAC1* PBM1 mut PBM2 mut); YAV119 (*cac1Δ*); YAV142 (*CAC1* PBM1 wt PBM2 wt *hir1Δ*); YAV144 (*CAC1* PBM1 mut PBM2 wt *hir1Δ*); YAV143 (*CAC1* PBM1 wt PBM2 mut *hir1Δ*); YAV145 (*CAC1* PBM1 mut PBM2 mut *hir1Δ*); YAV151 (*cac1Δhir1Δ*).

3.12.2.2 *cac1 PBM1* mutation in *hirΔ* background slightly increases mitotic chromosome loss rate

In order to determine whether the slow growth phenotype conferred by Cac1 PBM mutations was associated with defects in chromosome segregation, I measured the frequency of mitotic chromosome loss in each strain. For this purpose, I used yeast strains with a non-essential extra chromosome fragment whose presence can be inferred by a colony colour assay (Spencer et al., 1990; Chapter 2.9). The extra chromosome carries a tRNA gene (*SUP11*) that suppresses an *ade2-101* ochre stop codon mutation (see Figure 3.19 for a schematic representation). In media containing limiting amounts of adenine, yeast strains with the *ade2-101* mutation accumulate an intermediate in the biosynthesis of adenine that produces a red colony colour. The *SUP11* gene in the extra chromosome fragment suppresses the *ade2-101* mutation and leads to the formation of white colonies.

Cells were grown in minimal medium lacking uracil to select for the presence of the extra chromosome fragment, which carries a *URA3* marker. At that point, all the cells in the population contained the extra chromosome fragment and formed white colonies on plates containing uracil and limiting amounts of adenine (data not shown). Each culture was then diluted to 200 cells/ml and grown in rich medium to allow loss of the extra chromosome fragment during cell division. Cell density was recorded to determine the number of cell divisions that took place in the absence of selection for the extra chromosome fragment, then one thousand cells were plated on minimal media plates with uracil and limiting amounts of adenine.

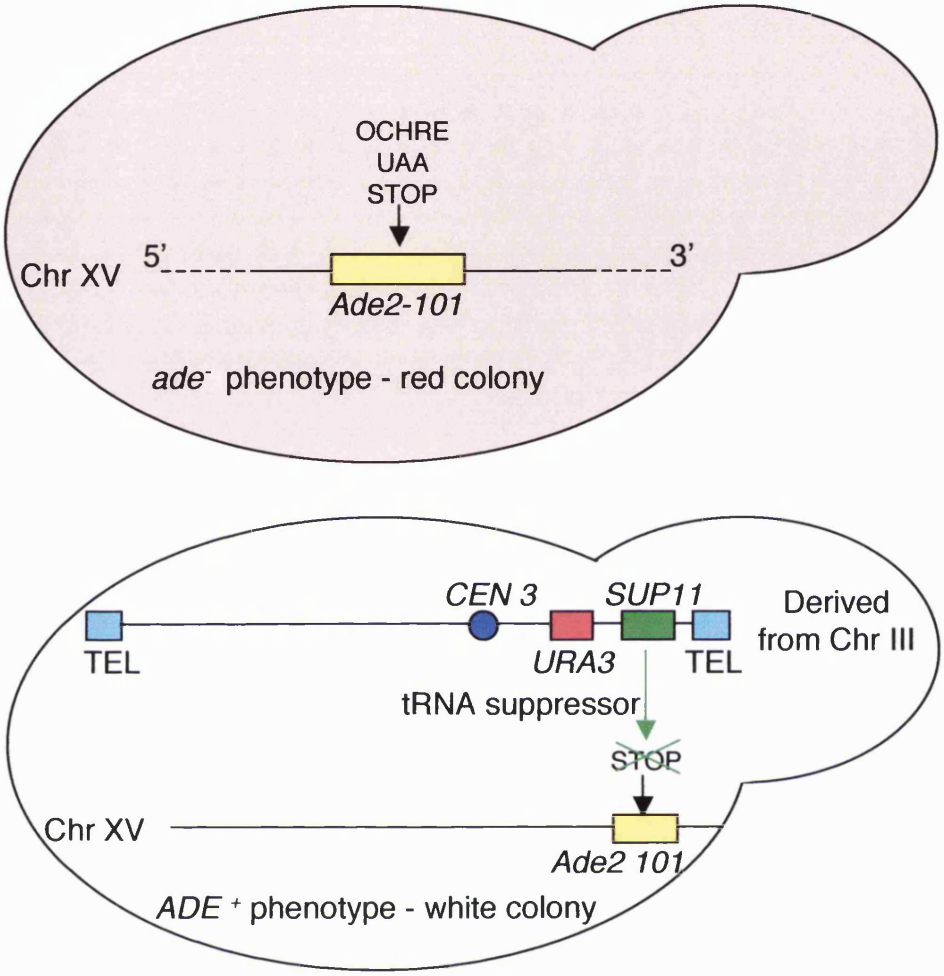

Figure 3.19: Assay to monitor the stability of a non-essential chromosome fragment
A chromosome fragment derived from the left arm of chromosome III (CF III.L) contains the *SUP11* gene which encodes a tRNA, that suppresses the ochre stop codon encoded by the *ade2-101* allele. After a known number of mitotic divisions in the absence of selection for CF III.L (growth in rich medium), the cells are plated onto minimal media plates with limiting amounts of adenine. Cells that retain CF III.L are *ADE* + and give rise to white colonies. Cells that lose CFIII.L are *ade* - and produce red colonies. Sectored colonies with more than 50% white cells are scored as having retained CF III.L (Spencer et al., 1990).

Most colonies were either uniformly white or red (data not shown). A small fraction of colonies contained both red and white sectors. Sectored colonies were scored as having lost the extra chromosome fragment when at least 50% of the colony was red. After determining the fraction of red and white colonies and taking into account the number of cell divisions that each culture underwent in the absence of selection, the chromosome loss rate per mitotic division was determined. Table 3.3 presents the average loss rates for at least three independent cultures of each strain.

Table 3.3: Frequency of chromosome fragment CF III.L loss per mitotic division in yeast strains with Cac1 PBM mutations

Strain	Genotype	Loss Rate per Division	Fold Increase
YAV134	*CAC1* PBM1wt PBM2wt *HIR1*wt	0.012	-
YAV136	*CAC1* PBM1mut PBM2wt *HIR1*wt	0.010	0.8
YAV135	*CAC1* PBM1wt PBM2mut *HIR1*wt	0.023	1.9
YAV137	*CAC1* PBM1mut PBM2mut *HIR1*wt	0.021	1.8
YAV87	*CAC1* PBM1wt PBM2wt *hir1Δ*	0.0047	-
YAV88	*CAC1* PBM1mut PBM2wt *hir1Δ*	0.030	6.4
YAV151	*cac1Δhir1Δ*	N.D.*	N.D.*

*N.D.: Not Determined. In this strain, individual Ura$^+$ colonies gave rise to either only white colonies (presumably due to *ade2-101* reversion to Ade$^+$ or integration of the *SUP11* suppressor into a natural chromosome) or only red colonies, *i.e.* all cells derived from the original Ura$^+$ colony had lost the extra chromosome fragment after growth in rich medium.

In *HIR1* WT cells, Cac1 PBM mutations had only marginal effects on the mitotic stability of the extra chromosome fragment (Table 3.3). This is to be expected because even a *cac1Δ* mutation only causes only a two-fold increase in chromosome loss frequency (Sharp et al., 2002). In *hir1Δ* cells, the PBM1 mutation increased the loss rate of the extra chromosome fragment by about 6.4-fold. Unfortunately, I was not able to perform the same assay in *hir1Δ* cells with other Cac1 PBM mutations (either PBM2 alone or both PBM1 and PBM2). In these strains, the colonies were either all white or had a very faint pink colour, making it impossible to monitor chromosome loss events accurately. Moreover, individual transformants of the *cac1Δhir1Δ* strain carrying the extra chromosome fragment gave rise to either red colonies alone (*i.e.* all cells in a given culture had lost the chromosome fragment after 24 hours in rich medium) or solely to white colonies (Table 3.3). The white colonies may be due to either a high frequency of mutations that revert the stop codon in the *ade2-101* reporter gene or integration of the *SUP11* suppressor into natural chromosomes, which have a much higher mitotic stability than the extra chromosome fragment used here. The latter possibility is quite likely because the left arm of the extra chromosome fragment contains extensive homology with chromosome III and the right arm contains the *URA3* gene (Figure 3.19), which could both direct integration of the *SUP11* suppressor into natural yeast chromosomes by homologous recombination (Aguilera et al., 2000). In support of this, defects in chromatin structure in *cacΔhirΔ* double mutant cells have been shown to result in substantially higher rates of transposition of Ty1 and Ty2 elements (Qian et al., 1998). In spite of these technical limitations, my results indicate that mutation of PBM1 alone slightly reduces the fidelity of mitotic chromosome segregation in *hir1Δ* cells, but not in wild type cells.

3.13 CONCLUSIONS AND FUTURE OBJECTIVES

3.13.1 Multiple PCNA binding sites on CAF1

In this chapter, I have shown that CAF1 is a genuine PCNA binding protein and identified motifs in CAF1 that play a role in its interaction with PCNA. Other laboratories have also reported that CAF1 interacts with PCNA (Moggs et al., 2000; Sharp et al., 2001; Shibahara and Stillman, 1999; Zhang et al., 2000). However, several questions regarding the exact sequences involved in CAF1 binding to PCNA (Krawitz et al., 2002; Moggs et al., 2000; Ye et al., 2003) and their importance for CAF1 function *in vivo* remained unanswered. My work reveals that the interaction between CAF1 and PCNA is far more complex than suspected, and some important issues are still unresolved.

First, I showed that CAF1 contains at least two distinct PBMs. In fact, given that CAF1 forms a dimer through the p150 subunit (Quivy et al., 2001), my results argue that the dimeric complex would contain at least four, and possibly up to six PBMs if the putative p60 PBM is included. I demonstrated that the two PBMs of p150 are functionally distinct. PBM1 binds tightly to PCNA *in vitro*, and can inhibit nucleosome assembly and DNA replication *in vitro*. Exchanging the PBM of Lig1 with hp150PBM1 converted this replication factor into a preferential inhibitor of nucleosome assembly. However, mutation of PBM1 within full-length human p150 had little effect on targeting this protein to replication foci *in vivo*. In addition, despite the fact that PBM1 binds strongly to PCNA *in vitro*, a deletion of this motif or even a much larger deletion of the first 296 residues of p150 (Kaufman et al., 1995) had no effect on the protein's ability to promote nucleosome assembly *in vitro*.

In yeast, I have shown that a short fragment derived from the N-terminus of Cac1 that only contains PBM1 binds to PCNA, and this interaction is abolished when the core hydrophobic residues of PBM1 are mutated. This motif is functional in *S. cerevisiae* because mutation of PBM1, but not PBM2, conferred a slow growth phenotype at 18°C. This phenotype was only observed in *hir1* mutant cells, showing that the presence of CAF1 lacking PBM1 or PBM2 does not interfere with the function of Hir proteins in wild type

background. In *hirΔ* cells, the Cac1 PBM1 mutation also conferred a 6.4-fold increase in the incidence of loss of a non-essential chromosome fragment.

In contrast, the PBM2 peptide did not bind to PCNA under any of the conditions tested in this work, and a deletion of PBM2 had no effect on the *in vitro* PCNA binding capacity of human p150. However, deletion of PBM2 in p150 abolished its ability to promote nucleosome assembly during DNA replication and greatly reduced the targeting of p150 to replication foci *in vivo*. As for the study in yeast, it is important to state that the slight increase in the incidence of non-essential chromosome loss is far less prominent than the 180-fold increase in chromosome loss previously reported in *cac1Δhir1Δ* cells (Sharp et al., 2002). Although these studies were performed with a different chromosome fragment from the one used here, the marked difference strongly argues that the mitotic chromosome loss caused by the Cac1 PBM1 mutation is not as pronounced as that resulting from a *cac1* null mutation. This may be because PBM2 is more important than PBM1 for pericentric chromatin assembly and preventing mitotic chromosome loss. Alternatively, PBM1 and PBM2 may be partially redundant for this function. However, the fact that the Cac1 PBM1 mutation resulted in slow growth at 18°C, which was not accentuated by the PBM2 mutation (Figure 3.18), argues that these two motifs are not fully redundant. A third possibility is that the defect in mitotic chromosome transmission in cells where both Cac1 PBMs and *hir1* are mutated may not be as severe as in *cac1Δhir1Δ* cells. This would suggest that CAF1 could promote nucleosome assembly in pericentric chromatin regions independently of its ability to bind PCNA. In *S. cerevisiae*, a fraction of CAF1 is stably associated with pericentric chromatin throughout the cell cycle via an interaction with Sir1 (Sharp et al., 2002). This is an exciting possibility because it suggests that CAF1 may promote nucleosome assembly at pericentric regions in a replication-independent manner. In agreement with this, CAF1 can promote nucleosome assembly in the absence of DNA replication in the SV40 system when present in sufficient amounts (Kaufman et al., 1997). Future studies, requiring more robust assays to quantitate mitotic chromosome loss

may address the relative contributions of the Cac1 PBMs and the Sir1 interaction motif to the function of CAF1 in pericentric chromatin assembly. Given that CAF1 plays a role in silencing of reporter genes integrated at telomeres and the rRNA gene cluster (Kaufman et al., 1997; Smith et al., 1999), it will be worthwhile evaluating the respective roles of the two Cac1 PBMs in the assembly of these other specialised forms of chromatin. Interestingly, the two PBMs are not fully redundant for telomeric silencing as the PBM2 mutation alone confers a significant defect in silencing (Krawitz et al., 2002). However, this defect is less prominent than the one observed in *cac1* null mutants (Krawitz et al., 2002), raising the possibility that PBM1 may also contribute to telomeric silencing.

I have also identified a putative PBM in p60 which is conserved from yeast to humans. However, it is not clear whether this sequence participates in CAF1 binding to PCNA. The only evidence presented here that supports the relevance of this sequence for PCNA binding, is the fact that a peptide derived from the putative PBM of the human p60 inhibits DNA replication. This inhibition is eliminated by mutating the two aromatic residues to alanines, as with other PBMs. Unlike p150, p60 by itself does not bind to PCNA *in vitro* and does not affect PCNA binding by the CAF1 complex under the conditions that I tested (data not shown). However, human p150PBM2 shows exactly the same characteristics *in vitro*, but this motif is clearly important for the interaction of CAF1 and PCNA *in vivo* (Ye et al., 2003), for targeting CAF1 to replication foci and for CAF1 function in yeast (Krawitz et al., 2002). Additional work is needed to address the function of the putative p60 PBM.

3.13.2 Unresolved puzzles

An intriguing dilemma arises from a comparison of the results presented here. In *S. cerevisiae*, the deletion of *cac1* is epistatic with a PCNA mutation known as *pol30-8* for telomeric silencing (Zhang et al., 2000). In contrast, the *pol30-8* mutation results in synergistic defects in telomeric silencing when combined with *hir1* gene disruption (Sharp et al., 2001). This genetic evidence argues that the *pol30-8* mutation interferes with the role of CAF1 in telomeric

silencing, but not that of Hir proteins. A mutation homologous to *pol30-8* in human PCNA bound p150 similarly to WT PCNA *in vitro* (Figure 3.4c). This is consistent with the fact that the *pol30-8* mutation (RD 61,63 AA in *S. cerevisiae* PCNA) affects a region on the edge of the PCNA ring that is not known to participate in interactions with PBM proteins. It is therefore possible that the *pol30-8* mutation inhibits CAF1 activity *in vivo* indirectly. For example, *pol30-8* may block a modification of PCNA or binding of an additional factor that is necessary for CAF1 activity. On the other hand, the *pol30-79* mutation does not block the function of CAF1 in telomeric silencing (Sharp et al., 2001), but *in vitro* both yeast and human PCNA carrying the 79 mutation were defective in binding p150 (Zhang et al., 2000; and Figure 3.4c). Thus, it is not clear why the *pol30-79* mutation does not prevent the contribution of CAF1 to telomeric silencing *in vivo*. For some PBPs the contacts with the central loop and the C-terminus of PCNA are more important for their interaction than the IDCL (Chapados et al., 2004; Eissenberg et al., 1997; Matsumiya et al., 2002). However, this does not seem to be the case with regards to human CAF1 binding to PCNA *in vitro* (Figure 3.4c).

Interestingly, mutations in the C-terminus of PCNA compromise the interaction of yeast FEN1 and Apn2 with PCNA loaded onto DNA, but do not affect the ability of these PBM proteins to bind PCNA in the absence of DNA (Gomes and Burgers, 2000; Unk et al., 2002). By analogy with FEN1 and Apn2, CAF1 may also have two distinct modes of interaction with PCNA in the absence or presence of DNA. In principle, the interaction of PBM1, PBM2 or both could be modulated by DNA. My result showing that CAF1 lacking only PBM2 is severely defective in nucleosome assembly during SV40 replication suggests that PBM2 is particularly important for CAF1 binding to PCNA in the presence of DNA. Additionally, a comparison of my results with those of Ye et al. (2003) suggests that there is a difference between the interaction of CAF1 and PCNA *in vitro* and *in vivo* in the mammalian system. Whereas mutation of PBM2 alone has no effect on PCNA binding *in vitro*, the same mutation dramatically reduces the association of p150 and PCNA *in vivo* (Ye et al., 2003). One prediction of such a model would be that mutations in the C-terminus of PCNA

should block CAF1 activity. Neither Zhang and Stillman nor Sharp et al. tested the *pol30-90* mutant for telomeric silencing in WT and *cac1Δ* cells.

3.13.3 The purpose of two distinct PBMs in CAF1

My work raises the issue of why CAF1 contains two distinct PBMs. In fact, a careful review of the literature reveals that several other PBPs also have more than one PBM: RFC (Fotedar et al., 1996; Montecucco et al., 1998), DNA polymerase δ (Ducoux et al., 2001; Lu et al., 2002; Zhang et al., 1995), DNA polymerase β (Kedar et al., 2002), and uracil DNA glycosylase (Yang et al., 2002). The arrangement of PBMs in RFC p140 is intriguingly similar to that of CAF1 p150. RFC p140 has two PBMs, one in the N-terminus (residues 1-24, Montecucco et al., 1998) and one in a central domain of RFC (NTSIKGFY, residues 695-702 in human p140). The latter domain competes with full-length RFC and inhibits SV40 DNA replication and PCNA loading *in vitro*, and blocks DNA replication *in vivo* (Fotedar et al., 1996). Interestingly, PCNA binding through the PBM located in the central domain is inhibited by CDK phosphorylation of T506 (Salles-Passador et al., 2003).

Several papers suggest that the multi-subunit DNA polymerase δ holoenzyme contains at least two distinct PBMs. Although the p125 catalytic subunit is devoid of PBM and cannot be stimulated by PCNA, a canonical PBM has been identified in the C-terminus of the human p66 subunit (Ducoux et al., 2001). This motif is conserved in non-catalytic subunits of yeast DNA polymerase δ, *S. pombe* Cdc27 (Reynolds et al., 2000) and *S. cerevisiae* Pol32 (Gerik et al., 1998). However, the fact that *POL32* is not an essential gene suggests the existence of at least one other PBM in the other subunits of the enzyme. A motif that resembles the consensus PBM has also been identified in the N-terminus of p50, the small subunit of human DNA polymerase δ (Lu et al., 2002). Notably, in both *S. cerevisiae* (Burgers and Gerik, 1998) and *S. pombe* (Zuo et al., 2000), a two-subunit sub-complex of DNA polymerase δ lacking the subunit equivalent to human p66 can be stimulated by PCNA. However much lower levels of PCNA are needed to stimulate the trimeric enzyme that

includes the p66 homologues. Curiously, the p50 motif is remarkably similar to PBM1b in CAF1 p150 (RLIQMRPFL in p50 and KLIQARLPF in CAF1 p150; Lu et al., 2002).

It may be of significance that both p150 PBMs are somewhat different from the canonical PBM (QXXLXXFF, where L is an aliphatic amino acid and F is an aromatic residue), suggesting that they may have a distinct mode of interaction with PCNA. It is therefore possible that the two CAF1 PBMs have different or only partially overlapping functions. Based on previous work (Krawitz et al., 2002; Ye et al., 2003) and data presented here using mouse and yeast model system (Figures 3.9-3.11 and 3.17 and 3.18), both PBMs contribute to CAF1 function *in vivo*. The synergistic effect of deleting both PBMs *in vivo* in mammalian cells suggests that the two PBMs co-operate in targeting CAF1 to replication foci.

It is tempting to speculate that certain steps in CAF1 function (targeting to DNA replication foci, histone deposition onto DNA, dissociation of CAF1 from histones or its binding to additional newly synthesised histones) may involve a switch from one PBM to the other. An example of a regulated interaction of PBPs with PCNA is involved in mismatch repair. The mismatch recognition heterodimer MSH2-MSH6 dissociates from PCNA upon recognition of a mismatch in DNA (Lau and Kolodner, 2003). Another example, already mentioned earlier is the dual mode of interaction between FEN1 and Apn2 and PCNA, depending on DNA (Gomes and Burgers, 2000; Unk et al., 2002). Recent crystalography work suggests that it is not only separate mutations in *POL30* that affect this interaction, but that different residues in FEN1 are important for interacting with PCNA on and off DNA (Chapados et al., 2004). Pol ε has also been suggested to have a dual mode of interaction involving the front or the back side of PCNA (Maga et al., 1999). Though it is the interaction with the front side that stimulates the DNA synthesis activity of pol ε, the interaction with the back side of PCNA has been postulated to serve a recruiting function, while the front side of the trimer is engaged with other replication factors.

3.13.4 Regulation of PCNA binding by CAF1

Many possible mechanisms may regulate the CAF1-PCNA interaction, some are schematically represented in Figure 3.20. PCNA binding by p21, FEN1 and RFC is negatively regulated by phosphorylation (Henneke et al., 2003b; Salles-Passador et al., 2003; Scott et al., 2000). Phosphorylation of single residues in FEN1 and RFC by cyclin-dependent kinases, in sites not immediately adjacent to the PBMs, is sufficient to inhibit their binding to PCNA, suggesting that phosphorylation inhibits PCNA binding through an allosteric mechanism.

In vitro, CAF1 p60 is phosphorylated by cyclin-dependent kinases that promote either S phase (cyclin A- or E-CDK2) or M phase (cyclin B1-CDK1). Interestingly, maximal nucleosome assembly activity of CAF1 is observed when both CDKs and Protein Phosphatase 1 (PP1) are active in the S100 extract (Keller and Krude, 2000). However, the mechanism by which CDKs and PP1 enhance CAF1 activity is not known. *In vivo*, both CAF1 p60 and p150 are phosphorylated during normal cell cycle progression (Marheineke and Krude, 1998; Smith and Stillman, 1991). In response to UV irradiation in G1 or G2 cells, CAF1 and PCNA are recruited to sites of nucleotide excision repair (Green and Almouzni, 2003; Martini et al., 1998). Interestingly, it is the phosphorylated form of p60 that is predominant in the Triton-resistant chromatin fraction of UV-irradiated cells, whereas in normal cells it is the hypophosphorylated form p60 that is more abundant in the chromatin fraction (Martini et al., 1998). In mitotic cells, the p60 subunit of CAF1 is not bound to chromatin and its low level of nucleosome assembly activity can be stimulated by dephosphorylation (Keller and Krude, 2000; Marheineke and Krude, 1998). By analogy with FEN1 and RFC, it is possible that the binding of CAF1 to PCNA is also modulated by CDK phosphorylation, though it is not clear whether phosphorylation would have a negative or a positive effect on this interaction. In my experiments, phosphorylation did not affect binding of p150 to PCNA, but I did not have an assay to directly measure the degree of p150 phosphorylation. To achieve a conclusive result a more thorough examination is needed.

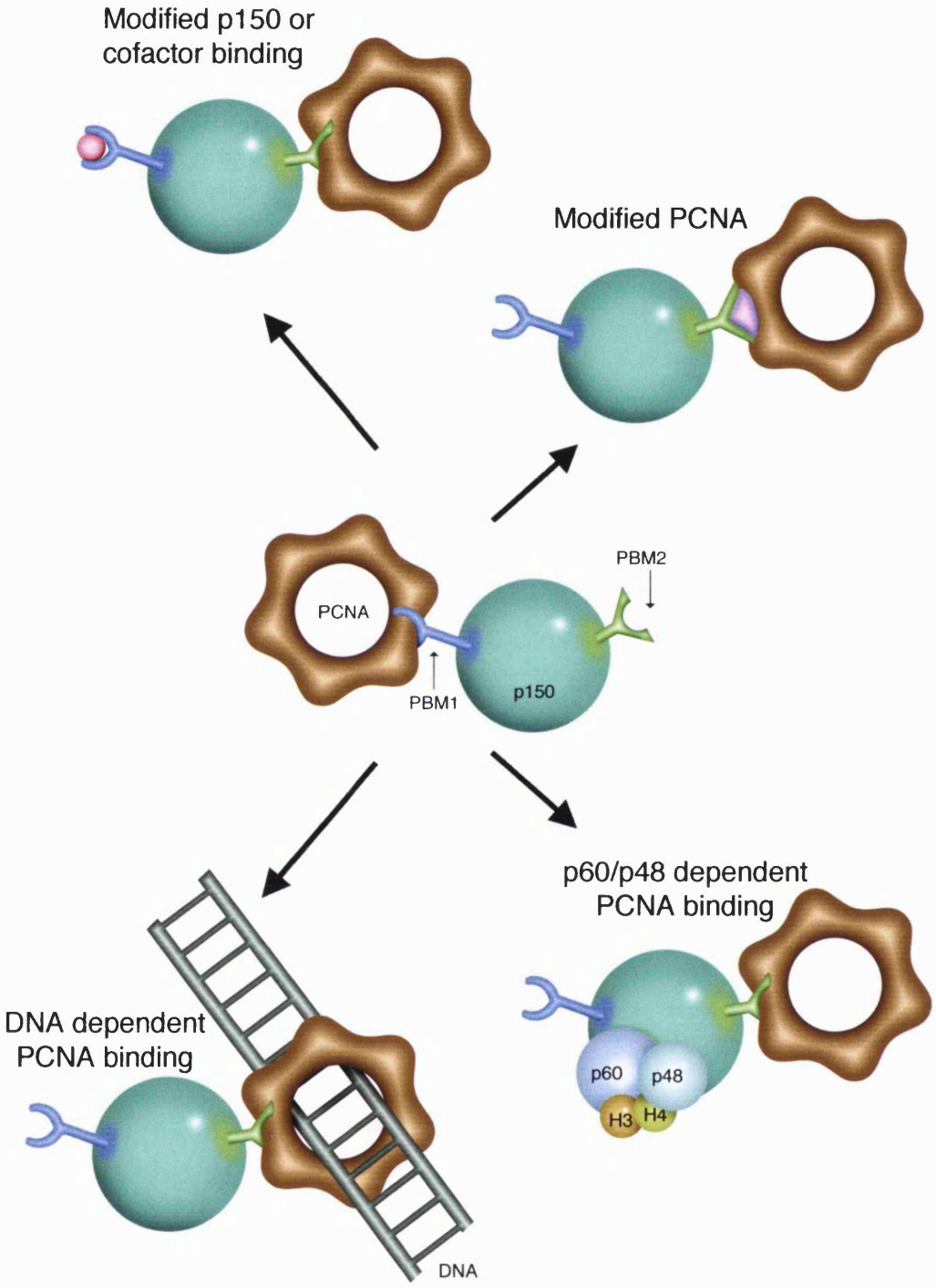

Figure 3.20: Putative mechanisms for PBM switching
I suggest a model whereby p150 binds to PCNA via one PBM and then switches to the other to regulate its activity. PBM switching may occur by modification of p150 or binding to a cofactor which blocks PBM1 or causes conformational changes or otherwise increases the affinity of the second PBM to PCNA. Switching may otherwise occur due to a modification on PCNA or binding of other factors to p150 such as p60 and p48 and/or histones H3/H4. A switch in binding could also occur after loading PCNA onto DNA, as is the case with scPCNA and scFEN1 (see discussion for details).

Another exciting possibility is that acetylation of lysine residues in the CAF1 PBMs is necessary to activate binding to PCNA. PBMs in many proteins usually have a glutamine as the first conserved residue of the motif (Figure 3.1a). In the complex of archaeal RFC and PCNA (Matsumiya et al., 2002), the amide group of the glutamine side chain contributes four hydrogen bonds to the interaction with PCNA. PBM2 inability to bind to PCNA *in vitro* may be due to the presence of a lysine, rather than a glutamine, as the first residue of this motif. By contrast, PBM1b, which binds tightly to PCNA *in vitro*, has a glutamine residue at the corresponding position (Figure 3.1a). Acetylation of the ε-amino group of the PBM2 lysine would mimic a glutamine at that position and thereby may activate PCNA binding.

Importantly, it is clear that CAF1 activity in the SV40 system is dependent on additional unidentified factors. Shibahara and Stillman demonstrated that in order to achieve nucleosome assembly onto pre-replicated DNA carrying PCNA, CAF1 and histones had to be added in the presence of S100 extract (Shibahara and Stillman, 1999). One attractive possibility is that PCNA post-translational modifications may be involved in regulating the interaction between CAF1 and PCNA. Recent studies have shown that a single lysine residue in PCNA can be subject to at least three distinct modifications: sumoylation, mono-ubiquitylation and multi-ubiquitylation (Hoege et al., 2002; Stelter and Ulrich, 2003). The mono- and multi-ubiquitylation of PCNA are respectively involved in two separate pathways of DNA damage tolerance during replication, error-free template switching and error-prone translesion DNA synthesis. PCNA exists also in three forms with regards to acetylation (Naryzhny and Lee, 2003; Naryzhny and Lee, 2004). Interestingly, the relative abundance of these PCNA forms changes as cells progress from G1 into S phase, suggesting that these modifications may contribute to the function of PCNA during S phase.

3.13.5 The dimerisation of p150 molecules

I have shown in this chapter that severe defects in GFP-p150 targeting to DNA replication foci only arose when the dimerisation domain was mutated in conjunction with PBM2 (Figure 3.12). This suggests that CAF1 is targeted to replication foci as a dimer, and that targeting can occur as long as the PBMs in either of the p150 monomers are intact.

In contrast, a mutation of the dimerisation domain that leaves the PBMs intact completely abolishes CAF1 activity *in vitro* (Quivy et al., 2001). In addition, the formation of heterodimers between human and *Xenopus* p150 interferes with CAF1 activity and embryonic development (Quivy et al., 2001). Thus, while a monomer of CAF1 can target to replication foci, dimerisation is important for CAF1 activity.

It is tempting to speculate that the presence of two PBMs in both monomers may allow CAF1 to contact simultaneously two PCNA rings associated with the leading and the lagging strand (see Figure 3.21 for a schematic model). This property may be important to achieve rapid histone deposition onto both sister chromatids behind the replication fork. During replication, parental histone H3/H4 tetramers can be transferred onto either the leading or the lagging (Sogo et al., 1986). Consistent with this, CAF1 is capable of promoting histone deposition onto both the leading and the lagging strand during SV40 DNA replication *in vitro* (Stillman, 1986).

Interestingly, overexpression of a p150 PBM2 mutant causes spontaneous DNA damage and S phase arrest in human cells (Ye et al., 2003). My results raise the possibility that p150 lacking PBM2 may give rise to this phenotype by forming a dimer with endogenous p150 and interfering with its function at the replication fork. This suggests that the active form of CAF1 at the replication fork is a dimer where both p150 subunits need to bind PCNA via PBM2 in order to prevent DNA damage during replication.

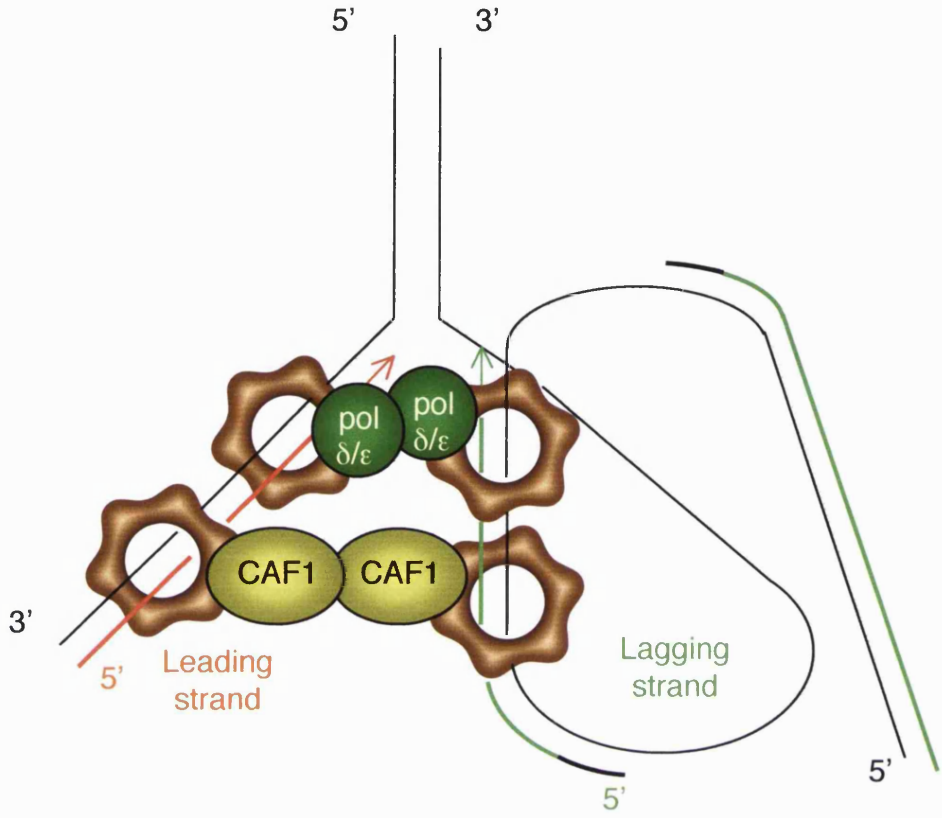

Figure 3.21: Model for simultaneous nucleosome assembly onto both sister chromatids
CAF1 p150 has been shown to dimerise. My work suggests that dimerisation occurs during S-phase and may play a role in targeting p150 to replication foci (Figure 3.12). Therefore, I suggest a model whereby two dimerised CAF1 complexes are bound to two separate PCNA ring on the leading and lagging strand, facilitating chromatin assembly onto both newly formed sister chromatids. The complexed PCNA and DNA polymerases represent the replication machinery. Black line represents parental DNA, red and green lines represent nascent DNA synthesised at a 5'-3' direction on leading and lagging strands, respectively.

3.13.6 The interaction of CAF1 with HP1

Outside of S phase, p150 is targeted to heterochromatin by its interaction with HP1 (Murzina et al., 1999), through the chromoshadow domain of HP1 and a PXVXL motif located within the N-terminal region of p150 (Thiru et al., 2004). Mutating this domain abolishes the recruitment of p150 to pericentric heterochromatin foci outside S phase, but does not influence the targeting of p150 to replication foci throughout S phase (Murzina et al., 1999). In contrast, deleting PBM1, PBM2 or the dimerisation domain does not impair the ability of p150 to associate with pericentric heterochromatin foci outside S phase (data not shown). Furthermore, p150 mutants that are unable to target to sites of DNA replication inappropriately accumulate in pericentric heterochromatin during early S phase. This is in agreement with the fact that HP1 is present in heterochromatin foci throughout S phase (Taddei et al., 1999). In my experiments, it is unclear whether the p150 molecules that accumulate in heterochromatin foci during early S phase were synthesised at that stage of the cell cycle or if they were synthesised prior to S phase and failed to re-localise to replication foci. This is because GFP-p150 was expressed from the CMV promoter, which is active at all stages of the cell cycle. Because HP1 seems to be more abundant in cells than CAF1 (Murzina et al., 1999), the affinity of PBMs for PCNA may be important to prevent the sequestration of CAF1 into pericentric heterochromatin during S phase.

In contrast to its role in nucleosome assembly, my results demonstrate that p150 dimerisation is not necessary for binding to HP1 in pericentric heterochromatin. Consistent with this, the structure of a p150 peptide bound to the chromoshadow domain of HP1 shows that a single p150 peptide binds to an HP1 dimer (Thiru et al., 2004). Additionally, unlike wild type GFP-p150, p150 carrying a PXVXL mutation (which prevents its interaction with HP1) fails to accumulate in pericentric heterochromatin foci even in cells that contain endogenous p150 (Murzina et al., 1999). This suggests either that only the monomeric form of p150 binds to HP1 proteins *in vivo* or that a single p150 PXVXL mutant in a p150 dimer is sufficient to abolish the targeting of the dimer to heterochromatin foci via HP1.

3.13.7 Understanding the sequence of events at the replication fork

During S phase, many distinct PCNA-binding proteins involved in replication, DNA methylation, DNA repair and nucleosome assembly function almost simultaneously at the replication fork.

The work initiated here presents an assay for exploring the mechanisms ensuring that these different PCNA-dependent processes are properly coordinated with each other. For instance, it is now clear that nucleosomes inhibit both uracil removal by UNG2 (Nilsen et al., 2002) and maintenance DNA methylation by DNMT1 (Okuwaki and Verreault, 2004). This suggests that these two PCNA-dependent processes may occur before CAF1-dependent nucleosome assembly behind the replication fork. It may be possible to test this hypothesis using DNA substrates containing uracil or CpG methylation to see if CAF1-dependent nucleosome assembly during replication interferes with uracil removal by UNG2 or with maintenance methylation by DNMT1. One interesting experiment would be to add catalytically inactive forms of UNG2 and DNMT1 that retain their ability to bind PCNA to see if a failure to remove uracil or methylate nascent DNA leads to a delay in histone deposition. This would argue that PCNA-dependent processes need to occur in a given temporal order and that a failure to complete early events such as DNA repair or methylation prevents the execution of subsequent steps such as nucleosome assembly. Interestingly, catalytically inactive mutants of yeast FEN1 exhibit more severe phenotypes than null mutants (Gary et al., 1999). Although other possibilities exist, this result may suggest that the presence of catalytically inactive FEN1 that binds to PCNA may interfere with other PCNA-dependent processes at the replication fork.

My results showing that, unlike p21 peptides, the CAF1 PBM peptides preferentially inhibited nucleosome assembly over DNA synthesis (Chapter 3.10) suggest that variations in the sequences of PBMs in individual proteins may contribute to the regulation of events taking place at the replication fork. Consistent with this, the crystal structures of three different PBM peptides bound to PCNA all show that, in addition to the hydrophobic residues of the PBM core, other residues make important contacts with PCNA (Chapados et

al., 2004; Gulbis et al., 1996; Matsumiya et al., 2002). This hypothesis can be further analysed using PBM peptides from other proteins that supposedly function behind the replication fork, such as DNMT1 and UNG2, in a similar manner to the work presented here. However, it is difficult to imagine that this is the sole mechanism ensuring that the numerous processes in which PCNA participates at the replication fork occur in a well-orchestrated manner. First, the preferential inhibition of nucleosome assembly by CAF1 PBM peptides was only observed in T Ag independent reactions, which result in low levels of DNA synthesis. Second, the range of peptide concentrations in which this effect was observed was very narrow. Within an increase of a few fold in the concentration of peptides, DNA synthesis is inhibited as well. Third, it seems unlikely that individual PBPs access PCNA in a sequential manner that is merely determined by their relative affinities for PCNA. This is because the differences in the affinity of individual proteins for PCNA are very modest and the off-rate of PBM peptides from PCNA is very slow (Maga and Hubscher, 2003). Fourth, cycles of binding and dissociation from PCNA would be incompatible with the known function of at least some PBPs. For instance, DNA polymerase δ most likely remains continuously bound to PCNA to ensure processive leading strand replication. These considerations make it unlikely that the numerous PBPs that contact PCNA at the replication fork all function by sequentially accessing a single PCNA ring.

I propose that multiple PCNA rings are continuously present at the replication fork (Figure 3.13b), and that each PCNA ring is dedicated to a single or to several specific functions (*e.g.* DNA synthesis, DNA methylation, uracil excision, mismatch repair or nucleosome assembly). The multiple rings may progress as carriages in a train-like formation, to enable constant feedback between the replication factors. The ability of pol ε to bind both the front and the back side of PCNA, for example, could involve interactions with two separate PCNA rings in front and behind the polymerase (Maga et al., 1999). This would imply the existence of a mechanism to ensure that each PCNA ring is somehow marked to interact with only one or a few PBPs. 'Marking' may involve modifications of both the PBPs and PCNA. Consistent with this, a

number of protein modifying enzymes are targeted to replication foci by binding to PCNA. These include protein kinases such as cyclin A-CDK2 (Koundrioukoff et al., 2000; Henneke et al., 2003a), histone deacetylases such as HDAC1 (Milutinovic et al., 2002) and p300, an enzyme that has both ubiquitylation and acetylation activities (Grossman et al., 2003; Hasan et al., 2001a). p300 can acetylate human FEN1 (Hasan et al., 2001b) at sites immediately adjacent to FEN1 PBM. Recently, the human bypass polymerase η has been demonstrated to specifically bind to mono-ubiquitilated PCNA following UV irradiation. This interaction was mediated by both a PBM and a putative "CUE domain", introducing a mechanism for identification of specifically marked PCNA (Kannouche et al., 2004).

As stated earlier, during S phase PCNA is sumoylated (Hoege et al., 2002) and subjected to acetylation (Naryzhny and Lee, 2003; Naryzhny and Lee, 2004). Future studies to identify sites of post-translational modifications on CAF1 and the forms of PCNA bound to CAF1 or other PBPs may shed some light over the mechanisms that prevent CAF1 and histone deposition from interfering with other PCNA-dependent processes at the replication fork.

CHAPTER 4 – A SEARCH FOR CAF1 BINDING PROTEINS

4.1 INTRODUCTION

The three subunits of the CAF1 protein interact with several partners. The p150 subunit binds to the other two subunits of CAF1, p60 (Kaufman et al., 1995) and p48 (Cac3 in *S. cerevisiae*; Krawitz et al., 2002) and histones H3/H4 (Shibahara et al., 2000). Mammalian p150 also binds directly to HP1 proteins (Murzina et al., 1999; Thiru et al., 2004). The function of this interaction is currently unknown. However, in *S. cerevisiae* the Cac1 subunit binds to the heterochromatin protein Sir1, which facilitates the role of CAF1 in pericentric chromatin function and mitotic chromosome segregation (Sharp et al., 2002). Sir1 is not conserved in higher eukaryotes, and the interaction between CAF1 p150 and HP1 proteins may have a functionally analogous role. As discussed in the previous chapter, p150 also binds to PCNA and this interaction is clearly important for the function of CAF1 in nucleosome assembly during replication (Sharp et al., 2001; Shibahara and Stillman, 1999; Zhang et al., 2000). The p60 subunit binds to histones H3/H4 (Shibahara et al., 2000) and to Asf1 (Mello et al., 2002; Tyler et al., 2001). This interaction is likely to play an important role in the stimulation of CAF1 activity by Asf1 (Krawitz et al., 2002; Tyler et al., 1999). In addition, CAF1 is clearly phosphorylated *in vivo* (Marheineke and Krude, 1998; Martini et al., 1998; Smith and Stillman, 1991), and can be phosphorylated *in vitro* by cyclin-dependent kinases (CDKs). CDK inhibitors interfere with CAF1 activity in the SV40 DNA replication system (Keller and Krude, 2000).

There were several motivations to look for additional CAF1 binding partners.
i. An exhaustive screen for CAF1-associated proteins has not yet been conducted and could potentially reveal some important insights into the mode of action of CAF1 during nucleosome assembly. For instance, the only known PCNA mutation that interferes with the contribution of CAF1 to telomere silencing in *S. cerevisiae* (*pol30-8*, which changes residues R61 and D63 to alanine) affects the edge of the PCNA ring, a region that according to the available crystal structures, is not involved in interactions with PBM proteins

(Chapados et al., 2004; Gulbis et al., 1996; Matsumiya et al., 2002). One possibility is that an as yet unidentified CAF1-associated protein is involved in contacting this region of PCNA. Another example is that although the three subunits of CAF1 bind very tightly to histones H3/H4 (Shibahara et al., 2000; Vermaak et al., 1999; Verreault et al., 1996), it is unclear how the histones are transferred from CAF1 to DNA and subsequently joined by H2A/H2B dimers to complete the formation of nucleosome core particles.

ii. The identification of CAF1-associated proteins is likely to provide some information regarding the more poorly understood functions of CAF1, such as its role in pericentric heterochromatin.

iii. Preliminary results suggest that CAF1 in the S100 extract may be phosphorylated in a CDK independent manner (S. Lorain and T. Rolef Ben-Shahar, unpublished).

iv. Sedimentation and immunoprecipitation studies have shown that both p60 (Kaufman et al., 1995; A. Verreault, unpublished) and p48 (Marheineke and Krude, 1998; Verreault et al., 1996) are present in excess over p150 in mammalian cell extracts, suggesting that these two subunits may be involved in additional functions as part of other complexes. This is clear in S100 extracts used for replication-dependent nucleosome assembly, which contain p60 and p48, but not p150 (Kaufman et al., 1995). Furthermore, a substantial fraction of the p60 and p48 subunits remain in the supernatant after immunodepletion of p150 from human cell nuclear extracts (Figure 4.2b and data not shown). Consistent with this, Cac3 in *S. cerevisiae* plays a unique role in suppression of the RAS pathway that is independent of the other two subunits of CAF1 (Johnston et al., 2001; Zhu et al., 2000). Remarkably, the role of Cac3/p48 in suppressing the RAS pathway is conserved in *C. elegans* (Lu and Horvitz, 1998; Solari and Ahringer, 2000). In higher eukaryotes, p48 also binds to the Rb tumour suppressor protein (Qian et al., 1993), and is a subunit of several HDAC complexes (Ahmad et al., 2001; Taunton et al., 1996; Zhang et al., 1997; Zhang et al., 1998).

In contrast, p60 has not been described in association with complexes other than CAF1. However, when budding yeast cell lysates were fractionated into soluble and chromatin fractions, the fraction of Cac2 that was bound to

chromatin was unaffected by PCNA mutations that prevented the association of Cac1 with chromatin (Zhang et al., 2000). This strongly suggests that Cac2, and perhaps p60 in higher eukaryotes, interacts with chromatin in a Cac1- and CAF1-independent manner. I decided to use a proteomics approach that could potentially identify many interacting partners by immunoprecipitation of either CAF1 or p60 from crude cell extracts and identifying the associated proteins by mass spectrometry.

4.2 MULTIPLE POLYPEPTIDES CO-PRECIPITATE WITH p60 AND p150

I prepared "nuclear extracts" and "chromatin extracts" as described in Chapter 2.10 from 80 litres of HeLa cells grown in suspension up to a cell density of roughly 6 x 10^5 cells/ml. These extracts were treated with polyethyleneimine (PEI) to precipitate DNA and RNA (Gegenheimer, 1990), and to prevent the non-specific co-precipitation of proteins associated with the same nucleic acid or chromatin fragments. PEI treatment removed DNA from the extracts (Figure 4.1a, right panel), while the protein content remained essentially similar (as detected by Bradford assay and by silver staining – Figure 4.1a left panel).

50 ml of each extract (corresponding to roughly 16-18 litres of starting material for the nuclear extract or 5-6 litres for the chromatin extract) were pre-incubated with anti-T Ag (419) mAb cross-linked to protein G-Sepharose beads to remove proteins that bind non-specifically to antibody beads. The supernatant from this step was then incubated with 0.5 ml of SS1 (anti-p150) mAb cross-linked to protein G-Sepharose beads or with non-specific rabbit IgG beads as control. After ON incubation, the supernatant from the SS1 beads was further incubated with SS24 (anti-p60) beads to identify proteins that bind to p60, but not CAF1. Beads were washed four times with 50 ml of binding buffer, eluted with high salt concentrations (5 M LiCl in binding buffer for SS1 and 3.5 M $MgCl_2$ in binding buffer for SS24 (Kaufman et al., 1995; Verreault et al., 1996), and then dialysed against S100 buffer (Figure 4.1.b). A fraction of each eluate (1-5%) was analysed in an SDS-10% polyacrylamide gel (Figure 4.2a). This gel showed that many polypeptides were present in the elution from

SS1 and SS24 but not the control antibody beads (compare lanes 3 and 4 with lane 5). Recombinant CAF1 was used as a point of reference in the gel. Samples were also analysed by Western blotting to examine the presence of CAF1 subunits and other known CAF1 binding proteins in the eluates. Figure 4.2b shows that SS1 co-precipitated p150, p60 as well as histone H3 from both the nuclear extract and the chromatin extract (lanes 2, 4 and 7). The subsequent purification with SS24 immunoprecipitated substantial amounts of p60 from both extracts, but did not co-precipitate any p150 or histone H3 (Figure 4.2b, lanes 3 and 5), suggesting that p60 is present in excess of CAF1 in these extracts and exists in a form that is devoid of histone H3. In addition to p150 and p60, SS1 beads also co-precipitated PCNA (Figure 4.2b, lane 7). After incubation with SS1 beads, no p150 was left in the extract, and further incubation with SS24 antibody beads confirmed that the residual p60 immunoprecipitated from these extracts was not bound to p150 (Figure 4.2b, lanes 3 and 5; see also Marheineke and Krude, 1998). For detection of p60, the membranes in these experiments were probed with SS53, a p60 antibody that recognises predominantly the hyperphosphorylated form of p60, and thus gives rise to a single band in Western blots. However, other modified forms of p60 are likely to be in the eluates as SS24 recognises all known forms of p60 indiscriminately (S. Lorain, unpublished).

a.

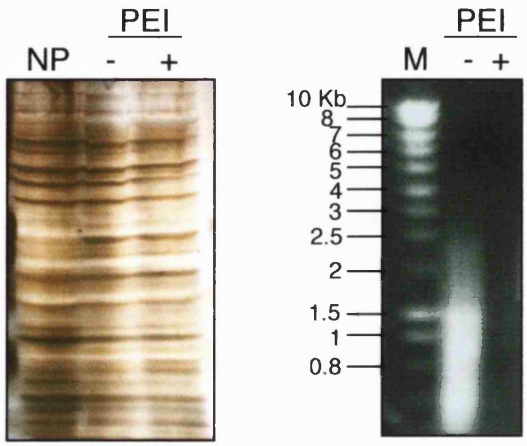

b.

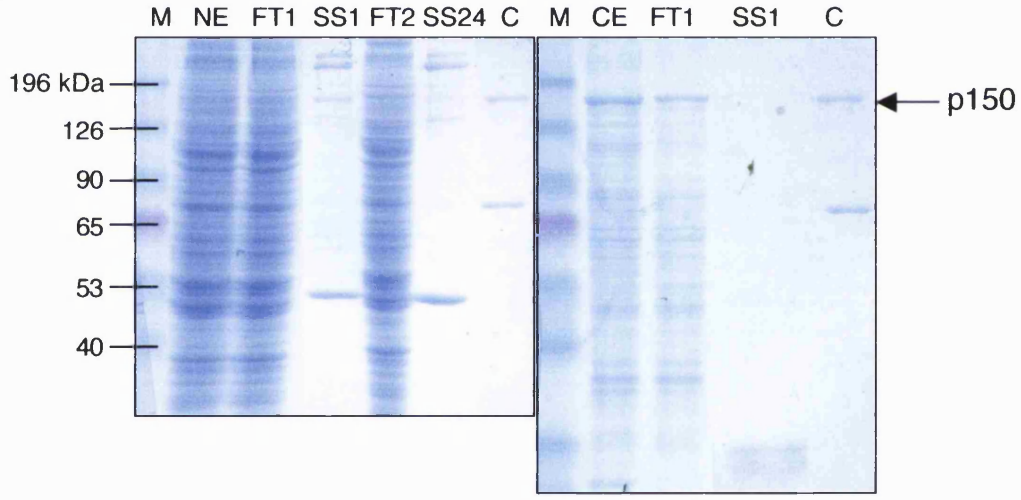

Figure 4.1: Immunoprecipitation of p150 and p60 from cell extracts

a. Preparation of chromatin extract. The pellet from preparation of nuclear extract (NP) was sonicated and spun down (see Chapter 2.10). The resulting extract was incubated with PEI and ultra-centrifugated to precipitate remaining DNA and RNA fragments. The silver stained SDS-PAGE in the left panel compares the protein composition in the extract before (-) and after (+) PEI treatment. The ethidium bromide stained agarose gel in the right panel shows DNA purified from the chromatin extract before (-) and after (+) PEI treatment and demonstrates that essentially all the DNA was removed from the extract. (M) DNA hyperladder.

b. Examples of the immunoprecipitates from nuclear (left panel) and chromatin extracts (right panel). (M) Protein marker. (NE) Nuclear extract. (FT1) Flow through after incubation with SS1 antibody beads. (SS1) 1% of the proteins bound to SS1 antibody beads. (FT2) Flow through after incubation with SS1 and SS24 beads. (SS24) 1% of the proteins bound to SS24 antibody beads. (C) Recombinant CAF1. (CE) Chromatin extract.

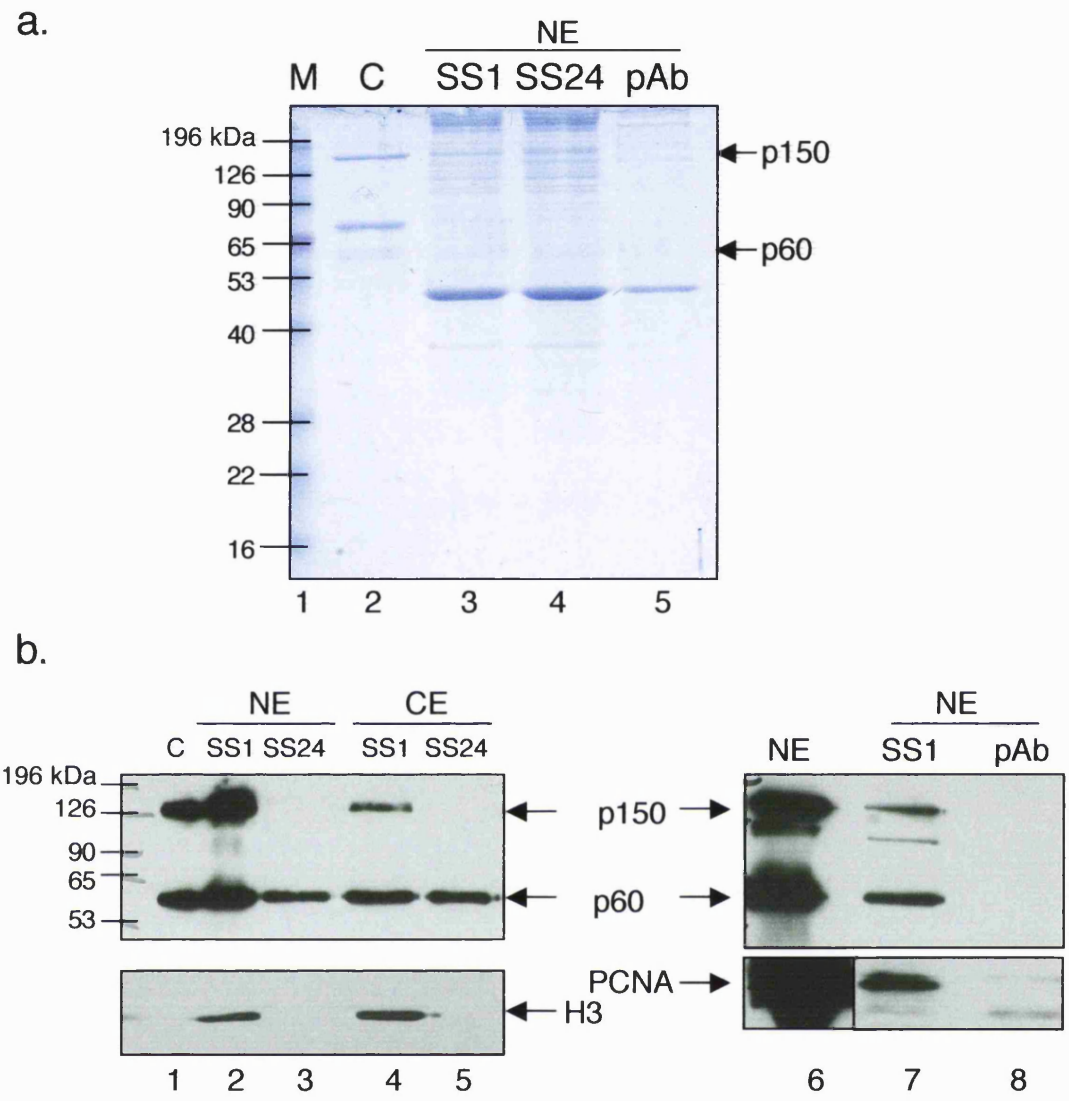

Figure 4.2: Preliminary analysis of immunprecipitated samples

a. A Coomassie staining of immunoprecipitates from nuclear extract (NE). (C) Recombinant CAF1. (SS1) 5% of the proteins bound to SS1 antibody beads. (SS24) 5% of the proteins bound to SS24 antibody beads. (pAb) 5% proteins eluted from control beads with non specific rabbit antibodies.

b. Immunoprecipitates were analysed by SDS-PAGE and Western blotting. Symbols are as in Figure 4.1c. Samples were probed with SS1, SS53, PC10 and H3C for detection of p150, p60, PCNA and H3, respectively.

4.3 2D GEL AND MASS SPECTROMETRY ANALYSIS

It was clear that there were too many bands in the affinity-purified samples to permit their unambiguous identification by mass spectrometry from standard SDS-polyacrylamide gels. Attempts to further separate CAF1 and associated proteins from proteins that bound non-specifically to the beads by gel filtration resulted in significant protein losses. Both p60 and p150 eluted in a very broad peak, which may suggest that they are involved in multiple complexes (data not shown). Therefore, rather than purifying the complexes further, I decided to resolve the protein mixtures eluted from the antibody beads by two-dimensional gel electrophoresis. The samples were first separated on a thin strip of gel according to their isoelectric point (pI). For the second dimension, the gel strip was rotated 90° and the proteins were resolved according to mass by conventional SDS-PAGE. The buffers and equipment used for 2D gel electrophoresis are described in Chapter 2.4. I used a strip with the broadest pH range available (pH 3-10) in order to keep most of the proteins in the sample within the gel. Although a strip with a narrower pH range would give better resolution, the proteins with pI outside the chosen range will migrate beyond the edges of the strip. Even with the pH 3-10 strip, histones (with a theoretical pI of 11.13 and 11.36 for H3 and H4, respectively) ran outside the strip. However, there are only a few other proteins that have such extreme pI.

Examples of 2D gels are presented in Figures 4.3-4.6. Similar patterns of protein spots were reproduced in at least two separate sets of experiments. Affinity-purified samples from the nuclear extract with p150 antibodies showed a line of consecutive protein spots that migrate between pI 5 and 6 and have a molecular mass between the 116 and 200 kDa markers (Figure 4.3a, purple square). This roughly corresponds to the calculated pI of p150 (5.77) and the multiple spots may reflect modified forms of p150. These spots were present in samples eluted from SS1 but not control (Figure 4.3b) or SS24 beads (Figure 4.4b). Based on Western blots, the p150 subunit was also present in samples affinity-purified from chromatin extracts (Figure 4.2b) but cannot be seen in Figure 4.5 because of faulty scanning.

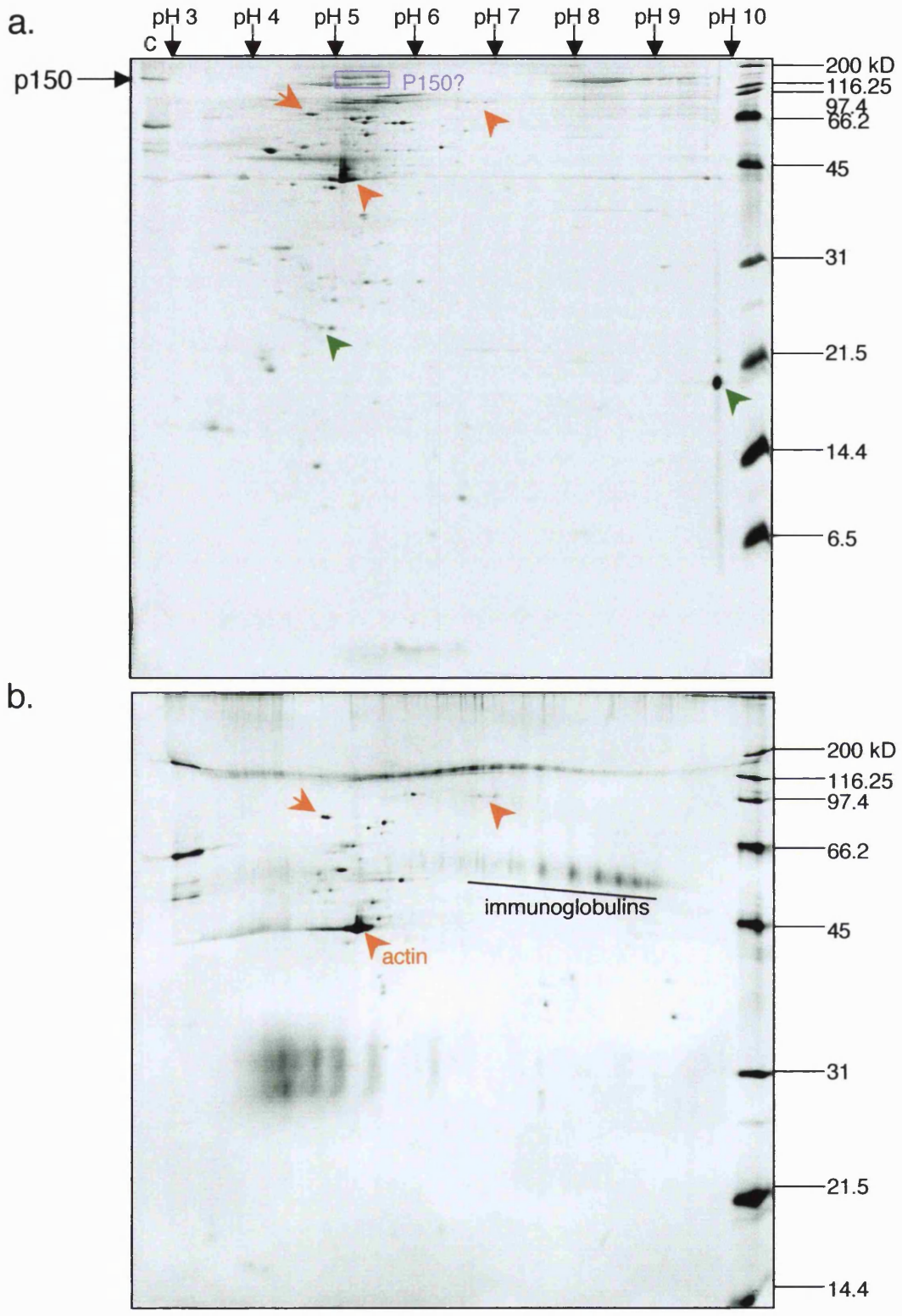

Figure 4.3: 2D gel analysis of proteins that co-immunoprecipitated with p150 from nuclear extract versus control

Proteins affinity purified from nuclear extract with either SS1 (**a.**) or control beads (**b.**) were analysed by 2D gels (see Chapter 2.4 for details). Red arrows indicate examples of protein spots present in both gels; green arrows indicate examples of proteins that are only present in one sample but not the other; purple square marks the possible spots of p150; residual antibodies eluted from the beads are also marked. Protein spots present in (a) but not (b) were excised for further analysis by mass spectrometry. Protein markers and recombinant CAF1 (c) were used for size reference at the right and left end of the gels, respectively.

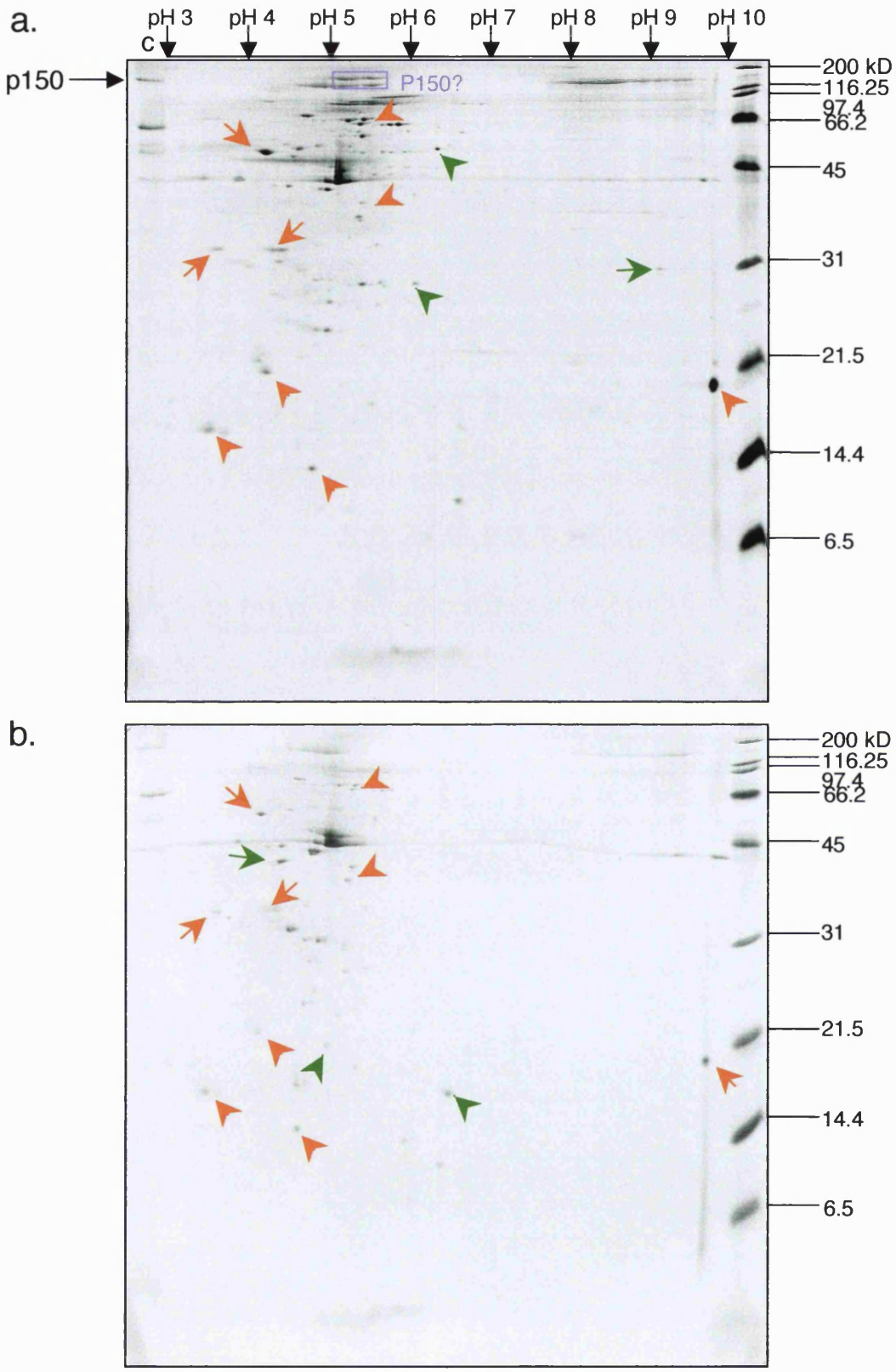

Figure 4.4: 2D gel analysis of proteins that co-immunoprecipitated with p150 or p60 from nuclear extract

Proteins affinity purified from nuclear extract with either SS1 (**a.**) or SS24 beads (**b.**) were analysed by 2D gels. Arrows are as in Figure 4.3. Protein spots were excised for further analysis by mass spectrometry.

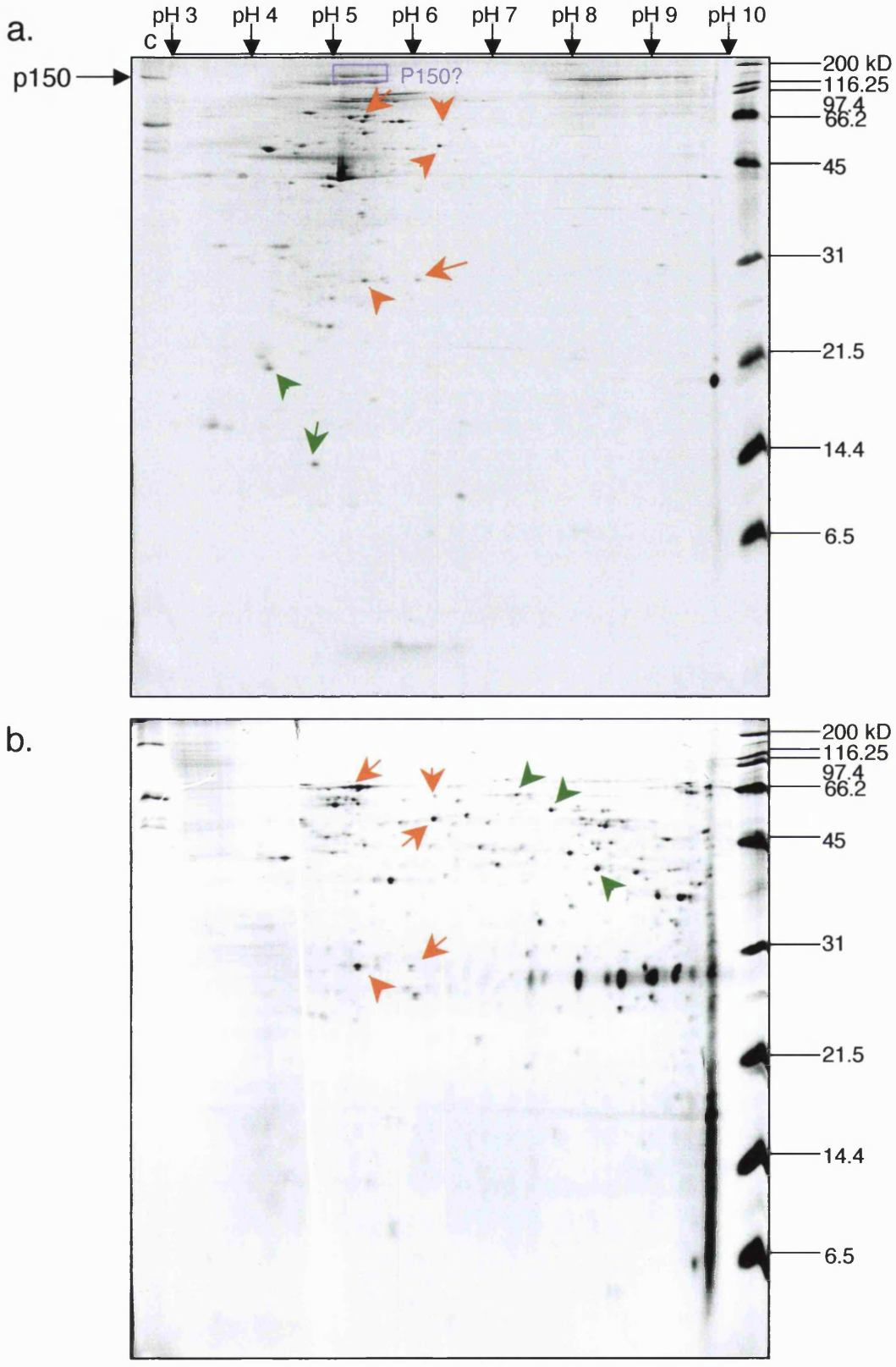

Figure 4.5: 2D gel analysis of proteins that co-immunoprecipitated with p150 from nuclear versus chromatin extract

Proteins affinity purified with SS1 beads from either nuclear extract (**a.**) or chromatin extract (**b.**) were analysed by 2D gels. Arrows are as in Figure 4.3. Protein spots were excised for further analysis by mass spectrometry.

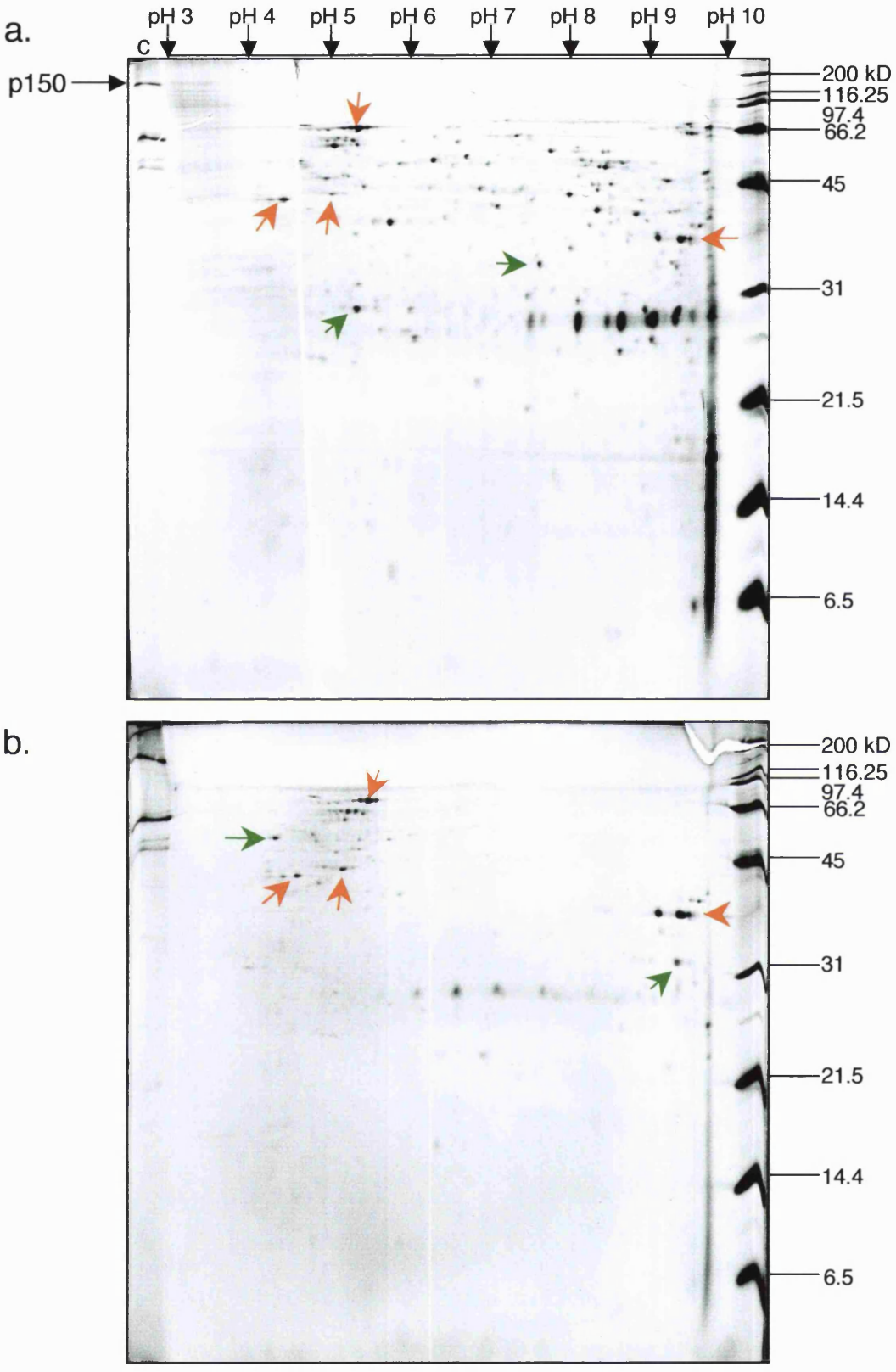

Figure 4.6: 2D gel analysis of proteins that co-immunoprecipitated with p150 or p60 from chromatin extract

Proteins affinity purified from chromatin extracts using either SS1 (**a.**) or SS24 beads (**b.**) were analysed by 2D gels. Arrows are as in Figure 4.3. Protein spots were excised for further analysis by mass spectrometry.

The spots corresponding to p60 (theoretical pI = 7.18) were not clearly visible in any of the gels. This is most likely due to multiple levels of phosphorylation (or other modifications) on this protein (Marheineke and Krude, 1998; Martini et al., 1998), which effectively reduces the amount of p60 present in each spot.

By comparing the eluates from p150 (SS1) and p60 (SS24) antibody beads with that from the control antibody beads, and examining both similarities and differences between the samples derived from nuclear extracts and chromatin extracts, I selected many protein spots that were analysed by mass spectrometry. In Figures 4.3-4.6, red arrowheads point at examples of protein spots common to both gels being compared, while green arrowheads show examples of proteins that were only present in one of the two gels. Unfortunately, although I excised over a hundred protein spots, most of the proteins were unidentifiable by mass spectrometry. Several proteins were presumably below the threshold of detection. Many other spots contained predominantly cytokeratins, which are a common contaminant. Other suggested identifications did not match the calculated mass and pI of the corresponding proteins and were not pursued further.

4.4 DNA POLYMERASE ∝ / PRIMASE

An interesting candidate that was identified among the proteins bound to p60 isolated from the nuclear extract was the large subunit of primase. A similar spot was excised from the gel derived by immunoprecipitation of p150 from nuclear extract, However this protein spot was not identified by mass spectrometry and it was therefore unclear whether primase was co-immunoprecipitated in this fraction as well. DNA polymerase a/primase (pol α/primase) synthesises short primers that consist of approximately 10 nt of RNA and 30 nt of DNA (Bullock et al., 1991; reviewed in Hubscher et al., 2002). These primers are essential both for the initiation of leading strand synthesis and the synthesis of each Okazaki fragment during lagging strand replication. Because CAF1 and pol α/primase are both present at the replication fork, it is possible that the interaction between pol α/primase and

CAF1 is indirect and bridged through DNA. Although only the large subunit of primase was identified by mass spectrometry other subunits may have also been present in the affinity purified fraction, but were not identified due to technical problems. Alternatively, it is possible that only this subunit was co-immunoprecipitated with CAF1.

Although recombinant DNA pol α/primase can be expressed and purified in an active form from a baculovirus expression system, the procedure is quite elaborate (Stadlbauer et al., 1994). I therefore used pol α/primase partially purified from human cells (Chapter 2.10) to rapidly test its binding to recombinant CAF1. However, the results of several such binding assays were inconclusive (data not shown). The possibility of a direct interaction needs to be investigated using purified subunits of the DNA polymerase a/primase holoenzyme (Stadlbauer et al., 1994) and specific antibodies (Tanaka et al., 1982).

4.5 DISCUSSION

I set out to look for novel binding partners of CAF1 p60 and p150 by immunoprecipitating the proteins from crude HeLa cell extracts and identifying co-precipitated proteins by mass spectrometry. Unfortunately, I was forced to abandon this approach because of technical difficulties. First, even though I started with 80 litres of HeLa cells, the relatively low abundance of CAF1-associated proteins made their identification by mass spectrometry rather difficult. In addition, at the time when I initiated this work, the Cancer Research UK mass spectrometry laboratory with which I collaborated was just starting. Many technical difficulties with the mass spectrometry equipment led to very frequent failure in protein identification. Therefore, the work presented here is very preliminary.

4.5.1 DNA polymerase α/primase, a potential CAF1 binding protein

I have identified pol α/primase as a potential partner of CAF1, but this result remains to be confirmed by pull down assays using purified proteins. My results cannot exclude the possibility that CAF1 may only bind to pol a/primase indirectly through other proteins or nucleic acids. Interestingly, a potential interaction between pol α/primase and CAF1 was also recently reported by another group (Muzi-Falconi et al., 2003). The authors identified many proteins that co-purified with pol a/primase, and it was therefore unclear whether CAF1 was co-purified through a direct interaction.

Pol α/primase synthesises primers for leading and lagging strand replication. For leading strand replication, DNA pol a/primase is required only once at the initiation step, whereas a new primer is needed for each Okazaki fragment during lagging strand replication. In contrast, CAF1 functions continuously to deposit histones onto either the leading or the lagging strand behind the replication fork. The *in vitro* assay for nucleosome assembly during SV40 DNA replication would be helpful to dissect the function of a putative interaction between pol a/primase and CAF1. However, because pol α/primase is essential for DNA replication on which CAF1 activity is dependent, the assay would have to be modified accordingly. If pol α/primase or indeed primase function with CAF1 is independent of it's primer synthesis function, this may be possible using primed single stranded circular DNA as substrate for leading strand synthesis in a purified system, such that pol α/primase is completely dispensable for synthesis of the complementary DNA strand by pol δ. The use of the complete SV40 system would first require the identification of pol α/primase mutants that do not interact with CAF1 but preserve the primase and DNA polymerase activities, which are essential for SV40 DNA replication, and the depletion of endogenous pol α/primase complexes. Alternatively, it may be easier to identify CAF1 mutants that do not bind to pol a/primase.

Interestingly, pol α is involved in heterochromatin structure and function. For instance, in budding yeast, pol α mutations cause telomere lengthening and

defects in rDNA silencing (Adams Martin et al., 2000; Smith et al., 1999). In fission yeast, a specific mutation in the catalytic subunit of pol α (*swi7-1*) disrupts heterochromatin-mediated transcriptional silencing at the mating-type region and at centromeres (Nakayama et al., 2001). This mutation is interesting, because it does not appear to affect the function of pol α in replication. Swi7 binds directly to the heterochromatin protein 1 (HP1) family member Swi6 (Eissenberg and Elgin, 2000; Lorentz et al., 1994) and this interaction is disrupted by the *swi7-1* mutation, resulting in reduced association of Swi6 with heterochromatin at the centromeres, telomeres and the mating-type regions, and in silencing defects in *swi7-1* cells (Nakayama et al., 2001). Intriguingly, the *swi7-1* mutation that abrogates Swi6 binding to pol a is located only 13 amino acids before a putative PXVXL motif, which is crucial for the interaction of CAF1 and other proteins with HP1 family members (Thiru et al., 2004). Hence, it may be possible to investigate the connection between CAF1 and pol α/primase using yeast as a model system.

FACT (Facilitates Chromatin Transcription) is an evolutionarily conserved and very abundant dimeric protein that is essential for transcription of cyclin genes (Belotserkovskaya et al., 2004). Human FACT was originally purified through its ability to promote transcription elongation by displacing H2A-H2B from nucleosomes in front of RNA polymerase (Belotserkovskaya et al., 2003; Orphanides et al., 1998; Orphanides et al., 1999). However, FACT was also recently shown to promote nucleosome re-assembly behind RNA polymerase (Belotserkovskaya et al., 2003). This is interesting because FACT binds to DNA polymerase a/primase (Belotserkovskaya et al., 2004) and in *S. cerevisiae*, hypomorphic mutations in the genes encoding the two subunits of FACT (*SPT16* and *POB3*) are lethal in combination with *hir* or *asf1* null mutations but, surprisingly, not a *cac1* mutation (Formosa et al., 2002). This suggests that FACT may have a role in replication-dependent nucleosome assembly, perhaps through its interaction with DNA polymerase a/primase.

4.5.2 Insights from 2D gel analysis

It is interesting to note that the 2D gel patterns obtained from each co-immunoprecipitation were reproducibly different, depending on whether I used nuclear or chromatin extracts and whether the immunoprecipitation was performed using p150 or p60 antibody beads. Some differences were not informative. For instance, actin, a very abundant protein and a common contaminant in immunoprecipitation experiments, was only found in samples immunoprecipitated from nuclear extracts and was absent from those derived from chromatin extracts. Interestingly, samples immunoprecipitated with p150 from chromatin extracts were repeatedly enriched in highly basic proteins in comparison to samples prepared from nuclear extracts (compare pI range 8-10 in Figure 4.5a and b), consistent with the chromatin fraction being enriched in basic DNA binding proteins. Other differences, such as those observed between the samples immunoprecipitated with p150 or p60 antibodies from the nuclear extract (Figure 4.4) may be functionally significant. Furthermore, the fact that samples immunoprecipitated with p60 from chromatin extracts (Figure 4.6) are not enriched in basic proteins suggests that these specifically associate with CAF1 but not p60 complexes that lack p150. With the continuous development of protocols for identifying proteins by mass-spectrometry from nanogram quantities of starting material, this method may still prove to be a useful tool to identify CAF1 interacting proteins.

CHAPTER 5 –
PRELIMINARY EXPRESSION ANALYSIS OF *caf1* AND *asf1* MUTANTS AND THE SEARCH FOR NOVEL NUCLEOSOME ASSEMBLY FACTORS

5.1 INTRODUCTION

In budding yeast, disruption of the genes encoding any one or all three subunits of the CAF1 protein causes minor defects in telomeric- (Enomoto et al., 1997; Kaufman et al., 1997), rDNA- (Smith et al., 1999a) and mating type silencing (Enomoto and Berman, 1998) as well as mild sensitivity to UV irradiation (Game and Kaufman, 1999). This strongly suggests that other nucleosome assembly factors are redundant with CAF1. One such pathway involves the participation of Asf1 and Hir proteins. Mutant strains lacking both CAF1 and any of the four *HIR* genes (*hir1*, *hir2*, *hir3* or *hpc2*) or *asf1* have much more pronounced silencing defects than either single mutant (Kaufman et al., 1998; Tyler et al., 1999). In contrast to the single mutants (Monson et al., 1997), the double mutant cells exhibit a slow growth phenotype and defects in chromatin structure (Kaufman et al., 1998). In spite of this, they remain viable (Kaufman et al., 1998). This led me to ask whether other nucleosome assembly factors can compensate for the loss of the CAF1 and Asf1/Hir–mediated nucleosome assembly pathways.

5.2 MICRO-ARRAY ANALYSIS

In organisms where the complete genome has been sequenced, such as *S. cerevisiae*, micro-array technology allows comprehensive analysis of gene expression. I used the GeneChip® yeast genome S98 array (Affymetrix) to compare the gene expression patterns of wild type (W303), *cac1Δ* (yeast strain YJB469; Enomoto et al., 1997), *asf1Δ* and *asf1Δcac1Δ* strains (ARY01 and YAV13; see Table I.III). The expression of the entire yeast genome can be monitored using this micro-array chip. The chip contains probes for approximately 6,400 Open Reading Frames (ORFs) of the *Saccharomyces cerevisiae* strain S288C including all the ORFs identified by the *Saccharomyces* Genome Database (SGD) and the Munich Information Centre for Protein Sequences (MIPS). A number of ORFs from other strains as well as

genes for mitochondrial proteins and Ty proteins are also represented. In addition, putative ORFs that have been tentatively identified by Serial Analysis of Gene Expression (SAGE; Velculescu et al., 1997) are also represented. In total, approximately 7,000 sequences are represented in a single 'Yeast Genome S98' chip, under nearly 10,000 entries, allowing for repetition as an additional internal control. Labelled RNA samples from each strain were prepared as described in Chapter 2.3, and then sent to the UK HGMP Resource Centre where hybridisation and data collection were carried out.

5.3 GENERAL ANALYSIS OF MICRO-ARRAY DATA

Together with Dr. Simon Tomlinson at the Cancer Research UK Computational Genome Analysis Laboratory, I analysed the expression profile of these strains using GeneSpring 6.0 software (Silicon Genetics). Proper statistical examination of micro-array requires replicas of the experiments, which are missing in this study because this analysis was only carried out as a pilot experiment. Consequently, the analysis described in this chapter is necessarily tentative and the changes in gene expression reported here should be confirmed either by repeating the micro-array experiments or using an independent approach such as Northern blotting.

Because many of the probes on the chip do not correspond to actual genes, and some genes have multiple probes for the detection of their expression, I will use the generic term "entry" to refer to a single micro-array probe.

In order to analyse the raw micro-array results it is essential to normalise the data. The GeneSpring software offers several normalisation procedures. We used the following steps in this order:

1. Data transformation: All measurements smaller than 0.01 were given the value 0.01. This was to eliminate negative values and very low measurements which are irrelevant in the context of this analysis.
2. Per chip: Data from each chip was normalised to the 50th percentile. Per chip normalisation accounts for chip-wide variations in intensity. Such variations may be due to inconsistent washing, inconsistent sample

preparation, or other micro-array production or microfluidics imperfections. In this procedure the middle point of each sample is determined (so half the measurements are lower than this value and half are higher) and so the deviation of each measurement on each chip from the median of that chip is known, allowing for a normalised comparison between chips.

3. Per gene: Each gene was normalised across the experiment to a specific sample. In this normalisation, each gene is divided by the intensity of that gene in a specific control sample or by the average intensity in several samples. This step has a strong effect on the representation of the results as each option puts an emphasis on a different aspect. After careful consideration we decided that for this study, normalising to the wild type strain was most appropriate.

By normalising all the samples to the profile of the wild type strain, it is immediately apparent that the expression profiles of all three mutants are very different from that of the wild type strain. At least in part, this may be due to the fact that I isolated RNA from asynchronous populations of yeast cells. Although *cac1Δ* cells do not have any apparent defect in cell cycle progression, *asf1Δ* and, to a greater extent, *asf1Δcac1Δ* cells exhibit a delay in progression through G2 and M phase of the cell cycle (Tyler et al., 1999). In these two strains, the transcripts derived from genes expressed in G2/M phase may therefore be falsely over-represented. According to Gene Ontology (GO) annotations (see below), RNAs derived from M phase-specific genes were not abnormally abundant in these two strains. This suggests that the defects in cell cycle progression in *asf1Δ* or *asf1Δcac1Δ* cells are not sufficiently pronounced to result in a marked accumulation of G2/M transcripts. This is in accordance with the doubling time of *asf1Δ* and *asf1Δcac1Δ* cells being only 130% and 160% longer than that of wild type cells (Tyler et al., 1999). However, it should be noted that the list of GO annotated genes is very limited. Furthermore, the M-phase GO category includes only M-phase regulators.

Because only one micro-array was analysed for each strain, it is not possible to ascertain whether small changes in expression are really significant.

However, relative to wild type cells, the magnitudes of the changes in expression of many genes were quite high even in the single mutant strains. This suggests that, although *cac1* or *asf1* single mutants do not have severe perturbations in chromatin structure, these mutations nonetheless have a significant impact on the expression of a large number of genes. The absence of nucleosome assembly factors such as Asf1 and CAF1 would be expected to result in a chromatin structure that is generally more permissive for transcription. However, many entries are down regulated, rather than overexpressed in the mutants.

Using the GeneSpring analysis tools, we tried to identify entries whose expression is significantly changed in the mutant strains relative to wild type cells. The results were filtered as a measure of confidence using a pseudo *t*-test P value of 0.2. The *t*-test gives a measure of the likelihood that the expression of a given gene is significantly different from the value one. Because the data was normalised according to the wild type strain, all entries in this strain will always give the value 1 while entries in other strains may give values that are significantly below or above 1 when a gene is either down or up regulated in the mutant strains. The *t*-test filters out all genes in the mutant strains that had a value of 1 or whose deviation from 1 is insignificant. However, since there are not enough samples in this experiment to determine the standard deviation for each gene, this is not a real *t*-test. To overcome this, the GeneSpring software offers a cross-gene error model known as 'deviation from one', which takes into account that there is a single chip for each strain. In this model, the standard deviation is calculated using measurements of a group of entries with similar expression patterns. Therefore, this filter screens out all the entries that do not seem to be strongly affected in any of the mutants, and entries with very low expression measurements which are bound to be inaccurate (generally this applies to measurements ≤ 20 before normalisation). We followed this by filtering out the entries that change by less than two-fold between the strains. A visualisation of such filtering is shown in Figure 5.1, where the selected entries after filtration by *t*-test are highlighted in pink, while the 2-fold filtering is marked by the parallel green lines.

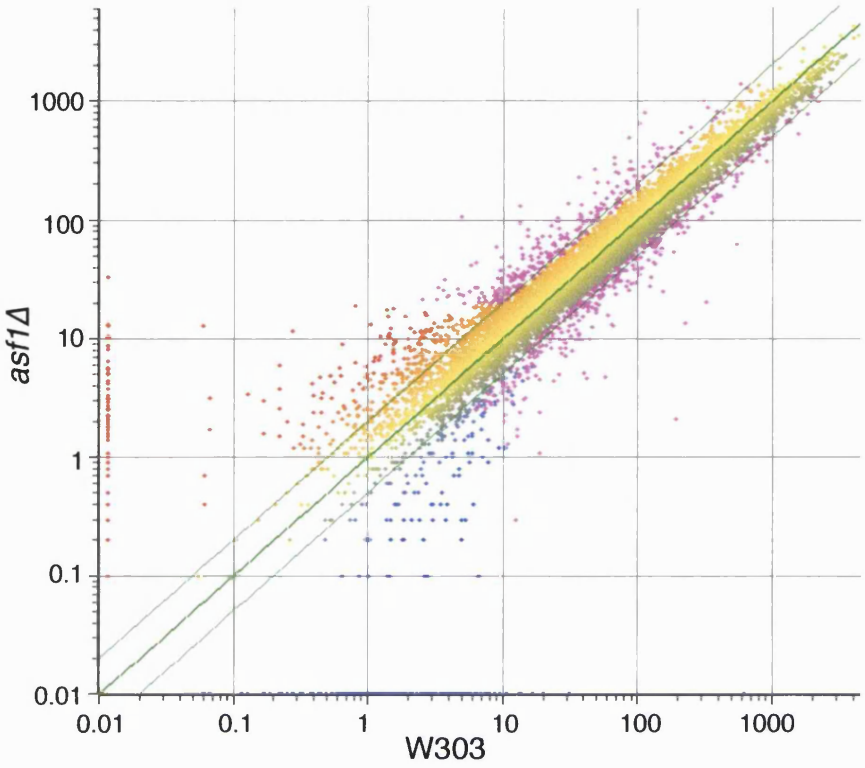

Figure 5.1: Comparison of expression in W303 versus *asf1Δ* cells
Using GeneSpring software, the expression of all Affymetrix entries in W303 (X axis) and *asf1Δ* (Y axis) strains were plotted in a logarithmic graph. Each dot represents a single normalised entry (see text for normalisation procedure). A gradient colour scheme is used to represent entries that are down regulated (blue) similar (yellow) or up regulated (red) in *asf1Δ* relative to wild type. The entries that are considered to have an altered expression in *asf1Δ* relative to wild type after filtration by a pseudo *t*-test with P value of 0.2, are coloured in pink. Filtration by 2-fold is represented by the parallel diagonal green lines.

After the use of these filters, the total fraction of all entries with significant changes in expression was around 33% and ranged from 19% in *cac1Δ* to 23% in *asf1Δ* cells and 22% in *asf1Δcac1Δ* cells. The Venn diagram in Figure 5.2a schematically shows the distribution of entries with altered expression in the three mutant strains relative to wild type cells. Many of these changes in expression were common to all three mutant strains. However there are also many entries that are specifically affected in each strain. Even though the expression of many entries seems to be affected in the mutant strains, analysis by "Clustering" demonstrated that all four strains were still similar to each other (data not shown). This is consistent with the fact that all mutant strains were constructed from W303, which was used as a wild type reference strain.

a.

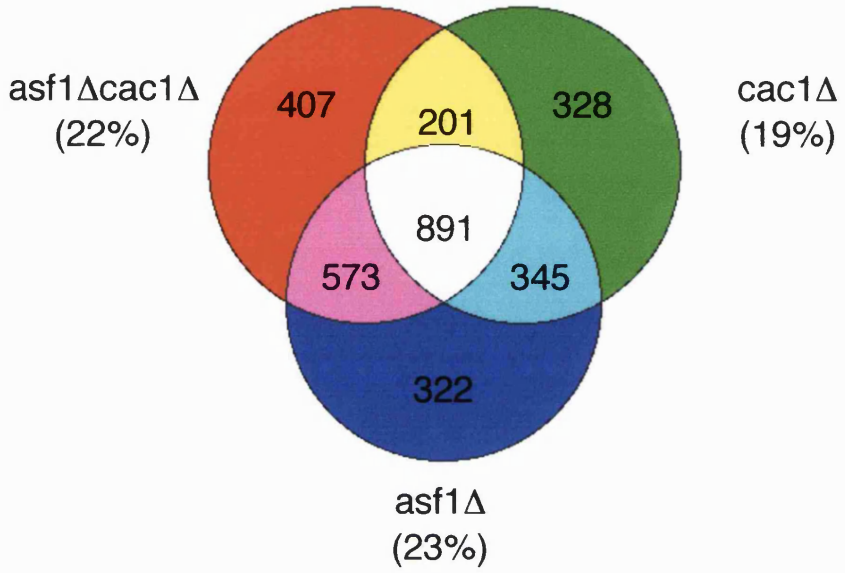

b.

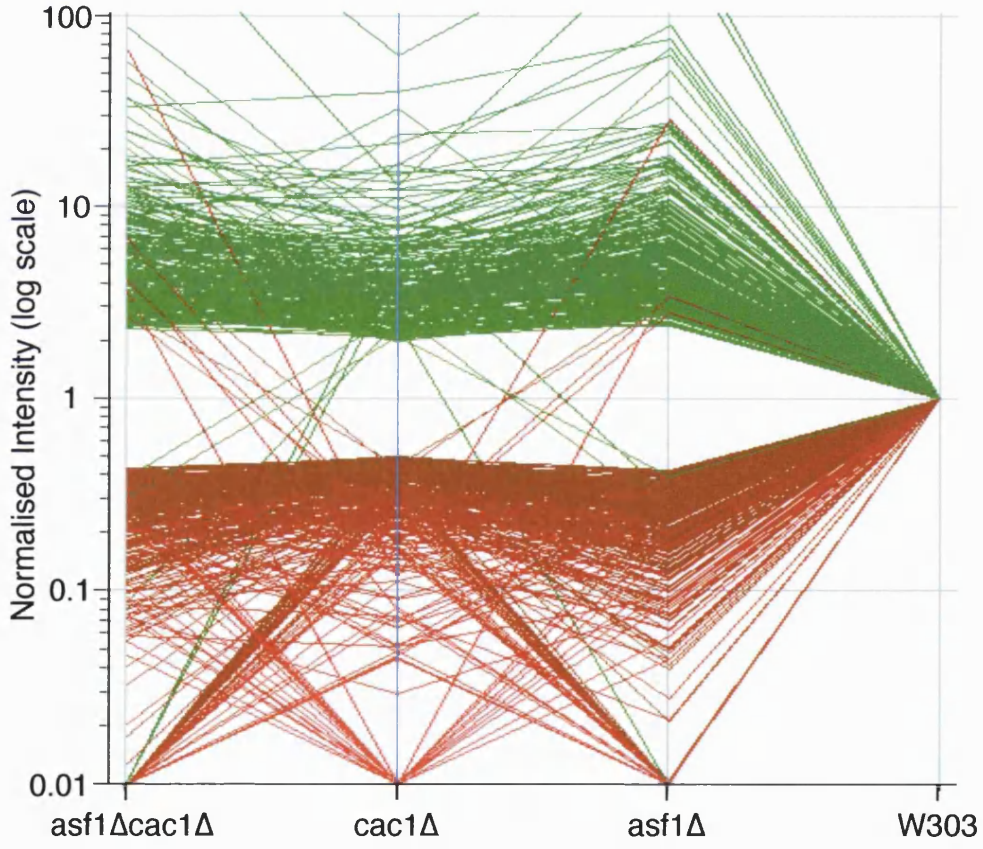

Figure 5.2: The distribution of entries with altered expression in the mutant strains
a. After filtration of P=0.2 followed by the removal of entries with less than 2-fold changes in their expression, all the remaining chip entries were plotted in a Venn diagram.
b. The relative expression level of entries whose expression is altered in all three mutants relative to W303 (891 entries) is plotted on a logarithmic scale graph. Green and red lines show the expression of entries that are mostly up or down regulated, respectively. Since the expression was normalised to W303 (see text for details), the level of expression of all entries in this strain is normalised to 1. Over 90% of entries follow a similar trend of expression in all mutants.

It is important to further emphasise that the filtration criteria were permissive and that some of these entries are probably false positive that would not show significant changes in expression if several replica of each strain were analysed. In spite of this, the fact that as many as 19% of all entries are affected in *cac1Δ* cells, which do not exhibit any defect in cell cycle progression (Kaufman et al., 1998), strongly suggests that a large number of transcripts are not affected simply as a result of cell cycle perturbations in the mutant cells. Assuming that Cac1 does not have a completely unknown function in gene expression unrelated to its chromatin assembly and maintenance function, and given that *cac1Δ* cells have an essentially normal chromatin structure (Kaufman et al., 1998), these results demonstrate that even subtle defects in nucleosome assembly can influence the expression of many genes.

Table 5.1 shows a general overview of the distribution of up regulated and down regulated entries in the three mutants relative to the wild type strain. Since the *asf1Δcac1Δ* double mutant has more pronounced silencing and cell cycle progression defects (Tyler et al., 1999) than either single mutant, I had expected these differences would be apparent in the micro-array results. Surprisingly, there are similar numbers of entries with altered expression patterns in all three mutant strains.

Table 5.1: General overview of alterations in gene expression in mutant strains normalised to wild type cells

	cac1Δ	*asf1Δ*	*asf1Δcac1Δ*
Up regulated ≥ 10 fold	37	83	62
Down regulated ≥ 10 fold	258	252	421
Up regulated ≥ 5 fold	109	236	178
Down regulated ≥ 5 fold	350	591	538
Up regulated ≥ 2 fold	680	836	723
Down regulated ≥ 2 fold	1085	1295	1349

Furthermore, as indicated in Table 5.1 and shown schematically in Figure 5.2b, many entries are either down regulated or up regulated in the mutant strains in comparison with wild type cells. Although this pilot experiment did not include replica of each strain, the three mutant strains can serve as qualitative controls for each other. Since all three mutants are defective in nucleosome assembly, it is possible that the change in expression of any given entry should be qualitatively similar in all three mutant strains. By this I mean that, if a given gene is overexpressed in one mutant background, the same gene may also be overexpressed in either of the other two mutant strains. This is, in fact, what we see. The graph in Figure 5.2b shows the normalised expression of all the entries with altered expression levels that are common to all three mutant strains (*i.e.* the entries in the centre of the Venn diagram in Figure 5.2a). This is plotted as a change in intensity in each of the different backgrounds. Green lines and red lines respectively represent entries that have a higher or lower expression in the mutant strains relative to wild type cells. Because normalisation was performed relative to the W303 strain, all entries converge to a normalised intensity of 1 in this background. Out of 891 entries in this group, less than 10% have a mixed pattern of expression among the three different mutants. Similar results were observed for groups of entries that were common to pairs of mutant strains (e.g. (*cac1Δ*)+(*asf1Δcac1Δ*)-(common to all three mutant strains); data not shown).

To filter the previous list further, I selected only the entries for which at least one of the mutant strains had an altered level of expression of 5-fold (or more) relative to the wild type strain, and excluded entries with very low levels of expression that may give rise to false positive results. Although a lot of data has been collected regarding many yeast genes, many of the micro-array entries are very poorly annotated. In order to make this list more accessible, I have omitted those entries from the final list. After this, I was left with 216 entries that were up regulated and 68 that were down regulated in mutant strains. This final result is represented in a Venn diagram in Figure 5.3, while the list of genes is in Appendix II.

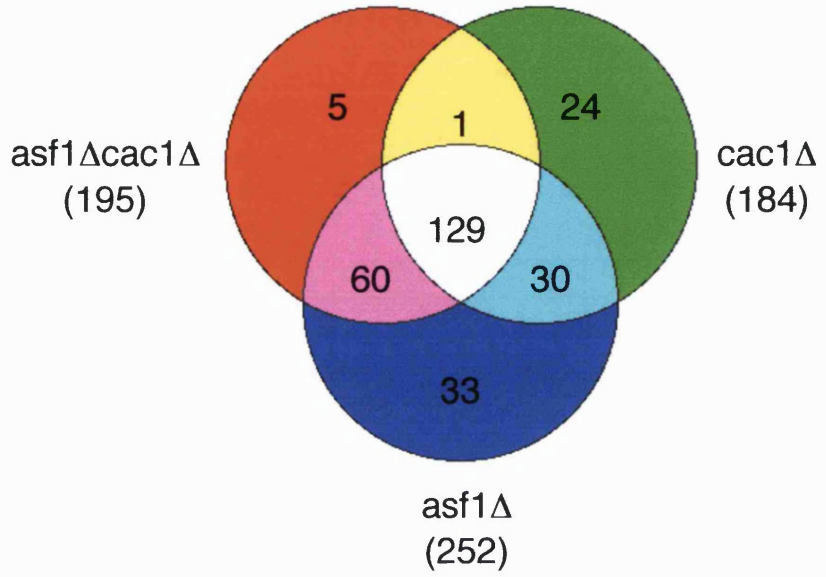

Figure 5.3: The distribution of annotated entries with strongly altered expression between the mutant strains
A Venn diagram similar to Figure 5.2a, except that only the entries with annotations and where expression is altered 5-fold or more in at least one of the mutant strains are represented.

5.4 EXPRESSION OF GENES OF INTEREST

5.4.1 Expression of genes in specific chromosomal domains

I looked at the expression level of genes in several distinct chromatin regions. Since *asf1* and *cac1* mutants exhibit silencing defects in telomeric regions, rDNA and the mating type loci (Enomoto and Berman, 1998; Enomoto et al., 1997; Kaufman et al., 1997; Monson et al., 1997; Smith et al., 1999a), I first analysed changes in gene expression in those chromosomal domains. For this, I identified the location of all the Open Reading Frames (ORFs) and non-ORF features from SGD (see useful web sites in Chapter 2.15). These were plotted in GeneSpring against the Affymetrix entries (taken from the annotated list at the Affymetrix web site which provides the accession number and gene name for each entry). Entries were visualised on a schematic representation of the yeast chromosomes. Figure 5.4 features all the mapped entries. Lines above each chromosome represent ORFs on the Watson strand and those below depict ORFs on the Crick strand. Blocks colour coded by a gradient from green to red represent entries that are expressed higher or lower in *asf1Δcac1Δ* compared to wild type cells,

respectively. Note that because Figure 5.4 includes all mapped entries, changes that are insignificant are also featured in this map. Nonetheless, this figure clearly illustrates that the absence of Asf1 and Cac1 affects gene expression throughout the genome.

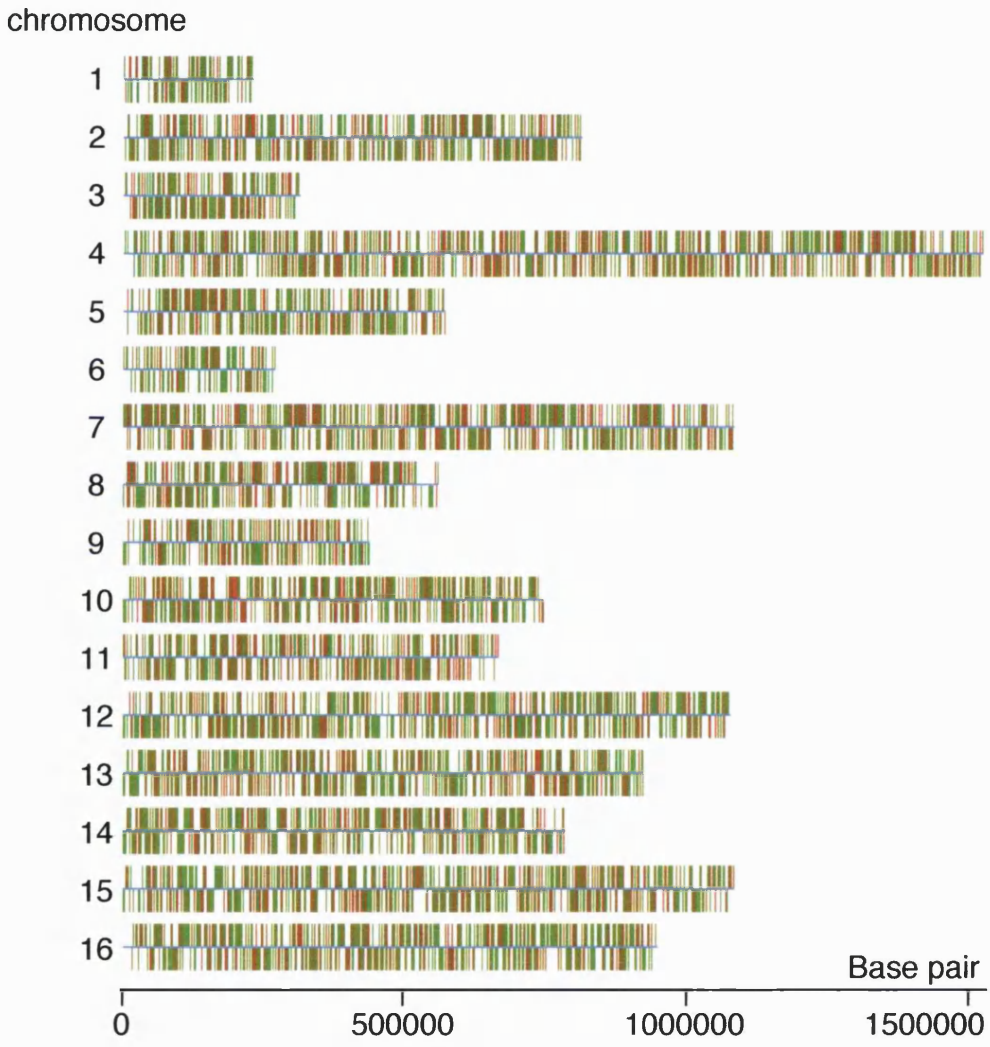

Figure 5.4: The genomic localisation of all available entries
The localisation of all entries on a chromosome map, and their level of expression in the *asf1Δcac1Δ* mutant relative to wild type cells are shown. A scale from green to red blocks represents up and down regulated entries. Blocks above and below the blue lines represent chromosomes entries found on the Watson and Crick strands respectively.

5.4.1.1 Subtelomeric regions

The Hda1-Affected SubTelomeric (HAST) domains are present in the vicinity of 22 of the 32 chromosome ends (at 10-25 kb) in haploid cells and span from 4 to 34 Kb in size (Robyr et al., 2002). Unlike telomeric heterochromatin, which is devoid of genes, HAST domains contain clusters of genes that are normally repressed under optimal growth conditions in the presence of glucose but activated in the presence of alternative carbon sources or environmental stress (*e.g.* changes in pH, osmotic shock or anaerobic growth). Under optimal growth conditions, the repressed state of these genes is maintained by deacetylation of the N-terminal tails of histones H3 and H2B by Hda1, although Rpd3 also contributes to histone deacetylation in HAST domains (Robyr et al., 2002; Suka et al., 2002). In addition, Ssn6-Tup1 plays an important role in the repression of genes located in HAST domains both by helping to recruit Hda1 and by binding to deacetylated histones.

Robyr *et al.* (2002) list 230 ORFs and intergenic sequences that reside within HAST domains. Out of these, we identified 186 Affymetrix entries that correspond to HAST sequences. The location of these entries is plotted on the chromosomes map in Figure 5.5. From the list of HAST entries, 84 out of 186 have an altered expression in mutant cells compared with the wild type strain, which is a little over 45%, compared with almost 33% when all entries were assessed. The statistical significance of this difference was calculated using the hypergeometric distribution. The probability to find 84 out of 186 HAST entries from a total of 3067 affected entries was low (P value $=1.8 \times 10^{-4}$), suggesting that the HAST domains are enriched in entries with altered expression in a statistically significant manner. The enrichment in entries whose expression is altered is concentrated at specific HAST regions. For example Figure 5.5, clearly shows that most HAST regions in *asf1Δcac1Δ* have both up and down regulated entries, however the right arms of chromosomes 6 and 9 both have a cluster of up regulated entries. In different mutant backgrounds, different "hot spots" appear, but the statistical significance of this was not determined.

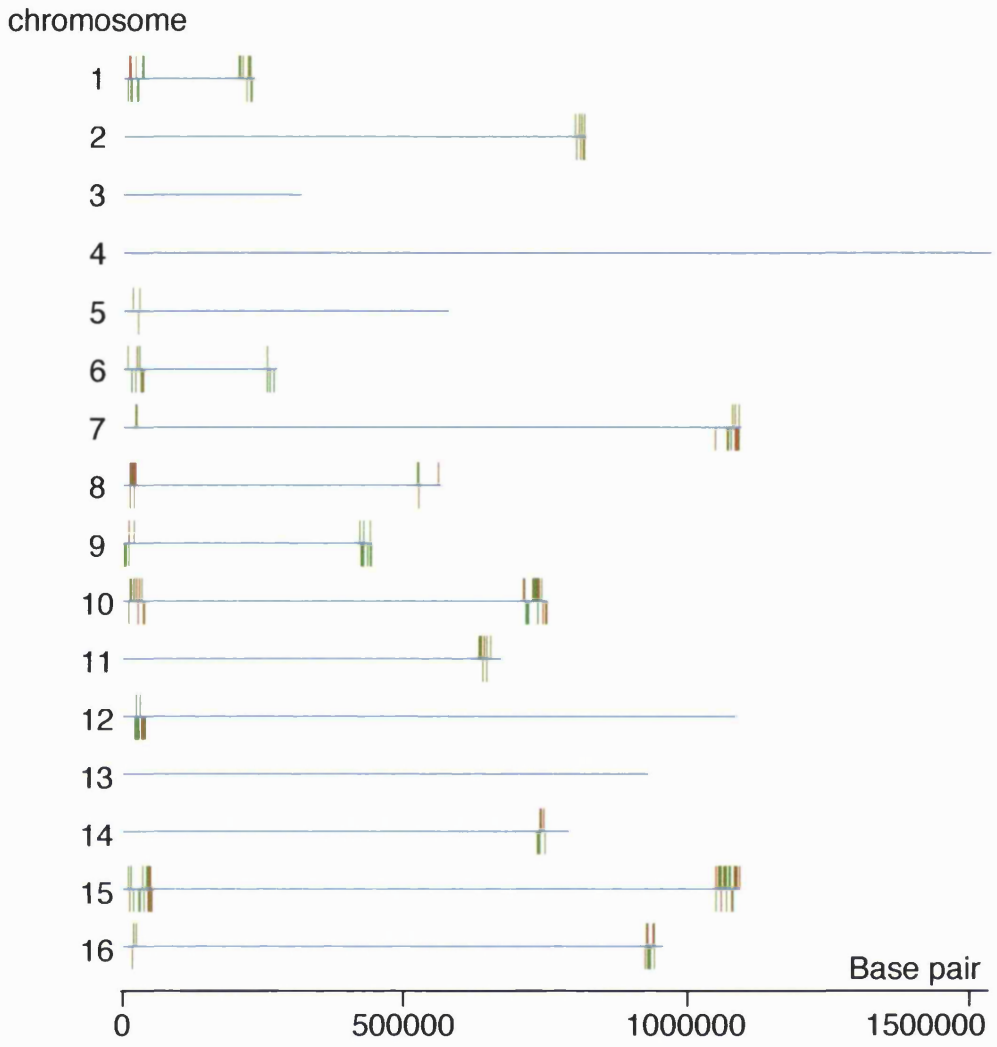

Figure 5.5: The genomic localisation and expression of HAST entries
The localisation of 186 HAST entries which could be mapped, and their relative level of expression in *asf1Δcac1Δ* compared with W303, are plotted against the chromosome map as in Figure 5.4. Entries are localised to most, but not all chromosome ends. The following subtelomeric regions are devoid of HAST domains: chr.2-L, 3-L and R, 4-L and R, 5-R, 11-L, 12-R, 13-L and 14-L. Although chr. 13R has a HAST domain, it is not represented in this figure, because out of 230 defined ORFs and intergenic sequences, none of the 186 entries identified in the affymetrix chip localise to this region.

Another way I looked at subtelomeric regions was by simply marking 30Kb spanning from each chromosome end as 'extended' subtelomeric regions. Altogether, these regions included 337 entries, which is roughly 3.8% of all mapped entries (337/8854). Out of 337, 151 entries were found to have altered expression in the mutant strains, corresponding to nearly 45%. Thus the results obtained using this approach resemble those derived by the analysis of HAST entries. The distribution of subtelomeric entries whose expression is affected in each mutant strain is illustrated in a Venn diagram in Figure 5.6.

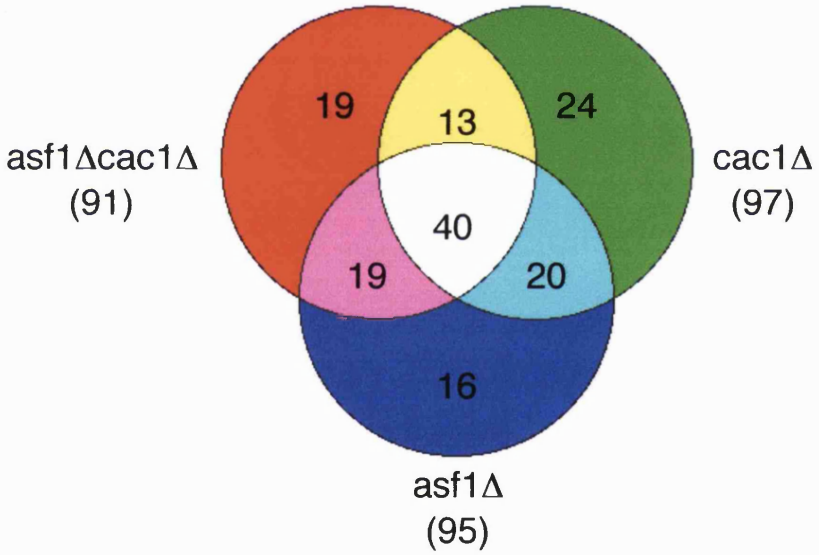

Figure 5.6: The distribution of subtelomeric entries with strongly altered expression between the mutant strains
Entries whose expression is altered in the mutant strains relative to W303, and which are localised within 30 Kbs from the chromosome ends are plotted in a Venn diagram. The representation is as in Figure 5.2a.

5.4.1.2 The *RDN1* locus

In *S. cerevisiae*, the *RDN1* locus encoding the ribosomal RNA gene cluster is located on chromosome 12 (Figure 5.7a) and consists of 100 – 200 copies of a 9.1Kb repeat containing the 35S rRNA precursor and 5S rRNA genes (over 1-2 Mb). A fraction of the rRNA gene repeats are packaged into a specialised form of chromatin that promotes transcriptional silencing (Smith et al., 1999a).

The fraction of active and silent rDNA repeats is determined by the requirement for ribosomes and protein synthesis (Dammann et al., 1993; Sandmeier et al., 2002). Silencing at the rDNA locus is dependent upon the histone deacetylases Sir2 and Rpd3, as well as a number of other proteins, including CAF1 (Sandmeier et al., 2002; Smith et al., 1999a).

In the S98 Array chip, the *RDN1* locus is represented in the following manner:

- 35S rDNA: the RDN37-1 primary transcript is represented in 7 probes. Additionally, RDN25-1 is represented 7 times and RDN18-1 6 times.
- 5S rDNA: RDN5-1 is represented twice.
- 5S variant rDNA: RDN5-3 is represented once.
- *ASP3* non-transcribed spacer: ASP3-1 is represented once.

The silencing at the RDN1 locus affects 35S and 5S rDNA but not 5S variant rDNA nor *ASP3* (Buck et al., 2002). Indeed, ASP3-1 was not highly up regulated in any of the mutant strains, yet RDN5-3 is up regulated by roughly 6 fold in *asf1Δcac1Δ*. 80% of ribosomal 35S and 5S entries are strongly up regulated by mutations in chromatin assembly factors. As expected, *cac1* single mutants exhibit elevated levels of ribosomal RNAs compared with wild type cells (appendix II). Surprisingly, *asf1* single mutants had a much more pronounced defect in rDNA silencing than *cac1* mutants (appendix II). This was unexpected because Asf1 and Hir proteins function in the same pathway for telomere silencing (Sharp et al., 2001), but *hir* mutants exhibit an increase in rDNA silencing (Smith et al., 1999a), whereas here *asf1* mutants display a defect in rDNA silencing. In over 80% of ribosomal RNA entries that were up regulated, the *asf1Δcac1Δ* double mutant strain exhibits a slightly greater rDNA silencing defect than the two single mutants. The expression of both the 35S precursor and the 5S rRNA, which are respectively transcribed by RNA polymerase I and III, is elevated in the mutant strains. Thus, mutations in chromatin assembly factors affect the expression of genes expressed by all three RNA polymerases.

The expression of genes flanking either the centromeric (*SMD3*, *SPE4* or *ACF2*) or the telomeric side (*MAS1*, *PUS5*, *SEC10* or *RPS31*) of the *RDN1*

locus is not significantly affected in the mutant backgrounds (data not shown). This suggests that the increase in rRNA expression in cells lacking chromatin assembly factors is not simply due to lateral spreading of a limiting pool of silencing factors on either side of the *RDN1* locus. Furthermore, expression of ribosomal proteins is also largely unaffected by the mutations. Unlike ribosomal RNA genes, the genes encoding ribosomal proteins are transcribed by RNA polymerase II and are distributed throughout the yeast genome. Out of 176 entries for ribosomal proteins, only two are strongly down regulated, and none is strongly up regulated in the deletion strains. Thus, only the RNA components of the ribosome are derepressed in cells lacking Asf1 or CAF1. This suggests that the elevated levels of ribosomal RNAs are due to loss of rDNA silencing, rather than to a non-specific effect of the mutations on all the components of the protein synthesis machinery.

5.4.1.3 Other RNA genes

The transcription level of some small nuclear RNAs and many tRNAs is reduced by 5-100 (which is the maximum value after normalisation) fold in the mutant cells. Not all known tRNA genes are represented in the S98 Affymetrix chip. Out of 95 different tRNA genes that are represented in the chip, 20 are strongly down regulated. These include 5 out of 11 tRNA-Ala, 3/16 tRNA-Gly, 2/3 tRNA-His, 5/16 tRNA-Arg and 5/12 tRNA-Ser genes on chromosomes 1, 2, 4, 5 and 10-13. This reduction in only some of the genes expressing a specific tRNA is not likely to cause a strong phenotype because within a given family, many tRNA genes are redundant with each other (Strathern et al., 1982). However, 62 out of 95 tRNA genes are reduced in mutant strains by 2 fold or more, while none are up regulated by 2 fold or more.

The tRNA genes are transcribed by RNA polymerase III and are scattered throughout the genome (Figure 5.7b). It is not clear whether this effect arises from a change in chromatin structure that affects the transcription of tRNA genes, or that it is an indirect effect (*e.g.* a change in cell metabolism) affecting the abundance of many different tRNAs.

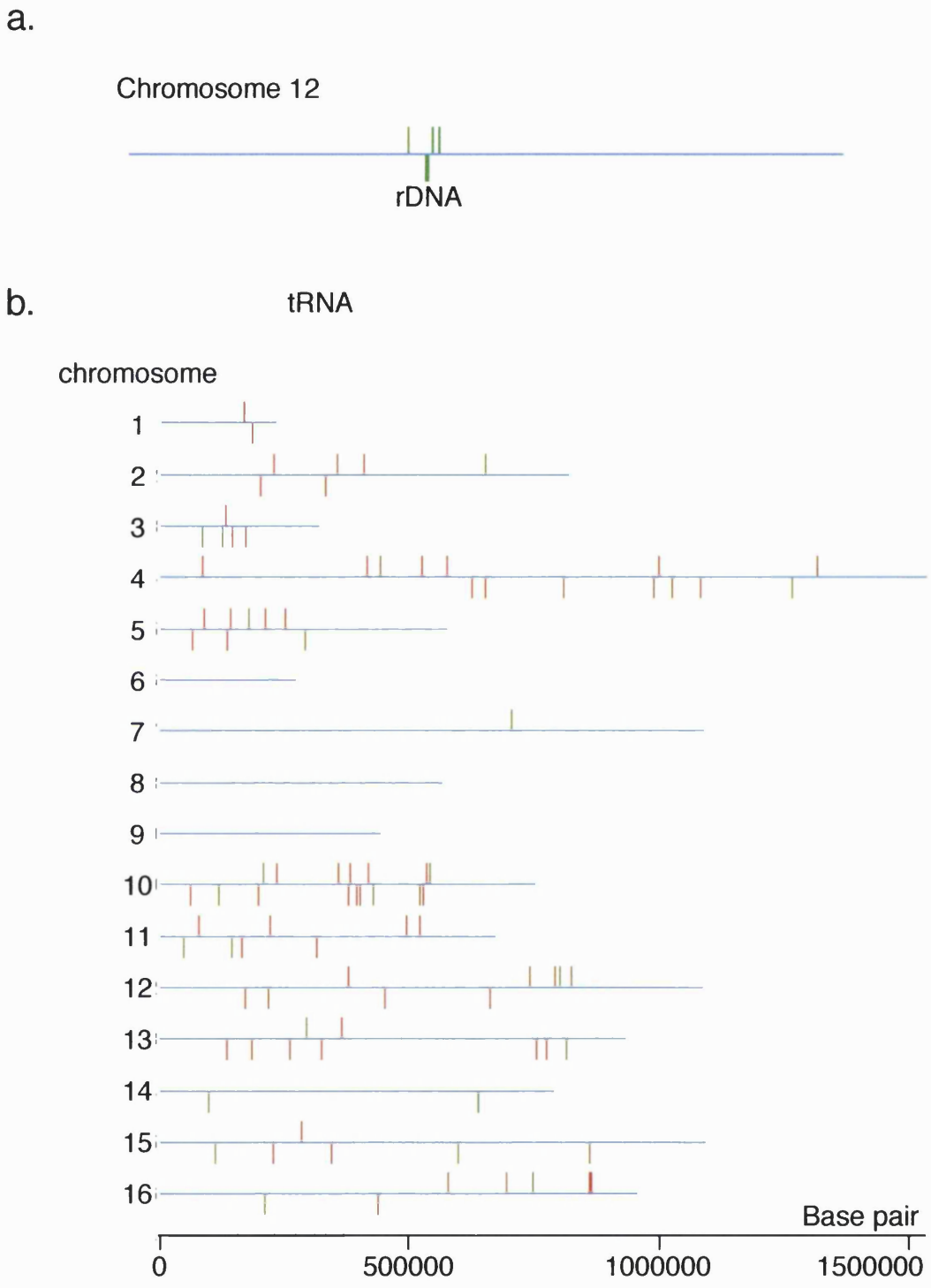

Figure 5.7: The genomic localisation and expression of ribosomal RNA and tRNA genes
a. The representing entries of the *RDN1* locus on chromosome 12 are schematically illustrated. The expression of rRNA genes in *asf1Δcac1Δ* relative to wild type is shown. In this background all the entries are up regulated relative to wild type.
b. A significant fraction of tRNA genes throughout the genome are down regulated in *asf1Δcac1Δ* relative to wild type.

5.4.1.4 The silent mating type loci

The silent mating type loci *HMLα* and *HMRa* are located on the left and right arms of chromosome 3, respectively (Figure 5.8a). In wild-type cells, the genes encoded by *HMLa* (a1 and a2) and *HMRa* (a1 and a2) are silenced through their packaging into heterochromatin that contains the Sir proteins (Sir2, Sir3 and Sir4) and unacetylated histones (Dhillon and Kamakaka, 2002). The silent chromatin domains extend beyond the structural genes. At *HMRa*, the silent domain spans ~3.5Kb, whereas *HMLα* is part of a much larger domain (~15Kb) that extends from the left telomere of chromosome 3 to the *CHA1* gene (Dhillon and Kamakaka, 2002).

The expression of genes at both mating type loci was not altered in any of the mutant strains relative to the wild-type cells. YCR099c and *GIT1* near the *HMRa* domain were slightly overexpressed in mutant strains, while near the *HMLα* silenced domain, the neighbouring YCL065w, *CHA1* and YCL063w were slightly down regulated. As expected in these silenced loci, the general level of expression of all these genes in the wild type strain was low. This was also true of the mutant strains and therefore the level of change in expression cannot be accurately determined. However, this demonstrates that genes in the silenced mating type domains remained repressed.

5.4.1.5 Other chromosomal regions

The chromosome maps can also be used to look for 'hot spots', which are chromosome segments with high density of genes showing alteration of expression in any of the mutants. In contrast, 'cold spots' are chromosome regions where only few genes are affected in the mutant strains. One particularly 'hot' domain spans the entire chromosome 11 in the group of changing entries common to *cac1Δ* and *asf1Δ* cells (Figure 5.8b). Surprisingly, these entries were only affected in the single mutants and not in *asf1Δcac1Δ* cells. 372 entries map to Chromosome 11. Out of these, 56 are significantly affected in *asf1Δ* and *cac1Δ* mutants but not in *asf1Δcac1Δ* , the vast majority of them (54) are up regulated.

a.

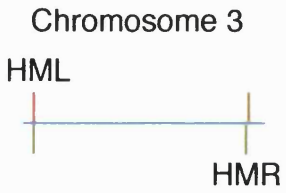

b.

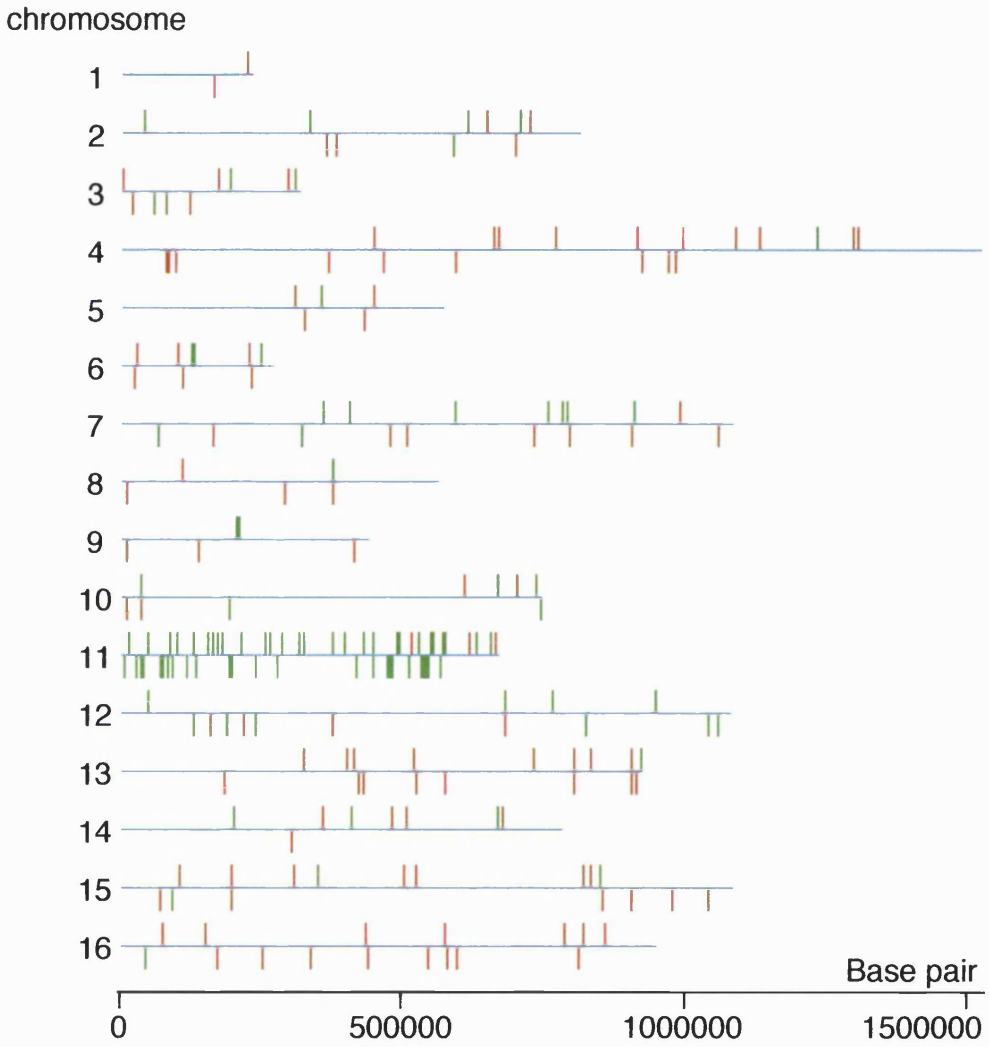

Figure 5.8: Genomic localisation and expression of specific groups of genes

a. The HML and HMR loci on chromosome 3 and their expression in *asf1Δcac1Δ* relative to W303 is schematically represented. Here the colour scheme is slightly misleading as the expression of genes in these loci is not significantly altered in the mutant background relative to wild type cells.

b. The 345 entries that have altered expression in both *asf1Δ* and *cac1Δ* but not in *asf1Δcac1Δ*, relative to wild type cells are plotted on a chromosome map. Specific "hot-spots" for up or down regulation of entries emerge. In particular, chromosome 11 has a high concentration of up regulated entries in this group.

However, most of these entries are only up regulated by 2-5 fold in the mutant strains and the expression level in wild type cells was not high.

Nonetheless, this represents roughly 15% of entries on chromosome 11 (56/372), while chromosome 11 carries only 4.2% of all yeast entries (372 entries on chromosome 11/8854 total mapped yeast entries). Genome-wide, there are 345 entries common to *cac1Δ* and *asf1Δ* single mutant cells, which represent 3.7% of all entries on the S98 chip (345/9335). Thus, the density of entries commonly affected by the *asf1Δ* or *cac1Δ* mutations is much higher on chromosome 11 than throughout the genome.

There were 102 entries derived from chromosome 11 that were up regulated in the *cac1* mutants, whereas only five were down regulated, In *asf1* mutant cells 122 entries from chromosome 11 were up regulated but only 9 were down regulated. This suggests that in these two mutant strains, the vast majority of chromosome 11 genes that have altered expression are up regulated relative to the wild type cells.

5.4.2 Expression of genes in related pathways

I was also interested in the expression of genes involved in specific cellular functions that may be affected by the deletion of genes encoding nucleosome assembly factors. These include:

- Genes encoding proteins that are directly involved in nucleosome assembly, such as the histones themselves, the Hir proteins that are involved in the regulation of histone gene expression as well as nucleosome assembly, and Trf4/Trf5, which have been shown in our laboratory to participate in histone mRNA polyadenylation.
- Genes involved in DNA replication, such as *POL30* (PCNA), *RAD27* (FEN1), *CDC45*, *CDC21* (thymidylate synthase, an enzyme involved in the conversion of dUMP to dTMP) and the genes encoding the subunits of ribonucleotide reductase (*RNR1*, *2*, *3* and *4*).
- Genes involved in various DNA repair pathways and the DNA damage checkpoint pathways such as *RAD1* and *RAD14* (nucleotide excision repair), *RAD5*, *RAD6*, *RAD18*, and *REV3* (DNA lesion bypass during

replication), *RAD51* and *RAD52* (homologous recombination), *RAD9*, *RAD53* and *DUN1* (DNA damage checkpoint).

- Genes involved in cell cycle regulation at the G1/S and G2/M transitions. These include: *CLN1*, *CLN2*, *CLB5*, *CLB6*, *MBP1* and *SWI4* (*MBP1* and *SWI4* respectively associate with *SWI6* to form the MBF and SBF transcription factors) for the G1/S transition, and *CLB1*, *CLB2*, *GIN4*, *TEL2*, *CDC20*, *SPO12*, *SWE1*, *APC1*, *TEM1*, *MCM1*, *SWI5*, *FKH1*, *FKH2*, *NDD1* and *ACE2* for the G2/M transition.
- I also included genes in the HAST group (Robyr et al., 2002), which were analysed previously as subtelomeric genes. These are generally stress response genes or genes required for growth in carbon sources other than glucose, including: *MAL11*, *MAL12*, *MAL13*, *MAL31*, *MAL32*, *MAL33*, *PEX11*, *HXK1*, *HXT8*, *HXT11*, *HXT12*, *BIO3*, *BIO4*, *BIO5*, *CAN1*, *DAN4*, *AQY1*, *AQY2*, *YPS6*, *FET4*, *FIT2*, *FIT3*, *PGU1* and*GRE2*.

Using the GO libraries and software (useful web-sites are listed in Chapter 2.15), annotated entries can be sorted according to their molecular function (such as kinases), the biological processes that they affect (such as cell cycle regulation) or their cellular localisation. Curiously, out of the functional groups mentioned above, only 'stress response' genes are significantly up regulated in the mutant background. Over 20% of all annotated entries that were up regulated belong to this group, constituting less then 10% of all annotated genes in the S98 chip (data not shown). It is important to stress that the usefulness of the GO libraries is limited by the fact that only about 40% of entries are annotated, and this annotation is, naturally, biased towards fields where extensive research has already been done.

5.4.3 Specific genes of interest have altered expression in *asf1 cac1* mutants

The micro-array experiment was performed in the hope of finding genes that are strongly up regulated in cells lacking Asf1 and CAF1. My hypothesis was that some of these genes may encode nucleosome assembly factors that are present in limiting amounts in wild type cells, but need to be up regulated to

compensate for the absence of Asf1 and CAF1. However, this approach was hampered by the fact that mutations in nucleosome assembly factors affect the expression of a large number of genes. In addition, none of the highly up regulated genes seemed like obvious candidates, although many are poorly annotated.

I was, however, intrigued by two specific proteins:

- *SRL3* (Suppressor of Rad53 Lethality – YKR091w) is slightly up regulated in all three mutant strains (3-6 fold). This non-essential (Giaever et al., 2002) cytoplasmic protein (Kumar et al., 2002) can suppress the lethality of a *rad53* null mutation when over expressed (Desany et al., 1998). It is of interest to us, because Rad53 has dual roles in regulating the synthesis of both histones and DNA precursors (Gunjan and Verreault, 2003; Zhao et al., 2001).
- *PWP1* (Periodic Tryptophan Protein 1 – YLR196w), whose expression is reduced by only 2 - 2.5 fold in *asf1Δ* or *cac1Δ* single mutants, and by 35.7 fold in *asf1Δ cac1Δ* double mutants. Pwp1 is a protein of unknown function with 7 WD (also known as WD40 repeats - http://bmerc-www.bu.edu/wdrepeat/) and a predicted mass of 63.8 kDa.

5.5 *PWP1* EXPRESSION IS REDUCED IN *asf1 cac1* DOUBLE MUTANTS

The family of WD repeat proteins contains more than 100 predicted members (reviewed in Smith et al., 1999b) and *S. cerevisiae* alone has 63 WD repeat proteins (Yu et al., 2000). WD repeat proteins are predicted to adopt a β-propeller structure, originally described in the crystal structure of the β subunit of transducin, a heterotrimeric G protein involved in light perception (Sondek et al., 1996). Proteins in this family are involved in functions as diverse as histone metabolism, signal transduction, RNA processing, transcriptional regulation, cytoskeletal assembly and mitotic spindle formation, control of vesicle formation and intracellular trafficking, control of cell division and the regulation of sulphur metabolism. It appears that the WD repeat propeller structures create a versatile platform that can form dynamic complexes with many different proteins. The extraordinary functional diversity of WD repeat proteins

likely stems from their ability to accommodate multiple interactions not only with partner proteins, but also with other ligands such as sugars, prosthetic groups and ions (Neer and Smith, 2000).

Remarkably, two subunits of CAF1 (p60 and RbAp48 in human cells; Cac2 and Cac3 in *S. cerevisiae*), a subunit of Hat1, the acetyltransferase that acetylates newly synthesised histone H4 (RbAp46 in human cells; Hat2 in *S. cerevisiae*) and vertebrate HIRA (Hir1 in *S. cerevisiae*) are all WD repeat proteins (Kaufman et al., 1998; Verreault et al., 1998). Furthermore, RbAp46 and p48 bind directly to core histones (Verreault et al., 1998) and both are part of the catalytic core of several histone deacetylase enzymes (Zhang et al., 1999). Intriguingly, Pwp1 exhibits significant amino acid sequence similarity with Hat2 and Cac3 (Figure 5.9a), although this does not necessarily imply that they are functionally related. Pwp1 is clearly conserved in human cells and studies with antibodies against the endogenous protein or cell lines expressing a GFP-PWP1 fusion protein demonstrated that human PWP1 localises both to the cytoplasm and the nucleolus, but is absent from the nucleoplasm (Andersen et al., 2002; Honore et al., 2002).

I was interested in Pwp1 because of its similarity to other nucleosome assembly factors. In addition, the fact that the expression of *PWP1* was strongly down regulated in cells lacking both Asf1 and CAF1 suggested that Pwp1 may function as a negative regulator of the nucleosome assembly pathway. Alternatively, Pwp1 may function together with Asf1 and CAF1, but its expression may become detrimental in cells lacking both Asf1 and CAF1.

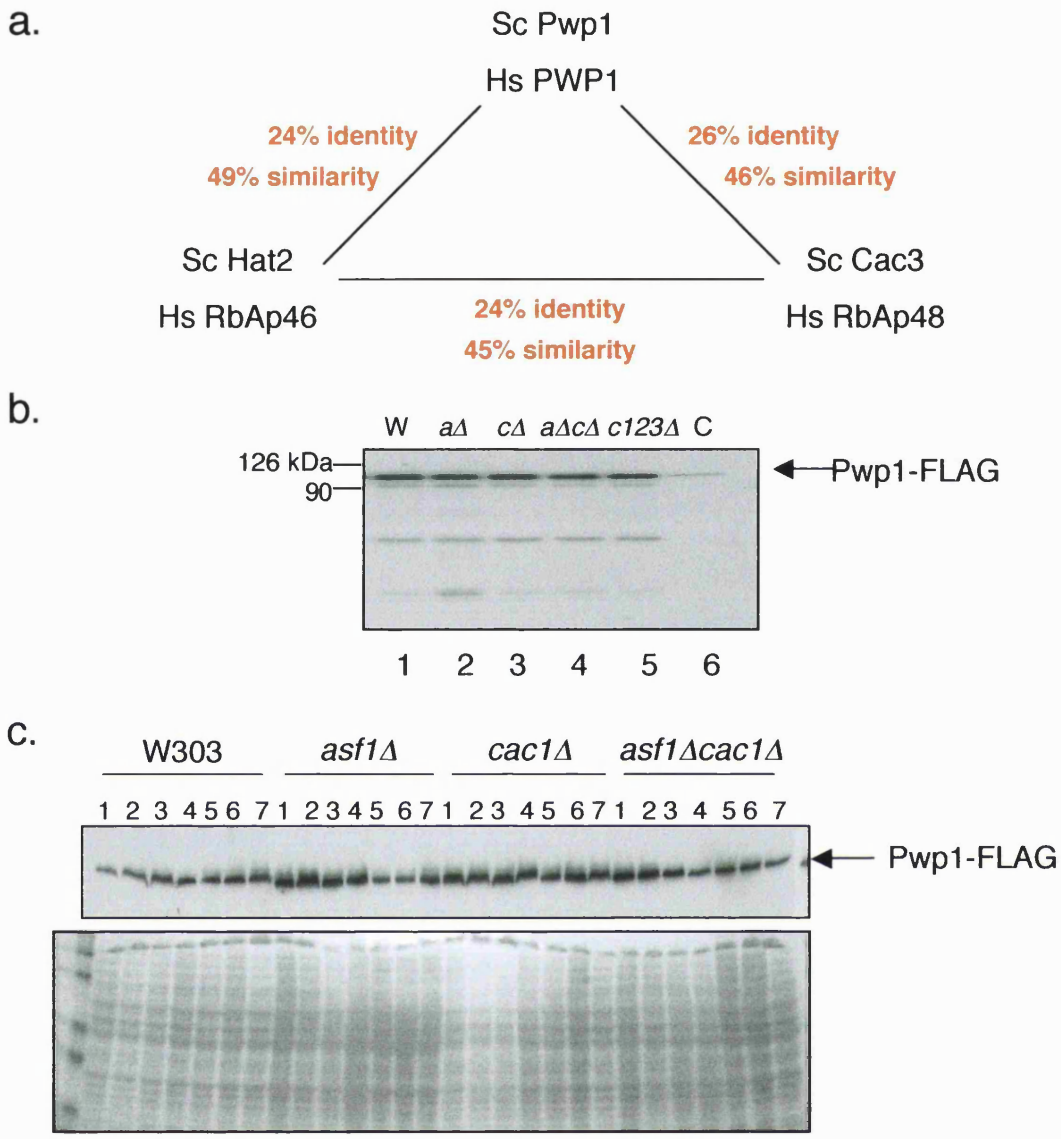

Figure 5.9: The expression of Pwp1 is not influenced by mutations in chromatin assembly factors or DNA damage

a. Pwp1 is a WD40 repeat protein which is roughly 25% identical and almost 50% similar to the core histone binding proteins RbAp46 and p48.

b. Pwp1 is present at similar levels in wild type and *cac* and *asf1* mutants. Pwp1 was tagged by FLAG-epitope at the C-terminus in different genetic backgrounds. Whole-cell extracts from these strains were analysed by SDS-PAGE and Western blotting with FLAG M2. Pwp1-FLAG was expressed in (W) W303, (*aΔ*) *asf1Δ*, (*cΔ*) *cac1Δ*, (*aΔcΔ*) *asf1Δcac1Δ* and (*c123Δ*) *cac1Δcac2Δcac3Δ* strains. (C) Extract from a W303 strain in which endogenous Pwp1 was not tagged by Flag was used as a negative control. Note that the protein band in this lane is an M2 cross-reacting band.

c. Expression of Pwp1 is not significantly altered in response to DNA damage. The strains presented in (b) were used to examine Pwp1-FLAG expression after treatment with DNA damaging agents. (1) arrested with α-factor for 3 h. (2) α-factor arrest for 3 h, release for 1 h. (3) α-factor arrest for 3 h, release into 0.4 M HU for 1 h. (4) Asynchronous cells treated with 0.4 M HU for 4 h. (5) Asynchronous cells treated with 0.1% MMS for 1 h. (6) Asynchronous cells treated with 100 J/m^2 UV. (7) Untreated asynchronous cells as control The top panel shows the results of Western blot analysis with FLAG M2 antibody. The bottom panel shows the protein loading control as obtained by Ponceau S staining of the membrane prior to the blocking step.

5.6 Pwp1 LEVELS UNDER DIFFERENT CONDITIONS

5.6.1 Pwp1 levels in wild type and mutant cells

The Micro-array results regarding the expression of PWP1 must be confirmed by Northern blot analysis. I was also interested in determining the levels of Pwp1 protein in the different backgrounds. For this purpose, I used yeast strains constructed by Dr. Munah Abdul-Rauf with whom I collaborated on this work. In these strains, a triple FLAG tag was inserted just before the stop codon of the endogenous *PWP1* gene. Equal numbers of cells grown to exponential phase in rich medium were harvested for each strain. Proteins were extracted and analysed by SDS-PAGE and Western blotting. The results are presented in Figure 5.9b. Surprisingly, the levels of Pwp1-FLAG seem to be constant among all the strains tested.

5.6.2 Pwp1 levels after treatment with DNA damaging agents

Since deletion of nucleosome assembly factors such as Asf1 or CAF1 often results in sensitivity to DNA damaging agents (Game and Kaufman, 1999; Tyler et al., 1999), I also monitored the levels of Pwp1 protein after treatment with hydoxyurea (HU, a drug that blocks replication by inhibiting ribonucleotide reductase and limiting dNTP availability), methyl methane sulphonate (MMS, a DNA alkylating agent which creates lesions that stall replication) and UV radiation (which causes bulky DNA adducts that also interfere with replication fork progression). To assess the effect of HU on Pwp1 expression, cells were first arrested in G1 with α-factor for 3 h, released into rich medium containing 0.4M HU for 1.5 h and then harvested. The effect of MMS was measured after adding 0.1% MMS to asynchronous cells for 1.5 h. To monitor the effect of UV radiation, asynchronous cells were exposed to a short wavelength UV-B light source (100 J/m^2) and left to recover for 30 min before harvesting. The results are presented in Figure 5.9c. There is no prominent change in Pwp1 level in response to any of these treatments. In *asf1Δ*, but not W303 or *cac1Δ* cells, there is a slight decrease in Pwp1 levels after exposure to MMS and UV in asynchronous cultures (compare lanes 5, 6 and 7 in each strain). However, this decrease is rather modest and the significance of this observation is currently unclear. After treatment with HU, Pwp1 protein levels are similar in

both cells released from a G1 arrest, which causes early S-phase arrest, and asynchronous cells, which results in arrest throughout S-phase (compare lanes 3 and 4 for each strain in Figure 5.9c).

5.7 DEGRADATION OF OVEREXPRESSED Pwp1

The reduced expression of *PWP1* transcripts in *asf1cac1* double mutant cells suggested that these cells may need to decrease the level of transcription or the stability of PWP1 mRNA in order to maintain the same level of Pwp1 protein as in the other strains (Figure 5.9b). Based on this, I reasoned that perhaps Pwp1 acts as an inhibitor of the nucleosome assembly pathway. Consequently, cells lacking abundant assembly factors such as CAF1 and Asf1 and perhaps even wild type cells, may not be able to tolarate high levels of Pwp1 protein.

To test this hypothesis, I used additional strains generated in our laboratory by Dr. Munah Abdul-Rauf. In addition to the endogenous *PWP1* gene, these cells contain a high copy 2μ plasmid from which Pwp1-HA3 can be overexpressed from a galactose-inducible promoter. Using these strains, I was able to overexpress Pwp1-HA3 in a regulated manner and follow the fate of the protein by Western blotting with a monoclonal antibody against the HA tag. Equal numbers of cells from different strains containing the 2μ pGAL *PWP1-HA3* plasmid were plated on minimal media plates, lacking uracil to select for the 2μ plasmid, but containing either glucose or galactose as a carbon source. Most strains gave rise to similar number of colonies in both glucose and galactose plates. The *cac1Δ* mutant strain produced fewer colonies, but this was true in both glucose and galactose, suggesting that the reduced number of colonies observed with this strain is unrelated to the overexpression of Pwp1, which should only occur in galactose (Figure 5.10a). Therefore, overexpression of Pwp1-HA3 is not extremely toxic even in *asf1cac1* double mutant cells. However, I observed that growth is slightly impaired in all the deletion strains tested in comparison to W303 (Figure 5.10a). After 72h on galactose plates, the colonies formed by the four deletion strains tested were visibly smaller than those derived from wild type cells. In contrast, most strains gave rise to similar colony sizes on glucose plates, with the exception of

asf1Δcac1Δ double mutants, which have a slow growth phenotype even in the absence of Pwp1 overexpression.

To follow Pwp1-HA3 overexpression, cells were grown ON in medium containing raffinose as the sole carbon source. Glucose but not raffinose actively represses the *GAL* promoter. Because of this, raffinose allows more rapid and higher expression upon addition of galactose. Cells were then grown for 3 h in the presence of 2% galactose to induce overexpression. After this period, 2% glucose was added to repress the *GAL* promoter and cells were harvested at 15 min intervals. The results are presented in Figure 5.10b. Interestingly, in comparison to W303 and *asf1Δ* single mutants, Pwp1-HA3 was expressed at significantly lower levels in *cac1Δ* mutants. This was true for several independent colonies of the *cac1Δ* mutant strain (Figure 5.10b shows three separate colonies). This reduced expression was due to degradation of Pwp1-HA3 in *cac1Δ* cells, as the levels of Pwp1-HA3 clearly declined as a function of time after addition of glucose in each of the three *cac1Δ* cultures (compare 0 and 60 min time points following glucose addition; lanes 1 and 5 in each strain). In contrast, overexpressed Pwp1-HA3 was stable in W303. The levels of Pwp1-HA3 also seemed to decrease slightly as a function of time following glucose addition in *asf1cac1* double mutants, but to a much lesser degree than in *cac1* mutants. I cannot, at this time, explain the difference in overexpressed Pwp1-HA3 degradation in *asf1Δcac1Δ* versus *cac1Δ* cells (see discussion).

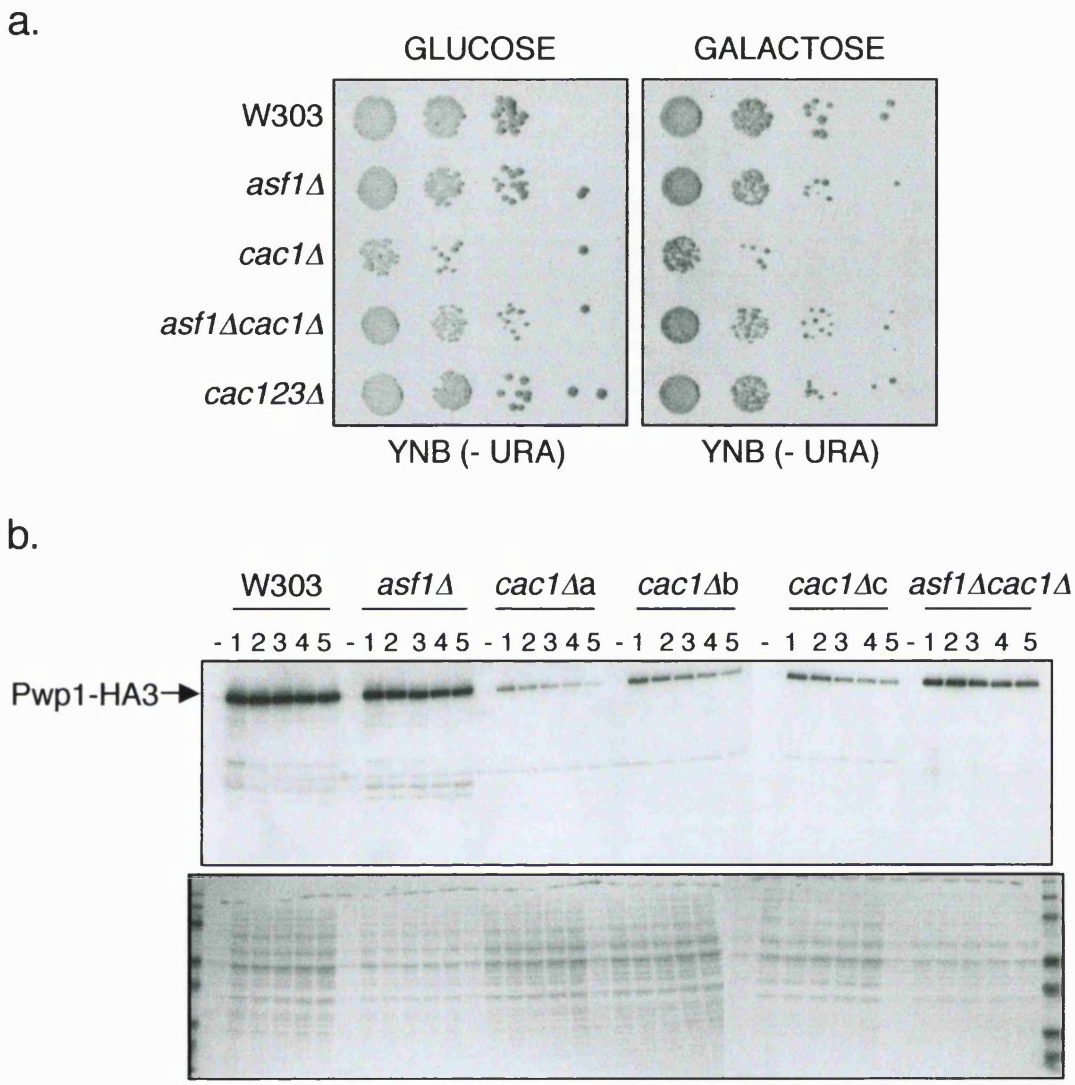

Figure 5.10: Overexpressed Pwp1-HA3 is degraded in *cac1* mutant cells

a. The indicated strains were transformed with a 2μ plasmid carrying a galactose inducible HA3-tagged *PWP1* gene and grown ON in minimal medium lacking uracil (to select for the plasmids), but containing 2% raffinose as the carbon source. Synthesis of tagged Pwp1 was induced by addition of 2% galactose for 3 h, after which 10-fold serial dilutions of each strain were plated on minimal agar minus uracil with either 2% glucose or 2% galactose as carbon source. The plates were incubated at 30°C and examined after 42 h (data not shown) and 72 h.

b. Asynchronous cells in exponential phase were induced with 2% galactose for 3 h, after which overexpression was blocked with 2% glucose. (-) Samples taken prior to induction by galactose demonstrate that *PWP1-HA3* was not expressed in raffinose containing media. After blocking expression, time points were taken from each sample at 15 min intervals (0-60 min corresponding to lane 1-5 in each strain). Whole cell extracts were analysed by SDS-PAGE and Western blotting with 12CA5 to detect the HA epitope.

5.8 Pwp1 BINDS HISTONE H3 *IN VIVO*

Because of the similarity between Pwp1 and the core histone-binding subunits of CAF1 (Cac3) and Hat1 (Hat2), I wanted to determine whether Pwp1 was also associated with histones *in vivo*. To address this possibility, 10 litres of exponential phase wild type cells expressing Pwp1-FLAG were harvested and lysed. Extracts were treated with ribonuclease A to remove RNA, ethidium bromide was added at 0.5mg/ml to disrupt complexes of proteins with DNA (Lai and Herr, 1992), and subjected to ultracentifugation. These steps were important since I was interested in finding out whether Pwp1 is associated with newly synthesised histones, rather than with DNA or chromatin. After these treatments, the extract was incubated ON with FLAG antibody beads (M2-agarose; Sigma). The beads were washed and eluted using repeated incubations with FLAG peptide (Chapter 2.9). The bound material was analysed by SDS-PAGE and Western blotting, and the results are shown in Figure 5.11a. Even after four sequential peptide elutions, some Pwp1-FLAG remained bound to the beads (lane 7). Interestingly, histone H3 also eluted with Pwp1 but, in contrast to Pwp1-FLAG, was only detectable in the fourth elution (lane 6). It is possible that some histone H3 was present in the earlier elutions as the histone H3 antibody used for detection is far less sensitive than the FLAG monoclonal antibody. However, it is clear that a substantial fraction of the Pwp1-FLAG protein eluted in the earlier fractions was not bound to histone H3, as similar levels of Pwp1-FLAG were eluted in all four elution steps.

I also tested whether Pwp1 was bound to histone H3 in strains lacking various chromatin assembly factors. For this, strains expressing Pwp1-FLAG (500ml) were harvested, lysed and treated as above. Although the *in vivo* levels of Pwp1 were similar in all strains (Figure 5.9b), the Pwp1-FLAG protein was susceptible to degradation during preparation of the crude cell extracts and immunoprecipitation of the protein. This degradation can be readily detected in all the strains with antibodies against the C-terminal FLAG epitope tag (Figure 5.11b, top panel). Pwp1-FLAG degradation was particularly striking in the extract prepared from *asf1Δcac1Δ* cells, where the full-length protein was

under-represented compared with the breakdown products (Figure 5.11b, top panel, lane 5). Similar amounts of histone H3 were co-precipitated with Pwp1-FLAG from both wild type cells and cells lacking Asf1 or CAF1 (Figure 5.11b, bottom panel). The detection of histone H3 in this assay was due to its association with Pwp1-FLAG because H3 was not detectable in a control immunoprecipitation performed from a strain lacking the FLAG tag (Figure 5.11b, bottom panel, lane 1). Co-precipitated histone H3 was not detected in the extract prepared from *asf1Δcac1Δ* cells (Figure 5.11b, bottom panel, lane 5). This is likely due to the more extensive degradation of Pwp1-FLAG during extract preparation and immunoprecipitation.

Because newly synthesised histone H3 and H4 are generally associated with each other (Tagami et al., 2004; Verreault et al., 1996), it seems reasonable to assume that Pwp1 binds to both H3 and H4. However, because of lack of sufficiently sensitive histone H4 antibodies, I have not been able to confirm the association of Pwp1 with H4. The results from mass spectrometry analysis may confirm or disprove this assumption (see below).

5.9 Pwp1 BINDING TO HISTONE H3 INCREASES IN *hat1Δ hat2Δ* CELLS

In *S. cerevisiae*, newly synthesised histones H3 and H4 are both acetylated by B-type HATs. The Hat1/Hat2 heterodimer is a very prominent B-type HAT that acetylates lysine 12 and, to a lesser extent, lysine 5 in newly synthesised histone H4 (Ai and Parthun, 2004; Kleff et al., 1995; Parthun et al., 1996; Poveda et al., 2004). Hat1/Hat2 is specific for newly synthesised histone H4 and cannot acetylate nucleosomal histones (Parthun et al., 1996; Verreault et al., 1998). However, cells lacking both Hat1 and Hat2 have no striking phenotype (Kleff et al., 1995; Parthun et al., 1996). This is because the acetylation of newly synthesised H4 is redundant with that of histone H3 (Ma et al., 1998). Acetylation of newly synthesised histone H3 can occur at up to five lysine residues (Kelly et al., 2000; Kuo et al., 1996). However, among the individual sites, mutation of lysine 14 (K14) in cells lacking Hat1/Hat2 has the most pronounced effect on telomeric silencing (Kelly et al., 2000). Because telomeric regions are generally deficient in acetylation at all sites in H3 and H4

(Suka et al., 2001), this silencing defect is most likely due to the involvement of K14 acetylation in chromatin assembly, rather than to a direct role of K14-acetylated H3 at the telomeres. The B-type HAT(s) responsible for acetylation of newly synthesised histone H3 is not known. Candidates for histone H3 K14 acetylation include Elongator and Gcn5, as both enzymes clearly acetylate this residue *in vitro* (Grant et al., 1999; Winkler et al., 2002). Because the acetylation sites in newly synthesised H3 and H4 are redundant with each other for nucleosome assembly (Kelly et al., 2000; Ling et al., 1996; Ma et al., 1998), one might expect that cells lacking Hat1/Hat2 would exhibit an increase in K14 acetylation of histone H3 bound to nucleosome assembly factors. To test this, extracts were prepared from either wild type or *hat1Δhat2Δ* mutant cells expressing Cac1- or Pwp1-FLAG. The levels of histone H3 and H3 K14 acetylation associated with Cac1- or Pwp1-FLAG were determined by Western blotting after immunoprecipitation with FLAG antibodies.

Similar amounts of both K14 acetylation and total histone H3 were found associated with Cac1 in wild type and *hat1Δhat2Δ* mutant cells (Figure 5.11c, lanes 2 and 4). Thus, perhaps acetylation of histone H3 bound to CAF1 does not increase to compensate for the absence of the B-type histone H4 HAT (Hat1/Hat2). Alternatively, it is possible that acetylation of newly synthesised histone H3 does increase but, due to the redundancy among the multiple acetylation sites, the increase in acetylation of K14 is very modest and undetectable in this assay.

In contrast, I observed a significant increase in the total amount of histone H3 bound to Pwp1-FLAG in cells lacking Hat1/Hat2. Consistent with this, I also detected an increase in K14 acetylation of histone H3 bound to Pwp1-FLAG (Figure 5.11c, compare lanes 1 and 3 in the two lower panels). The antibody used for the Western blot is very specific for K14 acetylation of histone H3 (Suka et al., 2001). Therefore, at least a fraction of the histone H3 bound to Pwp1 is acetylated at K14. Although K14 is a prominent site of acetylation in newly synthesised H3, this result does not prove that Pwp1 is bound to newly synthesised histone H3. This is because enzymes that acetylate nucleosomal histones such as Gcn5 can also modify histone H3 K14 (Grant et al., 1999).

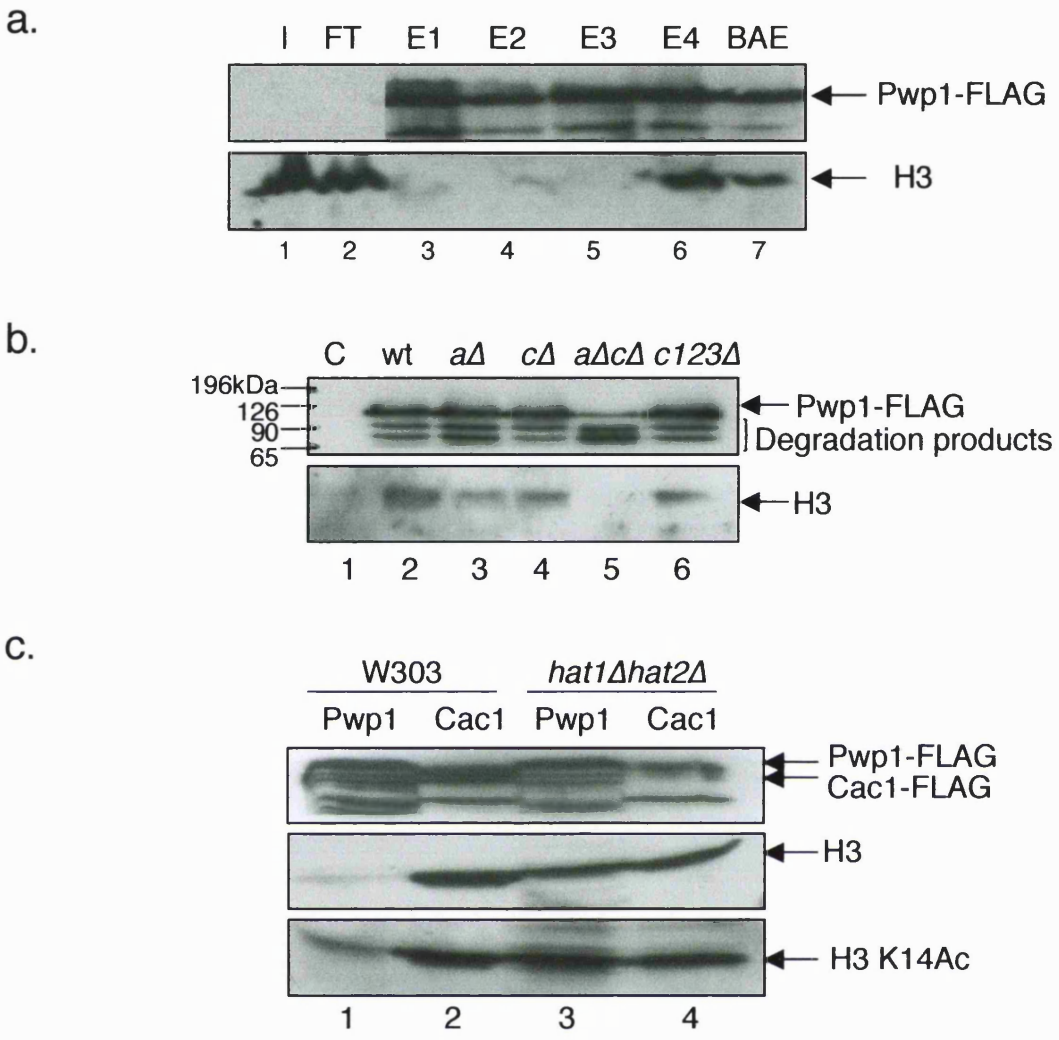

Figure 5.11: Pwp1 binds to higher amounts of histone H3 in *hat1Δhat2Δ* mutants than in wild type cells

a. FLAG-tagged Pwp1 was immunoprecipitated from extracts of W303 cells as described in Chapter 2.9 and in the text. FLAG-M2 antibody beads were washed and eluted with increasing levels of FLAG epitope peptide, followed by SDS-PAGE and Western blotting. The top panel shows Pwp1-FLAG detected using M2 as primary antibody. The bottom panel shows H3 detected by H3C antibody. (I) Input extract. (FT) Flow through after incubation with M2 beads. (E1-E4) Successive elutions with FLAG peptide. (BAE) M2 beads after the forth elution.

b. Co-immunoprecipitation experiments were carried out and analysed as in (a) using extracts from wild type and mutant strains. (W) W303, (*aΔ*) *asf1Δ*, (*cΔ*) *cac1Δ*, (*aΔcΔ*) *asf1Δcac1Δ* and (*c123Δ*) *cac1Δcac2Δcac3Δ* strains. (C) Imminoprecipitation from a W303 strain in which endogenous Pwp1 was not tagged by Flag. H3 was co-immunoprecipitated with Pwp1-FLAG from all extracts except for the control in which Pwp1 was not tagged, and the *asf1Δcac1Δ* extract in which Pwp1-FLAG was reproducibly unstable.

c. Pwp1-FLAG or Cac1-FLAG were immunoprecipitated from W303 (lanes 1 and 2) and *hat1Δhat2Δ* extracts (lane 3 and 4) as in (a). Bound proteins were analysed by SDS-PAGE and Western blotting with M2 antibody for detection of Flag (first panel), H3C antibody for detection of total H3 (second panel) and αH3 $K4_{Ac}$ antibody specific for detection of H3 acetylated on K14 (third panel).

Nonetheless, the fact that substantially higher amounts of H3 are bound to Pwp1 in *hat1Δhat2Δ* mutant cells suggests of a link between the degree of acetylation of newly synthesised histone H4 and the amounts of histones bound to Pwp1.

5.10 CONCLUSIONS AND FUTURE OBJECTIVES

5.10.1 Notes on the micro-array screen

Yeast cells lacking several chromatin assembly factors have heterochromatin-related phenotypes rather than global defects in chromatin structure. It has therefore been suggested that heterochromatin may be particularly sensitive to subtle alterations in chromatin structure or to delays in histone deposition during S phase. Such delays would occur in mutants lacking individual assembly factors. This may be because the deposition of acetylated H3/H4 and their subsequent deacetylation (Annunziato and Hansen, 2000; Jackson et al., 1976; Kuo et al., 1996; Ma et al., 1998; Parthun et al., 1996; Ruiz-Carrillo et al., 1975; Sobel et al., 1995; Taddei et al., 2001) appears to occur only once at heterochromatic loci - during S phase (Taddei et al., 1999), whereas dynamic acetylation and deacetylation processes operate continuously in euchromatin (Waterborg, 2002). However, the results from my pilot screen suggest that the fact that *cac1* and *asf1* mutants have mainly defects in heterochromatin mediated silencing does not imply that they are redundant for the assembly of euchromatin. A general overview on the micro-array results presented in this work suggests that many euchromatic genes have altered expression in *cac1Δ*, *asf1Δ* and *asf1Δcac1Δ* relative to the wild type strain (Table 5.1). The expression of around one fifth of entries located throughout the entire yeast genome (as represented in the Affymetrix chip – Figure 5.4) was found to significantly change in each of the three mutant strains tested. This is comparable with the change in expression in a *set1* mutant strain (Santos-Rosa et al., 2002; see introduction for chapter 6), but is higher than the sum of genes with altered expression in HDAC mutants such as *rpd3* or *sin3* (Bernstein et al., 2000).

Moreover, in the three mutant strains tested, different sets of genes were either up or down regulated relative to wild type cells. Interestingly, many genes are also down regulated when nucleosome assembly is inhibited by repression of histone H4 transcription during passage through S phase (Wyrick et al., 1999). Thus, defects in nucleosome assembly clearly affect the expression of many genes in either a positive or a negative fashion. Many of the effects of histone H4 repression or the disruption of nucleosome assembly factors are likely to be indirect (as opposed to being the direct consequence of alterations in nucleosome structure at the promoters of the affected genes). One illustration of this is the fact that, although histone deacetylases generally function as transcriptional repressors, mRNA expression profiles revealed that the numbers of down regulated and up regulated genes in histone deacetylase mutant cells are very similar (Bernstein et al., 2000). However, the vast majority of down regulated genes do not exhibit any changes in histone acetylation in the mutant cells, arguing that, in most cases, the deacetylase does not function directly at those promoters (Robyr et al., 2002). Based on these results, it seems possible that single mutations in *cac1* or *asf1* may affect gene expression globally because they perturb the expression or the activity of enzymes, such as histone deacetylases, that modify chromatin structure in a fairly global manner. For instance, the genome-wide deacetylation of newly synthesised histones H3/H4 that occurs shortly after their deposition at the replication fork may be disrupted or less efficient in cells lacking CAF1 or Asf1. As a result, the original acetylation pattern may not be restored even in euchromatin.

In asynchronous populations of *S. cerevisiae*, it has been estimated that as much as 50% of total histone H3 is methylated at K4 (Strahl et al., 1999 and V. Géli, personal communication) and as much as 90% is methylated at K79 (van Leeuwen et al., 2002). These modifications are present throughout most of the genome, with the notable exception of telomeres (Bernstein et al., 2002; van Leeuwen et al., 2002). Proliferating cells therefore need to methylate the majority of newly synthesised histones at lysines 4 and 79 either during or following replication in order to maintain these extremely abundant

modifications. As is the case for defects in histone deacetylation and nucleosome assembly, the absence of histone H3 K4 methylation alters the expression of many genes in both a positive and a negative manner (Santos-Rosa et al., 2002). It may therefore be worthwhile to determine whether the *cac1* or *asf1* mutations have an impact on the global levels of histone acetylation or histone H3 K4 and K79 methylation.

5.10.1.1 Expression in subtelomeric regions

It is possible that proteins whose ability to repress transcription is normally restricted to specific chromosomal domains in wild type cells are no longer confined to those domains in the absence of nucleosome assembly factors such as CAF1 or Asf1. For instance, the Sir complex formed by Sir2, Sir3 and Sir4 is normally restricted to telomeres and the silent mating type loci in wild type cells. However, because the Sir3 protein binds preferentially to non-acetylated histones (Carmen et al., 2002), mutations in several histone acetyltransferases allow the Sir complex to invade adjacent chromatin and repress transcription of many loci (Kimura et al., 2002; Kristjuhan et al., 2003; Suka et al., 2002). Interestingly, a fraction of the Rap1 protein, which is involved in nucleating the association of the Sir complex with telomeres, is delocalised from telomeres in *cac1* mutant cells (Enomoto et al., 1997). Yet, some Sir complexes remain at the telomeres in both *cac1* and *asf1* mutant cells (Enomoto et al., 1997), consistent with the fact that *cac1* and *asf1* mutants are much less defective in telomere silencing than *sir* mutant cells (Enomoto et al., 1997; Kaufman et al., 1997; Monson et al., 1997; Tyler et al., 1999). However, it is possible that the fraction of Sir complexes that dissociates from telomeres in *cac1* or *asf1* mutant cells, and is therefore free, is capable of repressing transcription at other loci. The exclusion of histone H3 K4 and K79 methylation from telomeres, and their nearly ubiquitous presence throughout the rest of the genome, has also been proposed to prevent the inappropriate silencing of non-telomeric loci (van Leeuwen et al., 2002), although there is no direct evidence that H3 K4 or K79 methylation directly interferes with Sir protein binding to histone H3. The above model would

predict that disruption of *sir* genes should restore normal expression to many genes that are down regulated in *cac1* or *asf1* mutant cells.

However, the preliminary analysis of gene expression in subtelomeric regions in this work, suggests that deleting *ASF1* or *CAC1* does not derepress the expression of all genes present in the HAST regions. Therefore, it seems unlikely that the absence of Asf1 and Cac1 affects chromatin structure uniformly throughout the HAST domains, for instance by increasing histone acetylation throughout the domain as occurs in *hda1* mutants (Robyr et al., 2002).

5.10.1.2 Expression from the *RDN1* locus

In contrast to subtelomeric regions, most rDNA entries were significantly up regulated in all three mutants, suggesting a general change in chromatin structure throughout the *RDN1* locus. Although this was expected in *cac1* single mutant cells, it was surprising that *asf1Δ* cells had a more pronounced rDNA silencing defect than *cac1Δ*, since *hir* mutants exhibit the opposite effect on rDNA silencing (Smith et al., 1999a). Furthermore, *asf1Δcac1Δ* strain had a slight increase in rDNA expression over the two single mutants. This preliminary result needs to be confirmed using direct assays for rDNA silencing (Smith et al., 1999a). However, it suggests that Asf1 plays a role in rDNA silencing that is independent of CAF1 or Hir proteins.

5.10.1.3 Expression of genes on chromosome 11

The fact that a significant number of entries on chromosome 11 were up regulated in *cac1Δ* and *asf1Δ* needs to be addressed. Using GO as an analysis tool, I was interested in finding out whether the chromosome 11 entries that are up regulated in *cac1Δ* and *asf1Δ* cells have any obvious connection with each other apart from their location on chromosome 11. However, the products of the ORFs for which annotations are available, localise to different compartments in the cell and do not seem to share a common function or act in one predominant pathway.

What could cause such a drastic effect? A comparative analysis of a large number of micro-array expression profiles revealed that as much as 8% of all deletion strains tested were aneuploid for whole chromosomes or chromosome segments. At least in some cases, the chromosome duplication was clearly important for growth of the mutant strain (Hughes et al., 2000). Interestingly, the authors found several strains were shown to have chromosome 11 di- or trisomy. In addition, extra chromosomes were found in a number of mutants that affect chromatin structure, including *rpd3Δ*, *sin3Δ*, *tup1Δ* and *hhf2Δ*.

It is possible that a similar scenario occurred in the analysis described here. This may be in agreement with the general low increase in expression of up regulated entries, which is more consistent with an increase in ploidy than changes in transcriptional regulation of individual genes. In *asf1Δ* and *cac1Δ* strains, only 122 and 102 entries were up regulated, respectively out of 372 entries for the whole chromosome. This means that the majority of entries on chromosome 11 (~65%) were not significantly affected, whereas whole chromosome aneuploidy was reported to affect the abundance of mRNAs derived from nearly all the genes on that chromosome (Hughes et al., 2000). However, because this experiment was not repeated, many entries whose expression is roughly 2-fold higher in the mutant strains relative to wild type cells (as would be expected for a disomic chromosome) would be filtered out as non-significant.

The up regulation of chromosome 11 entries was only observed in *asf1Δ* and *cac1Δ* single mutants, but not in the double mutant cells. Asf1 and CAF1 function in a largely redundant manner for nucleosome assembly of histones H3/H4 (Sharp et al., 2001; Tyler et al., 1999). Because *asf1cac1* double mutant generally has a more severe phenotype than either single mutants (Tyler et al., 1999), it seems unlikely that chromosome 11 duplication would have been selected for in both single mutants, but not in the double mutant. The fact that *asf1cac1* double mutant cells were not affected also suggests that these chromosome-wide changes in gene expression are not directly related to the degree of chromatin structural alteration, which would certainly be more severe in the double mutants than in *asf1* or *cac1* single mutants.

The karyotype of the mutant and wild type strains may be directly tested for the presence of disomic chromosome 11 by pulse-field gel electrophoresis.

5.10.2 Pwp1 and nucleosome assembly: an open question

In this chapter, I tried to identify novel proteins that promote or regulate nucleosome assembly. The micro-array experiments were based on the premise that the expression of genes encoding either assembly factors or regulators of nucleosome assembly would be altered in cells lacking Asf1 and CAF1. The fact that *PWP1* RNA levels were strongly down regulated in *asf1 cac1* double mutants, but less so in either single mutant, is consistent with the hypothesis that Pwp1 may be a negative regulator of the nucleosome assembly pathway. However, overexpression of Pwp1 from a galactose-inducible promoter did not have a striking cytotoxic effect in cells lacking either Asf1, CAF1 or both (Figure 5.10a). This may be due to the fact that cells lacking CAF1 can degrade a large fraction of the Pwp1 protein expressed from the galactose promoter (Figure 5.10b). Interestingly, this degradation was not observed in wild type or *asf1Δ* cells (Figure 5.10b), suggesting that the presence of excess Pwp1 only poses a problem in cells lacking CAF1. Surprisingly, although *asf1cac1* double mutants seem to have reduced levels of *PWP1* mRNA, they do not strongly degrade the overexpressed HA3 tagged Pwp1. It is possible that because *asf1Δcac1Δ* cells have less *PWP1* mRNA they stabilise the Pwp1 protein to maintain it at a constant level (as observed in Figure 5.9). Alternatively, the degradation of Pwp1-HA3 in this strain may occur at a slower pace. Supporting this, the level of Pwp1-HA3 is slightly reduced in *asf1Δcac1Δ* as a function of time. Moreover, a comparison of the first time point in each strain shows that the levels of overexpressed Pwp1 in *asf1Δcac1Δ* is intermediate between those seen in wild type and *asf1Δ* cells and those in *cac1Δ* cells (which clearly degrade Pwp1-HA3), suggesting that Pwp1 is kept at low levels. Consistent with this, Pwp1-FLAG seems particularly unstable in extracts made from *asf1Δcac1Δ* cells (Figure 5.11b).

A second link between Pwp1 and the nucleosome assembly pathway is that much higher amounts of H3 acetylated at lysine 14 are bound to Pwp1 in cells

lacking the B-type histone H4-specific acetyltransferase Hat1/Hat2. Although the precise significance of these results is not clear, they do suggest the existence of a link between Pwp1 and the nucleosome assembly pathway. The specific association of Pwp1 with newly synthesised histones could be validated by testing if tagged histone H3 induced from a *GAL* promoter is incorporated into the Pwp1 complex.

Two different groups isolated multiprotein complexes containing epitope-tagged Pwp1 by affinity purification (Gavin et al., 2002; Krogan et al., 2004). Neither group reported the presence of histones in the affinity-purified Pwp1 complexes. Surprisingly though, the polypeptide compositions of the two purified Pwp1 complexes are completely different (Table 5.2). This raises the possibility that Pwp1 may exist as part of several distinct protein complexes and perhaps the complex that contains histones is a minor one. In order to address this possibility, Dr. M. Abdul-Rauf in our lab purified Pwp1 complexes from a large amount of cells by using a Tandem Affinity Purification (TAP) tag (Rigaut et al., 1999). Surprisingly, none of the prominent bands in this purification corresponded to the apparent size of the protein subunits observed by others (Gavin et al., 2002; Krogan et al., 2004). The protein complexes purified in our lab remain to be analysed by mass spectrometry.

Table 5.2: PWP1 binding proteins

Protein	Description	MW	Localisation	reference
Act1	Actin	41,707	Cytoskeletal, nuclear	Gavin et al., 2002
Eno2	Enolase 2 (2-phosphoglycerate dehydrogenase) converts 2-phospho D-glycerate into phosphoenolpyruvate during glycolysis	46,773	Cytoplasmic	Ibid.
Fpr4	Nucleolar peptidylprolyl cis-trans isomerase	43,736	Nuclear, nucleolar	Ibid.
Nan1	Nucleolar protein associated with Net1, component of the U3 SnoRNA (small subunit processome), which is required for 18S rRNA biogenesis	101,088	Nuclear, nucleolar	Ibid.
Pol5	DNA polymerase V, member of the DNA polymerase B family	115,730	Nucleolar	Ibid.
Smc1	Coiled-coil protein of the SMC family involved in chromosome condensation and segregation	141,136	Nuclear	Ibid.
Yp1207w	Unknown function, contains a radical SAM superfamily domain and a flavodoxin domain	89,814		Ibid.
Brx1	Required for maturation of rRNA components of the 60S ribosomal subunit, member of the Imp4 superfamily containing a Sigma70-like motif	33,455	Nucleolar	Krogan et al., 2004
Nop12	Important for the synthesis of 25S pre-rRNA	51,830	Nucleolar	Ibid.

The only common feature in two distinct Pwp1 multiprotein complexes purified from *S. cerevisiae* previously (Gavin et al., 2002; Krogan et al., 2004), was that both complexes contain a number of nucleolar proteins, though each complex contains a different set of nucleolar proteins. This is consistent with the fact that Pwp1 itself has been localised in the nucleolus in both yeast (Huh et al., 2003) and human cells (Andersen et al., 2002; Honore et al., 2002). It is clear that some of the proteins associated with Pwp1 are involved in ribosomal RNA maturation and ribosome biogenesis (Table 5.2). Kap121 and Kap123 are nuclear import factors that, in addition to core histones (Mosammaparast et al., 2002; Mosammaparast et al., 2001), also transport ribosomal and signal recognition particle proteins (Grosshans et al., 2001; Rout et al., 1997). These proteins are normally directed to the nucleolus where they are assembled onto their cognate RNAs to form either ribosomal subunits or signal recognition particles, which are subsequently exported back to the cytoplasm. Therefore, it is tempting to speculate that newly synthesised histones may also be brought to the nucleolus by Kap121 and Kap123. Pwp1 may recognise newly synthesised histones during their normal transit through the nucleolus and thereby regulate the transfer of both ribosomal proteins and histones from Kap121/123 to downstream factors. Although the current dogma is that Ran-GTP releases protein cargoes from their import factors immediately upon entry into the nucleus, a number of Ran-independent nuclear import pathways also exist (Komeili and O'Shea, 2001). Arguably, at least for some protein cargoes, it may be advantageous to delay this dissociation. For instance, it may be preferable not to release ribosomal proteins from nuclear import factors until they can be assembled onto ribosomal RNA in the nucleolus. Free histones bind very strongly and non-specifically to DNA and can therefore potentially interfere with many processes that require access to genetic information (Gunjan and Verreault, 2003; Meeks-Wagner and Hartwell, 1986). It may therefore be necessary to delay their dissociation from import factors until the newly synthesised histones can be safely transferred to downstream nucleosome assembly factors.

Alternatively, Pwp1 may exert a negative influence on nucleosome assembly by diverting a fraction of newly synthesised histones to promote their assembly at the rDNA locus at the expense of other loci. This may interfere with nucleosome assembly throughout the genome and become particularly deleterious in cells lacking Asf1 and CAF1. In *S. cerevisiae*, the *RDN1* locus, which encodes both the large 35S rRNA precursor and the 5S rRNA, is present in the nucleolus and consists of 100-200 direct repeats that encompass 1-2 Mb of DNA, representing a significant fraction (7-14%) of the yeast genome (14 Mb). In rapidly proliferating cells, only about half of the repeats are transcriptionally active and appear to be devoid of nucleosomes (Dammann et al., 1993), but the fraction of repeats that are active in transcription can be adjusted in response to environmental conditions that affect the demand for protein synthesis and ribosome biogenesis. For instance, cells in stationary phase utilise fewer rRNA genes than exponentially growing cells (Dammann et al., 1993).

Dr. Munah Abdul-Rauf in our laboratory has disrupted the *PWP1* gene in W303 cells. In agreement with published work (Duronio et al., 1992), *pwp1Δ* cells are viable. This strain can now be analysed for phenotypes that may be consistent with a defect in nucleosome assembly such as reduced silencing at the telomeres, mating type and rDNA loci. Given the presence of Pwp1 in the nucleolus, it may be particularly instructive to analyse the chromatin structure of the *RDN1* locus. This can be achieved by comparing the accessibility of the *RDN1* locus to nucleases (*e.g.* DNase I, micrococcal nuclease or restriction enzymes). Alternatively, psoralen cross-linking can be used to distinguish rDNA repeats that are properly assembled into nucleosomes from those that are nucleosome-free (Dammann et al., 1993). In addition, the proposed role of Pwp1 as a negative regulator of nucleosome assembly suggests that disruption of the *PWP1* gene may suppress some of the phenotypes observed in *asf1cac1* double mutants, such as the defects in chromatin structure that interfere with telomere and mating type silencing.

CHAPTER 6 –
DOES *S. cerevisiae* Set1 FUNCTION IN S PHASE VIA PCNA?

6.1 INTRODUCTION

Set1 (Su(var)3-9 – Enhancer of zeste – Trithorax 1) is a histone methyltransferase and is the sole enzyme responsible for methylation of histone H3 lysine 4 (K4) in *S. cerevisiae*. In the past few years, there has been a lot of interest in the chromatin field regarding this enzyme and the methylation of histone H3 K4 as important elements of the so-called histone code hypothesis (Strahl and Allis, 2000). In higher eukaryotes, this modification of histone H3 has been proposed as a mark of chromosomal domains that are permissive for transcription (Litt et al., 2001). In an asynchronous population of human cells, at least 7% of histone H3 is methylated to some degree (Strahl et al., 1999). Histone H3 K4 methylation is even more abundant in *S. cerevisiae*, where ~50% of total histone H3 exhibit some degree of methylation, with roughly equal amounts of mono-, di- or tri-methylated histone H3 K4 (Pamblanco et al., 2004; Strahl et al., 1999). In other words, this implies that on average, one of the two histone H3 molecules in each nucleosome is mono-, di- or tri-methylated. Only a few chromosomal loci have been reported to lack histone H3 K4 methylation, including the silent mating type loci, the rDNA locus and telomere-proximal regions (Bernstein et al., 2002).

Consistent with the widespread distribution of histone H3 K4 methylation, the expression of about one fifth of all genes in *S. cerevisiae* is affected, either in a positive or in a negative manner, in cells lacking Set1 and histone H3 K4 methylation (Santos-Rosa et al., 2002). Despite the fact that histone H3 K4 methylation is regarded as a hallmark of transcriptionally competent chromatin in higher eukaryotes (Litt et al., 2001), over 800 genes were up-regulated in *S. cerevisiae* cells lacking Set1 (Santos-Rosa et al., 2002). However, the vast majority of the changes in gene expression are rather modest (less than two-fold) and are likely to be indirect.

The genome-wide distribution of histone H3 K4 methylation is reminiscent of K79 methylation, which occurs in about 90% of histone H3 molecules (again as a mixture of mono-, di- and tri-methylated species), and is catalysed by a different histone methyltransferase known as Dot1 (van Leeuwen et al., 2002). Paradoxically, although histone H3 K4 and K79 methylation are largely absent from heterochromatic loci such as telomere-proximal regions, both modifications are required for silencing of telomeric reporter genes (Nislow et al., 1997). Overexpression of Dot1, which results in nearly 100% of histone H3 being methylated at K79, also leads to defects in telomeric silencing (van Leeuwen et al., 2002). The fact that both loss of function and overexpression of Dot1 decrease the association of Sir proteins with telomere-proximal regions has led to a model in which genome-wide methylation of histone H3 K79 constrains the binding of Sir proteins to a few chromosomal loci that are devoid of K79 methylation, such as the telomeres (van Leeuwen and Gottschling, 2002). In other words, histone H3 K79 methylation serves to prevent the promiscuous binding of Sir proteins throughout the genome, which could potentially interfere with gene expression or other processes (van Leeuwen and Gottschling, 2002).

The ability to prevent inappropriate protein binding to certain chromosomal loci (rather than serving as a docking site) may be a property of other histone modifications. For example, acetylation of histone H4 K16 also occurs throughout the genome, but is excluded from telomere-proximal regions (Robyr et al., 2002). This is important because the region of the N-terminal tail of histone H4 containing K16 is part of the binding site for Sir3 and this interaction is required for telomeric silencing. The presence of K16 acetylation reduces the affinity of Sir3 for histone H4 (Carmen et al., 2002). Therefore, it seems likely that genome-wide histone H4 K16 acetylation may function to prevent promiscuous binding of Sir3. By analogy, it is possible that histone H3 K4 methylation may also serve a similar function, perhaps by discouraging the non-specific binding of Sir proteins and/or other general transcriptional repressors such as Ssn6-Tup1 (Smith and Johnson, 2000).

a.

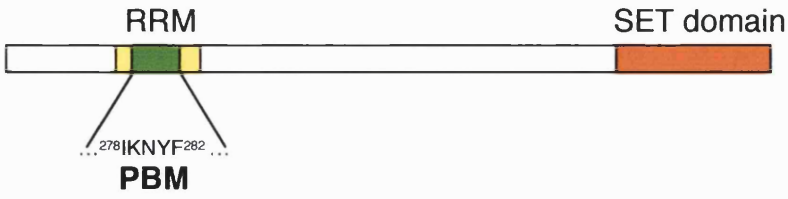

b.

S. cerevisiae Set1:	268	STTTNIQDISIKNYFKKYGE	287
Sc. pombe	100	NISPLVTSEQLRYHFKSFGE	119
S. mikatae	269	STTTSIQDISIKNYFKKYGE	288
S. castellil	276	INNTMIQDISIKNYFKKFGV	295
S. kudriavzevii	273	STTTGIQDVSIKNYFKKYGE	292
Kluyveromyces lactis	215	PIAAALSEAIIKNYFKSFGE	234
Candida glabrata	308	TQMANIPDISIKNYFRKFGE	327
Debaryomyces hansenii	256	DLPSTTSEVYLSNFFKSYGD	275
Yarrowia lipolytica	209	GLSSLTTSKTITAHFKTYGE	428

Figure 6.1: SET1 has a putative PCNA binding motif

a. A schematic representation of SET1, showing the positions of the SET domain, the RNA Recognition Motif (RRM) and the putative PBM.

b. Sequence alignment of several Set1 homologues from other yeast species, showing the partial conservation of the putative PBM sequence at the N-terminus. The conserved hydrophobic and aromatic residues are highlighted in yellow, the partially conserved glutamine in green, and the basic residues following the core PBM are underlined and in red. *S.* - *Saccharomyces*; *Sc.*: *Schizosaccharomycetes*.

The mechanisms that enable proliferating cells to propagate genome-wide modifications such as histone H3 K4 or K79 methylation are not known. Our laboratory showed that K4 methylation was undetectable in newly synthesised histone H3 before it is packaged into chromatin (A. Gunjan, unpublished data). I was interested in addressing how the newly synthesised histone H3 may acquire K4 methylation in proliferating cells.

6.2 Set1 CONTAINS A PUTATIVE PCNA BINDING MOTIF

Through sequence analysis, I found a putative PCNA Binding Motif (PBM) in Set1. As is the case in many other PCNA-binding proteins (Leonhardt et al., 1998; Warbrick, 2000), the putative PBM is not located within the catalytic SET domain, but is found instead near the N-terminus of the Set1 protein (Figure 6.1a). This region of Set1 is conserved across a number of different yeast species (Figure 6.1b) and exhibits sequence similarity to RNA recognition motifs (RRM; Burd and Dreyfuss, 1994; Noma and Grewal, 2002).

6.3 MUTATIONS IN THE PUTATIVE PBM OF Set1 CAUSE A STRONG DECREASE IN H3 K4 METHYLATION *IN VIVO*

Yeast strains were constructed in which the endogenous *SET1* gene was tagged to express Set1 with 9 Myc epitopes at the N-terminus. Based on the cDNA sequence, the predicted size of Set1 is 124 kDa. Tagging of wild type Set1 gave rise to a number of species that were absent from a control non-tagged strain (Figure 6.2a) The largest species ran between the 126 and 196 kDa markers and is probably the full-length tagged Set1. Because the *SET1* gene does not contain any introns, the shorter species most likely represent C-terminal breakdown products of Set1. The relative abundance of these breakdown products suggests that even wild type Set1 may be an unstable protein *in vivo*. Mutant strains were constructed where the $Y_{250}F_{251}$ residues that form the putative PBM core were substituted by YD, DD and AA residues. The stability of mutant proteins was analysed by Western blotting (Figure 6.2a). The YF/DD mutant was highly unstable and only a short breakdown product of ~90kDa was detected for this mutant.

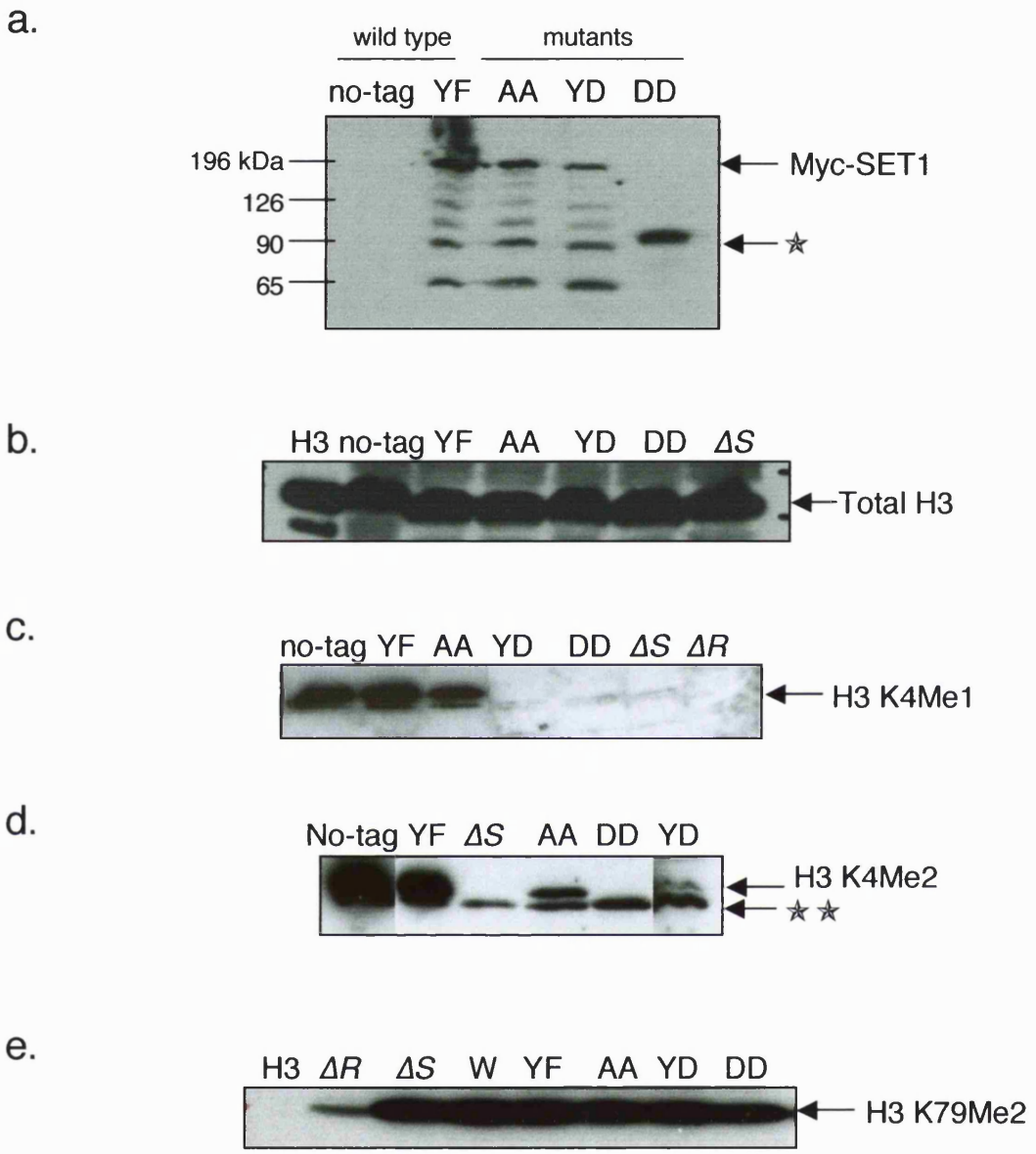

Figure 6.2: Mutations in the putative PBM of SET1 abolish H3 K4 methylation

Endogenous Set1 was tagged in W303 with 9 Myc epitopes on the N-terminus. Residues $Y_{250}F_{251}$of tagged Set1 were substituted by YD, DD and AA residues to create three distinct *set1* mutant strains. Whole-cell extracts were prepared from these strains and from a *set1* null mutant (*ΔS*) and a *rad6* null mutant (*ΔR*) strains used as a negative controls for H3 methylation. (H3) Recombinant histone H3 expressed in *E. coli*, which is devoid of methylation was used as a control for antibody specificity. Proteins were analysed by SDS-PAGE and Western blotting using 9E10, H3C, αH3 $K4_{Me1}$, αH3 $K4_{Me2}$ and αH3 $K79_{Me2}$ as primary antibodies for detection of Myc-set1 (**a**), histone H3 (**b**), H3 $K4_{Me1}$ (**c**), H3 $K4_{Me2}$ (**d**) and H3 $K79_{Me2}$ (**e**), respectively. (YF) A strain with wild type Myc-Set1. (AA) A strain with YF/AA mutation on Myc-Set1. (YD) A strain with YF/YD mutation on Myc-Set1. (DD) A strain with YF/DD mutation on Myc-Set1. (no-tag) W303 cells with no tag on Set1 were used as control. The YF/DD mutant was found to be highly unstable, (★) marks a degradation product of the YF/DD mutation. (★★) In panel (d), indicates what seems to be a αH3 $K4_{Me2}$ cross-reacting band, as it is also detected in set1Δ extracts. In panels c. and d. bands shown are from the same film and the same exposure time, but were from distant parts of the same membrane/gel.

The YF/YD and YF/AA mutations resulted in a slight, but reproducible decrease in the amount of full length Set1 protein (Figure 6.2a). The methylation of H3 K4 in wild type and mutant strains was analysed by Western blotting using antibodies against total histone H3 or antibodies specific for mono- (H3 $K4_{Me1}$) and di-methylated H3 K4 (H3 $K4_{Me2}$). Whereas the YF/AA mutation only slightly impaired mono- and di-methylation, the YF/YD and YF/DD mutations strongly reduced both types of H3 K4 methylation (Figure 6.2b, c and d). As expected, Dot1-dependent H3 K79 methylation was not affected by any of the *set1* mutations (Figure 6.2e). A quantitative analysis performed by N-terminal Edman sequencing of total histone H3 isolated from the mutant strains demonstrated the presence of residual levels of histone H3 K4 methylation in the YF/YD mutant strain (Pamblanco et al., 2004). Based on this criteria, the YF/AA mutant had 57% of the wild type activity, whereas the YF/YD mutant only showed less than 10% of the wild type activity (Pamblanco et al., 2004).

6.4 MUTATIONS IN PCNA MAY CAUSE SOME LOSS OF HISTONE H3 K4 METHYLATION

The phenotypes of many PCNA mutants have been extensively characterised in budding yeast (Ayyagari et al., 1995; Eissenberg et al., 1997). Because the *POL30* gene encoding PCNA is essential, these studies were performed by plasmid shuffling. In this system, the endogenous *POL30* gene was disrupted in cells carrying a *URA3*-marked plasmid encoding wild type *POL30* to maintain cell viability. These cells were transformed with a *TRP1*-marked plasmid encoding mutant forms of *pol30*. The plasmid encoding wild type *POL30* was selected against in the presence of 5-fluoro-orotic acid (FOA), a drug that is lethal to cells expressing the *URA3* gene. Only the cells that lost the URA3-marked plasmid encoding wild type *POL30*, but retained the *TRP1*-marked plasmid expressing mutant *pol30* were able to form colonies on FOA plates. These colonies were streaked on minimal media plates lacking tryptophan to ensure that the viability of the strains was indeed due to the *TRP1*-marked plasmids carrying the *pol30* mutations, rather than integration of the wild type *POL30* gene into the chromosome.

I reasoned that if Set1 was a *bona fide* PCNA-binding protein, its activity would be affected by *pol30* mutations that were previously shown to abolish or decrease the binding of PBPs to PCNA such *pol30-79* (LI 126,128 AA) and *pol30-90* (PK 252,253 AA), which respectively affect the inter-domain connector loop and the C-terminus of PCNA (Gomes and Burgers, 2000). Furthermore, I wished to test PCNA mutations that interfere with nucleosome assembly by either the Hir proteins (*pol30-6*, DD 41,42 AA) or CAF1 (*pol30-8*, RD 61,63 AA). In addition to these, *TRP1*-marked plasmids encoding wild type *POL30* and *pol30-22* (DE 256,257 AA) were used as controls.

In *S. cerevisiae*, a small fraction of PCNA is sumolated during normal S-phase progression and ubiquitylated in response to DNA damage (Hoege et al., 2002). Importantly, the ubiquitin-conjugating enzyme Rad6 is responsible for both PCNA and histone H2B K123 mono-ubiquitylation (Hoege et al., 2002; Sung et al., 1988). This is interesting because mutations of either *rad6* or the site of histone H2B ubiquitylation (K123) both abolish the methylation of histone H3 K4 and K79 (Briggs et al., 2002; Dover et al., 2002; Ng et al., 2002; Sun and Allis, 2002). This observation is puzzling because only a small fraction of H2B is ubiquitylated *in vivo*, whereas K4 and K79 methylation are extremely abundant modifications of histone H3. The mechanism linking Rad6, H2B ubiquitylation, and histone H3 K4 and K79 methylation is not known.
To investigate the potential roles of PCNA sumolation and ubiquitylation in histone methylation, I created two additional plasmids by site-directed mutagenesis. *pol30-K127R* and *pol30-K164R* alleles respectively, change lysine residues K127 (which is located in the inter-domain connector loop and is exclusively sumolated) and K164 (which can be either sumolated or ubiquitylated and is located on the back side of the PCNA ring, facing away from the direction of DNA synthesis) into arginine residues.

Eight strains (*pol30-wt/6/8/22/79/90/K127R/K164R*) were created by plasmid shuffling. Figure 6.3a shows the locations of these mutations on PCNA.

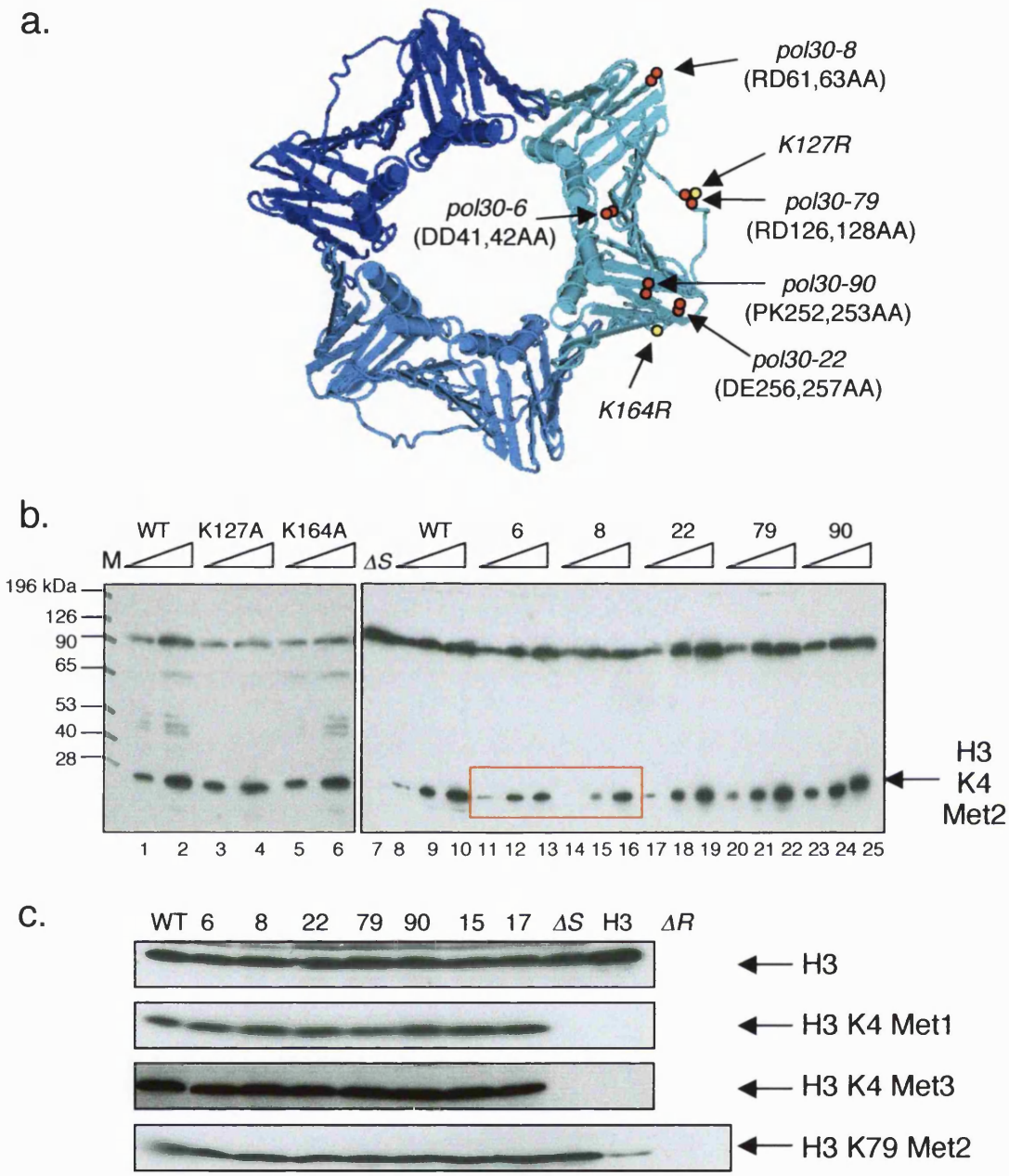

Figure 6.3: *pol30* mutations may affect H3 K4 methylation by SET1

a. Sites of PCNA mutations as described in the text. In each mutant, one (yellow dot) or two (red dots) residues were replaced by alanines. The PCNA structure is based on the coordinates from Gulbis et al. (1996).

b. Whole cell extracts derived from the different *pol30* strains were analysed by SDS-PAGE and Western blotting for H3 K4 di-methylation. (K127R) a strain where PCNA K127 was mutated to R. (K164R) a strain where PCNA K164 was mutated to R. (6) *pol30-6* strain. (8) *pol30-8* strain. (22) *pol30-22* strain. (79) *pol30-79* strain. (90) *pol30-90* strain. *pol30-6* and *pol30-8* (marked by the red square) seem to have slightly reduced levels of H3 K4 di-methylation. A *set1* null mutant (*ΔS*) was used as a control strain lacking H3 K4 methylation.

c. The *pol30* mutant strains were analysed by SDS-PAGE and Western-blotting for other H3 modifications, including K4 mono- and tri-methylation and K79 di-methylation. A *set1* null mutant (*ΔS*) was used as a control strain lacking H3 K4 methylation. A *rad6* null mutant (*ΔR*) was used as a control strain lacking H3 K79 methylation.

Detection of histones was as in Figure 6.2. αH3 $K4_{Me3}$ was used for detection of H3 $K4_{Me3}$.

These strains were grown under identical conditions in rich medium up to $1x10^7$ cell/ml, harvested, and analysed by SDS-PAGE and Western blotting. I also included *set1Δ* and *rad6Δ* mutants as negative control strains lacking histone H3 K4 methylation. Three different amounts of each cell lysate were analysed to ensure that the Western blotting signals were within the linear range. The *pol30-6* and *pol30-8* mutant strains showed slightly reduced levels of H3 K4 di-methylation (compare lanes 8-10 with lanes 11-16 in Figure 6.3b). In contrast, K4 mono- and tri-methylation as well as K79 methylation of histone H3 were not detectably affected by these mutations (Figure 6.3c). None of the other *pol30* mutations had any striking effect on histone H3 K4 or K79 methylation. However, using N-terminal Edman degradation to measure histone H3 K4 methylation quantitatively, our collaborators failed to detect any significant change in H3 K4 methylation levels in the *pol30-6* and *pol30-8* mutant strains (Pamblanco et al., 2004).

6.5 PULL DOWN ASSAYS

Using tagged proteins, I tried to detect an interaction between Set1 and PCNA. This was done by isolation of His-tagged PCNA from yeast extracts using nickel-agarose beads and probing for co-precipitation of Myc-tagged Set1. However, the results from numerous attempts were inconclusive as the Myc-Set1 protein was degraded during the incubation step (data not shown). Attempts to first immunoprecipitate Myc-Set1 or to use antibodies against non-tagged Set1 also failed. Therefore, I was not able to demonstrate an interaction between Set1 and PCNA.

6.6 CONCLUSIONS AND FUTURE OBJECTIVES

In this chapter, I set out to determine whether K4 methylation of newly synthesised histone H3 was coupled to DNA replication via PCNA. In higher eukaryotes, this is clearly the case for maintenance DNA methylation, which is mediated by a direct interaction between DNMT1 and PCNA (Chuang et al., 1997; Leonhardt et al., 1992). I hypothesised that S phase might represent an ideal opportunity to faithfully reproduce abundant histone post-translational modifications such as histone H3 K4 and K79 methylation, thereby allowing

their inheritance to daughter cells. I identified a putative PBM in Set1, which is conserved in a number of yeast species. Point mutations of the two conserved hydrophobic residues within this motif greatly reduced mono- and di-methylation of histone H3 K4, but not the Set1-independent methylation of histone H3 K79. However, I was not able to demonstrate a direct interaction between Set1 and PCNA. Importantly, a number of *pol30* mutants that I tested did not significantly affect histone H3 K4 methylation. This group included mutations in *POL30* known to block its interaction with PCNA-binding proteins (Tsurimoto, 1999), mutations that inhibit nucleosome assembly through CAF1 and Hir proteins (Sharp et al., 2001) and mutations that prevent PCNA ubiquitylation by Rad6 and sumolation by Ubc9 (Hoege et al., 2002). Although these results may indicate that Set1 simply does not interact with PCNA, they do not exclude this possibility entirely. For example, FEN1 was shown to be partly functional *in vivo*, even when its interaction with scPCNA seemed to be abolished by these mutations (Frank et al., 2001). Additionally, as is the case for CAF1 (Sharp et al., 2001), the binding of Set1 to PCNA may only be affected by PCNA mutations that do not localise to neither the inter-domain connector loop nor the C-terminal region of PCNA. Alternatively, cells may be able to compensate for the loss of this interaction.

Even if an interaction between Set1 and PCNA is not required for histone H3 K4 methylation, it is still possible that passage through S-phase may play an important role in methylation of newly synthesised histone H3. More direct experiments need to be carried out to test whether Set1 functions at the replication fork during S phase.

In order to study this further, it would be useful to create a yeast strain that allows conditional degradation of Set1 (Labib et al., 2000). Using this strain, Set1 could be degraded in G1 before the cells are allowed to progress through S-phase. Following S-phase, the cells should have no K4 methylation of newly synthesised histone H3. By re-expressing Set1, we could then ask whether the enzyme is able to promote K4 methylation of newly synthesised histone H3 in G2. Moreover, it would be interesting to test whether Set1 is present at the replication fork, in which case it would co-localises with sites of bromodeoxy-

uridine (BrdU) incorporation into nascent DNA. Although wild type yeast cannot incorporate BrdU supplied from the medium, strains that express a human nucleoside transporter and a thymidylate kinase gene were recently generated to allow pulse labelling of nascent DNA (Lengronne et al., 2001). This approach was recently used successfully to localise checkpoint proteins at the replication fork (Katou et al., 2003).

It may also be useful to study the methylation of epitope-tagged histone H3 expressed from a galactose-inducible promoter. The expression of the tagged H3 could be induced as cells synchronised in G1 are released into S phase. If Set1 can only function during S phase, K4 methylation will not occur in the G1 cells when the tagged H3 cannot be packaged into chromatin, nor will it be delayed until G2 phase, but will instead appear progressively as cells replicate their DNA during S phase.

While this work was in progress, several reports identified several components of the Paf1 complex as being required for genome-wide histone H3 K4 and K79 methylation (Krogan et al., 2003; Ng et al., 2003b) and H2B mono-ubiquitylation (Ng et al., 2003a; Wood et al., 2003). Though dispensable for viability, the Paf1 complex associates with elongating RNA polymerase II and participates in elongation (Squazzo et al., 2002). The requirement of the Paf1 complex for Set1-mediated histone H3 K4 methylation likely explains why actively transcribed genes are associated with high levels of tri-methylated histone H3 K4, whereas di-methylation of H3 K4 is more widespread throughout the genome (Santos-Rosa et al., 2002). A Paf1 subcomplex is also required for histone H3 K4 and K79 methylation in non-coding regions throughout most of the genome, through its effect on H2B ubiquitylation. One possibility to account for the severe reduction in histone H3 K4 methylation in the Set1 YF/YD mutant is that the mutation affects the ability of the Set1 RNA recognition motif to associate with the Paf1 complex or RNA during transcription. The critical role of the Paf1 complex in histone H3 K4 and K79 methylation therefore suggests that transcription, rather than replication, may be key to the maintenance of these abundant post-translational modifications of histone H3 in proliferating cells. However the function of the Paf1 subcomplex in this context needs to be elucidated.

REFERENCES

Abruzzi, K.C., Magendantz, M. and Solomon, F. (2002) An a-tubulin mutant demonstrates distinguishable functions among the spindle assembly checkpoint genes in *Saccharomyces cerevisiae. Genetics*, **161**, 983-994.

Adams, A., Gottschling, D.E., Kaiser, K.A. and Stearn T. (1997) Methods in Yeast genetics: A Cold Sping Harbor LAboratory Course Manual. Cold Spring Harbor laboratory press, New York.

Adams Martin, A., Dionne, I., Wellinger, R.J. and Holm, C. (2000) The function of DNA polymerase a at telomeric G tails is important for telomere homeostasis. *Mol Cell Biol*, **20**, 786-796.

Adkins, N.L., Watts, M. and Georgel, P.T. (2004) To the 30-nm chromatin fiber and beyond. *Biochim Biophys Acta*, **1677**, 12-23.

Aguilera, A., Chávez, S. and Malagón, F. (2000) Mitotic recombination in yeast: elements controlling its incidence. *Yeast*, **16**, 731-754.

Ahmad, A., Nagamatsu, N., Kouriki, H., Takami, Y. and Nakayama, T. (2001) Leucine zipper motif of chicken histone acetyltransferase-1 is essential for *in vivo* and *in vitro* interactions with the p48 subunit of chicken chromatin assembly factor-1. *Nucleic Acids Res*, **29**, 629-637.

Ahmad, K. and Henikoff, S. (2002a) Histone H3 variants specify modes of chromatin assembly. *Proc Natl Acad Sci U S A*, **12**, 12.

Ahmad, K. and Henikoff, S. (2002b) Histone H3 variants specify modes of chromatin assembly. *Proc Natl Acad Sci U S A*, **99 Suppl 4**, 16477-16484.

Ahmad, K. and Henikoff, S. (2002c) The histone variant H3.3 marks active chromatin by replication- independent nucleosome assembly. *Mol Cell*, **9**, 1191-1200.

Ai, X. and Parthun, M.R. (2004) The nuclear Hat1p/Hat2p complex: a molecular link between type B histone acetyltransferases and chromatin assembly. *Mol Cell*, **14**, 195-205.

Alexiadis, V., Varga-Weisz, P.D., Bonte, E., Becker, P.B. and Gruss, C. (1998) In vitro chromatin remodelling by chromatin accessibility complex (CHRAC) at the SV40 origin of DNA replication. *Embo J*, **17**, 3428-3438.

Andersen, J.S., Lyon, C.E., Fox, A.H., Leung, A.K., Lam, Y.W., Steen, H., Mann, M. and Lamond, A.I. (2002) Directed proteomic analysis of the human nucleolus. *Curr Biol*, **12**, 1-11.

Andersson, P., Goldfarb, M.P. and Weinberg, R.A. (1979) A defined subgenomic fragment of in vitro synthesized Moloney sarcoma virus DNA can induce cell transformation upon transfection. *Cell*, **16**, 63-75.

Ando, T., Kawabe, T., Ohara, H., Ducommun, B., Itoh, M. and Okamoto, T. (2001) Involvement of the interaction between p21 and proliferating cell nuclear antigen for the maintenance of G2/M arrest after DNA damage. *J Biol Chem*, **276**, 42971-42977.

Annunziato, A.T. and Hansen, J.C. (2000) Role of histone acetylation in the assembly and modulation of chromatin structures. *Gene Expr*, **9**, 37-61.

Ayyagari, R., Impellizzeri, K.J., Yoder, B.L., Gary, S.L. and Burgers, P.M. (1995) A mutational analysis of the yeast proliferating cell nuclear antigen indicates distinct roles in DNA replication and DNA repair. *Mol Cell Biol*, **15**, 4420-4429.

Azam, N., Vairapandi, M., Zhang, W., Hoffman, B. and Liebermann, D.A. (2000) Interaction of CR6 (GADD45{gamma}) with Proliferating Cell Nuclear Antigen (PCNA) impedes negative growth control. *J Biol Chem*, **5**, 5.

Azuara, V., Brown, K.E., Williams, R.R.E., Webb, N., Dillon, N., Festenstein, R., Buckle, V., Merkenschlager, M., and Fisher, A.G. (2003). Heritable gene silencing in lymphocytes delays chromatin resolution without affecting the timing of DNA replication. *Nature Cell Biol* **5**, 668-674.

Bannister, A.J., Schneider, R. and Kouzarides, T. (2002) Histone methylation: dynamic or static? *Cell*, **109**, 801-806.

Becker, P.B. and Horz, W. (2002) ATP-dependent nucleosome remodeling. *Annu Rev Biochem*, **71**, 247-273.

Bell, S.P. and Dutta, A. (2002) DNA replication in eukaryotic cells. *Annu Rev Biochem*, **71**, 333-374.

Belotserkovskaya, R., Oh, S., Bondarenko, V.A., Orphanides, G., Studitsky, V.M. and Reinberg, D. (2003) FACT facilitates transcription-dependent nucleosome alteration. *Science*, **301**, 1090-1093.

Belotserkovskaya, R., Saunders, A., Lis, J.T. and Reinberg, D. (2004) Transcription through chromatin: understanding a complex FACT. *Biochim Biophys Acta*, **1677**, 87-99.

Berezney, R., Dubey, D.D. and Huberman, J.A. (2000) Heterogeneity of eukaryotic replicons, replicon clusters, and replication foci. *Chromosoma*, **108**, 471-484.

Bernard, P., Maure, J.F., Partridge, J.F., Genier, S., Javerzat, J.P. and Allshire, R.C. (2001) Requirement of heterochromatin for cohesion at centromeres. *Science*, **294**, 2539-2542.

Bernstein, B.E., Humphrey, E.L., Erlich, R.L., Schneider, R., Bouman, P., Liu, J.S., Kouzarides, T. and Schreiber, S.L. (2002) Methylation of histone H3 Lys 4 in coding regions of active genes. *Proc Natl Acad Sci U S A*, **99**, 8695-8700.

Bernstein, B.E., Tong, J.K. and Schreiber, S.L. (2000) Genomewide studies of histone deacetylase function in yeast. *Proc Natl Acad Sci USA*, **97**, 13708-13713.

Biggins, S., Severin, F.F., Bhalla, N., Sassoon, I., Hyman, A.A. and Murray, A.W. (1999) The conserved protein kinase Ipl1 regulates microtubule binding to kinetochores in budding yeast. *Genes Dev*, **13**, 532-544.

Bird, A. (2002) DNA methylation patterns and epigenetic memory. *Genes Dev*, **16**, 6-21.

Boeke, J.D., LaCroute, F. and Fink, G.R. (1984) A positive selection for mutants lacking orotidine-5'-phosphate decarboxylase activity in yeast: 5-fluoro-orotic acid resistance. *Mol Gen Genet*, **197**, 345-346.

Bozhenok, L., Wade, P.A. and Varga-Weisz, P. (2002) WSTF-ISWI chromatin remodeling complex targets heterochromatic replication foci. *Embo J*, **21**, 2231-2241.

Bravo, R., Frank, R., Blundell, P.A. and Macdonald-Bravo, H. (1987) Cyclin/PCNA is the auxiliary protein of DNA polymerase-delta. *Nature*, **326**, 515-517.

Briggs, S.D., Xiao, T., Sun, Z.W., Caldwell, J.A., Shabanowitz, J., Hunt, D.F., Allis, C.D. and Strahl, B.D. (2002) Gene silencing: trans-histone regulatory pathway in chromatin. *Nature*, **418**, 498.

Brown, D.T. (2003) Histone H1 and the dynamic regulation of chromatin function. *Biochem Cell Biol*, **81**, 221-227.

Brown, W.C. and Campbell, J.L. (1993) Interaction of proliferating cell nuclear antigen with yeast DNA polymerase delta. *J Biol Chem*, **268**, 21706-21710.

Buck, S.W., Sandmeier, J.J. and Smith, J.S. (2002) RNA polymerase I propagates unidirectional spreading of rDNA silent chromatin. *Cell*, **111**, 1003-1014.

Buermeyer, A.B., Deschenes, S.M., Baker, S.M. and Liskay, R.M. (1999) Mammalian DNA mismatch repair. *Annu Rev Genet*, **33**, 533-564.

Bulger, M., Ito, T., Kamakaka, R.T. and Kadonaga, J.T. (1995) Assembly of regularly spaced nucleosome arrays by Drosophila chromatin assembly factor 1 and a 56-kDa histone-binding protein. *Proc Natl Acad Sci U S A*, **92**, 11726-11730.

Bullock, P.A., Seo, Y.S. and Hurwitz, J. (1991) Initiation of simian virus DNA synthesis *in vitro*. *Mol Cell Biol*, **32**, 503-568.

Burd, C.G. and Dreyfuss, G. (1994) Conserved structures and diversity of functions of RNA-binding proteins. *Science*, **265**, 615-621.

Burgers, P.M. (1991) Saccharomyces cerevisiae replication factor C. II. Formation and activity of complexes with the proliferating cell nuclear antigen and with DNA polymerases delta and epsilon. *J Biol Chem*, **266**, 22698-22706.

Burgers, P.M. and Gerik, K.J. (1998) Structure and processivity of two forms of Saccharomyces cerevisiae DNA polymerase delta. *J Biol Chem*, **273**, 19756-19762.

Cai, J., Gibbs, E., Uhlmann, F., Phillips, B., Yao, N., O'Donnell, M. and Hurwitz, J. (1997) A complex consisting of human replication factor C p40, p37, and p36 subunits is a DNA-dependent ATPase and an intermediate in the assembly of the holoenzyme. *J Biol Chem*, **272**, 18974-18981.

Cao, R., Wang, L., Wang, H., Xia, L., Erdjument-Bromage, H., Tempst, P., Jones, R.S. and Zhang, Y. (2002) Role of histone H3 lysine 27 methylation in Polycomb-group silencing. *Science*, **298**, 1039-1043.

Cardoso, M.C., Joseph, C., Rahn, H.P., Reusch, R., Nadal-Ginard, B. and Leonhardt, H. (1997) Mapping and use of a sequence that targets DNA ligase I to sites of DNA replication *in vivo*. *J Cell Biol*, **139**, 579-587.

Carmen, A.A., Milne, L. and Grunstein, M. (2002) Acetylation of the yeast histone H4 N terminus regulates its binding to heterochromatin protein Sir3. *J Biol Chem*, **277**, 4778-4781.

Cavalli, G. and Paro, R. (1999) Epigenetic inheritance of active chromatin after removal of the main transactivator. *Science*, **286**, 955-958.

Chang, L., Loranger, S.S., Mizzen, C., Ernst, S.G., Allis, C.D. and Annunziato, A.T. (1997) Histones in transit: cytosolic histone complexes and diacetylation of H4 during nucleosome assembly in human cells. *Biochemistry*, **36**, 469-480.

Chapados, B.R., Hosfield, D.J., Han, S., Qiu, J., Yelent, B., Shen, B. and Tainer, A. (2004) Structural basis for FEN-1 substrate specificity and PCNA-mediated activation in DNA replication and repair. *Cell*, **116**, 39-50.

Chen, I.T., Smith, M.L., O'Connor, P.M. and Fornace, A.J., Jr. (1995a) Direct interaction of Gadd45 with PCNA and evidence for competitive interaction of Gadd45 and p21Waf1/Cip1 with PCNA. *Oncogene*, **11**, 1931-1937.

Chen, J., Jackson, P.K., Kirschner, M.W. and Dutta, A. (1995b) Separate domains of p21 involved in the inhibition of Cdk kinase and PCNA. *Nature*, **374**, 386-388.

Chen, U., Chen, S., Saha, P. and Dutta, A. (1996) p21Cip1/Waf1 disrupts the recruitment of human Fen1 by proliferating- cell nuclear antigen into the DNA replication complex. *Proc Natl Acad Sci U S A*, **93**, 11597-11602.

Chicoine, L.G., Schulman, I.G., Richman, R., Cook, R.G. and Allis, C.D. (1986) Nonrandom utilization of acetylation sites in histones isolated from Tetrahymena. Evidence for functionally distinct H4 acetylation sites. *J Biol Chem*, **261**, 1071-1076.

Christmann, M., Tomicic, M.T., Roos, W.P. and Kaina, B. (2003) Mechanisms of human DNA repair: an update. *Toxicology*, **193**, 3-34.

Chuang, L.S., Ian, H.I., Koh, T.W., Ng, H.H., Xu, G. and Li, B.F. (1997) Human DNA-(cytosine-5) methyltransferase-PCNA complex as a target for p21WAF1. *Science*, **277**, 1996-2000.

Clark, A.B., Valle, F., Drotschmann, K., Gary, R.K. and Kunkel, T.A. (2000) Functional interaction of proliferating cell nuclear antigen with MSH2- MSH6 and MSH2-MSH3 complexes. *J Biol Chem*, **275**, 36498-36501.

Collins, N., Poot, R.A., Kukimoto, I., Garcia-Jimenez, C., Dellaire, G. and Varga-Weisz, P.D. (2002) An ACF1-ISWI chromatin-remodeling complex is required for DNA replication through heterochromatin. *Nat Genet*, **32**, 627-632.

Cook, H.A., Eldredge, N.T., Haley, M.I., Kupke, D.W., Luck, J.M. and Rasmussen, P.S. (1956) On the fractionation of thymus histone. *Arch Biochem Biophys*, **65**, 449-467.

Cooper, M.P., Balajee, A.S. and Bohr, V.A. (1999) The C-terminal domain of p21 inhibits nucleotide excision repair *in vitro* and *in vivo*. *Mol Biol Cell*, **10**, 2119-2129.

Corona, D.F. and Tamkun, J.W. (2004) Multiple roles for ISWI in transcription, chromosome organization and DNA replication. *Biochim Biophys Acta*, **1677**, 113-119.

Costa, R.M., Chigancas, V., Galhardo Rda, S., Carvalho, H. and Menck, C.F. (2003) The eukaryotic nucleotide excision repair pathway. *Biochimie*, **85**, 1083-1099.

Cremisi, C., Chestier, A. and Yaniv, M. (1977) Preferential association of newly synthesized histones with replicating SV40 DNA. *Cell*, **12**, 947-951.

Dammann, R., Lucchini, R., Koller, T. and Sogo, J.M. (1993) Chromatin structures and transcription of rDNA in yeast *Saccharomyces cerevisiae*. *Nucl. Acids Res.*, **21**, 2331-2338.

De Silva, H.. Lee, K., and Osley, M.A. (1998). Functional dissection of yeast Hir1p, a WD repeat-containing transcriptional corepressor. *Genetics* **148**, 657-667.

Desany, B.A., Alcasabas, A.A., Bachant, J.B. and Elledge, S.J. (1998) Recovery from DNA replicational stress is the essential function of the S-phase checkpoint pathway. *Genes Dev*, **12**, 2956-2970.

Dhillon, N. and Kamakaka, R.T. (2002) Breaking through to the other side: Silencers and barriers. *Curr Opin Genet Dev*, **12**, 188-192.

Dillon, N. and Festenstein, R. (2002) Unravelling heterochromatin: competition between positive and negative factors regulates accessibility. *Trends Genet*, **18**, 252-258.

Dilworth, S.M. and Dingwall, C. (1988) Chromatin assembly in vitro and in vivo. *Bioessays*, **9**, 44-49.

Dionne, I., Nookala, R.K., Jackson, S.P., Doherty, A.J. and Bell, S.D. (2003) A heterotrimeric PCNA in the hyperthermophilic archaeon *Sulfolobus solfataricus*. *Mol Cell*, **11**, 275-282.

Dotto, G.P. (2000) p21(WAF1/Cip1): more than a break to the cell cycle? *Biochim Biophys Acta*, **1471**, M43-56.

Dover, J., Schneider, J., Tawiah-Boateng, M.A., Wood, A., Dean, K., Johnston, M. and Shilatifard, A. (2002) Methylation of histone H3 by COMPASS requires ubiquitination of histone H2B by Rad6. *J Biol Chem*, **277**, 28368-28371.

Ducoux, M., Urbach, S., Baldacci, G., Hubscher, U., Koundrioukoff, S., Christensen, J. and Hughes, P. (2001) Mediation of proliferating cell nuclear antigen (PCNA)-dependent DNA replication through a conserved p21(Cip1)-like PCNA-binding motif present in the third subunit of human DNA polymerase delta. *J Biol Chem*, **276**, 49258-49266.

Duncan, T. (2001) Identifying substrates of CDK2:cyclinA. University of London PhD thesis.

Eissenberg, J.C., Ayyagari, R., Gomes, X.V. and Burgers, P.M. (1997) Mutations in yeast proliferating cell nuclear antigen define distinct sites for interaction with DNA polymerase delta and DNA polymerase epsilon. *Mol Cell Biol*, **17**, 6367-6378.

Eissenberg, J.C. and Elgin, S.C. (2000) The HP1 protein family: getting a grip on chromatin. *Curr Opin Genet Dev*, **10**, 204-210.

Emili, A., Schieltz, D.M., Yates, J.R., 3rd and Hartwell, L.H. (2001) Dynamic interaction of DNA damage checkpoint protein Rad53 with chromatin assembly factor Asf1. *Mol Cell*, **7**, 13-20.

Enomoto, S. and Berman, J. (1998) Chromatin assembly factor I contributes to the maintenance, but not the re-establishment, of silencing at the yeast silent mating loci. *Genes Dev*, **12**, 219-232.

Enomoto, S., McCune-Zierath, P.D., Gerami-Nejad, M., Sanders, M.A. and Berman, J. (1997) *RLF2*, a subunit of yeast Chromatin Assembly Factor-I, is required for telomeric chromatin function *in vivo*. *Genes Dev*, **11**, 358-370.

Fischle, W., Wang, Y., Jacobs, S.A., Kim, Y., Allis, C.D. and Khorasanizadeh, S. (2003) Molecular basis for the discrimination of repressive methyl-lysine marks in histone H3 by Polycomb and HP1 chromodomains. *Genes Dev*, **17**, 1870-1881.

Flickinger, R. (2001) Replication timing and cell differentiation. *Differentiation*, **69**, 18-26.

Formosa, T. (2003) Changing the DNA landscape: Putting a SPN on chromatin. *Curr Top Microbiol Immunol*, **274**, 171-201.

Formosa, T., Ruone, S., Adams, M.D., Olsen, A.E., Eriksson, P., Yu, Y., Rhoades, A.R., Kaufman, P.D. and Stillman, D.J. (2002) Defects in *SPT16* or *POB3* (yFACT) in Saccharomyces cerevisiae cause dependence on the Hir/Hpc pathway: Polymerase passage may degrade chromatin structure. *Genetics*, **162**, 1557-1571.

Fortini, P., Pascucci, B., Parlanti, E., D'Errico, M., Simonelli, V. and Dogliotti, E. (2003) The base excision repair: mechanisms and its relevance for cancer susceptibility. *Biochimie*, **85**, 1053-1071.

Fotedar, R., Mossi, R., Fitzgerald, P., Rousselle, T., Maga, G., Brickner, H., Messier, H., Kasibhatla, S., Hubscher, U. and Fotedar, A. (1996) A conserved domain of the large subunit of replication factor C binds PCNA and acts like a dominant negative inhibitor of DNA replication in mammalian cells. *EMBO J*, **15**, 4423-4433.

Fox, M.H., Arndt-Jovin, D.J., Jovin, T.M., Baumann, P.H. and Robert-Nicoud, M. (1991) Spatial and temporal distribution of DNA replication sites localized by immunofluorescence and confocal microscopy in mouse fibroblasts. *J Cell Sci*, **99 (Pt 2)**, 247-253.

Frank, G., Qiu, J., Zheng, L. and Shen, B. (2001) Stimulation of eukaryotic FEN-1 nuclease activities by PCNA is independent of its *in vitro* interaction via a consensus PCNA binding region. *J Biol Chem*, **26**, 26.

Fukuda, K., Morioka, H., Imajou, S., Ikeda, S., Ohtsuka, E. and Tsurimoto, T. (1995) Structure-function relationship of the eukaryotic DNA replication factor, proliferating cell nuclear antigen. *J Biol Chem*, **270**, 22527-22534.

Funk, J.O., Waga, S., Harry, J.B., Espling, E., Stillman, B. and Galloway, D.A. (1997) Inhibition of CDK activity and PCNA-dependent DNA replication by p21 is blocked by interaction with the HPV-16 E7 oncoprotein. *Genes Dev*, **11**, 2090-2100.

Fuss, J. and Linn, S. (2002) Human DNA polymerase epsilon colocalizes with proliferating cell nuclear antigen and DNA replication late, but not early, in S phase. *J Biol Chem*, **277**, 8658-8666.

Fyodorov, D.V., Blower, M.D., Karpen, G.H. and Kadonaga, J.T. (2004) Acf1 confers unique activities to ACF/CHRAC and promotes the formation rather than disruption of chromatin in vivo. *Genes Dev*, **18**, 170-183.

Gaillard, P.H., Martini, E.M., Kaufman, P.D., Stillman, B., Moustacchi, E. and Almouzni, G. (1996) Chromatin assembly coupled to DNA repair: a new role for chromatin assembly factor I. *Cell*, **86**, 887-896.

Gaillard, P.H., Moggs, J.G., Roche, D.M., Quivy, J.P., Becker, P.B., Wood, R.D. and Almouzni, G. (1997) Initiation and bidirectional propagation of chromatin assembly from a target site for nucleotide excision repair. *Embo J*, **16**, 6281-6289.

Game, J.C. and Kaufman, P.D. (1999) Role of Saccharomyces cerevisiae chromatin assembly factor-I in repair of ultraviolet radiation damage in vivo. *Genetics*, **151**, 485-497.

Gary, R., Kim, K., Cornelius, H.L., Park, M.S. and Matsumoto, Y. (1999a) Proliferating cell nuclear antigen facilitates excision in long-patch base excision repair. *J Biol Chem*, **274**, 4354-4363.

Gary, R., Ludwig, D.L., Cornelius, H.L., MacInnes, M.A. and Park, M.S. (1997) The DNA repair endonuclease XPG binds to proliferating cell nuclear antigen (PCNA) and shares sequence elements with the PCNA-binding regions of FEN-1 and cyclin-dependent kinase inhibitor p21. *J Biol Chem*, **272**, 24522-24529.

Gary, R., Park, M.S., Nolan, J.P., Cornelius, H.L., Kozyreva, O.G., Tran, H.T., Lobachev, K.S., Resnick, M.A. and Gordenin, D.A. (1999b) A novel role in DNA metabolism for the binding of Fen1/Rad27 to PCNA and implications for genetic risk. *Mol Cell Biol*, **19**, 5373-5382.

Gasser, R., Koller, T. and Sogo, J.M. (1996) The stability of nucleosomes at the replication fork. *J Mol Biol*, **258**, 224-239.

Gavin, A.C., Bosche, M., Krause, R., Grandi, P., Marzioch, M., Bauer, A., Schultz, J., Rick, J.M., Michon, A.M., Cruciat, C.M., Remor, M., Hofert, C., Schelder, M., Brajenovic, M., Ruffner, H., Merino, A., Klein, K., Hudak, M., Dickson, D., Rudi, T., Gnau, V., Bauch, A., Bastuck, S., Huhse, B., Leutwein, C., Heurtier, M.A., Copley, R.R., Edelmann, A., Querfurth, E., Rybin, V., Drewes, G., Raida, M., Bouwmeester, T., Bork, P., Seraphin, B., Kuster, B., Neubauer, G. and Superti-Furga, G. (2002) Functional organization of the yeast proteome by systematic analysis of protein complexes. *Nature*, **415**, 141-147.

Gegenheimer, P. (1990) Preparation of extracts from plants. *Methods Enzymol*, **182**, 174-193.

Gerik, K.J., Li, X., Pautz, A. and Burgers, P.M. (1998) Characterization of the two small subunits of *Saccharomyces cerevisiae* DNA polymerase delta. *J Biol Chem*, **273**, 19747-19755.

Giaever, G., Chu, A.M., Ni, L., Connelly, C., Riles, L., Veronneau, S., Dow, S., Lucau-Danila, A., Anderson, K., Andre, B., Arkin, A.P., Astromoff, A., El-Bakkoury, M., Bangham, R., Benito, R., Brachat, S., Campanaro, S., Curtiss, M., Davis, K., Deutschbauer, A., Entian, K.D., Flaherty, P., Foury, F., Garfinkel, D.J., Gerstein, M., Gotte, D., Guldener, U., Hegemann, J.H., Hempel, S., Herman, Z., Jaramillo, D.F., Kelly, D.E., Kelly, S.L., Kotter, P., LaBonte, D., Lamb, D.C., Lan, N., Liang, H., Liao, H., Liu, L., Luo, C., Lussier, M., Mao, R., Menard, P., Ooi, S.L., Revuelta, J.L., Roberts, C.J., Rose, M., Ross-Macdonald, P., Scherens, B., Schimmack, G., Shafer, B., Shoemaker, D.D., Sookhai-Mahadeo, S., Storms, R.K., Strathern, J.N., Valle, G., Voet, M., Volckaert, G., Wang, C.Y., Ward, T.R., Wilhelmy, J., Winzeler, E.A., Yang, Y., Yen, G., Youngman, E., Yu, K., Bussey, H., Boeke, J.D., Snyder, M., Philippsen, P., Davis, R.W. and Johnston, M. (2002) Functional profiling of the Saccharomyces cerevisiae genome. *Nature*, **418**, 387-391.

Gibbs, E., Kelman, Z., Gulbis, J.M., O'Donnell, M., Kuriyan, J., Burgers, P.M. and Hurwitz, J. (1997) The influence of the proliferating cell nuclear antigen-interacting domain of p21(CIP1) on DNA synthesis catalyzed by the human and Saccharomyces cerevisiae polymerase delta holoenzymes. *J Biol Chem*, **272**, 2373-2381.

Glikin, G.C., Ruberti, I. and Worcel, A. (1984) Chromatin assembly in Xenopus oocytes: in vitro studies. *Cell*, **37**, 33-41.

Gomes, X.V. and Burgers, P.M. (2000) Two modes of FEN1 binding to PCNA regulated by DNA. *EMBO J*, **19**, 3811-3821.

Gontijo, A.M., Green, C.M. and Almouzni, G. (2003) Repairing DNA damage in chromatin. *Biochimie*, **85**, 1133-1147.

Goren, A. and Cedar, H. (2003) Replicating by the clock. *Nat Rev Mol Cell Biol*, **4**, 25-32.

Graham, F.L., Smiley, J., Russell, W.C. and Nairn, R. (1977) Characteristics of a human cell line transformed by DNA from human adenovirus type 5. *J Gen Virol*, **36**, 59-74.

Grant, P.A., Eberharter, A., John, S., Cook, R.G., Turner, B.M. and Workman, J.L. (1999) Expanded lysine acetylation specificity of Gcn5 in native complexes. *J Biol Chem*, **274**, 5895-5900.

Green, C.M. and Almouzni, G. (2002) When repair meets chromatin. First in series on chromatin dynamics. *EMBO Rep*, **3**, 28-33.

Green, C.M. and Almouzni, G. (2003) Local action of the chromatin assembly factor CAF-1 at sites of nucleotide excision repair *in vivo*. *EMBO J*, **22**, 5163-5174.

Grewal, S.I. and Klar, A.J. (1996) Chromosomal inheritance of epigenetic states in fission yeast during mitosis and meiosis. *Cell*, **86**, 95-101

Grewal, S.I. and Rice, J.C. (2004) Regulation of heterochromatin by histone methylation and small RNAs. *Curr Opin Cell Biol*, **16**, 230-238.

Grosshans, H., Deinert, K., Hurt, E. and Simos, G. (2001) Biogenesis of the signal recognition particle (SRP) involves import of SRP proteins into the nucleolus, assembly with the SRP-RNA, and Xpo1p-mediated export. *J Cell Biol*, **153**, 745-761.

Grossman, S.R., Deato, M.E., Brignone, C., Chan, H.M., Kung, A.L., Tagami, H., Nakatani, Y. and Livingston, D.M. (2003) Polyubiquitination of p53 by a ubiquitin ligase activity of p300. *Science*, **300**, 342-344.

Gu, L., Hong, Y., McCulloch, S., Watanabe, H. and Li, G.M. (1998) ATP-dependent interaction of human mismatch repair proteins and dual role of PCNA in mismatch repair. *Nucleic Acids Res*, **26**, 1173-1178.

Guan, K.L., and Dixon, J.E. (1991) Eukaryotic proteins expressed in Escherichia coli: an improved thrombin cleavage and purification procedure of fusion proteins with glutathione S-transferase. *Anal Biochem* **192,** 262-267.

Gulbis, J.M., Kelman, Z., Hurwitz, J., O'Donnell, M. and Kuriyan, J. (1996) Structure of the C-terminal region of p21(WAF1/CIP1) complexed with human PCNA. *Cell*, **87**, 297-306.

Gunjan, A. and Verreault, A. (2003) A Rad53 kinase-dependent surveillance mechanism that regulates histone protein levels in S. cerevisiae. *Cell*, **115**, 537-549.

Hall, C., Nelson, D.M., Ye, X., Baker, K., DeCaprio, J.A., Seeholzer, S., Lipinski, M. and Adams, P.D. (2001) HIRA, the human homologue of yeast Hir1p and Hir2p, is a novel cyclin-cdk2 substrate whose expression blocks S-phase progression. *Mol Cell Biol*, **21**, 1854-1865.

Han, M., Chang, M., Kim, U.J. and Grunstein, M. (1987) Histone H2B repression causes cell-cycle-specific arrest in yeast: effects on chromosomal segregation, replication, and transcription. *Cell*, **48**, 589-597.

Haracska, L., Johnson, R.E., Unk, I., Phillips, B., Hurwitz, J., Prakash, L. and Prakash, S. (2001a) Physical and functional interactions of human DNA polymerase eta with PCNA. *Mol Cell Biol*, **21**, 7199-7206.

Haracska, L., Johnson, R.E., Unk, I., Phillips, B.B., Hurwitz, J., Prakash, L. and Prakash, S. (2001a) Targeting of human DNA polymerase iota to the replication machinery via interaction with PCNA. *Proc Natl Acad Sci U S A*, **98**, 14256-14261.

Haracska, L., Kondratick, C.M., Unk, I., Prakash, S. and Prakash, L. (2001b) Interaction with PCNA is essential for yeast DNA polymerase eta function. *Mol Cell*, **8**, 407-415.

Harlow, E. (1988) Antibodies: A Laboratory Manual, Cold Spring Harbor Laboratory Press, New York.

Harrison, T., Graham, F. and Williams, J. (1977) Host-range mutants of adenovirus type 5 defective for growth in HeLa cells. *Virology*, **77**, 319-329.

Hasan, S., Hasa, P.O., Imhof, R. and Hottiger, M.O. (2001a) Transcription coactivator p300 binds PCNA and may have a role in DNA repair synthesis. *Nature*, **410**, 387-391.

Hasan, S., Stucki, M., Hassa, P.O., Imhof, R., Gehrig, P., Hunziker, P., Hubscher, U. and Hottiger, M.O. (2001b) Regulation of human flap endonuclease-1 activity by acetylation through the transcriptional coactivator p300. *Mol Cell*, **7**, 1221-1231.

Haushalter, K.A. and Kadonaga, J.T. (2003) Chromatin assembly by DNA-translocating motors. *Nat Rev Mol Cell Biol*, **4**, 613-620.

He, H., Tan, C.K., Downey, K.M. and So, A.G. (2001) A tumor necrosis factor alpha- and interleukin 6-inducible protein that interacts with the small subunit of DNA polymerase delta and proliferating cell nuclear antigen. *Proc Natl Acad Sci U S A*, **98**, 11979-11984.

Henderson, D.S., Banga, S.S., Grigliatti, T.A. and Boyd, J.B. (1994) Mutagen sensitivity and suppression of position-effect variegation result from mutations in mus209, the Drosophila gene encoding PCNA. *Embo J*, **13**, 1450-1459.

Henneke, G., Friedrich-Heineken, E. and Hubscher, U. (2003a) Flap endonuclease 1: a novel tumour suppresser protein. *Trends Biochem Sci*, **28**, 384-390.

Henneke, G., Koundrioukoff, S. and Hubscher, U. (2003b) Multiple roles for kinases in DNA replication. *EMBO Rep*, **4**, 252-256.

Henneke, G., Koundrioukoff, S. and Hubscher, U. (2003c) Phosphorylation of human Fen1 by cyclin-dependent kinase modulates its role in replication fork regulation. *Oncogene*, **22**, 4301-4313.

Hennig, L., Taranto, P., Walser, M., Schonrock, N. and Gruissem, W. (2003) Arabidopsis MSI1 is required for epigenetic maintenance of reproductive development. *Development*, **130**, 2555-2565.

Herman, T.M., DePamphilis, M.L. and Wassarman, P.M. (1981) Structure of chromatin at deoxyribonucleic acid replication forks: Location of the first nucleosomes on newly synthesized simian virus 40 deoxyribonucleic acid. *Biochemistry*, **20**, 621-630.

Ho, Y., Gruhler, A., Heilbut, A., Bader, G.D., Moore, L., Adams, S.L., Millar, A., Taylor, P., Bennett, K., Boutilier, K., Yang, L., Wolting, C., Donaldson, I., Schandorff, S., Shewnarane, J., Vo, M., Taggart, J., Goudreault, M., Muskat, B., Alfarano, C., Dewar, D., Lin, Z., Michalickova, K., Willems, A.R., Sassi, H., Nielsen, P.A., Rasmussen, K.J., Andersen, J.R., Johansen, L.E., Hansen, L.H., Jespersen, H., Podtelejnikov, A., Nielsen, E., Crawford, J., Poulsen, V., Sorensen, B.D., Matthiesen, J., Hendrickson, R.C., Gleeson, F., Pawson, T., Moran, M.F., Durocher, D., Mann, M., Hogue, C.W., Figeys, D. and Tyers, M. (2002) Systematic identification of protein complexes in Saccharomyces cerevisiae by mass spectrometry. *Nature*, **415**, 180-183.

Hoege, C., Pfander, B., Moldovan, G.-L., Pyrowolakis, G. and Jentsch, S. (2002) *RAD6*-dependent DNA repair is linked to modification of PCNA by ubiquitin and SUMO. *Nature*, **419**, 135-141.

Hoek, M. and Stillman, B. (2003) Chromatin assembly factor 1 is essential and couples chromatin assembly to DNA replication in vivo. *Proc Natl Acad Sci U S A*, **100**, 12183-12188.

Hoffmann, A., Chiang, C.-M., Oelgeschläger, T., Xie, X., Burley, S.K., Nakatani, Y., and Roeder, R.G. (1996). A histone octamer-like structure within TFIID. *Nature* **380**, 356-359.

Hong, R. and Chakravarti, D. (2003) The human proliferating Cell nuclear antigen regulates transcriptional coactivator p300 activity and promotes transcriptional repression. *J Biol Chem*, **278**, 44505-44513.

Honore, B., Baandrup, U., Nielsen, S. and Vorum, H. (2002) Endonuclein is a cell cycle regulated WD-repeat protein that is up- regulated in adenocarcinoma of the pancreas. *Oncogene*, **21**, 1123-1129.

Hu, F., Alcasabas, A.A. and Elledge, S.J. (2001) Asf1 links Rad53 to control of chromatin assembly. *Genes Dev*, **15**, 1061-1066.

Huang, D. and Koshland, D. (2003) Chromosome integrity in *Saccharomyces cerevisiae*: the interplay of DNA replication initiation factors, elongation factors, and origins. *Genes Dev*, **17**, 1741-1751.

Hubscher, U., Maga, G. and Spadari, S. (2002) Eukaryotic DNA polymerases. *Annu Rev Biochem*, **71**, 133-163.

Hubscher, U. and Seo, Y.S. (2001) Replication of the lagging strand: a concert of at least 23 polypeptides. *Mol Cells*, **12**, 149-157.

Hughes, T.R., Roberts, C.J., Dai, H., Jones, A.R., Meyer, M.R., Slade, D., Burchard, J., Dow, S., Ward, T.R., Kidd, M.J., Friend, S.H. and Marton, M.J. (2000) Widespread aneuploidy revealed by DNA microarray expression profiling. *Nat Genet*, **25**, 333-337.

Huh, W.-K., Falvo, J.V., Gerke, L.C., Carroll, A.S., Howson, R.W., Weissman, J.S. and O'Shea, E.K. (2003) Global analysis of protein localization in budding yeast. *Nature*, **425**, 686-691.

Hyrien, O., Marheineke, K. and Goldar, A. (2003) Paradoxes of eukaryotic DNA replication: MCM proteins and the random completion problem. *Bioessays*, **25**, 116-125.

Imhof, A. and Wolffe, A.P. (1999) Purification and properties of the Xenopus Hat1 acetyltransferase: association with the 14-3-3 proteins in the oocyte nucleus. *Biochemistry*, **38**, 13085-13093.

Ito, T., Bulger, M., Pazin, M.J., Kobayashi, R. and Kadonaga, J.T. (1997) ACF, an ISWI-containing and ATP-utilizing chromatin assembly and remodeling factor. *Cell*, **90**, 145-155.

Ito, T., Bulger, M., Kobayashi, R. and Kadonaga, J.T. (1996a) Drosophila NAP-1 is a core histone chaperone that functions in ATP- facilitated assembly of regularly spaced nucleosomal arrays. *Mol Cell Biol*, **16**, 3112-3124.

Ito, T., Tyler, J.K., Bulger, M., Kobayashi, R. and Kadonaga, J.T. (1996b) ATP-facilitated chromatin assembly with a nucleoplasmin-like protein from Drosophila melanogaster. *J Biol Chem*, **271**, 25041-25048.

Jackson, V. (1990) In vivo studies on the dynamics of histone-DNA interaction: evidence for nucleosome dissolution during replication and transcription and a low level of dissolution independent of both. *Biochemistry*, **29**, 719-731.

Jackson, V., Shires, A., Tanphaichitr, N. and Chalkley, R. (1976) Modifications to histones immediately after synthesis. *J Mol Biol*, **104**, 471-483.

Jaenisch, R. and Bird, A. (2003) Epigenetic regulation of gene expression: how the genome integrates intrinsic and environmental signals. *Nat Genet*, **33 Suppl**, 245-254.

Jeppesen, P. and Turner, B.M. (1993) The inactive X chromosome in female mammals is distinguished by a lack of histone H4 acetylation, a cytogenetic marker for gene expression. *Cell*, **74**, 281-289.

Johnson, R.E., Kovvali, G.K., Guzder, S.N., Amin, N.S., Holm, C., Habraken, Y., Sung, P., Prakash, L. and Prakash, S. (1996) Evidence for involvement of yeast proliferating cell nuclear antigen in DNA mismatch repair. *J Biol Chem*, **271**, 27987-27990.

Johnston, S.D., Enomoto, S., Schneper, L., McClellan, M.C., Twu, F., Montgomery, N.D., Haney, S.A., Broach, J.R. and Berman, J. (2001) *CAC3* (*MSI1*) suppression of $RAS2^{G19V}$ is independent of chromatin assembly factor I and mediated by *NPR1*. *Mol Cell Biol*, **21**, 1784-1794.

Jones, D.L., Alani, R.M. and Munger, K. (1997) The human papillomavirus E7 oncoprotein can uncouple cellular differentiation and proliferation in human keratinocytes by abrogating p21Cip1-mediated inhibition of cdk2. *Genes Dev*, **11**, 2101-2111.

Jonsson, Z.O., Hindges, R. and Hubscher, U. (1998) Regulation of DNA replication and repair proteins through interaction with the front side of proliferating cell nuclear antigen. *Embo J*, **17**, 2412-2425.

Jonsson, Z.O. and Hubscher, U. (1997) Proliferating cell nuclear antigen: more than a clamp for DNA polymerases. *Bioessays*, **19**, 967-975.

Jonsson, Z.O., Podust, V.N., Podust, L.M. and Hubscher, U. (1995) Tyrosine 114 is essential for the trimeric structure and the functional activities of human proliferating cell nuclear antigen. *Embo J*, **14**, 5745-5751.

Kamakaka, R.T., Bulger, M., Kaufman, P.D., Stillman, B. and Kadonaga, J.T. (1996) Postreplicative chromatin assembly by *Drosophila* and human chromatin assembly factor 1. *Mol Cell Biol*, **16**, 810-817.

Kamakaka, R.T. and Kadonaga, J.T. (1993) Biochemical analysis of the role of chromatin structure in the regulation of transcription by RNA polymerase II. *Cold Spring Harb Symp Quant Biol*, **58**, 205-212.

Kannouche, P., Fernandez de Henestrosa, A.R., Coull, B., Vidal, A.E., Gray, C., Zicha, D., Woodgate, R. and Lehmann, A.R. (2003) Localization of DNA polymerases eta and iota to the replication machinery is tightly co-ordinated in human cells. *Embo J*, **22**, 1223-1233.

Kannouche, P.L., Wing, J. and Lehmann, A.R. (2004) Interaction of human DNA polymerase eta with monoubiquitinated PCNA: a possible mechanism for the polymerase switch in response to DNA damage. *Mol Cell*, **14**, 491-500.

Kass, S.U. and Wolffe, A.P. (1998) DNA methylation, nucleosomes and the inheritance of chromatin structure and function. *Novartis Found Symp*, **214**, 22-35; discussion 36-50.

Katou, Y., Kanoh, Y., Bando, M., Noguchi, H., Tanaka, H., Ashikari, T., Sugimoto, K. and Shirahige, K. (2003) S-phase checkpoint proteins Tof1 and Mrc1 form a stable replication-pausing complex. *Nature*, **424**, 1078-1083.

Kaufman, P.D., Cohen, J.L. and Osley, M.A. (1998) Hir proteins are required for position-dependent gene silencing in *Saccharomyces cerevisiae* in the absence of chromatin assembly factor I. *Mol Cell Biol*, **18**, 4793-4806.

Kaufman, P.D., Kobayashi, R., Kessler, N. and Stillman, B. (1995) The p150 and p60 subunits of chromatin assembly factor I: a molecular link between newly synthesized histones and DNA replication. *Cell*, **81**, 1105-1114.

Kaufman, P.D., Kobayashi, R. and Stillman, B. (1997) Ultraviolet radiation sensitivity and reduction of telomeric silencing in Saccharomyces cerevisiae cells lacking chromatin assembly factor-I. *Genes Dev*, **11**, 345-357.

Kawabe, T., Suganuma, M., Ando, T., Kimura, M., Hori, H. and Okamoto, T. (2002) Cdc25C interacts with PCNA at G2/M transition. *Oncogene*, **21**, 1717-1726.

Kaya, H., Shibahara, K.I., Taoka, K.I., Iwabuchi, M., Stillman, B. and Araki, T. (2001) FASCIATA genes for chromatin assembly factor-1 in arabidopsis maintain the cellular organization of apical meristems. *Cell*, **104**,131-142.

Kedar, P.S., Kim, S.J., Robertson, A., Hou, E., Prasad, R., Horton, J.K. and Wilson, S.H. (2002) Direct interaction between mammalian DNA polymerase b and proliferating cell nuclear antigen. *J Biol Chem*, **277**, 31115-31123.

Keller, C. and Krude, T. (2000) Requirement of Cyclin/Cdk2 and protein phosphatase 1 activity for chromatin assembly factor 1-dependent chromatin assembly during DNA synthesis. *J Biol Chem*, **275**, 35512-35521.

Kelly, T.J., Qin, S., Gottschling, D.E. and Parthun, M.R. (2000) Type B histone acetyltransferase Hat1p participates in telomeric silencing. *Mol Cell Biol*, **20**, 7051-7058.

Kelman, Z. (1997) PCNA: structure, functions and interactions. *Oncogene*, **14**, 629-640.

Kelman, Z. and Hurwitz, J. (1998) Protein-PCNA interactions: a DNA-scanning mechanism? *Trends Biochem Sci*, **23**, 236-238.

Khorasanizadeh, S. (2004) The nucleosome: from genomic organization to genomic regulation. *Cell*, **116**, 259-272.

Kim, S.M., Dubey, D.D. and Huberman, J.A. (2003) Early-replicating heterochromatin. *Genes Dev*, **17**, 330-335.

Kim, U.J., Han, M., Kayne, P. and Grunstein, M. (1988) Effects of histone H4 depletion on the cell cycle and transcription of Saccharomyces cerevisiae. *Embo J*, **7**, 2211-2219.

Kimura, A., Umehara, T. and Horikoshi, M. (2002) Chromosomal gradient of histone acetylation established by Sas2p and Sir2p functions as a shield against gene silencing. *Nature Genet*, **32**, 370-377.

Kleff, S., Andrulis, E.D., Anderson, C.W. and Sternglanz, R. (1995) Identification of a gene encoding a yeast histone H4 acetyltransferase. *J Biol Chem*, **270**, 24674-24677.

Knox, J.D., Araujo, F.D., Bigey, P., Slack, A.D., Price, G.B., Zannis-Hadjopoulos, M. and Szyf, M. (2000) Inhibition of DNA methyltransferase inhibits DNA replication. *J Biol Chem*, **275**, 17986-17990.

Kokoska, R.J., Stefanovic, L., Buermeyer, A.B., Liskay, R.M. and Petes, T.D. (1999) A mutation of the yeast gene encoding PCNA destabilizes both microsatellite and minisatellite DNA sequences. *Genetics*, **151**, 511-519.

Komeili, A. and O'Shea, E.K. (2001) New perspectives on nuclear transport. *Annu Rev Genet*, **35**, 341-364.

Koundrioukoff, S., Jonsson, Z.O., Hasan, S., de Jong, R.N., van der Vliet, P.C., Hottiger, M.O. and Hubscher, U. (2000) A direct interaction between proliferating cell nuclear antigen (PCNA) and Cdk2 targets PCNA-interacting proteins for phosphorylation. *J Biol Chem*, **275**, 22882-22887.

Krawitz, D.C., Kama, T. and Kaufman, P.D. (2002) Chromatin assembly factor I mutants defective for PCNA binding require Asf1/Hir proteins for silencing. *Mol Cell Biol*, **22**, 614-625.

Krishna, T.S., Kong, X.P., Gary, S., Burgers, P.M. and Kuriyan, J. (1994) Crystal structure of the eukaryotic DNA polymerase processivity factor PCNA. *Cell*, **79**, 1233-1243.

Kristjuhan, A., Wittschieben, B.O., Walker, J., Roberts, D., Cairns, B.R. and Svejstrup, J.Q. (2003) Spreading of Sir3 protein in cells with severe histone H3 hypoacetylation. *Proc Natl Acad Sci USA*, **100**, 7551-7556.

Krogan, N.J., Dover, J., Wood, A., Schneider, J., Heidt, J., Boateng, M.A., Dean, K., Ryan, O.W., Golshani, A., Johnston, M., Greenblatt, J.F. and Shilatifard, A. (2003) The Paf1 complex is required for histone H3 methylation by COMPASS and Dot1p: linking transcriptional elongation to histone methylation. *Mol Cell*, **11**, 721-729.

Krogan, N.J., Peng, W.-T., Cagney, G., Robinson, M.D., Haw, R., Zhong, G., Guo, X., Zhang, X., Canadien, V., Richards, D.P., Beattie, B.K., Lalev, A., Zhang, W., Davierwala, A.P., Mnaimneh, S., Starostine, A., Tikuisis, A.P., Grigull, J., Datta, N., Bray, J.E., Hughes, T.R., Emili, A. and Greenblatt, J.F. (2004) High-definition macromolecular composition of yeast RNA-processing complexes. *Mol Cell*, **13**, 225-239.

Krude, T. and Keller, C. (2001) Chromatin assembly during S phase: contributions from histone deposition, DNA replication and the cell division cycle. *Cell Mol Life Sci*, **58**, 665-72.

Krude, T. and Knippers, R. (1993) Nucleosome assembly during complementary DNA strand synthesis in extracts from mammalian cells. *J Biol Chem*, **268**, 14432-14442.

Krude, T. (1995) Chromatin assembly factor 1 (CAF-1) colocalizes with replication foci in HeLa cell nuclei. *Exp Cell Res*, **220**, 304-311.

Krude, T. (1999) Chromatin assembly during DNA replication in somatic cells. *Eur J Biochem*, **263**, 1-5.

Kumar, A., Agarwal, S., Heyman, J.A., Matson, S., Heidtman, M., Piccirillo, S., Umansky, L., Drawid, A., Jansen, R., Liu, Y., Cheung, K.H., Miller, P., Gerstein, M., Roeder, G.S. and Snyder, M. (2002) Subcellular localization of the yeast proteome. *Genes Dev*, **16**, 707-719.

Kuo, M.H., Brownell, J.E., Sobel, R.E., Ranalli, T.A., Cook, R.G., Edmondson, D.G., Roth, S.Y. and Allis, C.D. (1996) Transcription-linked acetylation by Gcn5p of histones H3 and H4 at specific lysines. *Nature*, **383**, 269-272.

Labib, K., Tercero, J.A. and Diffley, J.F.X. (2000) Uninterrupted *MCM2-7* function required for DNA replication fork progression. *Science*, **288**, 1643-1647.

Lai, J.-S. and Herr, W. (1992) Ethidium bromide provides a simple tool for identifying genuine DNA-independent protein associations. *Proc. Natl. Acad. Sci. USA*, **89**, 6958-6962.

Lau, P.J., Flores-Rozas, H. and Kolodner, R.D. (2002) Isolation and characterization of new proliferating cell nuclear antigen (POL30) mutator mutants that are defective in DNA mismatch repair. *Mol Cell Biol*, **22**, 6669-6680.

Lau, P.J. and Kolodner, R.D. (2003) Transfer of the MSH2-MSH6 complex from Proliferating Cell Nuclear Antigen to mispaired bases in DNA. *J Biol Chem*, **278**, 14-17.

Le, S., Davis, C., Konopka, J.B. and Sternglanz, R. (1997) Two new S-phase-specific genes from Saccharomyces cerevisiae. *Yeast*, **13**, 1029-1042.

Lebel, M., Spillare, E.A., Harris, C.C. and Leder, P. (1999) The Werner syndrome gene product co-purifies with the DNA replication complex and interacts with PCNA and topoisomerase I. *J Biol Chem*, **274**, 37795-37799.

Lee, S.H., Pan, Z.Q., Kwong, A.D., Burgers, P.M. and Hurwitz, J. (1991) Synthesis of DNA by DNA polymerase epsilon in vitro. *J Biol Chem*, **266**, 22707-22717.

Leonhardt, H., Page, A.W., Weier, H.U. and Bestor, T.H. (1992) A targeting sequence directs DNA methyltransferase to sites of DNA replication in mammalian nuclei. *Cell*, **71**, 865-873.

Leonhardt, H., Rahn, H.P. and Cardoso, M.C. (1998) Intranuclear targeting of DNA replication factors. *J Cell Biochem Suppl*, **30-31**, 243-249.

Armelle Lengronne, Philippe Pasero, Aaron Bensimon, and Etienne Schwob

Lengronne, A., Pasero, P., Bensimon, A. and Schwob, E. (2001) Monitoring S phase progression globally and locally using BrdU incorporation in *TK*$^+$ yeast strains. *Nucl Acids Res*, **29**, 1433-1442

Levin, D.S., Bai, W., Yao, N., O'Donnell, M. and Tomkinson, A.E. (1997) An interaction between DNA ligase I and proliferating cell nuclear antigen: implications for Okazaki fragment synthesis and joining. *Proc Natl Acad Sci U S A*, **94**, 12863-12868.

Li, E., Bestor, T.H. and Jaenisch, R. (1992) Targeted mutation of the DNA methyltransferase gene results in embryonic lethality. *Cell*, **69**, 915-926.

Li, R., Hannon, G.J., Beach, D. and Stillman, B. (1996) Subcellular distribution of p21 and PCNA in normal and repair-deficient cells following DNA damage. *Curr Biol*, **6**, 189-199.

Li, R., Waga, S., Hannon, G.J., Beach, D. and Stillman, B. (1994) Differential effects by the p21 CDK inhibitor on PCNA-dependent DNA replication and repair. *Nature*, **371**, 534-537.

Li, X., Li, J., Harrington, J., Lieber, M.R. and Burgers, P.M. (1995) Lagging strand DNA synthesis at the eukaryotic replication fork involves binding and stimulation of FEN-1 by proliferating cell nuclear antigen. *J Biol Chem*, **270**, 22109-22112.

Lichten, M. and Goldman, A.S. (1995) Meiotic recombination hotspots. *Annu Rev Genet*, **29**, 423-444.

Lindahl, T. and Wood, R.D. (1999) Quality control by DNA repair. *Science*, **286**, 1897-1905.

Ling, X., Harkness, T.A., Schultz, M.C., Fisher-Adams, G. and Grunstein, M. (1996) Yeast histone H3 and H4 amino termini are important for nucleosome assembly in vivo and in vitro: redundant and position-independent functions in assembly but not in gene regulation. *Genes Dev*, **10**, 686-699.

Litt, M.D., Simpson, M., Gaszner, M., Allis, C.D. and Felsenfeld, G. (2001) Correlation between histone lysine methylation and developmental changes at the chicken beta-globin locus. *Science*, **293**, 2453-2455.

Lorain, S., Quivy, J.P., Monier-Gavelle, F., Scamps, C., Lecluse, Y., Almouzni, G. and Lipinski, M. (1998) Core histones and HIRIP3, a novel histone-binding protein, directly interact with WD repeat protein HIRA. *Mol Cell Biol*, **18**, 5546-5556.

Lorentz, A., Otermann, K., Fleck, O. and Schmidt, H. (1994) Switching gene *swi6*, involved in repression of silent mating-type loci in fission yeast, encodes a homologues of chromatin-associated proteins from *Drosophila* and mammals. *Gene*, **143**, 139-143.

Loyola, A. and Almouzni, G. (2004) Histone chaperones, a supporting role in the limelight. *Biochim Biophys Acta*, **1677**, 3-11.

Lu, X. and Horvitz, H.R. (1998) *lin-35* and *lin-53*, two genes that antagonize a C. elegans Ras pathway, encode proteins similar to Rb and its binding protein RbAp48. *Cell*, **95**, 981-991.

Lu, X., Tan, C.K., Zhou, J.Q., You, M., Carastro, L.M., Downey, K.M. and So, A.G. (2002) Direct interaction of proliferating cell nuclear antigen with the small subunit of DNA polymerase delta. *J Biol Chem*, **277**, 24340-24345.

Luger, K., Mader, A.W., Richmond, R.K., Sargent, D.F. and Richmond, T.J. (1997) Crystal structure of the nucleosome core particle at 2.8 A resolution. *Nature*, **389**, 251-260..

Ma, X.J., Wu, J., Altheim, B.A., Schultz, M.C. and Grunstein, M. (1998) Deposition-related sites K5/K12 in histone H4 are not required for nucleosome deposition in yeast. *Proc Natl Acad Sci U S A*, **95**, 6693-6698.

MacKenney, V.J., Barnes, D.E. and Lindahl, T. (1997) Specific function of DNA ligase I in simian virus 40 DNA replication by human cell-free extracts is mediated by the amino-terminal non-catalytic domain. *J Biol Chem*, **272**, 11550-11556.

Maga, G., Jonsson, Z.O., Stucki, M., Spadari, S. and Hubscher, U. (1999) Dual mode of interaction of DNA polymerase epsilon with proliferating cell nuclear antigen in primer binding and DNA synthesis. *J Mol Biol*, **285**, 259-267.

Maga, G. and Hubscher, U. (2003) Proliferating cell nuclear antigen (PCNA): a dancer with many partners. *J Cell Sci*, **116**, 3051-3060.

Maldonado, E., Hampsey, M. and Reinberg, D. (1999) Repression: targeting the heart of the matter. *Cell*, **99**, 455-458.

Marheineke, K. and Krude, T. (1998) Nucleosome assembly activity and intracellular localization of human CAF-1 changes during the cell division cycle. *J Biol Chem*, **273**, 15279-15286.

Martinez-Balbas, M.A., Tsukiyama, T., Gdula, D. and Wu, C. (1998) Drosophila NURF-55, a WD repeat protein involved in histone metabolism. *Proc Natl Acad Sci U S A*, **95**, 132-137.

Martini, E., Roche, D.M., Marheineke, K., Verreault, A. and Almouzni, G. (1998) Recruitment of phosphorylated chromatin assembly factor 1 to chromatin after UV irradiation of human cells. *J Cell Biol*, **143**, 563-575.

Matsumiya, S., Ishino, S., Ishino, Y. and Morikawa, K. (2002) Physical interaction between proliferating cell nuclear antigen and replication factor C from Pyrococcus furiosus. *Genes Cells*, **7**, 911-922.

McKittrick, E., Gafken, P.R., Ahmad, K. and Henikoff, S. (2004) Histone H3.3 is enriched in covalent modifications associated with active chromatin. *Proc Natl Acad Sci U S A*, **101**, 1525-1530.

McNairn, A.J. and Gilbert, D.M. (2003) Epigenomic replication: linking epigenetics to DNA replication. *Bioessays*, **25**, 647-656.

Meeks-Wagner, D. and Hartwell, L.H. (1986) Normal stoichiometry of histone dimer sets is necessary for high fidelity of mitotic chromosome transmission. *Cell*, **44**, 43-52.

Meijer, M. and Smerdon, M.J. (1999) Accessing DNA damage in chromatin: insights from transcription. *Bioessays*, **21**, 596-603.

Meijsing, S.H. and Ehrenhofer-Murray, A.E. (2001) The silencing complex SAS-I links histone acetylation to the assembly of repressed chromatin by CAF-I and Asf1 in Saccharomyces cerevisiae. *Genes Dev*, **15**, 3169-3182.

Mello, J.A. and Almouzni, G. (2001) The ins and outs of nucleosome assembly. *Curr Opin Genet Dev*, **11**, 136-141.

Mello, J.A., Sillje, H.H., Roche, D.M., Kirschner, D.B., Nigg, E.A. and Almouzni, G. (2002) Human Asf1 and CAF-1 interact and synergize in a repair-coupled nucleosome assembly pathway. *EMBO Rep*, **3**, 329-334.

Mendez, J. and Stillman, B. (2003) Perpetuating the double helix: molecular machines at eukaryotic DNA replication origins. *Bioessays*, **25**, 1158-1167.

Milutinovic, S., Zhuang, Q. and Szyf, M. (2002) Proliferating Cell Nuclear Antigen associates with histone deacetylase activity, integrating DNA replication and chromatin modification. *J Biol Chem*, **277**, 29074-29078.

Moggs, J.G. and Almouzni, G. (1999) Chromatin rearrangements during nucleotide excision repair. *Biochimie*, **81**, 45-52.

Moggs, J.G., Grandi, P., Quivy, J.P., Jonsson, Z.O., Hubscher, U., Becker, P.B. and Almouzni, G. (2000) A CAF-1-PCNA-mediated chromatin assembly pathway triggered by sensing DNA damage. *Mol Cell Biol*, **20**, 1206-1218.

Monson, E.K., de Bruin, D. and Zakian, V.A. (1997) The yeast Cac1 protein is required for the stable inheritance of transcriptionally repressed chromatin at telomeres. *Proc Natl Acad Sci U S A*, **94**, 13081-13086.

Montecucco, A., Rossi, R., Levin, D.S., Gary, R., Park, M.S., Motycka, T.A., Ciarrocchi, G., Villa, A., Biamonti, G. and Tomkinson, A.E. (1998) DNA ligase I is recruited to sites of DNA replication by an interaction with proliferating cell nuclear antigen: identification of a common targeting mechanism for the assembly of replication factories. *Embo J*, **17**, 3786-3795.

Montecucco, A., Savini, E., Weighardt, F., Rossi, R., Ciarrocchi, G., Villa, A. and Biamonti, G. (1995) The N-terminal domain of human DNA ligase I contains the nuclear localization signal and directs the enzyme to sites of DNA replication. *EMBO J*, **14**, 5379-5386.

Moran, L., Norris, D. and Osley, M.A. (1990) A yeast H2A-H2B promoter can be regulated by changes in histone gene copy number. *Genes Dev*, **4**, 752-763.

Mosammaparast, N., Guo, Y., Shabanowitz, J., Hunt, D.F. and Pemberton, L.F. (2002) Pathways mediating the nuclear import of histones H3 and H4 in yeast. *J Biol Chem*, **277**, 862-868.

Mosammaparast, N., Jackson, K.R., Guo, Y., Brame, C.J., Shabanowitz, J., Hunt, D.F. and Pemberton, L.F. (2001) Nuclear import of histone H2A and H2B is mediated by a network of karyopherins. *J Cell Biol*, **153**, 251-262.

Mossi, R. and Hubscher, U. (1998) Clamping down on clamps and clamp loaders--the eukaryotic replication factor C. *Eur J Biochem*, **254**, 209-216.

Mozzherin, D.J., Tan, C.K., Downey, K.M. and Fisher, P.A. (1999) Architecture of the active DNA polymerase delta.proliferating cell nuclear antigen.template-primer complex. *J Biol Chem*, **274**, 19862-19867.

Muller-Weeks, S.J. and Caradonna, S. (1996) Specific association of cyclin-like uracil-DNA glycosylase with the proliferating cell nuclear antigen. *Exp Cell Res*, **226**, 346-355.

Munakata, T., Adachi, N., Yokoyama, N., Kuzuhara, T. and Horikoshi, M. (2000) A human homologue of yeast anti-silencing factor has histone chaperone activity. *Genes Cells*, **5**, 221-233.

Murray, A. and Hunt, T. (1993) The Cell Cycle: an introduction. New York: WH Freeman and Company, New York.

Murzina, N., Verreault, A., Laue, E. and Stillman, B. (1999) Heterochromatin dynamics in mouse cells: interaction between chromatin assembly factor 1 and HP1 proteins. *Mol Cell*, **4**, 529-540.

Muzi-Falconi, M., Giannattasio, M., Foiani, M. and Plevani, P. (2003) The DNA polymerase alpha-primase complex: multiple functions and interactions. *ScientificWorldJournal*, **3**, 21-33.

Myung, K., Pennaneach, V., Kats, E.S. and Kolodner, R.D. (2003) Saccharomyces cerevisiae chromatin-assembly factors that act during DNA replication function in the maintenance of genome stability. *Proc Natl Acad Sci U S A*, **100**, 6640-6645.

Nabatiyan, A. and Krude, T. (2004) Silencing of Chromatin Assembly Factor 1 in Human Cells Leads to Cell Death and Loss of Chromatin Assembly during DNA Synthesis. *Mol Cell Biol*, **24**, 2853-2862.

Nakanishi, M., Robetorye, R.S., Pereira-Smith, O.M. and Smith, J.R. (1995) The C-terminal region of p21SDI1/WAF1/CIP1 is involved in proliferating cell nuclear antigen binding but does not appear to be required for growth inhibition. *J Biol Chem*, **270**, 17060-17063.

Nakayama, J.-I., Allshire, R.C., Klar, A.J.S. and Grewal, S.I.S. (2001) A role for DNA polymerase a in epigenetic control of transcriptional silencing in fission yeast. *EMBO J*, **20**, 2857-2866.

Naryzhny, S.N. and Lee, H. (2003) Observation of multiple isoforms and specific proteolysis patterns of proliferating cell nuclear antigen in the context of cell cycle compartments and cell preparations. *Proteomics*, **3**, 930-936.

Naryzhny, S.N. and Lee, H. (2004) The post-translational modifications of proliferating cell nuclear antigen: acetylation, not phosphorylation, plays an important role in the regulation of its function. *J Biol Chem*, **279**, 20194-20199.

Neer, E.J. and Smith, T.F. (2000) A groovy new structure. *Proc Natl Acad Sci USA*, **97**, 960-962.

Nelson, D.M., Ye, X., Hall, C., Santos, H., Ma, T., Kao, G.D., Yen, T.J., Harper, J.W. and Adams, P.D. (2002) Coupling of DNA synthesis and histone synthesis in S phase independent of cyclin/cdk2 activity. *Mol Cell Biol*, **22**, 7459-7472.

Ng, H.H., Dole, S. and Struhl, K. (2003a) The Rtf1 component of the Paf1 transcriptional elongation complex is required for ubiquitination of histone H2B. *J Biol Chem*, **278**, 33625-33628.

Ng, H.H., Robert, F., Young, R.A. and Struhl, K. (2003b) Targeted recruitment of the Set1 histone methylase by elongating Pol II provides a localized mark and memory of recent transcriptional activity. *Mol Cell*, **11**, 709-719.

Ng, H.H., Xu, R.M., Zhang, Y. and Struhl, K. (2002) Ubiquitination of histone H2B by Rad6 is required for efficient Dot1- mediated methylation of histone H3 lysine 79. *J Biol Chem*, **277**, 34655-34657.

Nicolas, E., Ait-Si-Ali, S. and Trouche, D. (2001) The histone deacetylase HDAC3 targets RbAp48 to the retinoblastoma protein. *Nucl Acids Res*, **29**, 3131-3136.

Nicolas, E., Morales, V., Magnaghi-Jaulin, L., Harel-Bellan, A., Richard-Foy, H. and Trouche, D. (2000) RbAp48 belongs to the histone deacetylase complex that associates with the retinoblastoma protein. *J Biol Chem*, **275**, 9797-9804.

Nilsen, H., Lindahl, T. and Verreault, A. (2002) DNA base excision repair of uracil residues in reconstituted nucleosome core particles. *EMBO J*, **21**, 5943-5952.

Nislow, C., Ray, E. and Pillus, L. (1997) *SET1*, a yeast member of the trithorax family, functions in transcriptional silencing and diverse cellular processes. *Mol Biol Cell*, **8**, 2421-2436.

Noma, K. and Grewal, S.I. (2002) Histone H3 lysine 4 methylation is mediated by Set1 and promotes maintenance of active chromatin states in fission yeast. *Proc Natl Acad Sci U S A*, **99 Suppl 4**, 16438-16445.

Noma, K., Allis, C.D. and Grewal, S.I. (2001) Transitions in distinct histone H3 methylation patterns at the heterochromatin domain boundaries. *Science*, **293**, 1150-1155.

Nyberg, K.A., Michelson, R.J., Putnam, C.W. and Weinert, T.A. (2002) Toward maintaining the genome: DNA damage and replication checkpoints. *Annu Rev Genet*, **36**, 617-656.

O'Keefe, R.T., Henderson, S.C. and Spector, D.L. (1992) Dynamic organization of DNA replication in mammalian cell nuclei: spatially and temporally defined replication of chromosome-specific alpha-satellite DNA sequences. *J. Cell Biol.*, **116**, 1095-1110.

O'Reilly DR, Miller LK and Luckow VA. (1994) Baculovirus expression vectors: A Laboratory Manual WH Freeman, New York, NY.

Ohta, S., Shiomi, Y., Sugimoto, K., Obuse, C. and Tsurimoto, T. (2002) A proteomics approach to identify PCNA binding proteins in human cell lysates: identification of the human CHL12/RFCs2-5 complex as a novel PCNA binding protein. *J Biol Chem*, **8**, 8.

Okano, S., Lan, L., Caldecott, K.W., Mori, T. and Yasui, A. (2003) Spatial and temporal cellular responses to single-strand breaks in human cells. *Mol Cell Biol*, **23**, 3974-3981.

Oku, T., Ikeda, S., Sasaki, H., Fukuda, K., Morioka, H., Ohtsuka, E., Yoshikawa, H. and Tsurimoto, T. (1998) Functional sites of human PCNA which interact with p21 (Cip1/Waf1), DNA polymerase delta and replication factor C. *Genes Cells*, **3**, 357-369.

Okuwaki, M. and Verreault, A. (2004) Maintenance DNA methylation of nucleosome core particles. *J Biol Chem*, **279**, 2904-2912.

Orphanides, G., LeRoy, G., Chang, C.H., Luse, D.S. and Reinberg, D. (1998) FACT, a factor that facilitates transcript elongation through nucleosomes. *Cell*, **92**, 105-116.

Orphanides, G., Wu, W.-H., Lane, W.S., Hampsey, M. and Reinberg, D. (1999) The chromatin-specific transcription elongation factor FACT comprises human SPT16 and SSRP1 proteins. *Nature*, **400**, 284-288.

Osley, M.A. (1991) The regulation of histone synthesis in the cell cycle. *Annu Rev Biochem*, **60**, 827-861.

Osley, M.A. and Lycan, D. (1987) Trans-acting regulatory mutations that alter transcription of Saccharomyces cerevisiae histone genes. *Mol Cell Biol*, **7**, 4204-4210.

Otterlei, M., Warbrick, E., Nagelhus, T.A., Haug, T., Slupphaug, G., Akbari, M., Aas, P.A., Steinsbekk, K., Bakke, O. and Krokan, H.E. (1999) Post-replicative base excision repair in replication foci. *Embo J*, **18**, 3834-3844.

Owen, D.J., Ornaghi, P., Yang, J.C., Lowe, N., Evans, P.R., Ballario, P., Neuhaus, D., Filetici, P. and Travers, A.A. (2000) The structural basis for the recognition of acetylated histone H4 by the bromodomain of histone acetyltransferase gcn5p. *Embo J*, **19**, 6141-6149.

Pamblanco, M., Dehé, P.-M., Sollier, J., Lebrun, R., Moinier, D., Luciano, P., Galy, V., Nehrbass, U., Verreault, A., Sendra, R., Davie, J.K., Dent, S., Tordera, V. and Géli, V. (2004) Quantitative and qualitative determination of histone H3 lysine 4 methylation reveals an indirect role for Set1p in telomeric silencing. *J. Mol. Biol.*, **under review**.

Pan, Z.Q., Reardon, J.T., Li, L., Flores-Rozas, H., Legerski, R., Sancar, A. and Hurwitz, J. (1995) Inhibition of nucleotide excision repair by the cyclin-dependent kinase inhibitor p21. *J Biol Chem*, **270**, 22008-22016.

Parker, A., Gu, Y., Mahoney, W., Lee, S.H., Singh, K.K. and Lu, A.L. (2001) Human homolog of the MutY repair protein (hMYH) physically interacts with proteins involved in long patch DNA base excision repair. *J Biol Chem*, **276**, 5547-5555.

Parthun, M.R., Widom, J. and Gottschling, D.E. (1996) The major cytoplasmic histone acetyltransferase in yeast: links to chromatin replication and histone metabolism. *Cell*, **87**, 85-94.

Penny, G.D., Kay, G.F., Sheardown, S.A., Rastan, S. and Brockdorff, N. (1996) Requirement for Xist in X chromosome inactivation. *Nature*, **379**, 131-137.

Peters, A.H., Kubicek, S., Mechtler, K., O'Sullivan, R.J., Derijck, A.A., Perez-Burgos, L., Kohlmaier, A., Opravil, S., Tachibana, M., Shinkai, Y., Martens, J.H. and Jenuwein, T. (2003) Partitioning and plasticity of repressive histone methylation states in mammalian chromatin. *Mol Cell*, **12**, 1577-1589.

Peters, A.H., Mermoud, J.E., O'Carroll, D., Pagani, M., Schweizer, D., Brockdorff, N. and Jenuwein, T. (2002) Histone H3 lysine 9 methylation is an epigenetic imprint of facultative heterochromatin. *Nat Genet*, **30**, 77-80.

Philpott, A., Krude, T. and Laskey, R.A. (2000) Nuclear chaperones. *Semin Cell Dev Biol*, **11**, 7-14.

Plath, K., Fang, J., Mlynarczyk-Evans, S.K., Cao, R., Worringer, K.A., Wang, H., de la Cruz, C.C., Otte, A.P., Panning, B. and Zhang, Y. (2003) Role of histone H3 lysine 27 methylation in X inactivation. *Science*, **300**, 131-135.

Podust, V.N., Podust, L.M., Goubin, F., Ducommun, B. and Hubscher, U. (1995) Mechanism of inhibition of proliferating cell nuclear antigen-dependent DNA synthesis by the cyclin-dependent kinase inhibitor p21. *Biochemistry*, **34**, 8869-8875.

Poveda, A., Pamblanco, M., Tafrov, S., Tordera, V., Sternglanz, R. and Sendra, R. (2004) Hif1 is a component of yeast histone acetyltransferase B, a complex mainly localized in the nucleus. *J Biol Chem*, **279**, 16033-16043.

Prelich, G., Kostura, M., Marshak, D.R., Mathews, M.B. and Stillman, B. (1987) The cell-cycle regulated proliferating cell nuclear antigen is required for SV40 DNA replication in vitro. *Nature*, **326**, 471-475.

Prelich, G. and Stillman, B. (1988) Coordinated leading and lagging strand synthesis during SV40 DNA replication in vitro requires PCNA. *Cell*, **53**, 117-126.

Qian, Y.-W. and Lee, E.Y.-H.P. (1995) Dual retinoblastoma-binding proteins with properties related to a negative regulator of Ras in yeast. *Journal of Biological Chemistry*, **270**, 25507-25513.

Qian, Y.-W., Wang, Y.-C.J., Hollingsworth, R.E.J., Jones, D., Ling, N. and Lee, E.Y.-H.P. (1993) A retinoblastoma-binding protein related to a negative regulator of Ras in yeast. *Nature*, **364**, 648-652.

Qian, Z., Huang, H., Hong, J.Y., Burck, C.L., Johnston, S.D., Berman, J., Carol, A. and Liebman, S.W. (1998) Yeast Ty1 retrotransposition is stimulated by a synergistic interaction between mutations in chromatin assembly factor I and histone regulatory proteins. *Mol Cell Biol*, **18**, 4783-4792.

Qin, S. and Parthun, M.R. (2002) Histone H3 and the histone acetyltransferase Hat1p contribute to DNA double-strand break repair. *Mol Cell Biol*, **22**, 8353-8365.

Quivy, J.P., Grandi, P. and Almouzni, G. (2001) Dimerization of the largest subunit of chromatin assembly factor 1: importance in vitro and during Xenopus early development. *Embo J*, **20**, 2015-2027.

Ray-Gallet, D., Quivy, J.P., Scamps, C., Martini, E.M., Lipinski, M. and Almouzni, G. (2002) HIRA is critical for a nucleosome assembly pathway independent of DNA synthesis. *Mol Cell*, **9**, 1091-1100.

Recht, J., Dunn, B., Raff, A. and Osley, M.A. (1996) Functional analysis of histones H2A and H2B in transcriptional repression in Saccharomyces cerevisiae. *Mol Cell Biol*, **16**, 2545-2553.

Reynolds, N., Warbrick, E., Fantes, P.A. and MacNeill, S.A. (2000) Essential interaction between the fission yeast DNA polymerase delta subunit Cdc27 and Pcn1 (PCNA) mediated through a C-terminal p21(Cip1)- like PCNA binding motif. *EMBO J*, **19**, 1108-1118.

Rigaut, G., Shevchenko, A., Rutz, B., Wilm, M., Mann, M. and Séraphin, B. (1999) A generic protein purification method for protein complex characterization and proteome exploration. *Nature Biotech*, **17**, 1030-1032.

Riggs, A.D. and Pfeifer, G.P. (1992) X-chromosome inactivation and cell memory. *Trends Genet*, **8**, 169-174.

Roberts, C., Sutherland, H.F., Farmer, H., Kimber, W., Halford, S., Carey, A., Brickman, J.M., Wynshaw-Boris, A. and Scambler, P.J. (2002) Targeted mutagenesis of the Hira gene results in gastrulation defects and patterning abnormalities of mesoendodermal derivatives prior to early embryonic lethality. *Mol Cell Biol*, **22**, 2318-2328.

Robyr, D., Suka, Y., Xenarios, I., Kurdistani, S.K., Wang, A., Suka, N. and Grunstein, M. (2002) Microarray deacetylation maps determine genome-wide functions for yeast histone deacetylases. *Cell*, **109**, 437-446.

Roder, A. and Punter, J. (1977) [Interactions between nuclear polyhedrosis viruses and vertebrate cells (author's transl)]. *Zentralbl Bakteriol [Orig A]*, **239**, 459-464.

Rossi, R., Villa, A., Negri, C., Scovassi, I., Ciarrocchi, G., Biamonti, G. and Montecucco, A. (1999) The replication factory targeting sequence/PCNA-binding site is required in G(1) to control the phosphorylation status of DNA ligase I. *EMBO J*, **18**, 5745-5754.

Roth, S.Y., Denu, J.M. and Allis, C.D. (2001) Histone acetyltransferases. *Annu Rev Biochem*, **70**, 81-120.

Rougeulle, C., Chaumeil, J., Sarma, K., Allis, C.D., Reinberg, D., Avner, P. and Heard, E. (2004) Differential histone H3 Lys-9 and Lys-27 methylation profiles on the X chromosome. *Mol Cell Biol*, **24**, 5475-5484.

Rountree, M.R., Bachman, K.E. and Baylin, S.B. (2000) DNMT1 binds HDAC2 and a new co-repressor, DMAP1, to form a complex at replication foci. *Nat Genet*, **25**, 269-277.

Rousseau, D., Cannella, D., Boulaire, J., Fitzgerald, P., Fotedar, A. and Fotedar, R. (1999) Growth inhibition by CDK-cyclin and PCNA binding domains of p21 occurs by distinct mechanisms and is regulated by ubiquitin-proteasome pathway. *Oncogene*, **18**, 4313-4325.

Rout, M.P., Blobel, G. and Aitchison, J.D. (1997) A distinct nuclear import pathway used by ribosomal proteins. *Cell*, **89**, 715-725.

Ruiz-Carrillo, A., Wangh, L. and Allfrey, V. (1975) Assembly of newly replicated chromatin. *Science*, **190**, 117-128.

Salles-Passador, I., Munshi, A., Cannella, D., Pennaneach, V., Koundrioukoff, S., Jacquinod, M., Forest, E., Podust, V., Fotedar, A. and Fotedar, R. (2003) Phosphorylation of the PCNA binding domain of the large subunit of replication factor C on Thr506 by cyclin-dependent kinases regulates binding to PCNA. *Nucl. Acids Res.*, **31**, 5202-5211.

Sambrook J., Fritsch EF., and Maniatis T. (1989) Molecular Cloning: a Laboratory Manual, second edn, Cold Spring Harbor Laboratory press, New York.

Sandmeier, J.J., French, S., Osheim, Y., Cheung, W.L., Gallo, C.M., Beyer, A.L. and Smith, J.S. (2002) *RPD3* is required for the inactivation of yeast ribosomal DNA genes in stationary phase. *EMBO J*, **21**, 4959-4968.

Santos-Rosa, H., Schneider, R., Bannister, A.J., Sherriff, J., Bernstein, B.E., Emre, N.C., Schreiber, S.L., Mellor, J. and Kouzarides, T. (2002) Active genes are tri-methylated at K4 of histone H3. *Nature*, **419**, 407-411.

Schagger, H. and von Jagow, G. (1987) Tricine-sodium dodecyl sulfate-polyacrylamide gel electrophoresis for the separation of proteins in the range from 1 to 100 kDa. *Anal Biochem*, **166**, 368-379.

Scherer, W.F. and Hoogasian, A.F. (1954) Preservation at subzero temperatures of mouse fibroblasts (strain L) and human epithelial cells (strain HeLa). *Proc Soc Exp Biol Med*, **87**, 480-487.

Schmidt, K.H., Derry, K.L. and Kolodner, R.D. (2002) Saccharomyces cerevisiae RRM3, a 5' to 3' DNA helicase, physically interacts with proliferating cell nuclear antigen. *J Biol Chem*, **17**, 17.

Schmidt, S.L., Gomes, X.V. and Burgers, P.M. (2001) ATP utilization by yeast replication factor C. III. The ATP-binding domains of Rfc2, Rfc3, and Rfc4 are essential for DNA recognition and clamp loading. *J Biol Chem*, **276**, 34784-34791.

Schneider, C., Newman, R. A., Sutherland, D. R., Asser, U., and Greaves, M. F. (1982) A one-step purification of membrane proteins using a high efficiency immunomatrix, *J Biol Chem* **257**, 10766-9

Schubeler, D., Scalzo, D., Kooperberg, C., van Steensel, B., Delrow, J. and Groudine, M. (2002) Genome-wide DNA replication profile for Drosophila melanogaster: a link between transcription and replication timing. *Nat Genet*, **32**, 438-442.

Schwartz, M.F., Lee, S.J., Duong, J.K., Eminaga, S. and Stern, D.F. (2003) FHA domain-mediated DNA checkpoint regulation of Rad53. *Cell Cycle*, **2**, 384-396.

Scott, M.T., Morrice, N. and Ball, K.L. (2000) Reversible phosphorylation at the C-terminal regulatory domain of p21(Waf1/Cip1) modulates proliferating cell nuclear antigen binding. *J Biol Chem*, **275**, 11529-11537.

Senshu, T., Fukuda, M. and Ohashi, M. (1978) Preferential association of newly synthesized H3 and H4 histones with newly replicated DNA. *J Biochem (Tokyo)*, **84**, 985-988.

Sharp, J.A., Fouts, E.T., Krawitz, D.C. and Kaufman, P.D. (2001) Yeast histone deposition protein Asf1p requires Hir proteins and PCNA for heterochromatic silencing. *Curr Biol*, **11**, 463-473.

Sharp, J.A., Franco, A.A., Osley, M.A. and Kaufman, P.D. (2002) Chromatin assembly factor I and Hir proteins contribute to building functional kinetochores in S. cerevisiae. *Genes Dev*, **16**, 85-100.

Sharp, J.A., Krawitz, D.C., Gardner, K.A., Fox, C.A. and Kaufman, P.D. (2003) The budding yeast silencing protein Sir1 is a functional component of centromeric chromatin. *Genes Dev*, **17**, 2356-2361.

Sherr, C.J. and Roberts, J.M. (1999) CDK inhibitors: positive and negative regulators of G1-phase progression. *Genes Dev*, **13**, 1501-1512.

Sherwood, P.W. and Osley, M.A. (1991) Histone regulatory (hir) mutations suppress delta insertion alleles in Saccharomyces cerevisiae. *Genetics*, **128**, 729-738.

Sherwood, P.W., Tsang, S.V. and Osley, M.A. (1993) Characterization of HIR1 and HIR2, two genes required for regulation of histone gene transcription in Saccharomyces cerevisiae. *Mol Cell Biol*, **13**, 28-38.

Shibahara, K. and Stillman, B. (1999) Replication-dependent marking of DNA by PCNA facilitates CAF-1-coupled inheritance of chromatin. *Cell*, **96**, 575-585.

Shibahara, K., Verreault, A. and Stillman, B. (2000) The N-terminal domains of histones H3 and H4 are not necessary for chromatin assembly factor-1- mediated nucleosome assembly onto replicated DNA in vitro. *Proc Natl Acad Sci U S A*, **97**, 7766-7771.

Shivji, M.K., Ferrari, E., Ball, K., Hubscher, U. and Wood, R.D. (1998) Resistance of human nucleotide excision repair synthesis *in vitro* to p21Cdn1. *Oncogene*, **17**, 2827-2838.

Shivji, M.K., Grey, S.J., Strausfeld, U.P., Wood, R.D. and Blow, J.J. (1994) Cip1 inhibits DNA replication but not PCNA-dependent nucleotide excision-repair. *Curr Biol*, **4**, 1062-1068.

Shimizu, K., Kawasaki, Y., Hiraga, S., Tawaramoto, M., Nakashima, N. and Sugino, A. (2002) The fifth essential DNA polymerase phi in Saccharomyces cerevisiae is localized to the nucleolus and plays an important role in synthesis of rRNA. *Proc Natl Acad Sci U S A*, **99**, 9133-9138.

Sikorski, R.S., and Hieter, P. (1989). A system of shuttle vectors and yeast host strains designed for efficient manipulation of DNA in *Saccharomyces cerevisiae*. *Genetics* **122**, 19-27.

Simon, I., Barnett, J., Hannett, N., Harbison, C.T., Rinaldi, N.J., Volkert, T.L., Wyrick, J.J., Zeitlinger, J., Gifford, D.K., Jaakkola, T.S. and Young, R.A. (2001) Serial regulation of transcriptional regulators in the yeast cell cycle. *Cell*, **106**, 697-708.

Simpson, R.T., Thoma, F. and Brubaker, J.M. (1985) Chromatin reconstituted from tandemly repeated cloned DNA fragments and core histones: a model system for study of higher order structure. *Cell*, **42**, 799-808.

Singer, M.S., Kahana, A., Wolf, A.J., Meisinger, L.L., Peterson, S.E., Goggin, C., Mahowald, M. and Gottschling, D.E. (1998) Identification of high-copy disruptors of telomeric silencing in Saccharomyces cerevisiae. *Genetics*, **150**, 613-632.

Skibbens, R.V., Corson, L.B., Koshland, D. and Hieter, P. (1999) Ctf7p is essential for sister chromatid cohesion and links mitotic chromosome structure to the DNA replication machinery. *Genes Dev*, **13**, 307-319.

Smerdon, M.J. (1991) DNA repair and the role of chromatin structure. *Curr Opin Cell Biol*, **3**, 422-428.

Smith, G.E., Ju, G., Ericson, B.L., Moschera, J., Lahm, H.W., Chizzonite, R. and Summers, M.D. (1985) Modification and secretion of human interleukin 2 produced in insect cells by a baculovirus expression vector. *Proc Natl Acad Sci U S A*, **82**, 8404-8408.

Smith, J.S., Caputo, E. and Boeke, J.D. (1999a) A genetic screen for ribosomal DNA silencing defects identifies multiple DNA replication and chromatin-modulating factors. *Mol Cell Biol*, **19**, 3184-3197.

Smith, P.A., Jackson, V. and Chalkley, R. (1984) Two-stage maturation process for newly replicated chromatin. *Biochemistry*, **23**, 1576-1581.

Smith, R.L. and Johnson, A.D. (2000) Turning genes off by Ssn6-Tup1: a conserved system of transcriptional repression in eukaryotes. *Trends Biochem Sci*, **25**, 325-330.

Smith, S. and Stillman, B. (1989) Purification and characterization of CAF-I, a human cell factor required for chromatin assembly during DNA replication in vitro. *Cell*, **58**, 15-25.

Smith, S. and Stillman, B. (1991a) Immunological characterization of chromatin assembly factor I, a human cell factor required for chromatin assembly during DNA replication in vitro. *J Biol Chem*, **266**, 12041-12047.

Smith, S. and Stillman, B. (1991b) Stepwise assembly of chromatin during DNA replication in vitro. *EMBO J*, **10**, 971-980.

Smith, T.F., Gaitatzes, C., Saxena, K. and Neer, E.J. (1999b) The WD repeat: a common architecture for diverse functions. *Trends Biochem Sci*, **24**, 181-185.

Sobel, R.E., Cook, R.G. and Allis, C.D. (1994) Non-random acetylation of histone H4 by a cytoplasmic histone acetyltransferase as determined by novel methodology. *J Biol Chem*, **269**, 18576-18582.

Sobel, R.E., Cook, R.G., Perry, C.A., Annunziato, A.T. and Allis, C.D. (1995) Conservation of deposition-related acetylation sites in newly synthesized histones H3 and H4. *Proc Natl Acad Sci U S A*, **92**, 1237-1241.

Sogo, J.M., Stahl, H., Koller, T. and Knippers, R. (1986) Structure of replicating simian virus 40 minichromosomes. The replication fork, core histone segregation and terminal structures. *J Mol Biol*, **189**, 189-204.

Solari, F. and Ahringer, J. (2000) NURD complex genes antagonise Ras induced vulval development. *Curr Biol*, **10**, 223-226.

Sondek, J., Bohm, A., Lambright, D.G., Hamm, H.E. and Sigler, P.B. (1996) Crystal structure of a G_A protein bg dimer at 2.1Å resolution. *Nature*, **379**, 369-374.

Spector, D.L., Goldman, R.D. and Leinwand, L.A., (1997) Cells: a laboratory manual, Cold Spring Harbor Laboratory Press, Plainview New York.

Spector, D.L. (2003) The dynamics of chromosome organization and gene regulation. *Annu Rev Biochem*, **72**, 573-608.

Spencer, F., Gerring, S.L., Connelly, C. and Hieter, P. (1990) Mitotic chromosome transmission fidelity mutants in *Saccharomyces cerevisiae*. *Genetics*, **124**, 237-249.

Sporbert, A., Gahl, A., Ankerhold, R., Leonhardt, H. and Cardoso, M.C. (2002) DNA polymerase clamp shows little turnover at established replication sites but sequential de novo assembly at adjacent origin clusters. *Mol Cell*, **10**, 1355-1365.

Squazzo, S.L., Costa, P.J., Lindstrom, D.L., Kumer, K.E., Simic, R., Jennings, J.L., Link, A.J., Arndt, K.M. and Hartzog, G.A. (2002) The Paf1 complex physically and functionally associates with transcription elongation factors *in vivo*. *EMBO J*, **21**, 1764-1774.

Stelter, P. and Ulrich, H. (2003) Control of spontaneous and damage-induced mutagenesis by SUMO and ubiquitin conjugation. *Nature*, **425**, 188-190.

Stillman, B.W. and Gluzman, Y. (1985) Replication and supercoiling of simian virus 40 DNA in cell extracts from human cells. *Mol Cell Biol*, **5**, 2051-2060.

Stillman, B. (1986) Chromatin assembly during SV40 DNA replication *in vitro*. *Cell*, **45**, 555-565.

Strahl, B.D. and Allis, C.D. (2000) The language of covalent histone modifications. *Nature*, **403**, 41-45.

Strahl, B.D., Ohba, R., Cook, R.G. and Allis, C.D. (1999) Methylation of histone H3 at lysine 4 is highly conserved and correlates with transcriptionallyactive nuclei in *Tetrahymena*. *Proc Natl Acad Sci USA*, **96**, 14967-14972.

Strathern, J.N., Jones, E.W. and Broach, J.R. (1982) The molecular biology of the yeast *Saccharomyces*: metabolism and gene expression. Cold Spring Harbor Laboratory Press; New York.

Suka, N., Luo, K. and Grunstein, M. (2002) Sir2p and Sas2p opposingly regulate acetylation of yeast histone H4 lysine 16 and spreading of heterochromatin. *Nature Genet*, **32**, 378-383.

Suka, N., Suka, Y., Carmen, A.A., Wu, J. and Grunstein, M. (2001) Highly specific antibodies determine histone acetylation site usage in yeast heterochromatin and euchromatin. *Mol Cell*, **8**, 473-479.

Sun, Z.W. and Allis, C.D. (2002) Ubiquitination of histone H2B regulates H3 methylation and gene silencing in yeast. *Nature*, **418**, 104-108.

Sung, P., Prakash, S. and Prakash, L. (1988) The RAD6 protein of *Saccharomyces cerevisiae* polyubiquitinates histones, and its acidic domain mediates this activity. *Genes and Development*, **2**, 1476-1485.

Taddei, A., Maison, C., Roche, D. and Almouzni, G. (2001) Reversible disruption of pericentric heterochromatin and centromere function by inhibiting deacetylases. *Nat Cell Biol*, **3**, 114-120.

Taddei, A., Roche, D., Sibarita, J.B., Turner, B.M. and Almouzni, G. (1999) Duplication and maintenance of heterochromatin domains. *J Cell Biol*, **147**, 1153-1166.

Tagami, H., Ray-Gallet, D., Almouzni, G. and Nakatani, Y. (2004) Histone H3.1 and H3.3 complexes mediate nucleosome assembly pathways dependent or independent of DNA synthesis. *Cell*, **116**, 51-61.

Tan, C.K., Castillo, C., So, A.G. and Downey, K.M. (1986) An auxiliary protein for DNA polymerase-delta from fetal calf thymus. *J Biol Chem*, **261**, 12310-12316.

Tanaka, S., Hu, S.Z., Wang, T.S. and Korn, D. (1982) Preparation and preliminary characterization of monoclonal antibodies against human DNA polymerase alpha. *J Biol Chem*, **257**, 8386-8390.

Taunton, J., Hassig, C.A. and Schreiber, S.L. (1996) A mammalian histone deacetylase related to the yeast transcriptional regulator Rpd3p. *Science*, **272**, 408-411.

Thiru, A., Nietlispach, D., Mott, H.R., Okiwaki, M., Lyon, D., Nielsen, P.R., Hirshberg, M., Verreault, A., Murzina, N.V. and Laue, E.D. (2004) Structural basis of chromo shadow domain/PXVXL motif peptide interactions and HP1 localisation to heterochromatin. *EMBO J*, **23**, 489-499.

Thomas, B.J., and Rothstein, R. (1989). Elevated recombination rates in transcriptionally active DNA. *Cell* **56**, 619-630.

Tom, S., Henricksen, L.A. and Bambara, R.A. (2000) Mechanism whereby proliferating cell nuclear antigen stimulates flap endonuclease 1. *J Biol Chem*, **275**, 10498-10505.

Torres-Ramos, C.A., Yoder, B.L., Burgers, P.M., Prakash, S. and Prakash, L. (1996) Requirement of proliferating cell nuclear antigen in RAD6-dependent postreplicational DNA repair. *Proc Natl Acad Sci U S A*, **93**, 9676-9681.

Tsurimoto, T. (1998) PCNA, a multifunctional ring on DNA. *Biochim Biophys Acta*, **1443**, 23-39.

Tsurimoto, T. (1999) PCNA binding proteins. *Front Biosci*, **4**, D849-858.

Tsurimoto, T. and Stillman, B. (1991) Replication factors required for SV40 DNA replication in vitro. I. DNA structure-specific recognition of a primer-template junction by eukaryotic DNA polymerases and their accessory proteins. *J Biol Chem*, **266**, 1950-1960.

Tyler, J.K., Adams, C.R., Chen, S.R., Kobayashi, R., Kamakaka, R.T. and Kadonaga, J.T. (1999) The RCAF complex mediates chromatin assembly during DNA replication and repair. *Nature*, **402**, 555-560.

Tyler, J.K., Bulger, M., Kamakaka, R.T., Kobayashi, R. and Kadonaga, J.T. (1996) The p55 subunit of Drosophila chromatin assembly factor 1 is homologous to a histone deacetylase-associated protein. *Mol Cell Biol*, **16**, 6149-6159.

Tyler, J.K., Collins, K.A., Prasad-Sinha, J., Amiott, E., Bulger, M., Harte, P.J., Kobayashi, R. and Kadonaga, J.T. (2001) Interaction between the Drosophila CAF-1 and ASF1 chromatin assembly factors. *Mol Cell Biol*, **21**, 6574-6584.

Tyler, J.K. and Kadonaga, J.T. (1999) The "dark side" of chromatin remodeling: repressive effects on transcription. *Cell*, **99**, 443-446.

Umar, A., Buermeyer, A.B., Simon, J.A., Thomas, D.C., Clark, A.B., Liskay, R.M. and Kunkel, T.A. (1996) Requirement for PCNA in DNA mismatch repair at a step preceding DNA resynthesis. *Cell*, **87**, 65-73.

Unk, I., Haracska, L., Gomes, X.V., Burgers, P.M., Prakash, L. and Prakash, S. (2002) Stimulation of 3'-->5' exonuclease and 3'-phosphodiesterase activities of yeast Apn2 by proliferating cell nuclear antigen. *Mol Cell Biol*, **22**, 6480-6486.

Vairapandi, M., Azam, N., Balliet, A.G., Hoffman, B. and Liebermann, D.A. (2000a) Characterization of MyD118, Gadd45, and proliferating cell nuclear antigen (PCNA) interacting domains. PCNA impedes MyD118 AND Gadd45- mediated negative growth control. *J Biol Chem*, **275**, 16810-16819.

Vairapandi, M., Balliet, A.G., Fornace, A.J., Jr., Hoffman, B. and Liebermann, D.A. (1996) The differentiation primary response gene MyD118, related to GADD45, encodes for a nuclear protein which interacts with PCNA and p21WAF1/CIP1. *Oncogene*, **12**, 2579-2594.

Vairapandi, M., Liebermann, D.A., Hoffman, B. and Duker, N.J. (2000b) Human DNA-demethylating activity: a glycosylase associated with RNA and PCNA. *J Cell Biochem*, **79**, 249-260.

van Leeuwen, F., Gafken, P.R. and Gottschling, D.E. (2002) Dot1p modulates silencing in yeast by methylation of the nucleosome core. *Cell*, **109**, 745-756.

van Leeuwen, F. and Gottschling, D.E. (2002) Genome-wide histone modifications: gaining specificity by preventing promiscuity. *Curr Opin Cell Biol*, **14**, 756-762.

Velculescu, V.E., Zhang, L., Zhou, W., Vogelstein, J., Basrai, M.A., Bassett Jr, D.E., Hieter, P., Vogelstein, B. and Kinzler, K.W. (1997) Characterization of the yeast transcriptome. *Cell*, **88**, 243-251.

Vermaak, D., Wade, P.A., Jones, P.L., Shi, Y.B. and Wolffe, A.P. (1999) Functional analysis of the SIN3-histone deacetylase RPD3-RbAp48-histone H4 connection in the *Xenopus* oocyte. *Mol Cell Biol*, **19**, 5847-5860.

Verreault, A. (2000) De novo nucleosome assembly: new pieces in an old puzzle. *Genes Dev*, **14**, 1430-1438.

Verreault, A., Kaufman, P.D., Kobayashi, R. and Stillman, B. (1996) Nucleosome assembly by a complex of CAF-1 and acetylated histones H3/H4. *Cell*, **87**, 95-104.

Verreault, A., Kaufman, P.D., Kobayashi, R. and Stillman, B. (1998) Nucleosomal DNA regulates the core-histone-binding subunit of the human Hat1 acetyltransferase. *Curr Biol*, **8**, 96-108.

Vivona, J.B. and Kelman, Z. (2003) The diverse spectrum of sliding clamp interacting proteins. *FEBS Lett*, **546**, 167-172.

von Hippel, P.H. and Delagoutte, E. (2003) Macromolecular complexes that unwind nucleic acids. *Bioessays*, **25**, 1168-1177.

Waga, S., Hannon, G.J., Beach, D. and Stillman, B. (1994) The p21 inhibitor of cyclin-dependent kinases controls DNA replication by interaction with PCNA. *Nature*, **369**, 574-578.

Waga, S. and Stillman, B. (1994) Anatomy of a DNA replication fork revealed by reconstitution of SV40 DNA replication in vitro. *Nature*, **369**, 207-212.

Waga, S. and Stillman, B. (1998) The DNA replication fork in eukaryotic cells. *Annu Rev Biochem*, **67**, 721-751.

Wang, J.C. (2002) Cellular roles of DNA topoisomerases: a molecular perspective. *Nat Rev Mol Cell Biol*, **3**, 430-440.

Warbrick, E. (1998) PCNA binding through a conserved motif. *Bioessays*, **20**, 195-199.

Warbrick, E. (2000) The puzzle of PCNA's many partners. *Bioessays*, **22**, 997-1006.

Warbrick, E., Heatherington, W., Lane, D.P. and Glover, D.M. (1998) PCNA binding proteins in Drosophila melanogaster : the analysis of a conserved PCNA binding domain. *Nucleic Acids Res*, **26**, 3925-3932.

Warbrick, E., Lane, D.P., Glover, D.M. and Cox, L.S. (1995) A small peptide inhibitor of DNA replication defines the site of interaction between the cyclin-dependent kinase inhibitor p21WAF1 and proliferating cell nuclear antigen. *Curr Biol*, **5**, 275-282.

Warbrick, E., Lane, D.P., Glover, D.M. and Cox, L.S. (1997) Homologous regions of Fen1 and p21Cip1 compete for binding to the same site on PCNA: a potential mechanism to co-ordinate DNA replication and repair. *Oncogene*, **14**, 2313-2321.

Watanabe, H., Pan, Z.Q., Schreiber-Agus, N., DePinho, R.A., Hurwitz, J. and Xiong, Y. (1998) Suppression of cell transformation by the cyclin-dependent kinase inhibitor p57KIP2 requires binding to proliferating cell nuclear antigen. *Proc Natl Acad Sci U S A*, **95**, 1392-1397.

Waterborg, J.H. (2002) Dynamics of histone acetylation in vivo. A function for acetylation turnover? *Biochem Cell Biol*, **80**, 363-378.

Watson, J.D. and Crick, F.H. (1953) Molecular structure of nucleic acids; a structure for deoxyribose nucleic acid. *Nature*, **171**, 737-738.

Winkler, G.S., Kristjuhan, A., Erdjument-Bromage, H., Tempst, P. and Svejstrup, J.Q. (2002) Elongator is a histone H3 and H4 acetyltransferase important for normal histone acetylation levels *in vivo*. *Proc Natl Acad Sci USA*, **99**, 3517-3522.

Wold, M.S. (1997) Replication protein A: a heterotrimeric, single-stranded DNA-binding protein required for eukaryotic DNA metabolism. *Annu Rev Biochem*, **66**, 61-92.

Wolffe, A., (1992) Chromatin Structure and Function. San Diego: Academic Press, San Diego.

Wolffe, A.P. and Hayes, J.J. (1999) Chromatin disruption and modification. *Nucleic Acids Res*, **27**, 711-720.

Wood, A., Schneider, J., Dover, J., Johnston, M. and Shilatifard, A. (2003) The Paf1 complex is essential for histone mono-ubiquitination by the Rad6-Bre1 complex, which signals for histone methylation by COMPASS and Dot1p. *J Biol Chem*, **278**, 34739-34742.

Worcel, A., Han, S. and Wong, M.L. (1978) Assembly of newly replicated chromatin. *Cell*, **15**, 969-977.

Wyrick, J.J., Holstege, F.C., Jennings, E.G., Causton, H.C., Shore, D., Grunstein, M., Lander, E.S. and Young, R.A. (1999) Chromosomal landscape of nucleosome-dependent gene expression and silencing in yeast. *Nature*, **402**, 418-421.

Xiong, Y., Zhang, H. and Beach, D. (1992) D type cyclins associate with multiple protein kinases and the DNA replication and repair factor PCNA. *Cell*, **71**, 505-514.

Xu, H., Zhang, P., Liu, L. and Lee, M.Y. (2001) A novel pcna-binding motif identified by the panning of a random peptide display library. *Biochemistry*, **40**, 4512-4520.

Yamamoto, Y., Girard, F., Bello, B., Affolter, M. and Gehring, W.J. (1997) The cramped gene of Drosophila is a member of the Polycomb-group, and interacts with mus209, the gene encoding Proliferating Cell Nuclear Antigen. *Development*, **124**, 3385-3394.

Yang, H., Chiang, J.H., Fitz-Gibbon, S., Lebel, M., Sartori, A.A., Jiricny, J., Slupska, M.M. and Miller, J.H. (2002) Direct interaction between uracil-DNA glycosylase and a proliferating cell nuclear antigen homolog in the crenarchaeon *Pyrobaculum aerophilum*. *J Biol Chem*, **277**, 22271-22278.

Yao, N., Turner, J., Kelman, Z., Stukenberg, P.T., Dean, F., Shechter, D., Pan, Z.Q., Hurwitz, J. and O'Donnell, M. (1996) Clamp loading, unloading and intrinsic stability of the PCNA, beta and gp45 sliding clamps of human, E. coli and T4 replicases. *Genes Cells*, **1**, 101-113.

Ye, X., Franco, A.A., Santos, H., Nelson, D.M., Kaufman, P.D. and Adams, P.D. (2003) Defective S phase chromatin assembly causes DNA damage, activation of the S phase checkpoint and S phase arrest. *Mol Cell*, **11**, 341-351.

Yu, L., Gaitatzes, C., Neer, E. and Smith, T.F. (2000) Thirty-plus functional families from a single motif. *Protein Sci*, **9**, 2470-2476.

Zaika, A., Mozzherin, D.J., Tan, C.K., Downey, K.M. and Fisher, P.A. (1999) A two-dimensional support for selective binding of polyhistidine-tagged proteins: identification of a proliferating cell nuclear antigen point mutant with altered function in vitro. *Anal Biochem*, **268**, 193-200.

Zhang, P., Sun, Y., Hsu, H., Zhang, L., Zhang, Y. and Lee, M.Y. (1998a) The interdomain connector loop of human PCNA is involved in a direct interaction with human polymerase delta. *J Biol Chem*, **273**, 713-719.

Zhang, Q., Vo, N. and Goodman, R.H. (2000a) Histone binding protein RbAp48 interacts with a complex of CREB binding protein and phosphorylated CREB. *Mol Cell Biol*, **20**, 4970-4978.

Zhang, S.J., Zeng, X.R., Zhang, P., Toomey, N.L., Chuang, R.Y., Chang, L.S. and Lee, M.Y. (1995) A conserved region in the amino terminus of DNA polymerase delta is involved in proliferating cell nuclear antigen binding. *J Biol Chem*, **270**, 7988-7992.

Zhang, Y., Iratni, R., Erdjument-Bromage, H., Tempst, P. and Reinberg, D. (1997) Histone deacetylases and SAP18, a novel polypeptide, are components of a human Sin3 complex. *Cell*, **89**, 357-364.

Zhang, Y., LeRoy, G., Seelig, H.P., Lane, W.S. and Reinberg, D. (1998b) The dermatomyositis-specific autoantigen Mi2 is a component of a complex containing histone deacetylase and nucleosome remodeling activities. *Cell*, **95**, 279-289.

Zhang, Y., Ng, H.H., Erdjument-Bromage, H., Tempst, P., Bird, A. and Reinberg, D. (1999) Analysis of the NuRD subunits reveals a histone deacetylase core complex and a connection with DNA methylation. *Genes Dev*, **13**, 1924-1935.

Zhang, Z., Shibahara, K. and Stillman, B. (2000b) PCNA connects DNA replication to epigenetic inheritance in yeast. *Nature*, **408**, 221-225.

Zhao, X., Chabes, A., Domkin, V., Thelander, L. and Rothstein, R. (2001) The ribonucleotide reductase inhibitor Sml1 is a new target of the Mec1/Rad53 kinase cascade during growth and in response to DNA damage. *Embo J*, **20**, 3544-3553.

Zheleva, D.I., Zhelev, N.Z., Fischer, P.M., Duff, S.V., Warbrick, E., Blake, D.G. and Lane, D.P. (2000) A quantitative study of the in vitro binding of the C-terminal domain of p21 to PCNA: affinity, stoichiometry, and thermodynamics. *Biochemistry*, **39**, 7388-7397.

Zhu, X., Démolis, N., Jacquet, M. and Michaeli, T. (2000) *MSI1* suppresses hyperactive RAS via the cAMP-dependent protein kinase and independently of chromatin assembly factor-1. *Curr Genet*, **38**, 60-70.

Zuo, S., Bermudez, V., Zhang, G., Kelman, Z. and Hurwitz, J. (2000) Structure and activity associated with multiple forms of Schizosaccharomyces pombe DNA polymerase delta. *J Biol Chem*, **275**, 5153-5162.

APPENDICES

APPENDIX I – CLONING DATABASES

Table I.I: Oligonucleotides used for cloning and site directed mutagenesis in this work

Oligonucleotide	Sequence	use
mp1505'-Δ25-29	CCCGGGTTCCCACAAGCCCGCTTGC	Sense for deleting PBM1 in mp150 by site directed mutagenesis (SDM).
mp1503'-Δ25-29	GCAAGCGGGCTTGTGGGAACCCGGG	Antisense for deleting PBM1 mp150 by SDM.
5' mp150 Δ424-8	CGCATTAAGGCAGAAAAGGCAGAGCAGAAACCGAAGACTCCGCAGGC	Sense for deleting PBM2 in mp150 by SDM.
3' mp150 Δ424-8	GCCTGCGGAGTCTTCGGTTTCTGCTCTGCCTTTTCTGCCTTAATGCG	Antisense for deleting PBM2 mp150 by SDM.
5'hp150Δ11-15	CCAGCTTTTCCACAAGCCCGTCTGCCG	Sense for deleting PBM1 in hp150 by SDM.
3'hp150Δ11-15	CGGCAGACGGGCTTGTGGAAAAGCTGG	Antisense for deleting PBM1 in hp150 by SDM.
5'hp150Δ427-31	GCAGAGAAGGCCGAACAGAAACCAAAGACTCC	Sense for deleting PBM2 in hp150 by SDM.
3'hp150Δ427-31	GGAGTCTTTGGTTTCTGTTCGGCCTTCTCTGC	Antisense for deleting PBM2 in hp150 by SDM.
hp150Bgl-Nco	GAAGATCTGCCATGGATTGCAAAGATAGACCAG	Sense for cloning all pET28 hp150.
hp150Xho-2	GGGGTACCTCACTCGAGGCTGCCGCGCGGCACCAGCCCCTTTGGGAC AAGATTC	Antisense for cloning pET28 hp150 (1-31).
hp150Xho-3	GGGGTACCTCACTCGAGGCTGCCGCGCGGCACCAGGCCAACACCCTC CTCCTC	Antisense for cloning pET28 hp150 (1-171).
hp150Xho-4	GGGGTACCTCACTCGAGGCTGCCGCGCGGCACCAGGGTGGGGAAGGG ACTGGTAC	Antisense for cloning pET28 hp150 (1-296).
hp150Xho-5	GGGGTACCTCACTCGAGGCTGCCGCGCGGCACCAGGGCCAGGACCAT GTGCTC	Antisense for cloning pET28 hp150 (1-462).
hp150xho-6	CCCGCTCGAGGCTGCCGCGCGGCACCAGGGATGCACCCAGTGGGC	Antisense for cloning pET28 hp150 (full length)
IL-2	CGGGATCCAGGGGTCCCTCAGC	Sense for cloning pET16b p150 (1-32) LigI (20-263).
IL-3	CCCGCTCGAGGATTGCAAAGATAGACCAGCTTTTCCAGTTAAGAAGT TAATACAAGCCCGTCTGCCGTTTAAGCGCCTGAATCTTGTCCCAAAG GGGAAAGCCCCTGAGAAGGAGGCATCC	Antisense for cloning pET16b p150 (1-32) LigI (20-263).

mp150SacI	AAGGAAAAAAGAGCTCTGCACGAGTTCCGACTTGAAGC	Sense for deleting the dimerisation domain of mp150.
mp150 BamI	CGCGGATCCTCACTTGCAAAGTGTGGGAGC	Antisense for deleting dimerisation domain, mp150.
pCITE1rev	GCTTGCATGCCTGCAGGTCG	Antisense to sequence the end of p150 in pPK38.
PCNA-1	CTAGGCTAGCGTCGACATGGTGTTCGAGGCGCGCCTGGTCC	Sense to PCR the hPCNA and subclone as an NheI-XhoI fragment into the pDsRed-N1 vector.
PCNA-2	CGGGATCCCTACTCGAGAGATCCTTCTTCATCCTCG	Antisense to PCR the hPCNA and subclone as an NheI-XhoI fragment into the pDsRed-N1 vector.
5' PCNA-8	GGCTTCGACACCTACGCCTGCGCCCGCAACCTGGCCATGGGC	Sense for mutating hPCNA to PCNA-8 (RD61,63AA).
3' PCNA-8	GCCCATGGCCAGGTTGCGGGCGCAGGCGTAGGTGTCGAAGCC	Antisense for mutating hPCNA to PCNA-8 (RD61,63AA).
5'IDCLPCNALI->AA	GATGTTGAACAAGCCGGAGCCCCAGAACAGGAGTACAGC	Sense for mutating hPCNA to PCNA-79 (LI126,128AA).
3'IDCLPCNALI->AA	GCTGTACTCCTGTTCTGGGGCTCCGGCTTGTTCAACATC	Antisense for mutating hPCNA to PCNA-79 (LI126,128AA).
5'cPCNAPK->AA	CTACTTGGCTGCCGCGATCGAGGATGAAGAAGG	Sense for mutating hPCNA to PCNA-90 (PK253,254AA).
3'cPCNAPK->AA	CCTTCTTCATCCTCGATCGCGGCAGCCAAGTAG	Antisense for mutating hPCNA to PCNA-90 (PK253, 254AA).
CAC1PBM-1	CGGAATTCTAGAGCAACATCTCAAATCAATTCCTCTACAGGAC GACACTAAGAAAAAAGGCATACTATCTTTTTTCCAGAATACA	Sense for pGEXKG CAC1 PBM1 WT.
CAC1PBM-2	CATGCCATGGTTAGACATCCTTCTCTTTCGTGAGAAACTTAT TACTCTTTACCGTAGTTGTATTCTGGAAAAAAGATAGTAT	Antisense for pGEXKG CAC1 PBM1 WT.
CAC1PBM-3	CGGAATTCTAGAGCAACATCTCAAATCAATTCCTCTACAGGAC GACACTAAGAAAAAAGGCATACTATCTGCGGCCCAGAATACA	Sense for pGEXKG CAC1 PBM1 FF22,23AA.
CAC1PBM-4	CATGCCATGGTTAGACATCCTTCTCTTTCGTGAGAAACTTAT TACTCTTTACCGTAGTTGTATTCTGGGCCGCAGATAGTAT	Antisense for pGEXKG CAC1 PBM1 FF22,23AA.
CAC1-1	CGGGATCCCGGCGCCCAGTCAGCCTTTA	Sense for pRS305 CAC1 Pro+N PBM1 wt.
CAC1-2	CCGCTCGAGTGCTTTTTGTCTCGATAGCTATTAT	Antisense for pRS305 CAC1 Pro+N PBM1 wt.

CAC1-3	GAAAAAAGGCATACTATCTGCCGCTCAGAATACAACTACGGTAAAG	Sense for Cac1 PBM1 FF 22,23 AA by SDM.
CAC1-4	CTTTACCGTAGTTGTATTCTGAGCGGCAGATAGTATGCCTTTTTTC	Antisense for Cac1 PBM1 FF 22,23 AA by SDM.
CAC1-5	ATAAGAATGCGGCCGCATCCTAAAGAGGATGTCAGTG	Sense for Cac1 PBM2 wt FLAG3.
CAC1-6	CGGGATCCCAAAGACGGGGTTGGCATA	Antisense for Cac1 PBM2 wt FLAG3.
CAC1-7	CAATCCCGTATTGGTAACGCGGCTAAAAAACTAAGCGATTC	Sense for pRS304 CAC1 PBM2 FF233,234AA FLAG3 by SDM.
CAC1-8	GAATCGCTTAGTTTTTTAGCCGCGTTACCAATACGGGATTG	Antisense for pRS304 CAC1 PBM2 FF233,234AA FLAG3 by SDM.
PWP1-7	CTAGTCTAGACTTTCGATATTAGAAACAATG	Sense for tagging PWP1 with FLAG.
PWP1-8	CGGGATCCTGCCATGTCATCATGCTCATC	Antisense for tagging PWP1 with FLAG.
PWP1 FW	CTAGGATCCATGATTTCTGCTACTAAT	Sense for pYES-PWP1.
PWP1 RV	TAGGCGGCCGCATGCCATGTCATCATG	Antisense for pYES-PWP1
5'SET1YF-AA	CCAAGACATATCAATAAAAAACGCTGCTAAAAAGTATGGAGAAATTTC	Antisense to mutate YF to AA in putative PBM in scSet1.
3'SET1YF-AA	GAAATTTCTCCATACTTTTTAGCAGCGTTTTTTATTGATATGTCTTGG	Sense to mutate YF to AA in putative PBM in scSet1.
5'SET1YF-DD	CCAAGACATATCAATAAAAAACGATGATAAAAAGTATGGAGAAATTTC	Sense to mutate YF to DD in putative PBM in scSet1.
3'SET1YF-DD	GAAATTTCTCCATACTTTTTATCATCGTTTTTTATTGATATGTCTTGG	Antisense to mutate YF to DD in putative PBM in scSet1.
5'pol30k127r	CGATGCTGATTTCTTAAGGATTGAAGAATTACAGTACGACTCCACCC	Sense for mutating scPCNA (*pol30*) K127 to R by SDM.
3'pol30k127r	GGGTGGAGTCGTACTGTAATTCTTCAATCCTTAAGAAATCAGCATCG	Antisense for mutating scPCNA (*pol30*) K127 to R by SDM.
5'pol30k164r	CTATTAATATCATGATCACCAGAGAAACAATAAAGTTTGTAGC	Sense for mutating scPCNA (*pol30*) K164 to R by SDM.
3'pol30k164r	GCTACAAACTTTATTGTTTCTCTGGTGATCATGATATTAATAG	Antisense for mutating scPCNA (*pol30*) K164 to R by SDM.

Table I.II: plasmids used in this work

Plasmid	Vector*	Use	Source or cloning strategy
pPK38	pCITE1 (Novagen) Amp	*In vitro* translation reticulocyte lysate	Human p150 and C-terminal truncations expression from the T7 promoter (Kaufman et al., 1995).
hp150 Δ11-15	Same	Same	Human p150 ΔPBM1, constructed by site-directed mutagenesis of pPK38 using primers 5'hp150Δ11-15 and 3'hp150Δ11-15 (Table I.I).
hp150 Δ427-431	Same	Same	Human p150 ΔPBM2, constructed by site-directed mutagenesis of pPK38 using primers 5'hp150Δ427-31 and 3'hp150Δ427-31.
hp150 Δ2RFTS	Same	Same	Human p150 ΔPBM1+2, constructed by site-directed mutagenesis of hp150 Δ11-15 using primers 5'hp150Δ427-31 and 3'hp150Δ427-31.
pPK59	pCITE2a+ (Novagen) Amp	Same	Human p60 expression from the T7 promoter (Kaufman et al., 1995)
pGEM2β p48	pGEM2β (Promega) Amp	Same	Human p48 expression from the T7 promoter (A. Verreault, unpublished). p48 cDNA was subcloned as Nco I to Eco RI fragment into the same sites in the pGEM2β vector.
pCITE4a mp150 WT	pCITE4a+ (Novagen) Amp	Same	Mouse p150 WT expression from the T7 promoter (Murzina et al., 1999). cDNA is between the BamHI and NotI sites.
pCITE4a mp150 Δ25-29	Same	Same	Mouse p150 ΔPBM1 expression from the T7 promoter. Constructed by site-directed mutagenesis of pCITE4a mp150 WT using primers mp1505'-Δ25-29 and mp1503'-Δ25-29.
pCITE4a mp150 Δ424-428	Same	Same	Mouse p150 ΔPBM2 expression from the T7 promoter. Constructed by site-directed mutagenesis of pCITE4a mp150 WT using primers 5' mp150 Δ424-8 and 3' mp150 Δ424-8.

pCITE4a mp150 Δ2RFTS	Same	Same	Mouse p150 ΔPBM1+2 expression from the T7 promoter. Constructed by site-directed mutagenesis of pCITE4a mp150 Δ25-29 using primers 5' mp150 Δ424-8 and 3' mp150 Δ424-8.
pET23/C-His PCNA	pET23/C (Novagen) Amp	*E. coli* expression C-terminal His-tag	Human WT PCNA (Jónsson et al., 1998).
pET23/C-His PCNA-8	Same	Same	Human PCNA-8, constructed by site directed mutagenesis from WT plasmid using primers 5' PCNA-8 and 3' PCNA-8.
pET23/C-His PCNA-79	Same	Same	Human PCNA-79, constructed by site directed mutagenesis from WT plasmid using primers 5'IDCLPCNALI->AA and 3'IDCLPCNALI->AA.
pET23/C-His PCNA-90	Same	Same	Human PCNA-90, constructed by site directed mutagenesis from WT plasmid using primers 5'cPCNAPK->AA and 3'cPCNAPK->AA.
pQE30 N-His- PCNA	pQE30 (Qiagen) Amp	*E. coli* expression N-terminal His-tag	His6 human PCNA (Zaika et al., 1999).
pET28 hp150 (1-296)	pET28 (Novagen) Kan	*E. coli* expression C-terminal His-tag	Human p150 1-296. Primers hp150Bgl-Nco and hp150Xho-4 used to PCR a fragment encoding amino acid residues 1-296 of human p150. Product cloned into the NcoI and XhoI sites of pET28a+ vector.
pET28 hp150 (1-296) Δ11-15	Same	Same	Human p150 1-296 ΔPBM1. As above, using plasmid hp150 Δ11-15 as template.
pET28 hp150 (1-462)	Same	Same	Human p150 1-462. Primers hp150Bgl-Nco and hp150Xho-5 used to PCR a fragment encoding amino acid residues 1-462 of human p150. Product cloned into the NcoI and XhoI sites of pET28a+ vector.
pET28 hp150 (1-462) Δ11-15	Same	Same	Human p150 1-462 ΔPBM1. As above, using plasmid hp150 Δ11-15 as template.
pET28 hp150 (1-462) Δ427-431	Same	Same	Human p150 1-462 ΔPBM2. As above, using plasmid hp150 Δ427-431 as template.

pET28 hp150 (1-462) Δ2RFTS	Same	Same	Human p150 1-462 Δ11-15 Δ427-431 (ΔPBM1+2). As above, using plasmid hp150 Δ2RFTS as template.
pET28 hp150	Same	Same	Full length human p150 WT. Primers hp150Bgl-Nco and hp150Xho-6 used to PCR a fragment encoding residues 1-938 of human p150. Product cloned into the NcoI and XhoI sites of pET28a+ vector.
pET28 hp150 Δ11-15	Same	Same	Full length p150 ΔPBM1. As above, using plasmid hp150 Δ11-15 as template.
pET28 hp150 Δ427-431	Same	Same	Full length p150 ΔPBM2. As above, using plasmid hp150 Δ427-431 as template.
pET28 hp150 Δ2RFTS	Same	Same	Full length p150 Δ11-15 Δ427-431 (ΔPBM1+2). As above, using plasmid hp150 Δ2RFTS as template.
pET11 hLig I	pET11 (Novagen) Amp	*E. coli* expression N-terminal His-tag	Full length human DNA ligase I (MacKenney et al., 1997).
pET16b hLig I (2-263)	pET16b (Novagen) Amp	*E. coli* expression N-terminal His-tag	Human DNA ligase I N-terminal domain corresponding to residues 2-263 (MacKenney et al., 1997).
pET16b hLig I (262-919)	Same	Same	Human DNA ligase I catalytic domain. C-terminal region corresponding to residues 262-919 (MacKenney et al., 1997).
pET16b p150 (1-32) LigI (20-263)	Same	Same	Primers IL-3 and IL-2 were used to PCR a DNA fragment encoding resdiues 2-32 of human p150 (PBM1 region) fused in-frame to residues 20-263 of human ligase I (which removes the LIG I PBM). The PCR product was inserted between the XhoI and BamHI sites of plasmid pET16b hLIG I(262-919). The C-terminal domain of Lig I is absent from this construct.

pET16b p150 (1-32) Lig I (20-919)	Same	Same	Chimaera of p150 PBM1 (residues 2-32) fused in-frame with human ligase I residues 20-919 (which removes the Lig I PBM). The C-terminal domain of Lig I was isolated as a BamHI fragment from pET16b hLig I (262-919) and inserted into the BamHI site of pET16b p150 (1-32) LigI (20-263) to create the full-length chimaeric protein expression construct.
pGEX2TL hH4	pGEX2TL Amp	*E. coli* expression N-terminal GST	GST- human H4 (Hoffmann et al., 1996)
pGEX2TL hH3	Same	Same	GST- human H3 (Hoffmann et al., 1996).
pRED PCNA	pDsRed N1 (Clontech) Kan	Mammalian cell expression	PCNA-RFP. Human PCNA fused in-frame with Red Fluorescent protein. The human PCNA coding region was inserted into the NheI and XhoI sites of the pDsRed N1 vector (A. Verreault, unpublished).
GFP mp150 WT	EGFP-C1 (Clontech) Kan	Mammalian cell expression	GFP mouse p150 WT expression from CMV promoter (Murzina et al., 1999).
GFP mp150 Δ25-29	Same	Same	GFP mouse p150 ΔPBM1 expression from CMV promoter. Subcloned BamHI-NotI mp150 fragment from pCITE4a mp150 Δ25-29 into the BglII-BspNI sites of EGFP-C1 vector.
GFP mp150 Δ424-428	Same	Same	GFP mouse p150 ΔPBM2 expression from CMV promoter. Same subcloning strategy, starting with pCITE4a mp150 Δ424-428.
GFP mp150 Δ2RFTS	Same	Same	GFP mouse p150 ΔPBM1+2 expression from CMV promoter. Same subcloning strategy, starting with pCITE4a mp150 Δ2RFTS.
GFP mp150 ΔD	Same	Same	GFP mouse p150 ΔD expression from CMV promoter. A C-terminal fragment including the dimerisation motif was excised from GFP mp150WT as a SacI-BamHI fragment and replaced a shorter PCR product (lacking the dimerisation motif, residues 651-675) amplified by PCR from GFP mp150WT using primers mp150SacI and mp150BamI.

GFP mp150 ΔPBM1 ΔD	Same	Same	GFP mp150 ΔPBM1 ΔD expression from CMV promoter. Same subcloning strategy, starting with GFP mp150 Δ25-29.
GFP mp150 ΔPBM2 ΔD	Same	Same	GFP mp150 ΔPBM1 ΔD expression from CMV promoter. Same subcloning strategy, starting with GFP mp150 Δ424-428.
GFP mp150 Δ2RFTS ΔD	Same	Same	GFP mp150 ΔPBM1+2 ΔD expression from CMV promoter. Same subcloning strategy, starting with GFP mp150 Δ2RFTS.
pGEXKG CAC1 PBM1 WT	pGEXKG Amp	*E. coli* expression N-terminal GST	GST-Cac1 N-terminal region (residues 2-41) with WT PBM1. Primers CAC1PBM-1 and CAC1PBM-2 were annealed, the DNA filled-in with Klenow, digested with EcoRI and NcoI, and inserted into the EcoRI and NcoI sites of pGEXKG (Guan and Dixon, 1991).
pGEXKG CAC1 PBM1 FF22,23AA	Same	Same	GST-Cac1 N-terminal region (residues 2-41) with PBM1 mutation (FF 22,23 AA). Primers CAC1PBM-3 and CAC1PBM-4 were annealed, the DNA filled-in with Klenow, digested with EcoRI and NcoI, and inserted into the EcoRI and NcoI sites of pGEXKG.
pGEXKG MOD1	Same	Same	GST mouse MOD1 (HP1β). The cDNA was amplified by PCR from an EST cDNA clone and sub-cloned into the BamHI and SalI sites of the pGEX-KG vector (A. Verreault, unpublished).
pGEXKG MOD2	Same	Same	GST mouse MOD2 (HP1γ). The cDNA was amplified by PCR from an EST cDNA clone and sub-cloned into the BamHI and SalI sites of the pGEX-KG vector (A. Verreault, unpublished).
pGEXKG HP1α	Same	Same	GST mouse HP1α. The cDNA was amplified by PCR from an EST cDNA clone and sub-cloned into the BamHI and SalI sites of the pGEX-KG vector (A. Verreault, unpublished).
pRS305	pRS305 Amp *LEU2*	*S. cerevisiae* Integration vector	Yeast integration vector (Sikorski and Hieter, 1989).

pRS305 CAC1 Pro+N PBM1 wt	Same	Same	Cac1 PBM1 wt (no tag). A fragment encoding the CAC1 promoter (from -400) and N-terminal region (to +350) was amplified by PCR from yeast genomic DNA using primers CAC1-1 and CAC1-2 and sub-cloned into the BamHI and XhoI sites of pRS305. Linearise with HindIII for integration at CAC1 locus.
pRS305 CAC1 Pro+N PBM1 FF22,23AA	Same	Same	Cac1 PBM1 FF 22,23 AA (no tag). Construct derived by site-directed mutagenesis of pRS305 CAC1 Pro+N PBM1 wt using primers CAC1-3 and CAC1-4. Linearise with HindIII for integration at CAC1 locus.
pRS304 FLAG3	pRS304 Amp *TRP1*	*S. cerevisiae* Integration vector	Yeast integration vector (Sikorski and Hieter, 1989) modified by insertion of a FLAG3 epitope between the BamHI and XmaI sites (A. Verreault, unpublished).
pRS304 CAC1 PBM2 wt FLAG3	Same	Same	Cac1 PBM2 wt FLAG3. A CAC1 fragment (nt 139-1818, without STOP codon) was amplified by PCR from yeast genomic DNA using primers CAC1-5 and CAC1-6 and sub-cloned into the NotI and BamHI sites of pRS304 FLAG3. Linearise with BlpI for integration at the CAC1 locus.
pRS304 CAC1 PBM2 FF233,234AA FLAG3	Same	Same	Construct derived by site-directed mutagenesis of pRS304 CAC1 PBM2 wt FLAG3 using primers CAC1-7 and CAC1-8. Linearise with BlpI for integration at the CAC1 locus.
pRS304 CAC1 FLAG3	Same	Same	Cac1-FLAG3. A CAC1 fragment (nt 1158-1818, without STOP codon) was amplified by PCR from pSE1312, and sub-cloned into the NotI and BamHI sites of pRS304-FLAG3 (A. Verreault, unpublished). Linearise with EcoNI to integrate at the CAC1 locus.
pRS306 FLAG1	pRS306 Amp *URA3*	*S. cerevisiae* Integration vector	Yeast integration vector (Sikorski and Hieter, 1989) modified by insertion of a FLAG epitope between the BamHI and XmaI sites (A. Verreault, unpublished).

pRS306 PWP1 FLAG	Same	Same	Pwp1-FLAG. A C-terminal fragment of PWP1 (nt 1208-1728) was amplified by PCR from a cDNA clone using primers PWP1-7 and PWP1-8, and sub-cloned into the XbaI and BamHI sites of pRS306 FLAG1. Linearise with BglII to integrate at the PWP1 locus.
pYES2 HA3	pYES2 Amp *URA3* (Clontech)	*S. cerevisiae 2-μ GAL1 promoter*	High copy plasmid for expression of HA3-tagged proteins from the GAL1 promoter. The HA3 epitope was inserted into the NotI and XbaI sites of pYES2 (M. Abdul-Rauf, unpublished).
pYES2 PWP1 HA3	pYES2 HA3 Amp *URA3*	Same	High-copy plasmid for expression of Pwp1-HA3 from the GAL1 promoter. The full-length PWP1 cDNA was amplified by PCR and inserted into the EcoRI and NotI sites of pYES2 HA3 (M. Abdul-Rauf, unpublished).
pRS303 TAP	pRS303 *HIS3*	*S. cerevisiae* Integration vector	Yeast integration vector (Sikorski and Hieter, 1989) modified by insertion of a TAP epitope between the BamHI and XmaI sites (A. Verreault, unpublished).
pRS303 PWP1 TAP	Same	Same	Pwp1-TAP. A C-terminal fragment of PWP1 (nt 1208-1728) was amplified by PCR from a cDNA clone using primers PWP1-7 and PWP1-8, and sub-cloned into the sites of pRS303 TAP. Linearised with SnaBI to integrate at the PWP1 locus.
pYCF1/CEN3.L	YRp14 Amp *URA3*	*S. cerevisiae*	Plasmid to monitor the frequency of mitotic chromosome loss of fragments derived from the left arm of chromosome III (Spencer et al., 1990).
pBL230-WT	pRS314 Amp *TRP1*	*S. cerevisiae* CEN plasmid	*POL30* expressed from *POL30* promoter (Ayyagari et al., 1995).
pBL230-6	Same	Same	*pol30-6* (DD41,42AA) expressed from *POL30* promoter (Ayyagari et al., 1995).
pBL230-8	Same	Same	*pol30-8* (RD61,63AA) expressed from *POL30* promoter (Ayyagari et al., 1995).

pBL230-22	Same	Same	*pol30-22* (DE256,257AA) expressed from *POL30* promoter (Ayyagari et al., 1995).
pBL230-79	Same	Same	*pol30-79* (LI126,128AA) expressed from *POL30* promoter (Eissenberg et al., 1997).
pBL230-90	Same	Same	*pol30-90* (PK252,253AA) expressed from *POL30* promoter (Eissenberg et al., 1997).
pBL230-K127R	Same	Same	*pol30-K127R* expressed from POL30 promoter. Created by site-directed mutagenesis of pBL230-WT using primers 5'pol30k127r and 3'pol30k127r.
pBL230-K164R	Same	Same	*pol30-K164R* expressed from POL30 promoter. Created by site-directed mutagenesis of pBL230-WT plasmid using primers 5'pol30k164r and 3'pol30k164r.

* Including company, antibiotics and marker genes.

Table I.III: Yeast strains used in this work

Strain	Genotype	Reference or Source
WT (W303)	*MATa ho ade2-1 trp1-1 can1-100 leu2,3-112 his3-11,15 ura3-1*	(Thomas and Rothstein, 1999)
YAV1	*cac1::CAC1-FLAG3-TRP1* in W303	(Gunjan and Verreault, 2003)
YSTT3	*hat1::TRP1 hat2::HIS3*	(Le el al., 1997; Thomas and Rothstain, 1989)
ARY94	*cac1::CAC1-FLAG3-TRP1* in YSTT3	M. Abdul-Rauf, unpublidhes
YJB469	*cac1-Δ1::LEU2*	(Enomoto et al., 1997)
ARY01	*asf1:: loxP-KanMX-loxP*	M. Abdul-Rauf, unpublidhes
YAV13	*asf1Δ::kanMX cac1-Δ1::LEU2*	A. Verreault, unpublidhes
YJB1919	*cac1-Δ1::LEU2 cac2::TRP1 cac3Δ::FOA-R*	(Enomoto and Berman, 1998)
ARY79	*pwp1::PWP1-FLAG3-URA3* in W303	M. Abdul-Rauf, unpublidhes
ARY81	*pwp1::PWP1-FLAG3-URA3* in YJB469	M. Abdul-Rauf, unpublidhes
ARY80	*pwp1::PWP1-FLAG3-URA3* in ARY01	M. Abdul-Rauf, unpublidhes
ARY82	*pwp1::PWP1-FLAG3-URA3* in YAV13	M. Abdul-Rauf, unpublidhes
ARY83	*pwp1::PWP1-FLAG3-URA3* in YJB1919	M. Abdul-Rauf, unpublidhes
ARY93	*pwp1::PWP1-FLAG3-URA3* in YSTT3	M. Abdul-Rauf, unpublidhes
ARY94	*cac1::CAC1-FLAG3-URA3* in YSTT3	M. Abdul-Rauf, unpublidhes
ARY84	*2μ-pYES2 pGAL1-PWP1-HA3 (URA3)* in W303	M. Abdul-Rauf, unpublidhes
ARY86	*2μ-pGAL1-PWP1-HA3 (URA3)* in YJB469	M. Abdul-Rauf, unpublidhes
ARY85	*2μ-pGAL1-PWP1-HA3 (URA3)* in ARY01	M. Abdul-Rauf, unpublidhes
ARY87	*2μ-pGAL1-PWP1-HA3 (URA3)* in YAV13	M. Abdul-Rauf, unpublidhes
ARY88	*2μ-pGAL1-PWP1-HA3 (URA3)* in YJB1919	M. Abdul-Rauf, unpublidhes
ARY95	*pwp1::PWP1-TAP-HIS3* in W303	M. Abdul-Rauf, unpublidhes
YAV119	*cac1::TRP1* in W303	M. Abdul-Rauf, unpublidhes
YAV138	*cac1::CAC1 PBM1wt PBM2wt –FLAG3::TRP1::LEU2* in W303	M. Abdul-Rauf, unpublidhes

YAV139	*cac1::CAC1 PBM1wt PBM2mut –FLAG3::TRP1::LEU2* in W303	A. Verreault, unpublidhes
YAV140	*cac1::CAC1 PBM1mut PBM2wt –FLAG3::TRP1::LEU2* in W303	A. Verreault, unpublidhes
YAV141	*cac1::CAC1 PBM1mut PBM2mut –FLAG3::TRP1::LEU2* in W303	A. Verreault, unpublidhes
Δ1	*hir1::HIS3* in W303	(De Silva et al., 1998)
YAV142	*cac1::CAC1 PBM1wt PBM2wt –FLAG3::TRP1::LEU2* in Δ1	Dr Alain Verreault
YAV143	*cac1::CAC1 PBM1wt PBM2mut –FLAG3::TRP1::LEU2* in Δ1	A. Verreault, unpublidhes
YAV144	*cac1::CAC1 PBM1mut PBM2wt –FLAG3::TRP1::LEU2* in Δ1	A. Verreault, unpublidhes
YAV145	*cac1::CAC1 PBM1mut PBM2mut –FLAG3::TRP1::LEU2* in Δ1	A. Verreault, unpublidhes
YAV151	*cac1::FOA-R* in Δ1	A. Verreault, unpublidhes
PY37	pBL211 *(POL30 URA3)* in *Matα ura3-52 trp1Δ901 leu2-3, 112 can1 pol30Δ1*	(Ayyagari et al., 1995)
PY39-wt	pBL230-wt (*TRP1 pol30-wt*) in PY37 w/o pBL211 (*POL30 URA*)	ibid.
PY39-6	pBL230-6 (*TRP1 pol30-6*) in PY37 w/o pBL211 (*POL30 URA*)	ibid.
PY39-8	pBL230-8 (*TRP1 pol30-8*) in PY37 w/o pBL211 (*POL30 URA*)	ibid.
PY39-22	pBL230-22 (*TRP1 pol30-22*) in PY37 w/o pBL211 (*POL30 URA*)	ibid.
PY30-79	pBL230-79 (*TRP1 pol30-79*) in PY37 w/o pBL211 (*POL30 URA*)	(Eissenberg et al., 1997)
PY30-90	pBL230-90 (*TRP1 pol30-90*) in PY37 w/o pBL211 (*POL30 URA*)	ibid.
YRBS1	pBL230-K127R (*TRP1 pol30-K127R*) in PY37 w/o pBL211 (*POL30 URA*)	This work, made by shuffling plasmid pBL230-K127R into PY37
YRBS2	pBL230-K164R (*TRP1 pol30-K164R*) in PY37 w/o pBL211 (*POL30 URA*)	This work, made by shuffling plasmid pBL230-K164R into PY37
YSJ208	*POL30-Myc3::KanMX4* in DF5α: *Matα MTR10 lys2-801 leu2-3, 2-112 ura3-52 his3Δ200 trp1-1*	(Hoege et al., 2002)
YPL917	*set1::p9MycSET1-TRP1* in W303	(Pamblanco et al., 2004)
YPL918	*set1::p9MycSET1-LEU2* in W303	ibid.
YPL919	*set1::p9MycSET1 YF->AA-TRP1* in W303	ibid.
YPL920	*set1::p9MycSET1 YF->YD-LEU2* in W303	ibid.
YPL921	*set1::p9MycSET1 YF->DD-LEU2* in W303	ibid.

Unless stated otherwise, all strains are MATa and in the W303 background (Thomas and Rothstein, 1999).

In the genotype column, null mutations are indicated by the gene name in small letters and italics, *e.g. hat1::TRP1* is identical to *hat1Δ::TRP1* and refers to a null mutation of the *HAT1* gene produced with a *TRP1* nutritional marker.

For strains YAV138-145, PBM1 mut indicates the PBM1 mutation FF22,23AA, whereas PBM2 mut refers to the PBM2 mutation FF232,233AA.

All strains were created by transformation of yeast strains with either linearised plasmids or PCR products to direct DNA integration at the desired locus by homologous recombination. Integration at the correct locus was selected with the indicated nutritional markers (*HIS3*, *TRP1*, *LEU2*, *URA3* or KanMX) and verified by PCR.

The *asf1Δ cac1Δ* strain was created by crossing the *asf1Δ::KanMX* and *cac1Δ::LEU2* single mutant strains and selecting the LEU+ and KanMX+ progeny.

Strains 36-43 were obtained by plasmid shuffling (Ayyagari et al., 1995). The mutant *pol30* alleles on a *TRP1* plasmid were transformed into strains containing the wild type *POL30* gene on a *URA3* plasmid. The plasmid expressing wild type *POL30* was then selected against using 5-FOA, a drug that kills cells that express the *URA3* gene.

APPENDIX II – MICRO-ARRAY SCREEN RESULTS

Table II.I: Annotated genes whose expression is significantly altered in all three mutant strains relative to wild type

Affymetrix name	Expression value normalized to W303				Common name	Genbank name	Description
	asfΔ cac1Δ	*cac1Δ*	*asf1Δ*	W303			
3768_i_at	6560.9	1540.6	10254	1	*RDN5-1*	RDN5-1	RDN5-1 5S ribosomal RNA
4859_at	4558.3	4951.3	3343.5	1	*MTR3*	YGR158C	Involved in mRNA transport
5087_at	4503	5755.5	4040.8	1	*ALG2*	YGL065C	Glycosyltransferase
11301_i_at	4326	116.3	3155.8	1	*FLO1*	YAR050W	FLO1 putative cell wall glycoprotein
4584_at	3927.7	1153	4201.7	1	*RIM4*	YHL024W	RNA binding domain (N-term) with asparagine rich region?
4212_g_at	3153.2	1472.8	3844.1	1	*SGA1*	YIL099W	Intracellular glucoamylase
10099_at	3153.2	2422.4	4720.2	1		YLR251W	Similarity to peroxisomal rat membrane protein PMP22
10072_at	2832.3	968.9	2458.5	1		YLR267W	Bypass of PAM1
3810_s_at	2300.2	83.1	1520.2	1	*RDN37-1*	RDN37-1	RDN37-1 35S ribosomal RNA
8596_at	2246	1317.8	3862	1	*THI20*	YOL055C	Similarity to B. subtilis transcriptional activator tenA
10858_s_at	2168.5	9398.8	15430	1	*THI11*	YJR156C	Thiamine biosynthetic enzyme
9313_at	1659.6	116.3	2905.4	1			Protein with similarity to Gls1p and Gls2p (GB:Z49212)
4336_at	1504.7	3003.7	2306.5	1	*FMO*	YHR176W	Dimethylaniline monoxygenase
9515_at	1283.4	484.5	2807.1	1			Strong similarity to succinate dehydrogenase
4284_at	1183.8	474.8	2887.6	1		YIL167W	serine dehydratase
9196_s_at	1040	1501.9	4568.3	1			Similarity to M.verrucaria cyanamide hydratase, identical to hypothetical protein YFL061w

3614_f_at	785.5	1763.5	2825	1		YORCDELTA18	Ty1 LTR
AFFX-25srRnac_at	749.7	62.3	357.9	1			Z73326 SGD:YLR154C Yeast S.cerevisiae 25S ribosomal RNA corresponds to complement of 4212-7605 in Z73326 (regions a-e represent transcript regions 5 prime to 3 prime respectively)
AFFX-18srRnaa_at	85.4	6.55	67.75	1			Z75578 SGD:YLR154C Yeast S. cerevisiae 18S ribosomal RNA corresponds to 1-1799 in Z75578 (regions a-e represent transcript regions 5 prime to 3 prime respectively)
8599_at	47.4	5.8	24.5	1		YOL053C-A	DNA Damage Responsive
4209_at	45.4	5.9	20.5	1	*XBP1*	YIL101C	DNA-binding transcriptional repressor
8784_s_at	43.15	55.9	137.1	1		YNR073C	Strong similarity to E.coli D-mannonate oxidoreductase, identical to YEL070w
4573_at	40.3	41.4	38.8	1		YHL035C	ABC transporter
11287_f_at	33.1	40.0	75.7	1	*PAU7*	YAR020C	Strong similarity to members of the srp1p/Tip1p family
10551_at	26.3	3.7	11.3	1	*DAL80*	YKR034W	Negative regulator of multiple nitrogen catabolic genes
7295_at	24.9	6.9	38.1	1	*HSP26*	YBR072W	Heat shock protein 26
9388_at	24.3	7.6	22.35	1			Similarity to glutamate decarboxylases
5372_at	20.1	2.25	11.85	1	*HSP12*	YFL014W	12 kDa heat shock protein
8725_g_at	18.5	14.7	28.0	1		YOL155C	Similarity to glucan 1,4-alpha-glucosidase Sta1p and YAR066w
11068_at	18.0	14.9	43.45	1		YJL045W	Strong similarity to succinate dehydrogenase flavoprotein
10962_at	17.3	13.4	25.25	1	*BNA2*	YJR078W	Similarity to mammalian indoleamine 2,3-dioxygenase

7944_at	16.4	21.7	62.0	1	*OYE3*	YPL171C	NAD(P)H dehydrogenase
8375_at	16.2	5.0	10.9	1		YOR173W	Strong similarity to YLR270w
10078_at	14.5	5.2	23.7	1	*PIG1*	YLR273C	Protein similar to Gac1p, a putative type 1 protein phosphatase targeting subunit
7367_at	14.2	8.0	17.4	1	*FLR1*	YBR008C	Major Facilitator Transporter
4752_at	13.5	12.3	11.8	1	*NAS6*	YGR232W	Possible homolog of human 26S proteasome regulatory subunit p28
9538_at	12.8	15.2	16.0	1			Encodes highly conserved 35 kDa protein that shows increased expression after entry into stationary phase
8724_at	12.6	8.8	18.7	1		YOL155C	Similarity to glucan 1,4-alpha-glucosidase Sta1p and YAR066w
10501_at	12.6	8.5	25.4	1	*ECM4*	YKR076W	ExtraCellular Mutant
4768_at	12.2	4.1	7.8	1		YGR248W	Similar to SOL3
5633_at	11.5	4.8	10.2	1	*HOR2*	YER062C	DL-glycerol-3-phosphatase
7604_at	11.3	2.3	6.5	1	*GPH1*	YPR160W	Glycogen phosphorylase
8412_at	10.8	3.4	6.9	1	*GCY1*	YOR120W	Similar to mammalian aldoVketo reductases
9980_at	10.5	4.1	8.1	1			Similarity to SCM4 protein
11060_at	10.0	3.13	10.7	1	*TDH1*	YJL052W	Glyceraldehyde-3-phosphate dehydrogenase 1
9519_at	9.8	6.2	16.9	1			5-aminoimidazole-4-carboxamide ribonucleotide (AICAR) transformylaseVIMP cyclohydrolase
8683_at	9.8	12.6	18.0	1	*GRE2*	YOL151W	Induced by osmotic stress\; similar to dihydroflavonol 4-reductase from plants
10158_at	9.2	3.35	6.3	1	*TFS1*	YLR178C	Suppressor of cdc25
8659_at	9.2	4.4	7.7	1	*PHM7*	YOL084W	Similarity to A.thaliana hyp1 protein
9757_at	9.1	2.4	7.6	1			C-terminal part starting with aa 262 cause growth inhibition when overexpressed
10681_at	8.75	6.0	12.0	1	*LAP4*	YKL103C	Vacuolar aminopeptidase ysc1

4074_at	8.7	2.6	5.8	1	*GTT1*	YIR038C	Glutathione transferase
4969_at	8.7	3.7	7.8	1		YGR043C	Strong similarity to transaldolase
4924_at	8.6	4.9	10.0	1	*CTT1*	YGR088W	Cytoplasmic catalase T
4241_at	8.6	2.25	12.6	1	*POT1*	YIL160C	Peroxisomal 3-oxoacyl CoA thiolase
9996_at	8.5	3.0	6.2	1			Strong similarity to Stf2p
4236_at	8.4	11.8	11.9	1	*QDR1*	YIL120W	Similarity to antibiotic resistance proteins
6598_at	8.4	3.1	5.6	1	*STF1*	YDL130W-A	ATPase stabilizing factor
4732_at	8.3	4.3	17.5	1	*GND2*	YGR256W	6-phosphogluconate dehydrogenase
10060_at	8.2	7.9	6.8	1	*GSY2*	YLR258W	Glycogen synthase (UDP-gluocse--starch glucosyltransferase)
4075_at	8.2	2.0	13.1	1	*YPS6*	YIR039C	GPI-anchored aspartic protease
5253_g_at	8.2	3.6	12.5	1	*YPS5*	YGL259W	GPI-anchored aspartic protease
7432_at	8.1	4.7	8.6	1	*PRX1*	YBL064C	Homolog to thiol-specific antioxidant
4198_at	8.1	6.0	8.9	1	*SDP1*	YIL113W	Strong similarity to dual-specificity phosphatase Msg5p
8669_at	7.8	4.15	6.9	1	*MCH4*	YOL119C	Similarity to monocarboxylate transporter proteins
8988_at	7.6	5.7	4.9	1			Similarity to C.carbonum toxD gene
10626_at	7.4	4.9	26.0	1		YKL070W	Similarity to B.subtilis transcriptional regulatory protein
9120_at	7.15	3.75	6.15	1			Similarity to glycerate- and formate-dehydrogenases
7321_at	7.1	2.4	4.6	1		YBR053C	Similarity to rat regucalcin
5400_at	7.1	4.85	6.35	1		YFL030W	Similarity to several transaminases
9059_at	7.1	2.7	3.5	1			Strong similarity to human TGR-CL10C
9743_at	7.05	6.3	7.7	1			123 kD regulatory subunit of trehalose-6-phosphate synthaseVphosphatase complex\; homologous to TPS3 gene product

10080_at	7.0	4.4	22.1	1	*EST1*	YLR233C	Telomere elongation protein (ever shorter telomeres)
9482_g_at	7.0	3.0	5.7	1			Aldehyde Dehydrogenase (NAD(P)+)
3252_s_at	6.8	66.0	14.9	1		YGRWTY3-1	YGRWTY3-1 Full length Ty3
6462_at	6.8	2.2	4.1	1	*NTH1*	YDR001C	Neutral trehalase (alpha,alpha-trehalase)
7274_at	6.8	0.2	3.4	1	*PHO5*	YBR093C	Acid phosphatase, repressible
9801_at	6.5	5.95	15.7	1			similarity to human leukotriene b4 12-hydroxydehydrogenase
8359_at	6.3	32.7	2.9	1	*HIS3*	YOR202W	Imidazoleglycerol-phosphate dehydratase
10758_at	6.3	5.9	12.8	1		YKL161C	Probable serineVthreonine-specific protein kinase (EC 2.7.1.-)
5735_at	6.2	2.5	5.9	1	*GLC3*	YEL011W	1,4-glucan-6-(1,4-glucano)-transferase
4070_at	6.2	2.6	3.2	1	*LYS1*	YIR034C	Saccharopine dehydrogenase
6012_at	6.2	6.3	17.1	1	*TSA2*	YDR453C	Strong similarity to thiol-specific antioxidant proteins
9481_at	6.2	2.8	7.0	1			Aldehyde Dehydrogenase (NAD(P)+)
5357_at	6.0	3.9	4.5	1	*GSY1*	YFR015C	Glycogen synthase (UDP-gluocse--starch glucosyltransferase)
8593_at	5.9	3.8	3.2	1	*ARG1*	YOL058W	Arginosuccinate synthetase
6902_at	5.9	3.4	4.35	1	*HIS4*	YCL030C	Histidinol dehydrogenase
10581_at	5.9	4.8	7.3	1	*GPX1*	YKL026C	Strong similarity to glutathione peroxidase
6273_at	5.8	3.7	6.65	1	*ADR1*	YDR216W	Positive transcriptional regulator of ADH2 and peroxisomal protein genes
6710_at	5.75	7.8	21.8	1	*AAD4*	YDL243C	Hypothetical aryl-alcohol dehydrogenase
6937_at	5.7	2.2	4.15	1	*GLK1*	YCL040W	Glucokinase
9460_at	5.7	5.8	5.25	1			Glycine decarboxylase complex (P-subunit), glycine synthase (P-subunit), Glycine cleavage system (P-subunit)

11032_at	5.6	3.35	4.65	1	*MET3*	YJR010W	ATP sulfurylase
9668_at	5.6	4.3	8.3	1			Carnitine O-acetyltransferase, peroxisomal and mitochondrial
5749_at	5.5	3.5	13.9	1		YEL041W	Strong similarity to Utr1p
8173_at	5.5	2.2	3.8	1	*ALD4*	YOR374W	Aldehyde dehydrogenase (E.C. 1.2.1.5) (sold by SIGMA under the catalogue number A5550, according to A. Blomberg)
5588_at	5.5	2.5	7.45	1	*SSA4*	YER103W	Member of 70 kDa heat shock protein family
4992_at	5.5	2.6	3.3	1	*UGA1*	YGR019W	Gamma-aminobutyrate (GABA) transaminase (4-aminobutyrate aminotransferase)
10614_at	5.3	5.4	10.5	1	*RGT1*	YKL038W	Transcriptional repressor and activator
6480_at	5.3	6.1	6.5	1	*GCV1*	YDR019C	Glycine cleavage T protein (T subunit of glycine decarboxylase complex
7037_s_at	5.25	3.7	4.1	1	*UGA2*	YBR006W	Probable aldehyde dehydrogenase (EC 1.2.1.-)
6428_at	5.1	2.3	2.9	1	*UBC5*	YDR059C	Ubiquitin-conjugating enzyme
4526_at	4.9	3.6	5.65	1	*SOD2*	YHR008C	Manganese-containing superoxide dismutase
7244_at	4.8	3.8	8.0	1		YBR108W	Probable transcription factor
8437_at	4.8	2.8	9.1	1	*CRC1*	YOR100C	Similarity to mitochondrial carrier proteins
6794_at	4.7	2.0	8.6	1		YCR099C	Strong similarity to Pep1p
4068_at	4.6	0.08	0.01	1	*DAL3*	YIR032C	Ureidoglycolate hydrolase
3721_s_at	4.6	4.2	5.0	1		YLRWTY2-1	Full length Ty2
10532_at	4.5	3.4	6.6	1	*KTR2*	YKR061W	Putative mannosyltransferase\; type 2 membrane protein
10244_at	4.5	2.8	8.9	1	*EMP46*	YLR080W	Strong similarity to Emp47p
6899_at	4.4	2.2	5.1	1		YCL033C	Transcription regulator
11385_s_at	4.3	2.2	7.65	1	*FLO9*	YAL063C	Putative Flo1p homolog
9287_s_at	4.3	3.5	9.2	1			Strong similarity to YPL280w, YOR391c and YDR533c

10794_at	4.15	5.0	5.6	1		YKL218C	Threonine dehydratase
9762_at	4.1	0.2	2.8	1			Inorganic phosphate transporter, transmembrane protein
10505_at	3.9	6.4	5.95	1	*MTD1*	YKR080W	NAD-dependent 5,10-methylenetetrahydrafolate dehydrogenase
5751_at	3.9	2.1	6.3	1	*CYC7*	YEL039C	Iso-2-cytochrome c
7109_at	3.8	9.95	16.5	1	*GPX2*	YBR244W	Probable glutathione peroxidase (EC 1.11.1.9)
11253_s_at	3.7	2.8	9.95	1	*HXT9*	YJL219W	High-affinity hexose transporter
8420_at	3.5	24.15	26.5	1	*ADE2*	YOR128C	Phosphoribosylamino-imidazole-carboxylase
9537_at	3.5	5.8	12.0	1			SNZ1 proximal ORF, stationary phase induced gene
11251_s_at	3.5	2.9	8.7	1	*FSP2*	YJL221C	Homology to maltase(alpha-D-glucosidase)
6799_at	3.4	2.9	6.95	1	*ADH7*	YCR105W	Alcohol dehydrogenase
9057_at	3.3	3.2	5.9	1			Peroxisomal 2,4-dienoyl-CoA reductase
11185_at	3.0	16.8	9.5	1	*INO1*	YJL153C	L-myo-inositol-1-phosphate synthase
10470_at	2.9	3.3	5.9	1	*SRL3*	YKR091W	Suppressor of rad53 lethality
10795_at	2.8	3.2	7.2	1	*JEN1*	YKL217W	Carboxylic acid transporter protein homolog
9309_at	2.8	4.5	12.2	1			Alcohol dehydrogenase II
6797_at	2.8	3.6	15.6	1		YCR102C	Alcohol dehydrogenase
7314_at	2.8	3.6	5.05	1	*ZTA1*	YBR046C	Homolog to quinone oxidoreductase (*E. coli*)
8192_at	2.6	0.2	0.3	1	*PUT4*	YOR348C	Putative proline-specific permease
9885_at	2.6	11.2	3.1	1			Ornithine aminotransferase
10563_at	2.45	5.3	3.3	1	*MET14*	YKL001C	Adenylylsulfate kinase
10494_at	2.3	5.2	5.0	1	*MET1*	YKR069W	Siroheme synthase
6077_at	2.2	6.45	4.0	1	*ARO10*	YDR380W	Similarity to Pdc6p, Thi3p and to pyruvate decarboxylases
6906_at	2.15	2.0	11.8	1	*FRM2*	YCL026C-A	Protein involved in the integration of lipid signaling pathways with cellular homeostatis

6798_f_at	2.15	2.0	8.3	1	*PAU3*	YCR104W	Member of the seripauperin proteinVgene family (see Gene_class PAU)
4844_at	2.1	3.15	10.1	1	*THI4*	YGR144W	Component of the biosynthetic pathway producing the thiazole precursor of thiamine
10748_at	2.0	9.3	9.8	1		YKL171W	Probable serineVthreonine-specific protein kinase (EC 2.7.1.-)
10478_at	2.0	4.5	8.8	1	*PCK1* ***	YKR097W	phosphoenolpyruvate carboxylkinase
8592_at	0.4	0.4	0.2	1	*GPD2*	YOL059W	Glycerol-3-phosphate dehydrogenase (NAD+)
3404_f_at	0.4	0.2	0.1	1		YDRWDELTA10	Ty1 LTR
3924_f_at	0.3	0.3	0.2	1		TS	TS(AGA)A tRNA-Ser
3794_f_at	0.3	0.3	0.1	1		TS	TS(AGA)L tRNA-Ser
6515_at	0.3	0.3	0.2	1	*BSC1*	YDL037C	Strong similarity to glucan 1,4-alpha-glucosidase
3869_f_at	0.3	0.01	0.01	1		TG	TG(GCC)J1 tRNA-Gly
3863_f_at	0.3	0.5	0.2	1		TR	TR(UCU)J2 tRNA-Arg
3862_f_at	0.3	0.5	0.2	1		TR	TR(UCU)J1 tRNA-Arg
7398_at	0.3	0.3	0.2	1		YBL054W	Homolog to myb transforming proteins
6923_at	0.25	0.2	0.2	1	*SPB1*	YCL054W	Methyltransferase
6707_at	0.25	0.4	0.2	1	*TRM8*	YDL201W	Strong similarity to human D1075-like protein
3514_f_at	0.2	0.3	0.1	1		TS	TS(AGA)B tRNA-Ser
6049_at	0.2	0.25	0.3	1	*UTP5*	YDR398W	Similarity to human KIAA0007 gene
11389_at	0.2	0.3	0.15	1	*ECM1*	YAL059W	ExtraCellular Mutant
6025_at	0.15	0.2	0.3	1	*RMT2*	YDR465C	Protein arginine methyltransferase
3821_f_at	0.15	0.3	0.1	1		TH	TH(GUG)K tRNA-His
3372_f_at	0.1	0.25	0.2	1		TH	TH(GUG)E1 tRNA-His
3361_f_at	0.1	0.2	0.1	1		TS	TS(AGA)E tRNA-Ser
4893_at	0.1	0.4	0.2	1	*NOP7*	YGR103W	Similarity to zebrafish essential for embryonic development gene pescadillo

9027_at	0.1	0.5	0.1	1		Adenosine deaminaseVadenine aminohydrolase
3508_f_at	0.1	0.01	0.01	1	TG	TG(GCC)B tRNA-Gly
4605_s_at	0.1	0.3	0.1	1	SNR39b	SNR39b snRNA
3803_f_at	0.1	0.3	0.1	1	TR	TR(ACG)L tRNA-Arg
3710_f_at	0.04	0.3	0.2	1	TA	TA(AGC)M1 tRNA-Ala
3438_f_at	0.03	0.3	0.1	1	TR	TR(ACG)D tRNA-Arg
3251_s_at	0.01	34.15	3.2	1	YGRWTY3-1	Full length Ty3
3819_f_at	0.01	0.4	0.1	1	TA	TA(AGC)K1 tRNA-Ala
3358_f_at	0.01	0.01	0.01	1	TG	TG(GCC)E tRNA-Gly

Table II.II : Annotated genes whose expression is significantly altered in *asf1Δ* and *asf1Δcac1Δ* relative to wild type

Affymetrix name	**Expression value normalized to W303**				**Common name**	**Genbank name**	**Description**
	asfΔ cac1Δ	***cac1Δ***	***asf1Δ***	**W303**			
3982_at	65.7	0.1	28.9	1		KANMX4	Kanamycin resistance casette
10416_at	14.0	0.7	2.4	1	*GTT2*	YLL060C	YLL060C Glutathione transferase
7981_at	13.95	1.8	15.4	1	*GRE1*	YPL223C	Induced by osmotic stress
11387_at	12.8	1.4	7.3	1		YAL061W	Similarity to alcohol/sorbitol dehydrogenase
3766_s_at	11.4	1.8	9.65	1	*RDN25-1*	RDN25-1	RDN25-1 25S ribosomal RNA
7322_at	10.5	1.2	5.2	1	*YRO2*	YBR054W	Homolog to HSP30 heat shock protein YRO1 (*S. cerevisiae*) 7
7422_at	10.4	1.9	6.9	1	*SSA3*	YBL075C	Heat-inducible cytosolic member of the 70 kDa heat shock protein family
5179_at	9.7	1.8	9.9	1	*AMS1*	YGL156W	Vacuolar alpha mannosidase
7254_at	7.6	1.7	9.4	1	*TKL2*	YBR117C	Transketolase, homologous to tkl1
10172_at	6.3	0.8	2.2	1	*PUT1*	YLR142W	Proline oxidase
4884_i_at	6.2	1.65	2.6	1	*TPO2*	YGR138C	Similarity to multidrug resistance proteins

7582_at	5.95	1.9	4.5	1	*GDB1*	YPR184W	Similarity to human 4-alpha-glucanotransferase (EC 2.4.1.25)/amylo-1,6-glucosidase (EC 3.2.1.33)
6607_at	5.55	1.6	5.4	1		YDL124W	Similarity to aldose reductases
9008_at	5.5	1.6	3.2	1			YGP1 encodes gp37, a glycoprotein synthesized in response to nutrient limitation which is homologous to the sporulation-specific SPS100 gene
5423_s_at	5.1	1.5	5.4	1	*AAD16*	YFL057C	Strong similarity to aryl-alcohol dehydrogenases
10373_at	4.75	0.8	14.0	1		YLL057C	Similarity to E.coli dioxygenase
10154_at	4.7	1.0	5.1	1	*IDP2*	YLR174W	Cytosolic form of NADP-dependent isocitrate dehydrogenase
6427_at	4.4	1.8	5.6	1	*TGL2*	YDR058C	TriGlyceride Lipase
7613_at	3.7	1.9	5.9	1		YPR127W	Similarity to C-term. of N.tabacum auxin-induced protein
8387_at	3.5	1.9	5.1	1	*GSP2*	YOR185C	GTP binding protein, almost identical to Gsp1p
9771_at	2.95	1.9	7.0	1			Predicted protein is very hydrophobic, has many membrane-spanning regions, several potential glycosylation sites, potential ATP-binding site
5786_f_at	2.7	1.0	6.4	1	*PAU2*	YEL049W	Member of the seripauperin proteinVgene family (see Gene_class PAU)
10853_at	2.7	1.8	5.2	1	*DAN4*	YJR151C	Similarity to mucin proteins, YKL224c, Sta1p
9958_at	2.6	1.7	7.2	1			Fructose-1,6-bisphosphatase
6795_at	2.6	1.6	5.0	1	***	YCR100C	Strong similarity to Pep1p
8922_at	0.45	0.6	0.2	1			Protein involved in the aging process
4522_at	0.44	0.7	0.2	1	*GPA1*	YHR005C	Alpha subunit of G protein coupled to mating factor receptors

5571_at	0.4	0.55	0.2	1	*RPS26B*	YER131W	Ribosomal protein S26B
3310_s_at	0.3	0.6	0.2	1		YERWDELTA18	Ty1 LTR
3814_f_at	0.3	0.7	0.1	1		TR	TR(UCU)K tRNA-Arg
3688_f_at	0.2	0.6	0.2	1		TA	TA(AGC)M2 tRNA-Ala
5034_at	0.2	0.65	0.2	1	*SCW11*	YGL028C	Glucanase gene family member
9900_at	0.2	0.55	0.3	1			Strong similarity to S. pombe beta-transducin
7413_at	0.1	0.75	0.4	1	*URA7*	YBL039C	CTP synthase, highly homologus to URA8 CTP synthase
6950_at	0.1	0.7	0.25	1		SNR56	SNR56 snRNA
3473_f_at	0.06	0.8	0.01	1		TA	TA(AGC)D tRNA-Ala
3885_f_at	0.04	0.7	0.2	1		TA	TA(AGC)J tRNA-Ala
10131_at	0.03	0.6	0.4	1	*PWP1*	YLR196W	A WD40 repeat protein
11134_at	0.01	0.7	0.01	1	*ASF1*	YJL115W	Anti-silencing protein that causes depression of silent loci when overexpressed

Table II.III: Annotated genes whose expression is significantly altered in *cac1Δ* and *asf1Δcac1Δ* relative to wild type

Affymetrix name	**Expression value normalized to W303**				**Common name**	**Genbank name**	**Description**
	asfΔ cac1Δ	***cac1Δ***	***asf1Δ***	**W303**			
10957_at	6.6	3.5	1.95	1	*OPI3*	YJR073C	Methylene-fatty-acyl-phospholipid synthase (unsaturated phospholipid N-methyltransferase)

Table II.IV: Annotated genes whose expression is significantly altered in *asf1Δ* and *cac1Δ* relative to wild type

Affymetrix name	Expression value normalized to W303				Common name	Genbank name	Description
	asfΔ cac1Δ	*cac1Δ*	*asf1Δ*	W303			
3247_s_at	1.1	10513	625.8	1		NC_001139	TY3B protein Found forward in NC_001139 between 707604 and 708461 with 100% identity.
7308_at	1.1	8468.6	1698.6	1	*FIG1*	YBR040W	Integral membrane protein
3966_i_at	1.1	5726.5	1099.6	1		NC_001224	Similarity to T.brucei mitochondrion protein SGC6 Found reverse in NC_001224 between 34032 and 34430 with 88.28% identity.
3816_f_at	1.4	82.7	37.5	1		YKLWDELTA 3	Ty1 LTR
3259_at	0.8	44.0	5.6	1		YGLCDELTA 5	Ty1 LTR
3137_s_at	1.1	15.7	2.0	1		YILWTY3-1	Full length Ty3
4184_s_at	0.95	13.0	2.4	1		YIL080W	Ty3-2 orf C fragment
8802_at	1.0	8.4	2.0	1	*AGA1*	YNR044W	Anchorage subunit of a-agglutinin
4386_at	1.9	7.5	6.3	1	*ARO9*	YHR137W	Aromatic amino acid aminotransferase II
9902_at	1.5	6.85	3.15	1			Copper Transporter
3851_s_at	1.0	6.2	3.2	1	*COS5*	YJR161C	Protein with similarity to members of the Ybr302pVYcr007pVCos8pVCos9p family, coded from subtelomeric region
10879_at	1.75	5.9	6.2	1	*MNS1*	YJR131W	Specific alpha-mannosidase
10804_at	1.9	5.8	6.7	1	*CBT1*	YKL208W	Subunit of complex involved in processing of the 3' end of cytochrome b pre-mRNA
10793_at	1.3	5.0	2.7	1	*COS9*	YKL219W	Protein with similarity to subtelomerically-encoded proteins such as Cos5p, Ybr302p, Cos3p, Cos1p, Cos4p, Cos8p, Cos6p, Cos9p

9864_at	1.9	2.9	10.3	1	***		Similarity to C.carbonum toxD protein
3476_f_at	0.7	0.5	0.1	1		TS	TS(AGA)D1 tRNA-Ser
8505_at	0.9	0.5	0.1	1	*HMS1*	YOR032C	Myc-family transcription factor homolog
9567_at	1.2	0.3	0.2	1			May regulate NAM7 function, possibly at level of mRNA turnover
7626_at	0.7	0.25	0.2	1	*MEP3*	YPR138C	NH4+ transporter, highly similar to Mep1p and Mep2p
6907_at	1.5	0.2	0.2	1	*AGP1*	YCL025C	Amino acid permease
4428_at	0.65	0.1	0.3	1	*HXT4*	YHR092C	High-affinity glucose transporter
3959_at	1.0	0.1	0.03	1		NC_001224	F1F0-ATPase complex, FO A subunit Found forward in NC_001224 between 28487 and 29266 with 97.564% identity.
3958_r_at	1.5	0.1	0.03	1		NC_001224	Similarity to mouse Gcap1 Found forward in NC_001224 between 28122 and 28444 with 88.59% identity.
5409_at	0.8	0.1	0.15	1	*GAT1*	YFL021W	Transcriptional activator with GATA-1-type Zn finger DNA-binding motif
9026_at	1.05	0.07	0.1	1			Ammonia transport protein
10511_at	1.3	0.06	0.06	1	*GAP1*	YKR039W	General amino acid permease
3960_at	0.7	0.01	0.01	1		NC_001224	Endonuclease SCEI, small subunit Found forward in NC_001224 between 46046 and 46361 with 69.394% identity.
10933_at	0.6	0.01	0.01	1	*RPL43B*	YJR094W-A	Ribosomal protein L43B

Table II.V: Annotated genes whose expression is significantly altered in *asf1Δ* only relative to wild type

Affymetrix name	Expression value normalized to W303				Common name	Genbank name	Description
	asfΔ cac1Δ	*cac1Δ*	*asf1Δ*	W303			
10486_s_at	0.9	1.2	7.7	1		YKR105C	Strong similarity to Sge1p and hypothetical protein YCL069w
8720_f_at	0.7	1.35	7.3	1		YOL161C	Strong similarity to members of the Srp1p/Tip1p family
10704_at	1.1	2.0	7.25	1	*SSH4*	YKL124W	Suppressor of SHR3\; confers leflunomide resistance when overexpressed
3988_at	0.6	1.6	7.05	1	*BI3*	Q0115	Cytochrome-c oxidase chain III
8816_at	3.4	2.05	6.6	1	*BIO4*	YNR057C	Dethiobiotin synthetase
6057_at	1.5	2.0	6.5	1	*PDR15*	YDR406W	Probable multidrug resistance transporter
9124_at	3.9	3.6	5.8	1			Protein highly homologous to permeases Can1p and Lyp1p for basic amino acids
10792_at	1.0	1.9	5.5	1	*FRE2*	YKL220C	Ferric reductase, similar to Fre1p
6761_at	3.3	3.5	5.4	1		YCR068W-A	Similarity to starvation induced pSI-7 protein of C. fluvum
10789_f_at	1.1	1.6	5.0	1		YKL224C	Strong similarity to members of the Srp1p/Tip1p family
5627_at	1.7	2.8	5.0	1	*SHC1* ***	YER096W	Sporulation-specific homolog of csd4
11181_at	0.6	1.6	0.2	1	*FAR1*	YJL157C	Factor arrest protein

Table II.VI: Annotated genes whose expression is significantly altered in *cac1Δ* only relative to wild type

Affymetrix name	Expression value normalized to W303				Common name	Genbank name	Description
	asfΔ cac1Δ	*cac1Δ*	*asf1Δ*	W303			
6784_at	1.15	8.4	1.2	1	*FIG2*	YCR089W	Predicted GPI-anchored cell wall protein
11213_at	0.6	7.1	0.6	1	*ASG7* ***	YJL170C	An a-specific gene that is induced to a higher expression level by alpha factor
7478_s_at	0.7	0.2	0.8	1		YBL109W	Similarity to subtelomeric encoded proteins
3752_f_at	1.2	0.2	0.9	1		YLRCDELTA19	Ty1 LTR
7546_at	1.0	0.2	0.55	1	*OPT2*	YPR194C	Similarity to S.pombe isp4 protein
8228_at	1.45	0.15	0.6	1		YOR338W	Similarity to YAL034c
7273_at	1.5	0.15	0.7	1	*PHO3*	YBR092C	Acid phosphatase, constitutive
5064_at	0.6	0.15	0.8	1	*DST1*	YGL043W	RNA polymerase II elongation factor
5724_at	0.9	0.1	0.7	1	*URA3*	YEL021W	Orotidine-5'-phosphate decarboxylase
4562_at	1.1	0.02	1.5	1	*ARN2*	YHL047C	Similarity to C.carbonum toxin pump
10185_s_at	2.2	0.01	1.45	1	*ASP3-1*	YLR155C	Nitrogen catabolite-regulated cell-wall L-asparaginase II
3189_i_at	1.6	0.01	0.9	1	*COS8*	YHL048W	Protein with similarity to subtelomerically-encoded proteins such as Cos5p, Ybr302p, Cos3p, Cos1p, Cos4p, Cos8p, Cos6p, Cos9p
3954_at	1.16	0.01	0.9	1		2mic_REP2	2 micron plasmid rep2 protein
3952_at	1.0	0.01	1.0	1		2mic_REP1	2 micron plasmid rep1 protein
3953_at	1.7	0.01	2.1	1		2mic_D_protein	2 micron plasmid D protein
3955_at	1.0	0.01	1.5	1		2mic_FLP1	2 micron plasmid recombinase

Table II.VII: Annotated genes whose expression is significantly altered in *asf1Δcac1Δ* only relative to wild type

Affymetrix name	Expression value normalized to W303				Common name	Genbank name	Description
	asfΔ cac1Δ	***cac1Δ***	***asf1Δ***	**W303**			
4220_at	19.1	0.55	1.2	1	*OM45*	YIL136W	45-kDa mitochondrial outer membrane protein
3770_i_at	6.6	1.3	1.72	1	*RDN5-3* ***	RDN5-3	RDN5-3 5S ribosomal RNA
10703_at	0.1	0.8	0.8	1	*RRN3*	YKL125W	DNA-independent RNA Polymerase I transcription factor